Targeting Lipid Metabolism as a Therapeutic Approach for Gulf War Illness

Thesis

Roskamp Institute

A thesis submitted for the degree of Doctor of Philosophy
in the discipline of Neuroscience

Targeting Lipid Metabolism as a Therapeutic Approach for Gulf War Illness

Supervisors: Dr. Laila Abdullah and Dr. Fiona Crawford

Utsav Joshi
Personal identifier (PI): E5018112
Roskamp Institute, Sarasota, Florida, USA (ARC)
Open University, Milton Keynes, UK

July 2019

Declaration

I, Utsav Joshi, hereby submit this original work as a part of partial requirement for the degree of Doctor of Philosophy in Neuroscience

Utsav Joshi

Publications

Abdullah, L., Evans, J. E., Joshi, U., Crynen, G., Reed, J., Mouzon, B., Stephan Baumannd , Montaguee H., Zakirova Z., Emmerich T., Bachmeiera C., Klimas N., Sullivani K., Mullan M., Crawford F., 2016. Translational potential of long-term decreases in mitochondrial lipids in a mouse model of Gulf War Illness. *Toxicology* 372, 22–33. doi: 10.1016/j.tox.2016.10.012

Joshi, U., Evans, J.E., Joseph, R., Emmerich, T., Saltiel, N., Lungmus, C., Oberlin, S., Langlois, H., Ojo, J., Mouzon, B., Paris, D., Mullan, M., Jin, C., Klimas, N., Sullivan, K., Crawford, F., Abdullah, L., 2018. Oleoylethanolamide treatment reduces neurobehavioral deficits and brain pathology in a mouse model of Gulf War Illness. Sci. Rep. 8, 12921. doi:10.1038/s41598-018-31242-7

Joshi U., Pearson A., Evans J.E., Langlois H., Saltiel N., Ojo J., Klimas n., Sullivan k., Keegan A., Oberlin S., Darcey T., Cseresznye A., Raya B., Paris D., Hammock B., Vasylieva N., Hongsibsong S., Stern L., Mullan M., Crawford F., Abdullah L., 2019 A permethrin metabolite is associated with adaptive immune responses in Gulf War Illness. July 17 2019, Brain Behavior and Immunity DOI: 10.1016/j.bbi.2019.07.015

ACKNOWLEDGEMENT

This work would not have been possible without the help, support and patience of my supervisors Dr. Laila Abdullah, Senior Scientist III, Roskamp Institute and Dr. Fiona Crawford, President and CEO, Roskamp Institute. I thank them for their brilliant advice, valuable suggestions and supreme knowledge of comparative analysis to complete this thesis. Their enthusiasm for science, high standards, and good humor has created a phenomenal work environment with an inspiring and collaborative atmosphere. I have immense respect for their scientific vision, exceptional knowledge, and for the fact that they were never too busy to answer a question and always corrected my blunders. I am grateful for their patience, support, and valuable insights during my PhD. I would especially like to thank Dr. Abdullah, for challenging me and setting an incredible example for a career in academia.

I would also like to take this opportunity to extend my sincere thanks to Prof. Jim Evans, Director of Mass spectrometry, Roskamp Institute. His enthusiasm, encouragement, and insightful suggestions have been instrumental in making this work possible. I also take this opportunity to thank Mr. Jon Reed, former Head of proteomics, Roskamp Institute for your support and guidance on my early days and for helping shape my scientific and analytical skills. You are such a wonderful person, and I have been lucky to learn so much from you!

I also like to extend my acknowledgement to Dr. Joseph Ojo, Dr. Daniel Paris and Dr. Benoit Mouzon Principle Investigator, Roskamp Institute for their help and encouragement in conducting this research work.

To the lab –Ross Joseph, Sarah Oberlin, Adam Cseresznye and Anastasia Edsell thank you for your hard-collaborative work without which this project would have been stranded in the middle.

Finally, I would like to thank all the staff and PhD students of Roskamp Institute specially Moustafa Algamal, Cillian Lynch, Charis Ringland Ariana Menden, Alexander Morin, Jonas Schweig, Maxwell Eisenbaum and Claire Huguenard. Many more thanks to Andrew Pearson,

Teresa Darcey, Heather Langlois, Mackenzie Browning and Nicole Saltiel for their assistance with reviewing & editing the thesis.

Many thanks to Dr. Michael Mullan, executive director Roskamp Institute for his valuable advice and support which not only helped improved my scientific skills but also my public speaking and presentation skills.

Special thanks to our external collaborators Prof. Bruce Hammock, Dr. Surat Hongsibsong, Dr. Nancy Klimas and Dr. Kimberly Sullivan, who have provided clinical samples.

This dissertation would also not have been possible without the unwavering support from facility people of Roskamp Institute– especially Christopher McGuinness. Thank you for creating a comfortable work environment and making sure that I am safe at all time even during weekends. Chris is also a great friend, and I would like to thank him for his endless support in times of hardship.

This work is supported by two CDMRP awards (GW1300045 and GW150056) and a VA Merit award (1I01RX002260-01A1) to Dr. Laila Abdullah and a CDMRP award (GW080094) to Dr. Fiona Crawford, and by the Roskamp Foundation. Plasma samples from GW veterans were made possible through a CDMRP GWI consortium award (GW120037) to Dr. Kimberly Sullivan, and a VA merit and a CDMRP award to Dr. Nancy Klimas. Partial support for this work came from NIEHS/R01 ES002710, NIEHS/Superfund Research Program P42 ES004699 and the Counter Act Program NIH/U54 NS079202 award to Prof. Bruce Hammock.

At last many thanks to my parents and my brother for their love and unwavering support over the many years and for always being interested in my work.

Table of Contents

Table of Figures

Tables

List of Abbreviations

Chapter 1:

Gulf War Illness (GWI)

Gulf War (GW)

Chronic fatigue syndrome/ Myalgic Encephalomyelitis (CFS/ME)

Central nervous system (CNS)

Magnetic resonance spectroscopy (MRS)

N-acetyl aspartate–to-creatine (NAA/Cr)

Magnetic Resonance Imaging (MRI)

Diffusion Tensor Imaging (DTI)

Pyridostigmine bromide (PB)

Permethrin (PER)

Organophosphate (OP)

N, N-Diethyl-meta-toluamide (DEET)

Chlorpyrifos (CPF)

Ionized calcium-binding adapter molecule 1 (IBA-1)

Diisopropyl fluorophosphate (DFP)

Corticosterone (CORT)

dentate gyrus (DG)

Reactive oxygen species (ROS)

Phospholipids (PL)

Very long chain fatty acids (VLCFA)

Ether phospholipids (ePL)

Sphingomyelin (SM)

Ether phosphatidylcholine (ePC)

Oxidative phosphorylation (OXPHOS)

Adenosine triphosphate (ATP)

nicotinamide adenine dinucleotide (NAD+)

Electron transport chain(ETC)

Tricarboxylic acid cycle (TCA)

Uncoupling proteins (UCP)

Acyl coenzyme A (acyl-CoA)

Carnitine palmitoyltransferase (CPT)

T helper (Th)

Interleukin-1beta (IL-1 β)

Interferon-gamma (IFN)-γ

Tumor necrosis factor (TNF-α)

Interleukin (IL)-2

Coenzyme Q10 (CoQ10)

Transcranial Magnetic Stimulation (rTMS)

Peroxisome proliferator-activated receptors (PPAR)

Nicotinamide Riboside (NR)

Ketogenic diet (KD)

Acyl-coenzyme A oxidase 1 (ACOX1)

17β-hydroxysteroid dehydrogenase 4 (HSD17β4)

Myelin basic protein (MBP)

Glial fibrillary acid protein (GFAP)

Chapter 2:

Branched chain fatty acid(BCFAs)

Oleoylethanolamide (OEA)

Veterans Administration Medical Center (VAMC)

Dimethylformamide (DMF)

Dichloromethane (DCM)

Forced swim test(FST)

Bicinchoninic acid (BCA)

LifeSpan Biologicals (LSBio)

Polyvinylidene fluoride (PVDF)

Meso Scale Discovery (MSD)

Malondialdehyde assay (MDA)

Thiobarbituric Acid Reactive Substances (TBARS)

American Type Culture Collection (ATCC)

One-way analysis of variance (ANOVA)

Least significant difference (LSD)

Target hole (TH)

Liquid chromatography–mass spectrometry (LC-MS)

Lipopolysaccharides (LPS)

Prostaglandin E2 ethanol amide (PGE2EA)

Docosahexaenoyl ethanolamide (DHEA)

Lactate dehydrogenase (LDH)

Mammalian protein extraction reagent (mPER)

Chemokine receptor type 2 (CCR2)

Chemokine ligand type 2 (CCL2)

Elevated Plus Maze(EPM)

Peroxisome proliferator-activated receptors-gamma (PPARγ)

PPARγ co-activator 1α (PGC-1α)

Enzyme-Linked Immunosorbent Assay (ELISA)

Tetramethylbenzidine (TMB)

Benjamini Hochberg correction (BH)

Chapter 3:

Reduction oxidation (redox)

Nicotinamide riboside kinase (NRK)

Nicotinamide mononucleotide adenylyltransferase (NMNAT)

Institutional Review Board (IRB)

Red blood cells (RBC)

Uncoupling protein 2(UCP-2)

Triethylammonium bicarbonate (TEAB)

β-Hydroxybutyrate (β-HB

fatty acid oxidation (FAO)

Kolmogorov-Smirnov test (K-S test)

Trimethylamine *N*-oxide (TMAO)

Short-chain acylcarnitine species (SCAC)

Medium-chain acylcarnitine (MCAC)

Long-chain acylcarnitine species (LCAC)

Very long-chain acylcarnitine species (VLCAC)

Gamma-butyrobetaine hydroxylase (GBBH)

Gamma-butyrobetaine (GBB)

Sirtuin(SirT)

Chapter 4:

3-phenoxybenzoic acid (3-PBA)

Systemic lupus erythematosus (SLE)

Blood-brain barrier (BBB)

N-methyl-D-aspartate (NMDA)

Peripheral blood mononuclear cells (PBMC)

Gulf War Illness Consortium (GWIC)

Parallel reaction monitoring (PRM)

Gas chromatography–mass spectrometry (GC-MS)

Glectron capture detector (ECD)

1,1,1,3,3,3-Hexafluoroisopropanol (HFIP)

N,N'-Diisopropylcarbodiim (DIC)

Magnetic activated cell sorting (MACS)

Abstract:

Upon returning from the 1991 Gulf War (GW), veterans from this conflict exhibited a persistent multisymptomatic illness which is now defined as Gulf War Illness (GWI). There is ample evidence that the presentation of GWI is associated with exposure to an anti-nerve agent pyridostigmine bromide (PB) and pesticides, such as permethrin (PER), that were used as prophylactic measures by veterans during the war. The prevalence of GWI is about 30% in US veterans and 15% in UK veterans who were deployed during this conflict. Clinical presentation of GWI is heterogenous, and veterans with this condition display a wide range of symptoms such as memory impairment, fatigue, gastrointestinal disorder and chronic pain. Current treatment strategies for GWI are limited and provide only symptomatic relief. Due to the multifactorial nature of this illness, quest for appropriate treatment strategies is difficult and further complicated by the fact that many of the GW veterans are also facing age-related chronic health problems. I utilized a mouse model of GWI previously developed using combined exposure to PB and PER (GWI mice) which exhibits neurobehavioral features that are similar to the symptoms reported by GWI veterans. This model displays glia activation and neuroinflammation, pathological features that are reported in other GWI rodent models, representing a common chronic outcome associated with GW chemical exposure. The main objectives of this thesis are to find effective therapies against GWI that target the underlying pathology of GWI.

Many clinical and imaging studies have suggested a possible central nervous system (CNS) involvement in GWI. However, even after two decades, there is no approved medication for treating the CNS pathology of GWI. Much of our previous work suggests dysregulation of lipid homeostasis and metabolism. These results pointed to both mitochondrial and peroxisomal abnormalities in GWI mice as well as in veterans with GWI. As part of my thesis work, I

explored whether targeting mitochondrial and peroxisomal function can reduce abnormal brain lipid accumulation and improve chronic neurobehavioral deficits and the accompanying neuropathology in a mouse model of GW chemical exposure. I examined oleoylethanolamide, which targets peroxisome function via activation of peroxisome proliferator-activated receptors (PPAR) and also decreases inflammation. I examined another strategy using two different treatment regimens, nicotinamide riboside and a ketogenic diet, both of which target different aspects of mitochondrial bioenergetics. In addition to peroxisome and mitochondria dysfunction, recent evidence suggests that the symptoms of GWI resemble those of patients with autoimmune disorders, but it is unknown how GW chemicals could have caused immune dysfunction in GWI. Therefore, I focused on a PER metabolite, 3-phenoxybenzoic acid (3-PBA), which is previously shown to form adducts with endogenous proteins. I observed the presence of 3-PBA modified lysine on protein peptides in GWI mice acutely post-exposure and also detected autoantibodies against 3-PBA-albumin conjugates in plasma of GWI mice and in veterans with GWI at chronic post-exposure timepoints. These studies suggest that pesticide exposure associated with GWI may have resulted in the activation of the peripheral and CNS adaptive immune responses, possibly contributing to an autoimmune-type phenotype in veterans with GWI. I hope that the work described in this thesis provides novel avenues for the development of objective biomarkers and therapies for GWI.

Chapter 1: Introduction

1.1 Background

Gulf War Illness (GWI) is a complex and chronic, multi-symptom condition, which affects approximately 30% of the 700,000 US military personnel who were deployed to the 1990-1991 Gulf War (GW)[1,2]. It is also believed that about 33,000 UK GW veteran are living with GWI[3]. Almost three decades have passed since a United Nations resolution act officially ended this war, yet GW veterans with GWI continue to suffer from poor health and report a wide range of symptoms that include fatigue, muscle pain, sleep disturbance and memory problems. The clinical presentation of GWI resembles that of other multi-symptom conditions including chronic fatigue syndrome/Myalgic Encephalomyelitis (CFS/ME) and fibromyalgia, which affect roughly 3% and 2% of the general population in the USA, respectively. Although the clinical presentations of both CFS/ME and fibromyalgia have many similarities with GWI, such as chronic pain, fatigue, sleep disturbance and memory problems, the causative agents of GWI are unique to those encountered during the 1991 GW and include overexposure to pesticides, insecticides and other chemicals. Veterans with GWI experience symptoms chronically, with no improvement over time[2,4]. Furthermore, the underlying pathology remains unknown which makes it particularly difficult to diagnose and treat GWI. The key objectives of my thesis work were to identify biological targets that are downstream of GW chemical exposure to develop therapies and identify potential biomarkers for diagnosing GWI.

1.2 Clinical evidence of central nervous system involvement in GWI

Gulf War veterans were deployed for 2 months in Gulf during 1991 Operation Desert Storm. It is now well-established that deployment to the GW theatre or it's vicinities strongly influenced GWI symptom profiles and severity. The chronic multi-symptom illness is more prevalent in deployed GW veterans than in their non-deployed counterparts[1,5]. Steele and colleagues reported that the prevalence of GWI in US veterans was directly proportional to the time period and location in which they served [6]. Symptoms of GWI are reported more

frequently by veterans deployed to the combat theater compared to those deployed to other locations. Of the veterans deployed to the 1991 GW, 23% continue to suffer from fatigue, 32% report suffering from memory problems, and 17% report chronic pain[1,7,8]. Among GWI veterans, 62% report suffering from at least two of these chronic symptoms (fatigue, mood-cognition, and musculoskeletal)[2,9]. Nearly 67% of US GW veterans report that the onset of these symptoms occurred with two years of their return from the conflict[6,7]. Among UK veterans diagnosed with GWI, 23% continue report suffering from fatigue, 28% from memory problems and 17% from chronic pain[3]. Many epidemiologic studies have reported that GW veterans who served in the US Army and US Marines have higher rates of multi-symptom illness than those in the Navy and Air Force[6,10,11]. The prevalence of GWI was lowest among GW veterans who served in the US Navy (21%) or the US Air Force (13%) and highest among ground troops in Iraq and/or Kuwait (42%)[6,9], further supporting that deployed GW veterans were particularly affected by GWI. Among GW veterans diagnosed with GWI, those who were deployed to Iraq and Kuwait reported a higher prevalence and severity of multiple symptoms compared to veterans with GWI deployed elsewhere[12]. Also, several studies have reported that GWI prevalence differs depending on the locations where veterans served during the war. For instance, GW veterans who served in some areas of theater, such as Khamisiyah, have higher rates of GWI than veterans who were in other locations[6,10,13,14].

Among the multitude of symptoms experienced by veterans with GWI, chronic fatigue, memory problems, gastrointestinal problems and musculoskeletal pain are the most commonly reported symptoms. Memory impairment is a major complaint among GWI veterans, and many studies suggest that this may be due to damage to the brain regions involved in cognition. Veterans with GWI had significantly lower scores on tests of verbal memory, verbal learning, motor speed, and attention than non-deployed veterans[15]. Janulewicz and colleagues reported significantly decreased performance in attention and executive function, visuospatial skills and learning/memory in symptomatic vs. non-symptomatic GW veterans[16]. Other reports state that

nearly 40% of GW veterans with GWI reported fatigue-related issues along with memory problems[1,17]. These clinical findings suggest that GWI may involve central nervous system (CNS) dysfunction. This is supported by brain imaging studies which provide substantial support for a CNS component in GWI. For instance, a proton magnetic resonance spectroscopy (MRS) imaging study revealed a lower ratio of neuronal metabolite *N*-acetyl aspartate–to-creatine (NAA/Cr) in the basal ganglia and brainstem, suggesting neuronal loss in the brains of veterans with GWI compared to control GW veterans [18]. Another proton MRS imaging study showed that NAA/Cr ratios were also significantly lower in the hippocampi of veterans with GWI compared to control GW veterans [19]. Magnetic Resonance Imaging (MRI) using voxel-based morphometric analysis showed reduced volume in both the gray matter and white matter in GWI veterans compared to GW healthy veterans [20]. Magnetic resonance imaging studies showed the loss of gray matter and hippocampal volume in GW veterans who were stationed at Khamisiyah compared to GW veterans who were stationed elsewhere [21]. In a subset of GWI veterans, a reduction of grey matter volume was reported using functional Diffusion Tensor Imaging (DTI)[22]. Hence, these studies show that clinical symptoms of GWI correspond with metabolic disturbances in the brain and support the role of CNS disturbances in GWI.

1.3 Chemical exposure implicated in the pathogenesis of GWI

While no single etiological factor has been definitively linked to GWI[1], reports compiled by the Veterans' Administration Research Advisory Committee (RAC) on GWI, based on self-reported systematic retrospective data collection from GW veterans, implicate exposure to GW chemicals, such as the anti-nerve agent pyridostigmine bromide (PB) and insecticides like permethrin (PER), in the pathogenesis of GWI. In particular, PB is a reversible acetylcholinesterase (AChE) inhibitor which was taken by combat soldiers as a prophylactic measure against the organophosphate (OP) nerve agent sarin[1]. Pyridostigmine bromide is used for treating myasthenia gravis[23]. Comparing GW veterans who were exposed to PB to those

who reported not being exposed to PB, the exposed group performed significantly worse in motor and executive functioning[21,24]. Memory impairment was greater among GW veterans who reported being exposed to chemical weapons along with higher intake of PB than veterans who did not take PB[6,25]. Along with significant hippocampal dysfunction among GW veterans deployed to Khamisiyah, self-reported surveys revealed that GW veterans deployed to Khamisiyah had higher exposure to both PB and PER[6,26,27]. During the GW, the recommended dose of PB was 3 pills (90 mg) per day[1]. However, research studies report that veterans used 6 or more PB pills per day which was twice the recommended daily dose[27]. Several epidemiological studies have indicated that exposure to PB was directly proportional to the severity of GWI [28,29]. For instance, veterans who took PB more than 3 times a day had a higher overall symptom severity than those who had moderately severe symptoms and reported taking PB pills less than 3 times a day[27,30]. Using a case-control design, Steele and colleagues reported that being stationed at Kuwait or Iraq coupled with a high intake of PB (consumption of greater than 3 pills per day) increased the odds of GW veterans having GWI[28]. Also, memory impairment was greater among GW veterans who reported being exposed to chemical weapons along with higher intake of PB than in veterans who did not take PB[25,28]. These epidemiological studies indicate that exposure level to PB was directly proportional to the severity of GWI[28].

Permethrin was also used as a pesticide by veterans deployed to the 1991 GW. It is a synthetic chemical that belongs to the pyrethroid family. These compounds exert their neurotoxic effects by prolonging the activation of voltage-gated sodium channels that are present on the neuronal membranes[31]. To protect soldiers from insect-borne illnesses, uniforms of the US and British soldiers were saturated with PER, using a 0.5% spray. Permethrin was also used far more than recommended[1]. For instance, the average recommended use for PER on clothing was once every month. However, GW veterans reported that they used PER almost 30 times per month [1,27]. GW veterans who sprayed their uniforms with 0.5% PER reported

developing multiple symptoms, such as dermatological problems, gastrointestinal complaints and neurological and psychiatric symptoms[25,27]. Cognitive impairment was more common among veterans who frequently sprayed their uniforms with PER than in those who never used it[25]. Hence, exposure to PER may represent a GW exposure which was common to many deployed GW veterans and may have played a significant role in the pathogenesis of GWI.

There are other chemicals which are indicated to have played a significant role in the pathogenesis of GWI. Along with PER, N, N-Diethyl-meta-toluamide (DEET) was also used as an insect repellent, which is thought to inhibit the olfactory senses by targeting the ionotropic receptors of insects[32]. Regular use of DEET was associated with more severe symptoms of GWI than infrequent use[25]. Arthromyoneuropathy (joint and muscle pain and muscle fatigue) in GWI patients increased with higher use of insect repellents containing DEET in either a 33% cream or 70% liquid [25]. Collectively, these studies suggest a dose-dependent relationship between pesticide/insect repellent use and the clinical severity of GWI. Organophosphates pesticides such as chlorpyrifos were issued for personal use to service members deployed in the GW[33]. Exposure to OP pesticides can affect the CNS, autonomic nervous system, and skeletal muscles; and they have neurotoxic effects through mechanisms other than acetylcholinesterase inhibition [34–37]. Other studies have shown that repeated exposure to OP is associated with neurochemical and behavioral alterations that do not occur with single exposures at similar doses[37–42]. It has been suggested that these persistent symptoms are associated with neuronal oxidative injury and neuronal cell death in multiple brain regions following OP exposure[43]. Acute OP poisoning usually develops within minutes to hours and persists for hours to a few days. Acute exposure to OP can be toxic, producing symptoms that are similar to those seen in GWI[44–46]. Veterans were also exposed to chemicals from burning oil wells, vaccines and depleted uranium that may be capable of accumulating in the brain and affecting learning and behavior in animal studies, but the evidence does not suggest that GWI symptoms predominantly originated from these factors[1,2].

1.4 A role of combined GW chemical exposure in the pathogenesis of GWI

It is also hypothesized that combined exposure to PB and pesticides may be a major contributing factor to GWI pathology. Combined exposure to these compounds may have had a synergistic effect on GW veterans, resulting in the subsequent development of GWI symptoms. An increased risk for GWI was seen among veterans who reported taking higher than recommended doses of PB and used uniforms treated with pesticides[1,2,5,28,47]. In many studies, GWI was strongly associated with the use of PB pills, exposure to PER and proximity to exploding missiles[5,6,11,48,49]. Among GW veterans who reported using PB pills above the recommended dose, 62% of them reported using some form of a pesticide where nearly 44% used pyrethroid sprays almost 30 times per month and 26% used pesticide lotions almost 20 times per month [27]. Among the GW veterans serving on the ground, 25% reported that they had applied pesticides ranging from 50 to 120 times in a month and had also used an average of 15-19 PB pills in the same month[27]. As such, combined exposure to PB and multiple pesticides represents a key etiological factor potentially causal to the pathogenesis of GWI.

A causal role of combined pesticide and PB exposure in GWI comes from animal studies which show that exposure to these chemicals results in neurobehavioral deficits which resemble the symptoms reported by veterans with GWI. There are now several GWI animal models available that consistently show adverse effects of GW chemicals on the brain. Most of the animal models developed by different groups have focused on exposure to PB and pesticides such as PER and DEET. A rat model using combined exposure to PB, PER and DEET along with restraint stress was developed by Abdel-Rahman et al., (2004)[50]. In this model, PB was administered through oral gavage while DEET and PER were applied dermally. This model exhibits neurobehavioral changes such as motor function impairment and reduced locomotion[50]. In this model, Parihar et al (2013) showed mood and cognitive dysfunction at 4 weeks post-exposure in rats using the same GW chemical exposure paradigm[51]. Also, in the same model, hippocampal-dependent and hippocampal-independent memory impairments were

observed, as well as mood dysfunction[52]. Terry and colleagues showed that exposure to OP pesticides such as chlorpyrifos (CPF) every other day over 30 days resulted in impaired spatial learning when examined using the radial arm maze test [42]. In the Roskamp Institute laboratories, our most commonly used mouse model of GWI was developed using combined exposure to PB and PER. These chemicals are administered intraperitoneally (i.p.) daily for 10 days and characterization of these mice to 22-months post-exposure demonstrates chronic neurobehavioral and neuropathological changes. Exposed mice showed learning and memory impairment, and disinhibition[53,54]. Hence, the major neurobehavioral changes associated with this mouse model are cognitive impairment, anxiety, motor function impairment and impaired spatial learning and memory. Thus, many of these GWI rodent models exhibit neurobehavioral features that are similar to the symptoms reported by ill GW veterans. However, fatigue or pain, which are also major symptoms of GWI, have not been examined in these rodent models. Nevertheless, the availability of these GWI animal models has been helpful in characterizing the long-term consequences of exposure to GW chemicals and provide experimental evidence for a potential role of these chemicals in the pathogenesis of GWI.

In our PB and PER animal model of GWI we observed a chronic and persistent presence of astroglial activation ranging from 5 to 22-months post-exposure [53,54]. To best model the current human patient population, most relevant animal models have explored the chronic consequences of relatively acute exposures. Collectively, these studies suggest that astroglial activation is a consistent feature of GWI[51,53,55]. Even though microglial activation was observed in the rat model by Parihar and colleagues[51], other studies did not observe microglia activation or proliferation using ionized calcium-binding adapter molecule 1 (IBA-1) staining in animal models at a similar time point[50,53,56]**.** Instead, Iba12 staining of microglia was detected at 16-months post-exposure in PB+PER exposed mice model [54]. In addition, Iba1 is expressed by other myeloid cells and infiltrating monocytes[57,58]. Very little is known about monocyte and

myeloid cell infiltration in the brain and their contribution to the neuroinflammation observed in GWI mouse models.

Some degree of neuronal loss, especially in the hippocampal region, is reported in a rat model of GWI[51,59]. O'Callaghan and colleagues showed that exposure to PB and pesticides such as DEET in addition to corticosterone (CORT) resulted in astroglia activation, along with an increase in proinflammatory cytokines and chemokines, but no neurodegeneration[60]. This study also showed that di-isopropyl fluorophosphate (DFP) with and without CORT+PB/DEET does not cause remarkable neurodegeneration[60]. Studies have shown that an increase in cytokines in the brain corresponds with increased macrophages in the brain. Grigoryan et al., showed that OP binds to tubulin which affects axonal transport[61], bilaterally this model also had altered myelin structure along with astroglial activation[62]. Exposure to an OP pesticide, individually or in combination with other GW chemicals (PB+PER), causes brain pathology associated with GWI[55,60,63,64]. Taken together this indicates that mild chronic neuroinflammation is predominant over neuronal loss or neurodegeneration in these GWI mouse models.

1.5 Pathophysiology of GWI

As can be seen from the above studies, animal models of GWI display many clinical features of GWI and have yielded invaluable insights. While animal models have their limitations, they have advanced translational research given the complex clinical presentation of this illness and unknown etiological origins in humans. These mouse models have provided a wealth of information for understanding the molecular mechanisms behind the illness. They have been most useful in the search for objective biomarkers and for testing candidate therapies. As our previous and current work shows, these animal models have helped by providing an understanding of the brain pathology of GWI that would be inaccessible in humans. This aspect of our work is particularly valuable since human brain samples for GWI largely remain unavailable. Our translational studies included the use of omics technologies to examine GWI

rodent models and samples from GW veterans to identify biological disturbances that are associated with GWI in both. These studies identified the alteration of many biological pathways that pointed to peroxisomal dysfunction, mitochondrial dysfunction and immune and inflammation-related biological functions as major contributors to the pathogenesis of GWI[54,65,66]. Each of these critical areas of GWI pathogenesis will be discussed in greater detail below.

1.6 Peroxisomal dysfunction associated with GWI

Peroxisomes are ubiquitously distributed cellular organelles that carry out synthesis and metabolism of many lipids and participate in scavenging of reactive oxygen species (ROS)[67–69]. Some of these lipids include ether phospholipids (PL), sterols, and fatty acids[70]. Peroxisomes perform both catabolic and anabolic functions on lipids. β-oxidation and α-oxidation of fatty acids are major catabolic functions, whereas anabolic functions include ether lipid synthesis [71]. Peroxisomes have specific enzymes that are required for performing β-oxidation of fatty acids with 22 or more carbons, very long chain fatty acids (VLCFA), and α–oxidation of 3-methyl branched FA (phytanic acid and pristanic acid). Synthesis of ether PL, synthesis of docosahexaenoic acid (DHA), glyoxylate detoxification and synthesis of bile acids also occurs in the peroxisomes[72]. For instance, peroxisomal acyl-coenzyme A oxidase 1 (ACOX1) and 17β-hydroxysteroid dehydrogenase 4 (HSD17β4) are not present in mitochondria and, as such, metabolism of VLCFA initiates in the peroxisomes[73]. Phytanic acid, which has a branched methyl group on the third carbon, undergoes α-oxidation to pristanic acid (phytanoyl-CoA dioxygenase) that undergoes several cycles of β-oxidation in the peroxisomes after which it is transferred to mitochondria for its complete oxidation. Furthermore, chain shortening of these VLCFA results in the production of acetyl-CoA. Since, peroxisomes do not have the Krebs

cycle, these acetyl-CoA are transferred back to mitochondria[74]. An accumulation of VLCFA, as well as phytanic and/or pristanic acids in tissues and body fluids, is usually used as an indicator of peroxisomal dysfunction in genetically inherited diseases associated with peroxisome biogenesis dysfunction, such as Zellweger Syndrome and adrenoleukodystrophy[75].

Previous work on lipids gives a strong indication of peroxisomal dysfunction which coincides with abnormal lipid profiles in several GWI mouse models[54,65,76]. In a previous study of a GWI mouse model of PB+PER exposure, immunohistochemical analyses of our PB+PER showed that staining of peroxisome-specific catalase was increased in the dentate gyrus (DG) of GWI mice[65]. It is possible that this increase in catalase may reflect increased proliferation of peroxisomes following GW chemical exposure. However, other studies have suggested that such increases in catalase could be an indicator of abnormal accumulation of non-functional peroxisomes due to impaired recycling of these organelles through autophagy[77]. There was also an increase in ether phosphatidylcholine (ePC) in the brains of GW chemical exposed mice[65]; other lipid changes including altered levels of omega-3 fatty acids and VLCFA-containing sphingomyelin (SM) species in the brains of GWI mice compared to control mice also indicate peroxisomal dysfunction[65]. As such, there is an increasing evidence connecting peroxisomal dysfunction to the pathogenesis of GWI in mouse models.

Translating these studies, Emmerich and colleagues reported an increase in ether PL in the blood of veterans with GWI compared to healthy GW veterans as well as rodent models of GWI[76]. Additional evidence for possible impairment of peroxisome function also comes from same studies which showed an increase in DHA containing PL specially PC, LPC and PE[76]. More recently, my own work showed that VLCFA were increased in the plasma of veterans with GWI[78]. Overall, these studies suggest possible peroxisomal dysfunction in both ill GW veterans and in mouse models of GWI. Therefore, targeting peroxisomal lipid metabolism might be a possible therapeutic route to treating this illness.

1.7 Mitochondria dysfunction in GWI

Mitochondria are cellular organelles that perform several complex functions including; 1) fatty acid ß-oxidation, 2) oxidative phosphorylation (OXPHOS), 3) production and consumption of ROS, and 4) the generation of adenosine triphosphate (ATP). Due to their critical role in energy production mitochondria are commonly referred to as the "powerhouse of the cell". The substrate is provided to mitochondria in the form of pyruvate or fatty acids, which are metabolized to acetyl-coenzyme A (Co-A)[79]. These acetyl-Co-A molecules condense with oxaloacetate to form citric acid, finally entering the Krebs cycle[79]. During the Krebs cycle, 3 molecules of nicotinamide adenine dinucleotide (NAD+) are reduced to NADH. Along, with NAD+, the Krebs cycle reduces flavin adenine dinucleotide (FAD+) to FADH2 by redox reaction[80]. FADH2 is a reduced electron carrier of FAD+, it also donates its electron to the electron transport chain (ETC)[80]. This process also transfers protons to the inner membrane of mitochondria to generate a proton gradient[80]. The inner membrane of mitochondria contains protein complexes I, II, III and IV [80]; together these protein complexes transfer electrons from electron donors to electron acceptors via redox reaction and act as an electron shuttle [80]. Complex V, an ATP-synthase, uses the energy generated by the protons as they pass through the inner mitochondrial membrane to generate ATP from ADP[80]. In this way the mitochondrial redox reaction helps to maintain the cellular NAD^+/NADH ratios for normal cellular processes[81]. A major consequence of this event is the generation of unpaired electrons which interact with O_2 to form ROS. Under pathological conditions, or during cellular stress, high concentrations of ROS could lead to lipid peroxidation and damage the cellular membrane, subsequently leading to inflammation[82,83]. The inner mitochondrial membrane also has uncoupling proteins (UCP), which act as channels to pass the protons from the inner mitochondrial membrane to the mitochondrial matrix[80]. In this way, the proton gradient is dissipated to the mitochondrial matrix resulting in the production of heat. As such, mitochondrial membrane potential and OXPHOS is regulated by UCP.

The mitochondrial outer membrane is impermeable to fatty acids, so the carnitine shuttle system is used to transport these fatty acids inside mitochondria. The acyl group of acyl coenzyme A (acyl-CoA) is conjugated to carnitine by the enzyme carnitine palmitoyltransferase (CPT). These conjugates of fatty acids and carnitines are called fatty acid acylcarnitine. Long chain fatty acid acylcarnitines are transported to the inner membrane of mitochondria for β-oxidation. β-oxidation results in cleavage of 2 carbons from fatty acids as acetyl-CoA and resynthesizes the carnitine conjugate of the chain-shortened fatty acids and the process is repeated for complete conversion of the fatty acids to acetyl-CoA [84,85]. Another important mitochondrial lipid is cardiolipin (CL), it is exclusively located in mitochondria and represents almost 25% of total mitochondrial lipid [86]. Cardiolipins maintain and stabilize the inner mitochondrial complex such as ATP synthase and UCP [87]. Mitochondrial membranes have a high cardiolipin content, which maintains mitochondrial membrane integrity and mitochondrial morphology. As such they also play major role in regulating mitochondrial membrane potential[87].

Many of the GWI symptoms suggest a possible involvement of oxidative stress and mitochondrial dysfunction[25]. Evidence of mitochondrial dysfunction is also seen in GWI animal models. In a rat model of GWI, transcriptomics analysis showed increased expression of the genes involved in mitochondrial respiration [88]. These genes include NADH dehydrogenase 1 alpha subcomplex, succinate dehydrogenase and cytochrome C oxidase, and especially control the function of complexes I, II, III and IV[88]. This effect might be ascribed to a hyperactive mitochondrial electron transport chain compensating for increased ROS due to mitochondrial dysfunction[89]. These findings are also supported by results from another study showing a decrease in complex I and II activity in the brains of GWI mice [66]. Also, lipid analysis showed lower mitochondria specific lipids such as CL and acylcarnitine in the brains of GWI mice[54]. Exposure to pesticides (dimethoate and zineb) has also been shown to lower CL levels in the brain of pesticide exposed mice[90].

The clinical presentation of GWI veterans shows many features that can be related to mitochondrial dysfunction. Both clinical and preclinical studies suggest targeting mitochondrial biogenesis and function might be a useful treatment for GWI. Recent studies found that mitochondrial DNA damage was 20 percent higher in GWI veterans[91]. Also, a study from our laboratories showed a change in mitochondrial specific acylcarnitine in human plasma[54]. Hokama et al., in a pilot study, showed that GW veterans had higher plasma levels of anti-CL antibody compared to healthy controls from the general population[92]. Koslik et al. showed that post-exercise recovery of phosphocreatine levels in the muscle of GWI veterans is affected, as measured by ^{31}P phosphorus magnetic resonance spectroscopy[93]. In another study, using ^{1}H MRS, veterans with GWI had increased levels of lactate in their prefrontal cortex following an exercise challenge[94]. These results suggest the inability of brain cells responsible for the catalytic conversions between pyruvate and lactate, which results in Krebs cycle impairment[95]. A possible cause of this might be a lower level of NAD+ substrate which is used in glycolysis to generate ATP in mitochondria[84,96]. Additional support for mitochondrial dysfunction in GWI comes from our own pilot study showing increased products of lipid peroxidation in the blood of veterans with GWI[78]. All these studies suggest mitochondrial dysfunction is involved in the pathobiology of GWI and should continue to be investigated. Therefore, therapies that target restoration of mitochondrial function and bioenergetics may prove beneficial for alleviating GWI pathology.

1.8 Immune and inflammation as key pathologies of GWI

The immune system is comprised of a network of cells, tissues, and organs that work in unison to defend the body against pathogens or antigens. The immune system should correctly identify and respond to potentially harmful organisms, and it must also differentiate between the non-antigenic substances and antigens that present potential harm[97]. The immune system can be divided into two classes, the innate and the adaptive immune system. The innate immune system is the body's first line of defense and is able to respond immediately upon

encountering antigens; while this immune response is rapid, it does not confer specific, long term protection as it does not generate an immunological memory[97]. The adaptive immune response is performed by lymphocytes which respond to pathogens via either humoral or cell-mediated immunity. In humoral immunity, B lymphocytes secrete antibodies that mark target antigens or microbes for elimination. In cell mediated immunity, T lymphocytes activate cytotoxic T-cells to engulf antigens or kill infected host cells[97]. Furthermore, T-lymphocytes also provide a helper function for B cells by the help of T helper (Th) cells. While the adaptive immune system is slower to respond to pathogens it generates an immunological memory, enabling it to respond more rapidly in cases of future re-infection by the same pathogen[97]. In general, Th-1 cells secrete pro-inflammatory cytokines, such as interleukin-1beta (IL-1 β), interferon (IFN)-γ, tumor necrosis factor (TNF-α) and interleukin (IL)-2, cytokines which promote inflammation to fight against foreign or other pathological stimuli. On the other hand, Th-2 cells release anti-inflammatory cytokines such as IL-4, IL-5, and IL-10,[97] which essentially limit and antagonize the effects of inflammation to help restore the natural state of the tissue[98]. Th-17 cells play a role in adaptive immunity, protecting the body against pathogens and stimulating generation of cytokines, such as IL-17, IL-21 and IL-23[99]. Recent studies have suggested that Th-17 cells are involved in the pathogenesis of autoimmune disorders[100]. A homeostatic balance between pro- and anti-inflammatory cytokines is necessary to maintain normal physiological function in the body. Chronic inflammation involves dysregulation of pro- and anti-inflammatory cytokines[101].

GWI veterans were potentially exposed to many hazards such as prophylactic medications, multiple vaccinations and pesticides [1]; it is likely that these resulted in immune function alterations. Previously, it was hypothesized that veterans with GWI had their immune response shifted towards a Th-2 cytokine pattern due to multiple vaccination [102]. However, this is not supported by recent literature[103,104]. The current hypothesis is that various chemical exposures during the 1991 GW, together with battle stress, may have caused a chronic

dysregulation of the immune system [1]. In fact, studies have shown an irregular activation of Th-1 and Th-17 mediated immune responses in GWI[104]. Evidence for a Th1 immune response comes from studies showing an elevation of TNF-α and IL-2 cytokines produced by CD4+ T-cells in GWI patients compared with healthy controls[105]. Additional evidence for a Th1-like immune response is evident from studies showing prolonged elevation of plasma pro-inflammatory cytokines, such as IFN-γ and TNF-α, in subjects with GWI compared to healthy controls[104,106]. Plasma cytokine profiles show a significant upregulation of IL-17A and IL-17F in GWI cases compared to controls, suggesting a Th-1/Th-17 immune shift[104]. Veterans with GWI not only showed T-cell dysregulation but also an increased population of B cells and monocytes in their blood[107,108]. Defective regulation of B- and T-cells results in a loss of the immune system's ability to discriminate self- and non-self-antigens leading to autoantibody production[109]. Characterization of the immune profiles suggests a presence of autoantibodies against brain-specific proteins, such as glial fibrillary associated protein (GFAP), myelin basic protein (MBP) and tau – all produced in GWI veterans, which was absent in healthy veterans[110]. However, mechanisms behind generation of these autoantibodies following exposure to GW chemicals and their contribution to immune dysfunction and neuroinflammation are currently unknown in the literature. Future research must focus on mechanisms that show how exposure to GW chemicals leads to the production of autoantibodies which then contribute to the chronic debilitating symptoms experienced by veterans with GWI.

1.9 Currently available treatment strategies in GWI

Currently, there are no approved treatments for GWI which target the underlying pathologies, and therefore there is a continual need for research into better understanding the pathological mechanisms associated with GWI in order to better inform the treatment development process. Various approaches have been utilized thus far which are focused on symptom management. For instance, yoga or acupuncture clinical trials have been conducted in

GWI patients which provided some relief in pain reduction[111,112] but benefits from these treatments are modest and do not change the underlining pathology of the disease. Donta et al., hypothesized that GWI was caused by an systemic infection with *Mycoplasma* species[113]. They tried antibiotic treatment and exercise to improve cognitive behavior, neither intervention had any long lasting effects[113,114]. Many studies conducted on GWI veterans have targeted mitochondrial dysfunction[54,93,115]. In a preliminary analysis of 46 GW veterans, treatment of GWI veterans with Coenzyme-Q10 (CoQ10) did show improvement in physical function and other symptoms related to GWI [116]. CoQ10 is involved in significant metabolic pathways where it receiving electron from redox enzymes and provides these electrons to ETC (specially Complex III)[117]. As such, CoQ10 was suggested to improve bioenergetics by increasing ATP production in the cells and also protects cells against oxidative damage[118,119].

Others have shown that CoQ10 exerts a favorable effect on GWI-relevant symptoms such as fatigue[120,121]. Although this study had improvements reducing commonly reported symptoms of fatigue, dysphoric mood, and pain, some adverse effects were observed such as 2 case of seizures and ischemic attacks on treatment group[116]. Another study treating GWI patients with carnosine (a dipeptide of alanine and histidine) reported a beneficial cognitive effect but no improvement in other clinical symptoms such as fatigue and pain[122]. Although the mechanism of action of L-carnosine is not well understood, carnosine has been known to protect against ROS and improve memory in adults and children[123,124]. Previous pilot studies found that use of carnosine supplements was effective in improving memory and neurologic function in autism and schizophrenia,[124–126].

In another GWI treatment study, the glucocorticoid receptor antagonist mifepristone resulted in an improvement in verbal learning, but no improvement in cognition or mental health was reported by veterans[127]. Out of 67 GWI veterans recruited in this study, 32 received treatment while 35 were placebo[127]. Treatment of chronic pain in GW veterans with repetitive Transcranial Magnetic Stimulation (rTMS) was terminated as it failed to meet recruitment

criteria. This study could only recruit 17 participant which did not meet recruitment goal (source: clinicaltrial.gov). Recently, many clinical trials are recruiting GWI veterans, which are focused on changing the diet to treat the digestive problems associated with the illness, such as a low-glutamate diet or a probiotic diet (source: clinicaltrial.gov). Few other clinical trials are completed or are recruiting patients but very few trials look promising. As such, more research studies are needed that identify the underlying mechanisms associated with GWI. As GW veterans are ageing, finding effective treatments for GWI is a high priority. The research in this thesis was directed towards identifying potential therapies that target peroxisomal and mitochondrial dysfunction observed in GWI. The work described in this thesis has resulted in identification of several therapeutic approaches that will be investigated further in veterans with GWI in the near future. The ultimate goal of all these interventions are to provide the patient with relief of symptoms, stop the progression of disease and improve the quality of life of GW veterans suffering from this chronic and debilitating multisymptomatic illness.

1.10 Hypothesis & Synopsis of following chapters.

My working hypothesis is therapeutic targeting of lipid remodeling pathways can reduce abnormal brain lipid accumulation and improve chronic neurobehavioral deficits and the accompanying neuropathology in a mouse model of GWI. One of my aim is to target peroxisomal and mitochondrial lipid metabolism in order to identify possible therapies for treating GWI. I will examine several compounds such as bioactive lipids, especially ethanolamides, which target peroxisome function via activation of peroxisome proliferator-activated receptors (PPAR) and also decrease inflammation. I will also examine a different strategy which targets mitochondrial function and/or biogenesis using nicotinamide riboside and ketogenic diet.

Another main objective of this thesis is to further characterize the PB+PER mouse model for other key pathologies of GWI. As inflammation is major hallmark of GWI, I further wanted to

analyze systemic inflammation related to GW agent exposure in our GWI mouse model as well as in humans. I therefore hypothesize that peripheral immune cell activation and infiltration in the brain following GW agent exposure may be associated with brain inflammation and memory impairment.

1.11 The aim of the thesis research

1) **To target peroxisomal lipid metabolism in order to identify possible therapies for treating GWI**

   Using our mouse model of GWI I targeted peroxisome function via activation of peroxisome proliferator-activated receptors (PPAR) to determine if this approach can improve the behavioral phenotype and decrease the inflammation associated with exposure to agents known to have caused GWI.

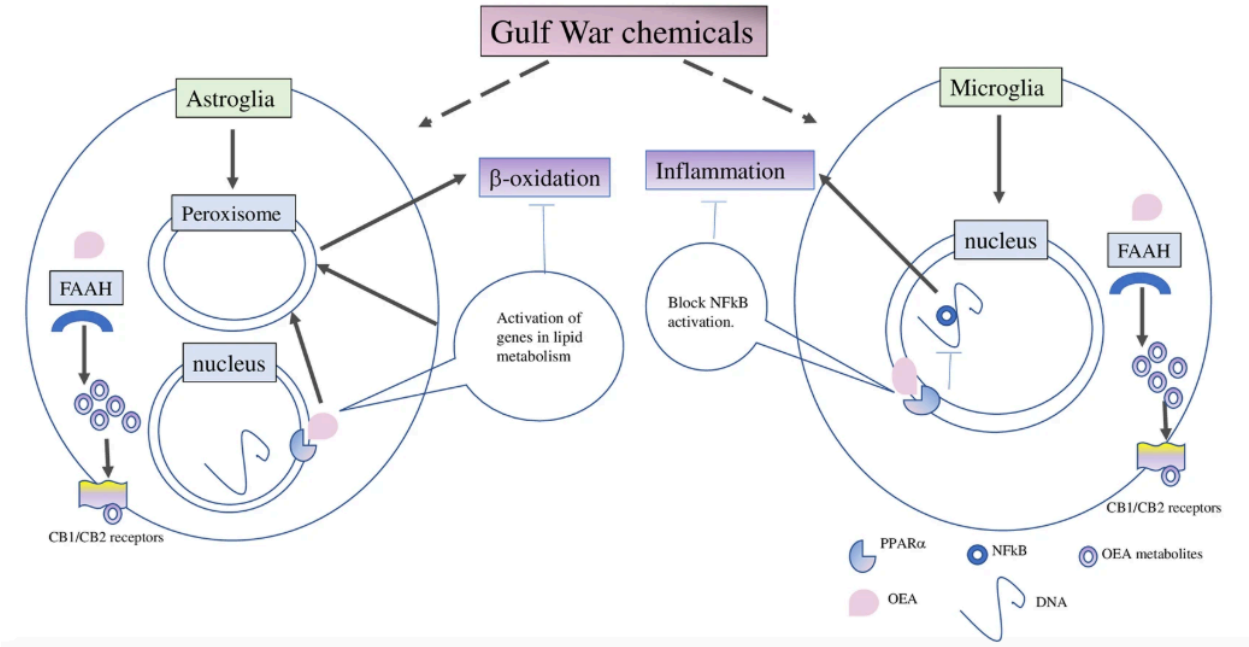

Figure 1.1: PPAR-α as a new therapeutic target for GWI (source: nature publishing group)

2) **Mitochondrial function and/or biogenesis as a potential target for therapeutics of Gulf War Illness (GWI)**

The main aim of this study was to assess the efficacy of nicotinamide riboside (NR) or a ketogenic diet (KD) in reducing the brain pathology and mitochondrial disturbances in a mouse model of GWI.

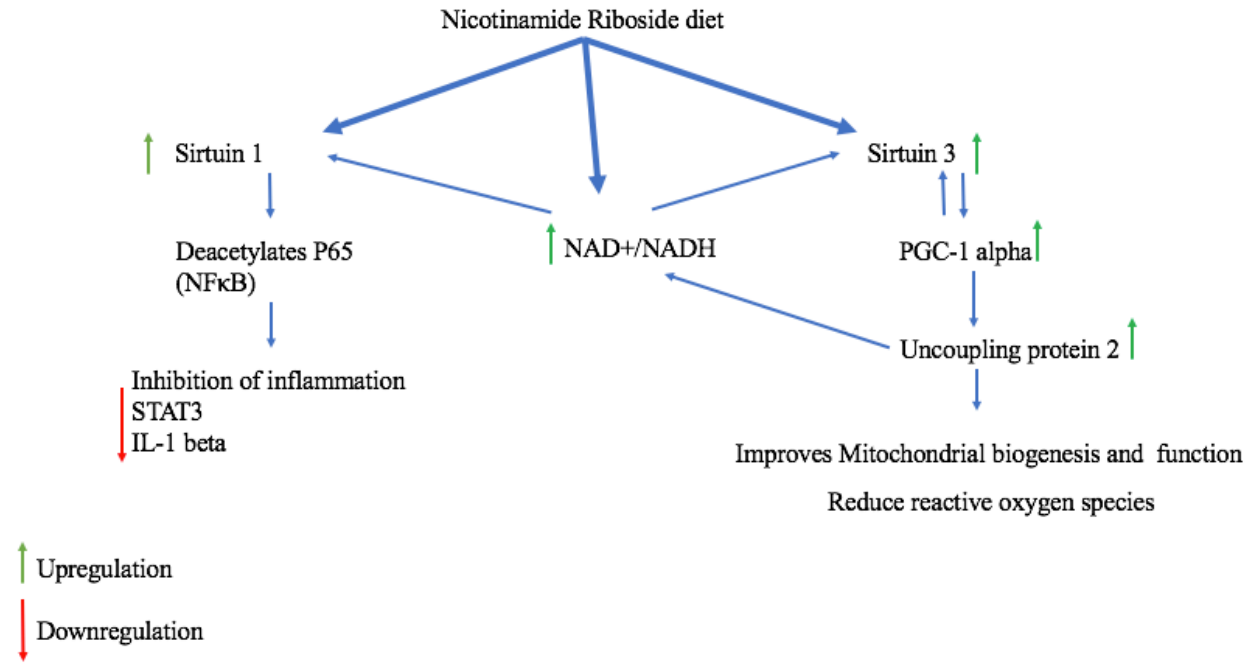

Figure 1.2: Metabolic pathways involved in Nicotinamide riboside (NR) treatment

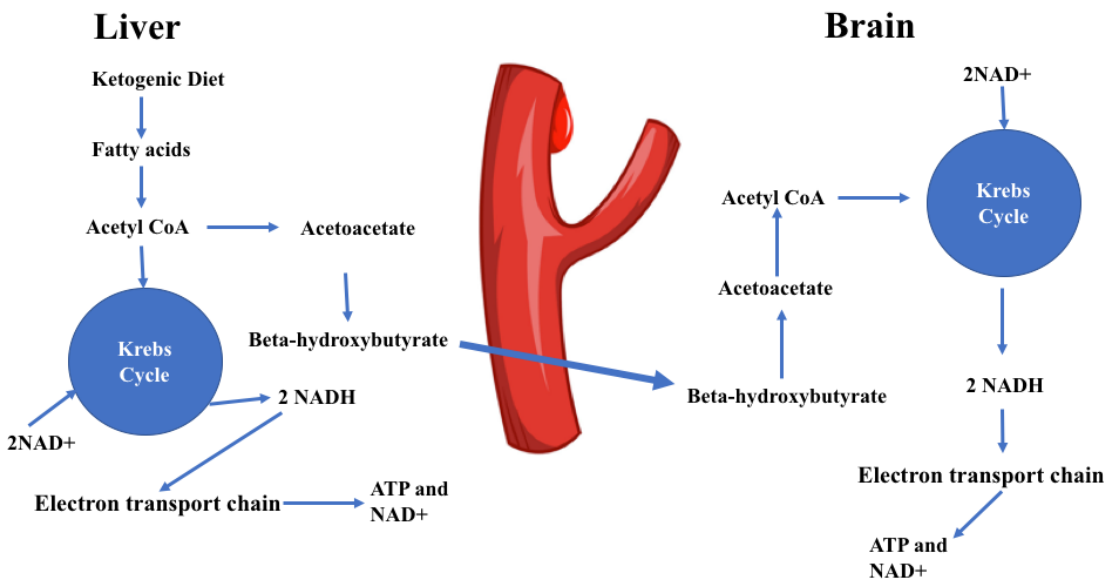

Figure 1.3: Metabolic pathways involved in ketogenic diet (KD) treatment

3) To examine peripheral and brain inflammation and immune-related changes in the PB+PER GWI mouse model

The key aspect of this project was to identify the underlying immune dysfunction that drives the brain pathology in our GWI mouse model in order to develop appropriate biomarkers and therapies for treating this condition.

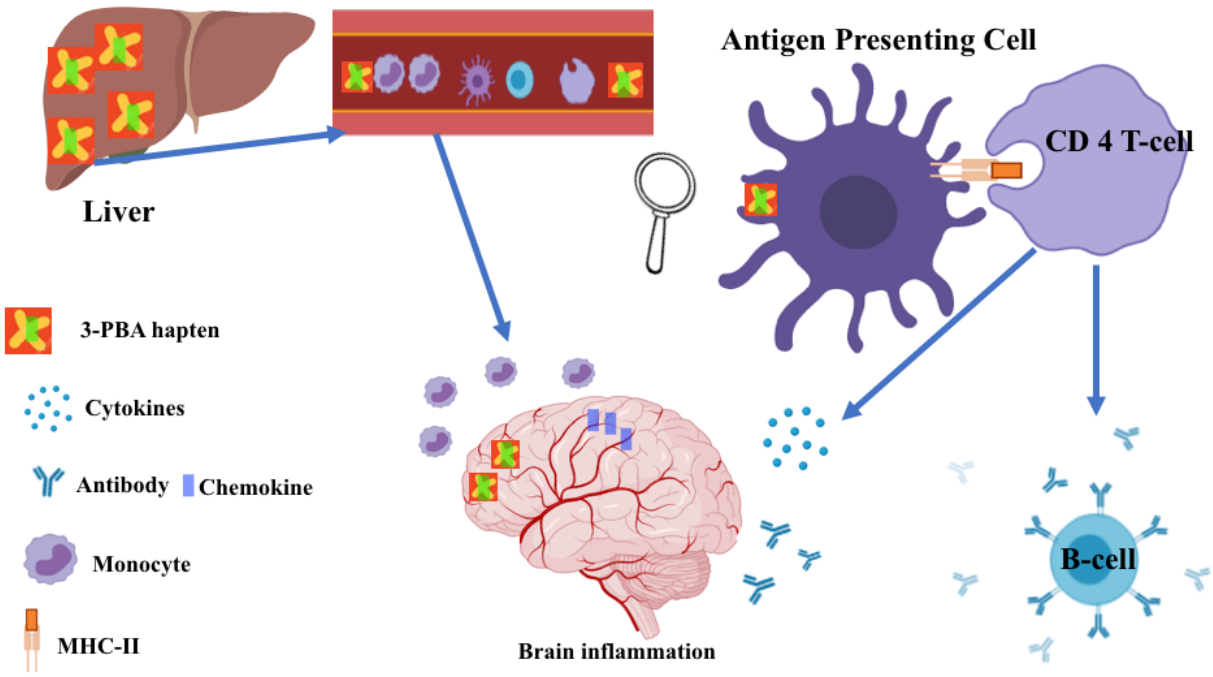

Figure 1.4: PER induced immune dysfunction (source: Elsevier).

Chapter 2: Oleoylethanolamide treatment reduces neurobehavioral deficits and brain pathology in a mouse model of Gulf War Illness

2.1 Introduction

As previously described, a common feature noted consistently across animal models and amongst patients affected by GWI are distinct differences in blood lipid profiles with regards to ether PLs, VLCFAs and BCFAs[65,76,78]. It has been reported in several studies that these changes in lipid profiles are indicative of peroxisomal dysfunction ([128]). Peroxisomes are small cellular organelles, which contain several enzymes involved in oxidative metabolism [128]. Traditionally, their function was believed to be purely a site for the oxidation of fatty acids such as VLCFA and BCFA, a vital source of metabolic energy for cellular processes [128]. Furthermore, recent evidence suggests that in addition to their role in oxidative metabolism, peroxisomes are involved in ether PL and bile acid synthesis[73,129,130]. In GWI, peroxisomal dysfunction is believed to promote incomplete ß-oxidation of VLCFAs, resulting in the overproduction or inadequate detoxification of ROS. The dysfunctional processing of ROS has been shown to trigger oxidative stress and upregulate proinflammatory responses[131–133]. Reactive oxygen species are involved in activation of the signaling pathway leading to NF-κB activation and production of proinflammatory cytokines [134,135].

Support for a role of inflammation in GWI has been reported in several animal models where exposure to GWI chemicals has been described to increase the expression of genes related to oxidative stress and inflammation[88], potentially increasing glial cell activation and the production of proinflammatory cytokines in the brain[136]. Subsequent evidence from clinical studies reporting increases in pro-inflammatory cytokines, such as TNF-α, IFN-γ, IL-2 and IL-1β on immune cells and in the plasma of veterans with GWI compared to healthy veterans further suggest that disturbances in peroxisomal β-oxidation may be associated with the oxidative stress and

inflammation observed in GWI[104,107,137,138]. Together these studies suggest that targeting and increasing peroxisome function and thereby reducing inflammation may be a potentially viable therapeutic avenue in GWI research.

One strategy to increase peroxisomal activity is by targeting peroxisome proliferator-activated receptor alpha (PPARα), which is a nuclear hormonal receptor that stimulates peroxisome proliferation, thereby regulating lipid biosynthesis, β-oxidation of fatty acids and scavenging ROS[139–143]. Recent studies have shown that PPARα activation promotes normal cognitive function [144] and that the pharmacological stimulation of PPARα improves cognitive function in mice[145]. Furthermore, several studies have reported that PPARα agonists inhibit glial cell activation and enhance memory function in a rodent model of neurodegeneration[146,147]. Conversely, studies which have pharmacologically inhibited PPAR-α reported the accumulation of VLCFA and increases in inflammatory markers[148]. As such, PPARα has emerged as a promising molecular target for many CNS related diseases [149,150].

With respect to lipid metabolism, PPARα activates transcription of genes encoding for the enzymes required in ß-oxidation. Furthermore, PPARα agonists are also shown to reduce inflammation through genetic regulation of NFκB in various CNS disorders[151–154]. One such natural occurring PPARα agonist is oleoylethanolamide (OEA) which is shown to have potent anti-inflammatory, antioxidant, neuroprotective and antidepressant-like properties. OEA ais a monosaturaed class of lipid compound that constitute ethanolamide of oleic acid. Therapeutic intervention with OEA has demonstrated considerable pre-clinical efficacy in the treatment of neuroinflammatory and psychological disorders[150,155]. We, therefore, hypothesize that GW chemicals disturb peroxisome function, which subsequently impair β-oxidation or aberrantly increases VLCFA synthesis. As such, targeting peroxisome function through OEA may be beneficial for treating GWI and improving disease outcomes.

The main goal of this study is to examine the fatty acid (FA) profiles associated with peroxisome function in the blood plasma of veterans with GWI compared to healthy veteran control samples. Furthermore, this study investigated the efficacy of the PPARα agonist OEA, to determine if treatment can beneficially alter peroxisomal lipid metabolism and treat the chronic neurobehavioral deficits and glial activation shown in our mouse model of GWI. The work detailed below is now published in the journal Scientific Reports[78].

Hypothesis: Lipids play a key role in neuronal survival by both supporting neuronal architecture and biological functions and by serving as a source of energy. Accumulating evidence suggests that dysfunctional lipid metabolism is a major hallmark of GWI. Lipid metabolism is upstream of many immune/inflammatory and neuroendocrine responses that are affected in GWI. Previous lipidomic data support a potential role of peroxisomal specific lipid metabolism dysfunction in GWI. We therefore hypothesize that restoring lipid homeostasis in the brain will treat the CNS symptoms of GWI.

Specific aim 1: To determine if therapeutic targeting of lipid remodeling pathways can reduce abnormal brain lipid accumulation in a mouse model of GW agent exposure.

Specific aim 2: To determine if PPAR agonists can decrease chronic inflammation and accompanying cytokine and chemokine production in a mouse model of GW agent exposure.

Specific aim 3: To determine if supplementing PPAR agonists can treat chronic neurobehavioral deficits and accompanying neuropathology in a mouse model of GW agent exposure.

2.2 Methods

2.2.1 Human subjects

This study was approved by the Institutional Review Board (IRB) with all protocols conducted in accordance with relevant guidelines and regulations. Plasma samples from age- and gender-matched control health GW deployed veterans (n = 10) and veterans with GWI (n = 12) were compared in this study. It is assumed that all the subject were fasting when blood was withdrwan, no data on Diabetes medation were avilable. A biorepository of plasma samples from GW veterans who previously consented to share their blood samples for future studies from the Boston Gulf War Illness Consortium (GWIC) and the Dynamic Modeling of GWI study were provided by our collaborators at the Boston University and NOVA Southeastern University sites. The GWI biorepository is approved by the institutional review boards (IRBs) at Boston University, NOVA Southeastern University and Miami Veterans Administration Medical Center (VAMC). All experiments were performed in accordance to the guidance from these oversight committees. Informed consent was obtained from all participating subjects. The GWI biorepository samples were all collected using the same written standard operating procedures for performing phlebotomy, plasma separation and aliquoting. All samples were stored at -80^{o}C and were not previously thawed and refrozen. The Kansas GWI criteria were used to determine cases of GWI and controls. The Kansas GWI criteria require that GW deployed veterans show symptoms in at least 3 of 6 symptom domains (fatigue/sleep problems, pain, cognitive impairment, mood symptoms, gastrointestinal symptoms, respiratory symptoms, and skin abnormalities). Study participants were excluded if they reported being diagnosed with another medical condition that could explain their chronic health symptoms. The Kansas GWI case definition exclusions include veterans with a history of prior CNS or major psychiatric disorders that could affect cognitive function (e.g., epilepsy, stroke, brain tumor, multiple sclerosis, Parkinson's Disease, Alzheimer's disease, schizophrenia). Controls were deployed veterans from the 1991 GW who did not meet the Kansas GWI criteria or exclusionary criteria listed above. Subjects also completed demographic and health symptom questionnaires. The recruitment strategy for the biorepository also excludes subjects currently participating in

clinical trials to minimize immediate interferences from these medications at the time of the blood draw. Subjects are also asked if they are on any steroid treatments and, to the best of our knowledge, subjects have reported no. However, no other medication information is currently obtained. A detailed demographic table is provided in table 1.

Table1. Demographics of the Gulf War veteran cohort.

	Control (GW veteran)	**GWI**
N total	10	12
Age (Mean ± SE)	49.3 ± 2.6	46.1 ± 1.6 SE
Male (%)	100	100
Ethnicity		
Caucasian	5(50%)	4(28.5%)
African American	1(10%)	5(35.7%)
Hispanic	2(20%)	2(15%)
Asian	2(20%)	3(23%)

2.2.2 In vitro study to find potent PPAR-alpha agonist which reduces LPS induced inflamation:

The main aim of this experiments was to study anti-inflamatory properties of natural PPAR-alpha ligan and similar strutural compounds. Murine macrophage RAW 264.7 cells were obtained from the American Type Culture Collection (ATCC) and grown in Dulbecco's Modified Eagle Medium (DMEM) F12 medium (life science St. Louis, MO) containing 10% fetal bovine serum (FBS) and 1% mixture of antibiotics (penicillin, streptomycin sulfate) and

antimycotics (amphotericin B). Cells were incubated in a humidified 5% CO_2 atmosphere at 37°C and subsequently challenged with lipopolysaccharide (LPS) from E. coli (Sigma Aldrich, St. Louis, MO) at 10μg/ml to induce NFκB activation. Oleoylethanolamide, docosahexaenoyl ethanolamide (DHEA), Prostaglandin E2 ethanolamide (PGE2EA) (Cayman chemical, Ann Arbor, MI) at 10μM, 1μM, 100nM each were used to investigate possible inhibition of NFκB phosphorylation by these compounds. Cells were incubated with either DMSO alone, with LPS and DMSO, or with each test compound in combination with LPS and DMSO. Conditioned media were collected and analyzed for the quantification of cytokines. The cells were lysed with mammalian protein extraction reagent (mPER) along with protease inhibitor to quantify pNFκB and total NFκB expression in these cells. Cytotoxicity was estimated by the presence of lactate dehydrogenase (LDH) using an LDH assay (Roche, Basel, Switzerland) which was performed according to manufacturer's instructions. Subsequently in another experiment, cells were pretreated by PPARα inhibitor (GW 6471) and PPARγ inhibitor (GW 1929) at 10μm 3 hours before LPS and OEA treatment. The main aim of this experiments was to confrom OEA mechanism of action was dependend on PPAR-alpha. Western blot analyses were performed as above to examine NFκB (**Ser 536**), Janus kinase (JAK2, **Tyr1008**) and STAT3 (**Tyr 705**) phosphorylation as inflammation associated outcomes. JAK-STAT pathway is a signaling pathway that involves several tyrosine kinases and transduce cytokine-mediated signals[156].

2.2.3 Animal Handling:

All procedures on mice were approved by Roskamp Institute's Institutional Animal Care and Use Committee and were in compliance with the Office of Laboratory Animal Welfare and Laboratory animal care guidelines as described previously [54].Eight-week-old male C57BL6 mice(Jackson Laboratory, Bar Harbor, ME, USA) were purchased from Jackson Laboratory and

allowed to acclimate to the new environment. All mice were placed on Standard rodent diet (Envigo, IN, USA) routine diet upon arrival. At 9 weeks of age (n = 48), 0.7mg/kg of pyridostigmine bromide (PB) (Fisher Scientific) and 200 mg/kg of PER (Sigma Aldrich) in 50ul 100% Dimethyl sulfoxide (DMSO) was administered via intraperitoneal (i.p.) injection daily for 10 days, while the control group received only 100% DMSO [53,54,157]. All animals were randomized to the various groups. Subsequently, mice were allowed to age for 5-months post-exposure, a timepoint when we have observed cognitive impairment [53,65]. Mice were again randomly assigned to either the OEA treatment or the control group. Mice in the OEA group were fed standard rodent chow (Envigo, MD, USA) containing a daily dose of 10mg/kg OEA (based on the consumption of 5g daily food intake) for up to 6 months, while the control group mice received standard chow only (11-months post-exposure). After GW chemical exposure, mice underwent testing with the FST at 3- and 5-months post-exposure to establish the presence of GW chemical induced changes in exposed relative to control mice. Control and GWI mice were divided into groups which either received oral OEA treatment in diet daily or normal diet for a total of six months. The Barnes Maze test was used to assess learning in control and GWI mice after 1-month of oral OEA treatment (6-months post-exposure to GW chemicals) and long-term memory after 2-months of treatment (7-months post-exposure). Learning was assessed during the acquisition trials in which mice were allowed to freely explore the maze for 3 min and escape into the target box through one of the holes in the platform. After 6 months of treatment, animals were euthanized for lipidomics, neuropathological, and biochemical studies. Randomization was performed in all neuro behavioural experiment, experimenter were blinded GW treatment but not diet. Mice were not deprived of food before euthenesia. A timeline of the study procedures is provided as Figure 2.1.

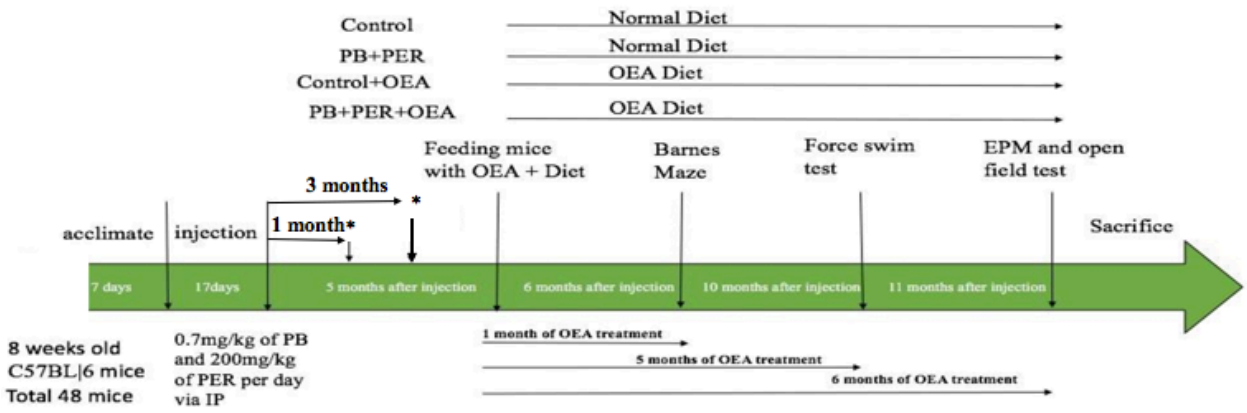

Figure 2.1: Timeline of the study

2.2.4 OEA Synthesis method

A 1-L round-bottom flask was charged with a mixture of benzene and hexanes (360 mL, 1:1, v/v) and oleic acid (25 g, 88 mmol). The above solution was cooled on an ice-bath to which oxalyl chloride (20 mL, 232 mmol) was slowly added over a period of 30 minutes via an addition funnel. This was followed by an addition of a catalytic amount of Dimethylformamide (DMF) (1 mL, 13 mmol). The above reaction mixture was removed from ice and then stirred at room temperature for 5 hrs. The solvents were then removed under reduced pressure and replaced with anhydrous Dichloromethane (DCM) (360 mL). To this solution, triethylamine (50 mL, 359 mmol) and 2-aminoethanol (22 g, 360 mmol) was added. The reaction solution was stirred overnight at room temperature and was quenched with H_2O (360 mL). Layers were separated and then the organic layer was washed with H_2O (360 mL × 3) and brine (360 mL) and dried with

anhydrous $MgSO_4$. After drying, the resulting residue was dissolved in n-hexane (500 mL) and was left in the refrigerator under -10°C overnight. The resulting product was filtered, washed, and dried in vacuo to a constant weight as a white solid (24.5 g, 86%). ^{1}H and ^{13}C NMR of this product conform to literature reports.

2.2.5 The Barnes Maze test to access memory

The Barnes Maze test was conducted according to previously described procedures[53,54]. Briefly, at 1-month post-treatment with OEA, the Barnes maze trial was performed for assessing learning. Acquisition trials were conducted over 4 days where each trial was conducted for 3 min, and 4 trials were conducted for each mouse per day. Briefly, each mouse was placed in the middle of the maze and the trial ended when the mouse entered the escape box through the target hole (TH) or after 3 min. Bright flood lamps were used as motivators for mice to enter the escape box, where they stayed for 1 min. If a mouse did not reach the TH within 3 min, the experimenter guided it to the escape box. A probe trial was conducted 24 hrs after the last training session. The escape box was removed for the probe trials. Each mouse was placed in the middle of the maze and allowed to explore for a fixed interval of 1.5 min. Another probe trial was administered at 2 months post-treatment to assess long-term memory. The Ethovision software was used to track mouse movement, and total distance traveled by each mouse on the platform was used to calculate the path length.

2.2.6 Forced Swim Test to examine fatigue like behavior

Forced swim test (FST) was performed to measure fatigue-like behavior, according to the protocol published by Can and colleagues [158] and was administered at 1- and 3-months post-exposure to GW chemicals and then subsequently at 10-months post-exposure, corresponding with 5-months after OEA treatment. Furthermore, repeated exposure to FST is used to induce fatigue in mice [159]. Mice were brought to the behavior testing room at least 30 minutes prior to

the initiation of the testing in order to acclimate them to the testing conditions. The FST apparatus was comprised of a cylindrical tank (30 cm height x 20 cm diameters) which was filled with warm tap water (approximately 22 °C) to a depth of 25 cm, preventing the tail and feet to reach the apparatus. Each animal was placed in the tank for 6 minutes, after which the mouse was removed to a warm and dry environment. Data were recorded and captured using the Ethovision XT software version 7, and latency to stop swimming and time spent being immobile were recorded as the outcome measures. Due to technical problems, data were lost for few mice(n=2/3 per group)

2.2.7 The Elevated Plus Maze test to determine anxiety

The elevated plus maze (EPM), used to determine anxiety, consisted of two open arms and two closed arms surrounded by high walls (40cm) across from each other. The middle section that allows the animal to transit from arm to arm consisted of a square with dimensions of 12 × 12 cm. Mice were allowed to move freely within the maze for 5 min. Entries to each arm were recorded using the Ethovision system. Only one trial per mouse was administered. The distance travelled in the maze, the number of entries into each arm, and the percentage of entries to open arms were calculated. The time spent in open and closed arms were analyzed as the outcome measures.

2.2.8 Sample preparation

Mice were euthanized via cardiac puncture under anesthesia and all animals were transcardially perfused with PBS. Half brains (right hemisphere) and plasma were immediately frozen in liquid nitrogen and transferred to a -80˚C freezer until further use. Using a dounce homogenizer, each brain hemisphere was homogenized in chilled lysis buffer containing protease (Roche, Indianapolis IN) and phosphatase inhibitor (Pierce, Grand Island, NY) cocktails.

2.2.9 Immunohistochemistry and confocal microscopy

The left-brain hemispheres were fixed in 4% paraformaldehyde and embedded in paraffin. Sagittal sections (8 μm) were prepared and rehydrated in an ethanol gradient before the staining procedure. Glial fibrillary acid protein (GFAP; 1: 1000, Wako, Carpinteria, CA, USA) and ionized calcium binding adaptor molecule 1 (Iba1) antibodies (1: 5,000; Abcam, Cambridge, MA, USA) were used to stain astroglia and microglia, respectively. Primary antibodies were localized using respective fluorescent labeled secondary antibodies. Slides were mounted in mounting media with DAPI (Abcam). The Image J software was used to analyze the stained sagittal sections. The stained areas were calculated and expressed as a percentage of the field of view.

2.2.10 Enzyme-Linked Immunosorbent Assay

Brain samples were homogenized using a dounce homogenizer, in chilled lysis buffer containing protease (Roche, Indianapolis IN) and phosphatase inhibitor (Pierce, Grand Island, NY) cocktails. Enzyme-Linked Immunosorbent Assay (ELISA) kits for mouse CCR2 and CCL2 protein (LifeSpan Biologicals [LSBio], Seattle, USA) were used to study levels of these proteins in the brain. Chemokine receptor type 2 is involved in chemotaxis of myeloid cells in response to CCL2 [160]. Brain homogenates were diluted 1:4 with the sample diluent provided with the kits, and all procedures were performed as per the manufacturer's instructions. The total protein content of each sample was determined by the bicinchoninic acid (BCA) assay (ThermoFisher, Waltham, MA USA). Results were expressed in ng/mg of protein. The detection limit is typically < 0.156 ng/ml and < 10000 pg/ml for both of these ELISA kits, respectively. Intra-Assay: CV<4.6% Inter-Assay: CV<7.6% for CCR2 and Intra-Assay: CV<5.6% Inter-Assay: CV<6% for CCL2. There was no reported cross reactivity with other proteins for the primary antibody used in these kits.

Brain cytokine specially IFN-γ, IL-1 β, IL-10, IL-6, and TNF-α were quantified using commercially available ELISA kit. LifeSpan Biologicals kit was used to quantify IFN-γ (LS-F5065), IL-10(LS-F9770) and IL-6 (LS-F2478) according to manufacture protocol (LSBio Seattle, USA). IL-1 β and TNF-α (KMC0011and BMS607-3) were quantified by using commercial ELISA (ThermoFisher, Waltham, MA USA). All procedures were performed as per the manufacturer's instructions. Final protein concentrations were measured, which were then normalized to total protein content in the brain homogenate. Protein were normalized against total protein content determined by BCA. Results were then expressed as percentage to control. There was no reported cross reactivity with other proteins for the primary antibody used in these kits.

2.2.11 Western blot

Following the BCA, equal amounts of protein (20 μg) from each sample were heated with Laemmli buffer containing beta-mercaptoethanol (BioRad, Hercules, CA, USA) and separated by 4-20% PAGE using a Tris-HCL buffer system and 18-well Criterion gels (Biorad) and then transferred to a polyvinylidene fluoride (PVDF) membrane (Biorad) overnight at 90 mA. The membrane was blocked for 1 hour in 5% blocking milk (BioRad, Hercules, CA, USA). Then, each membrane was individually immunoprobed with a primary antibody against total p65 (NFκB) (1:1000, cell signaling), NFκB (pNFκB) phosphorylated at Ser536 (1:1000, Cell Signaling), PPARα (1:1000, cell signaling), pSTAT3 (1:1000, Cell Signaling) phosphorylated at Tyr 705, or tubulin (1:1000, abcam) in blocking buffer overnight. After each primary antibody incubation, each membrane was incubated with the recommended dilution (1:5000) of corresponding horseradish peroxidase-conjugated secondary antibody (cell signaling) in blocking buffer at room temperature for 1hr. Protein bands were visualized using enhanced chemiluminescence detection reagents (Thermo Scientific, MA USA). Band intensities were analyzed using the ChemiDoc imaging system (Bio-Rad). Results were

calculated using Image Lab software and normalized to the expression of tubulin protein in the sample.

2.2.12 Multiplex cytokine Assay

Selected cytokine levels in the plasma were analyzed using Meso Scale Discovery (MSD) 96-Well MULTI-SPOT®Ultra-Sensitive V-PLEX Proinflammatory Panel 1 mouse Kit, using electrochemiluminescence detection on an MSD Sector Imager™ 6000 with Discovery Workbench software (version 3.0.18) (MSD®, Gaitherburg, MD, USA). Cytokines were measured using the TH1/TH2 8-plex kit, which included 8 markers: IFN-γ, IL-1 β, IL-2, IL-4, IL-5, IL-10, IL-13, and TNF-α. All assays were performed according to manufacturer's instructions, in duplicates. Samples were diluted 1:2 and added to the plate which contains capture antibody immobilized on a working electrode. Following incubation for 1 hour, SULFO_TAG labelled detection antibodies were added to the wells. Finally, MSD buffer was added which developed electrochemiluminescence and the plate was loaded into an MSD instrument for reading. Data were acquired using a SECTOR S 6000 plate reader (MSD). Results were then expressed as percentage to control

2.2.13 Malondialdehyde assay

Malondialdehyde (MDA) levels in brain homogenates were measured using a Thiobarbituric Acid Reactive Substances (TBARS) Assay Kit (Cayman Chemical, 10009055) according to manufacturer protocol. Malondialdehyde is an organic compound used as marker for lipid peroxidation, since it is a byproduct of lipid peroxidation. At boiling temperature, oxidized lipids produce MDA which can be measured calorimetrically at 530–540 nm.

2.2.14 Fatty acid analysis Assay

Total lipid extracts were prepared from brain homogenate and plasma samples by the Folch et al., [161] and modified to minimize the sample volume used. Briefly, a 5 µL aliquot of internal standard containing C17 fatty acid was spiked into 10 µL of brain or plasma. Methanol (70 µL) and chloroform (120 µL) were then added. This mixture was centrifuged at 20,000 x g for 10 minutes to pellet proteins and other cell debris, and the supernatant was transferred to a clean tube. Next, 0.88% KCl was added (40 µL) at a volume of approximately 25% of the total reaction volume. This mixture was then vortexed for 1 minute and centrifuged as above to separate the phases. The upper phase was discarded, and the lower phase was dried into a clean tube under vacuum. Samples were cleaned using 750 µL, PVDF, 0.2 µm centrifuge filters (Thermo Scientific) prior to analysis. Filters were conditioned by centrifuging with 1:1 chloroform: methanol (v/v) (200µL) at 10,000 x g for 5 minutes and discarding the flow-through. Dried lipid extracts were resuspended in 1:1 chloroform: methanol (v/v) loaded onto the conditioned centrifuge filters and centrifuged as above. Flow-through was then dried directly into an autosampler vial under vacuum and stored at -80°C until further processing. Cleaned lipid extracts were resuspended in LC solvents (50 µL) at a ratio of 70% solvent A (27 % IPA, 42 % water, 21% ACN, 0.1 % formic acid, 10mM ammonium formate), and 30% solvent B (90% IPA, 10% ACN, 0.1% formic acid, 10mM ammonium formate) for LCMS analysis of total lipids. A Thermo EASY nLC 1000 liquid chromatograph coupled with a Thermo LTQ/Orbitrap mass spectrometer with nanoflex ESI source was used for nano-HPLC-MS sample analysis. Samples were injected onto an Acclaim PepMap™ 100, 75 µm X 2 cm, nanoViper, C18, 3 µm, 100 A trapping column using mobile phase A as the loading solvent with the outlet flow directed to waste. Following sample loading, the outlet flow was directed to the analytical column (Acclaim PepMap™ RSLC, 75 µm X 15 cm, nanoViper, C18, 2 µm, 100 A) for chromatographic separation of lipid species. Gradient elution was carried out by the gradient programs shown below in Tables 1 and 2. All samples were kept at 7°C in a cooled autosampler tray for the duration of the analysis. Data was acquired by full scan MS in both

positive and negative modes with a mass range of 130-2000 m/z (13μ scans/sec, spray voltage: 1500V, resolution: 30,000, max inject time: 200msec). Tracefinder™ software (Thermo Scientific) was used for peak identification and integration for lipid species in each run. Target compound lists of expected analytes for each chosen lipid class were used to find peaks of interest with ion windows of 5 ppm mass accuracy for the expected ions.

Table 2: Gradient Program for Positive and negative Total Lipid Runs

Time	**% Solvent A**	**% Solvent B**	**Flow Rate (nl/min)**
00:00	70	30	250
01:00	50	50	250
40:00	2	98	250
50:00	2	98	250
50:01	70	30	250
65:01	70	30	250

2.2.15 Statistical analyses

Data are expressed as mean ± SEM.There were total 12 mice per groups N=12. Mice were excluded from analysis if they were outlier. In some experiment technical error led to decreased in mice number. Differences between means were assessed using one-way analysis of variance (ANOVA) or t-tests as appropriate. Neuropathological, western blot, and ELISA data for protein markers described above were analyzed using ANOVA to determine statistical significance. For the lipidomics studies, a mixed linear model regression (MLM), Fisher's least significant difference (LSD) correction, and the Benjamini–Hochberg procedure (B-H) were

used for multiple-test corrections and to control the false discovery rate (FDR) for hypothesis testing of primary outcomes and as applicable. Barnes Maze data were analyzed using MLM for the acquisition trials and ANOVA for the probe trials. All other behavior tests were analyzed using ANOVA. All data were analyzed using SPSS version 22.0.0 (IBM Corporation, Armonk, NY). B-H ($\alpha = 0.05$) was calculated using excel. $P < 0.05$ was considered to be significant.

2.3 Results:

2.3.1 Peroxisome-associated VLCFA and BCFA are altered in plasma from veterans with GWI

In a pilot cross-sectional study of age- and gender-matched healthy GW veterans and those with GWI, we examined pristanic acid (a BCFA), VLCFAs, and several other free fatty acids (FFA). Figure 2.2A shows that levels of VLCFA were significantly increased ($F_{(5,18)} = 2.64$, $p = 0.034$) in plasma from veterans with GWI compared to control GW veterans. Plasma TBARS levels were used as surrogate for MDA measurements since TBARS are formed following MDA's reaction with thiobarbituric acid. Levels of TBARS were two-fold higher in GWI compared to control GW veterans (t-test (df= 7) = 2.7, $p = 0.004$, Figure 2.2B). Pristanic acid levels were decreased in GWI compared to controls ($F_{(2,10)} = 3.4$, $p = 0.053$, Figure 2.2C). An increase in several omega-3 (FA18:3, FA20:5n3, FA 22:5n3) and omega-6 (FA18:2, FA20:4, FA22:4 and FA 22:5) FFA was observed in plasma from GWI compared to control subjects (Figure 2.2C). Absolute concentration of these human plasma free fatty acid is provided in appendix.

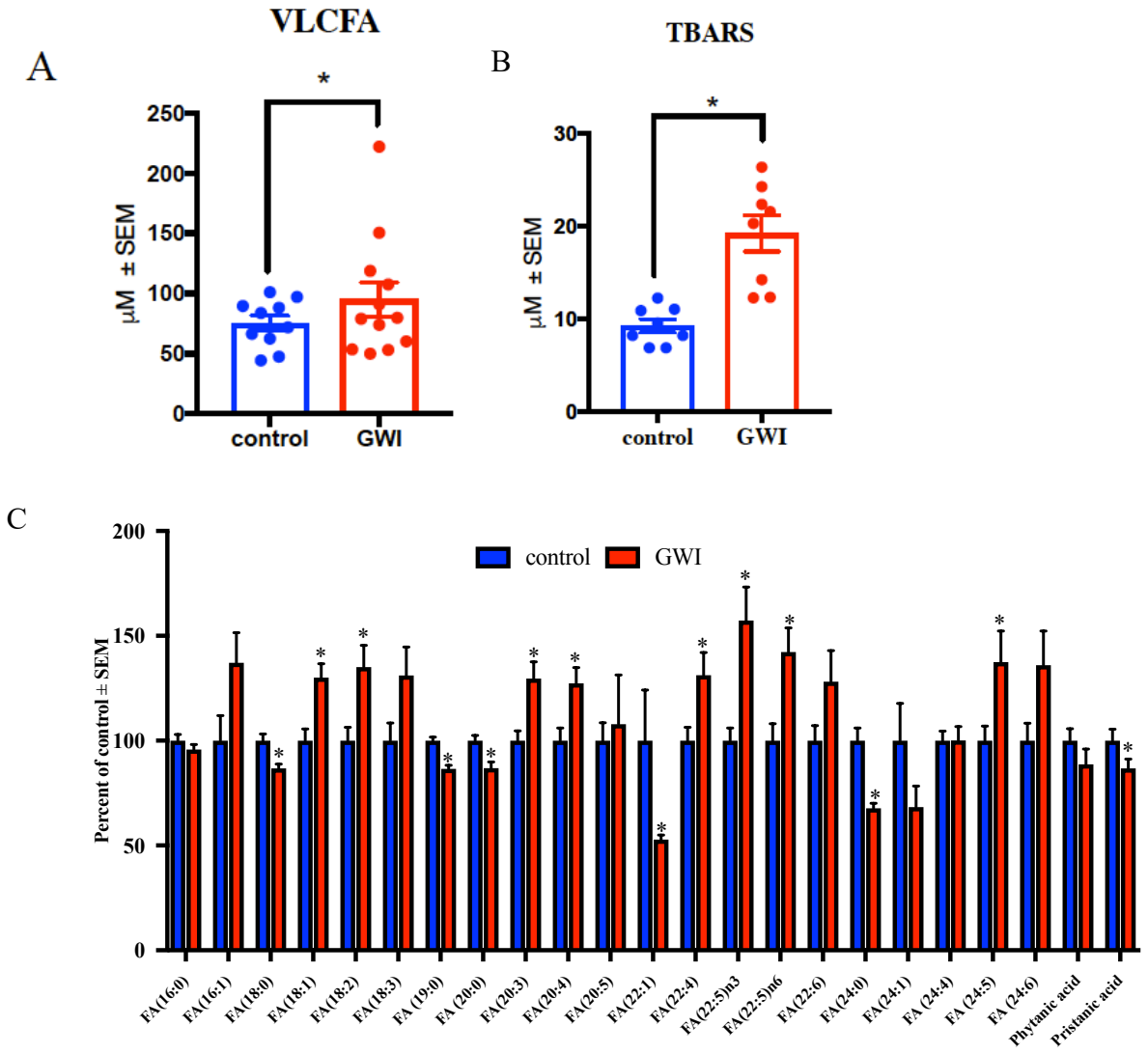

Figure 2.2. Plasma free fatty acid profiles in veterans with GWI compared to GW control veterans. Plasma free fatty acid were measured using LC/MS. Mean ± SEM (n = 10 for controls and n = 12 for GWI). (A) When all VLCFA (≥ C22 fatty acids), were combined as one category, there was an overall increase in GWI compared to control GW veterans T-test*$p \leq 0.05$. (B) Quantification of lipid peroxidation product TBARS (n = 8 per group for these analyses only) showed that levels were significantly elevated in GWI plasma compared to control veterans. T-test*$p \leq 0.05$. (C) Profiling of FFA showed that while several saturated (no double-bonds) and monounsaturated fatty acids (one double-bond) were decreased in blood of veterans with GWI compared to controls. Pristianic acid was decreased in GWI compared to controls. The remaining long-chain fatty acids (14-21 carbons) and VLCFA species particularly omega-3 and omega-6 species, were significantly elevated in veterans with GWI compared to controls. MLM along with BH correction *$p \leq 0.05$.

2.3.2 OEA treatment improves neurobehavioral deficits in a GWI mouse model

Based on the suggestion of possible peroxisomal β-oxidation dysfunction shown in blood samples from GWI subjects described above, I tested whether targeting peroxisomal β-oxidation with OEA (administered orally in chow at 10mg/kg daily dose) can improve the chronic learning and memory deficits observed in a well-characterized mouse model of GWI. After GW chemical exposure, mice underwent testing with the FST at 3- and 5-months post-exposure to establish the presence of GW chemical induced changes in exposed relative to control mice. Control and GWI mice were divided into groups which either received oral OEA treatment in diet daily or normal diet for a total of six months. Average food intake was 5.75 ± 0.07 g/day/mouse, and the average consumption of diets was not affect by OEA treatment(p=). There was no significant change in body weight among all four groups(Figure 2.4 C). The Barnes Maze test was used to assess learning in control and GWI mice after 1-month of oral OEA treatment (6-months post-exposure to GW chemicals) and long-term memory after 2-months of treatment (7-months post-exposure). Learning was assessed during the acquisition trials in which mice were allowed to freely explore the maze for 3 min and escape into the target box through one of the holes in the platform. On days 1 and 2, GWI mice travelled a longer distance to reach the TH than control mice. However, GWI mice treated with OEA had the best performance compared to all other groups ($F_{(1,10)} = 12$, $p = 0.03$, Figure 2.3A), having the shortest travel time when compared to controls treated with OEA ($p < 0.05$) as well as compared to controls ($p < 0.05$) and GWI mice on the normal chow diet ($p < 0.05$). During the probe trial at 2-months post-treatment, GWI mice had lowest frequency of visit to the TH compared to all other groups ($F_{(1,16)}= 11.1$, $p = 0.02$, Figure 2.3B). Oleoylethanolamide treated GWI mice had a higher frequency of visiting the TH compared to GWI mice on a normal diet ($p < 0.05$, Figure 2.3B).

To test whether OEA corrected fatigue-like behavior in GWI mice, I performed the FST at 5-months post-treatment. While this test can be used for assessing depression, it is also helpful in quantifying fatigue by examining immobility, particularly when mice are repeatedly assessed with the FST apparatus [162,163], as is the case here, where all mice were subjected to the FST at 1- and 3-months post-exposure (figure 2.4). I also observed at 3-months post-exposure, immobility was similar between control and GWI mice for the first 2 min, but the immobility increased in GWI mice with time, further suggesting that fatigue emerges with some time delay. At 5-months post-treatment (10-months post-exposure), GWI mice treated with OEA were less immobile compared to all other groups ($F_{(1,6)} = 10.2$, $p = 0.018$; 2.3C), while *post-hoc* analysis showed that OEA treated GWI mice had less fatigue type presentation than GWI mice on the control diet ($p < 0.05$) but mean velocity did not differ between the groups ($F_{(2,6)} = 5.2$, $p = 0.318$, Figure 2.3C). However, OEA treated control mice were more immobile than control mice on normal diet ($p < 0.05$; Figure 2.3C). Anxiety/disinhibition was tested at 6-months post-treatment using the elevated plus maze (EPM) test, in which the amount of time spent in the closed arm indicates increased anxiety, whereas time spent in the open arms is indicative of disinhibition. Relative to all other groups, GWI mice spent more time in the open arms ($F_{(2,6)} = 9.2$, $p = 0.018$, Figure 2.3E); and an influence of OEA treatment was observed whereby the time spent in the open arms was reduced in OEA-treated GWI mice ($p < 0.001$, Figure 2.3E and 2.3F). Control mice on the OEA diet exhibited disinhibition when compared to control mice on the normal diet, but no anxiety-like behavior was observed. There was no significant change in weight across all 4 groups.

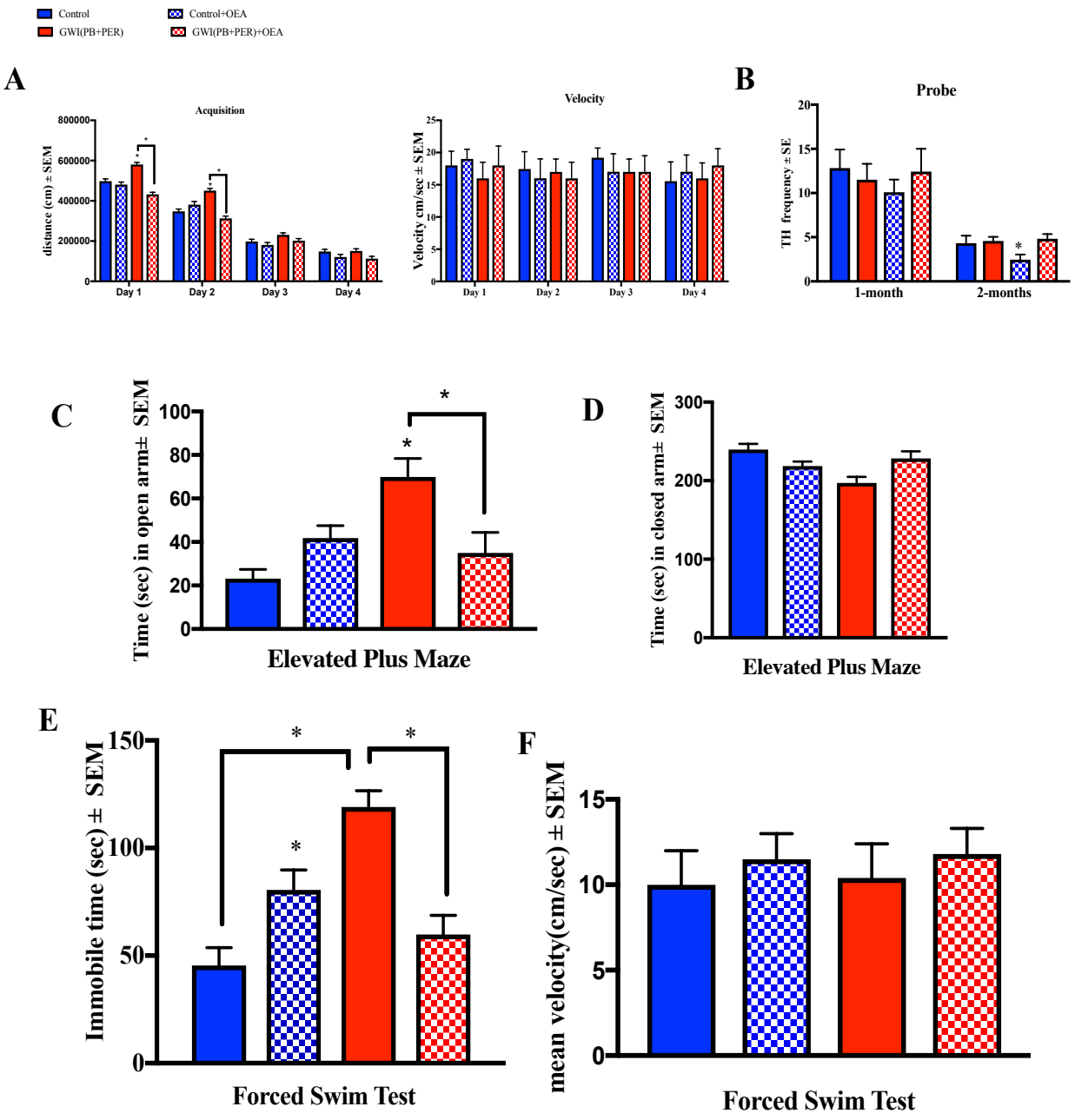
Control
Control+OEA
GWI(PB+PER)
GWI(PB+PER)+OEA
A
Acquisition
distance (cm) ± SEM
800000
600000
400000
200000
0
Day 1
Day 2
Day 3
Day 4
Velocity
Velocity cm/sec ± SEM
25
20
15
10
5
0
Day 1
Day 2
Day 3
Day 4
B
Probe
TH frequency ± SE
20
15
10
5
0
1-month
2-months
C
Time (sec) in open arm± SEM
100
80
60
40
20
0
Elevated Plus Maze
D
Time (sec) in closed arm± SEM
300
200
100
0
Elevated Plus Maze
E
Immobile time (sec) ± SEM
150
100
50
0
Forced Swim Test
F
mean velocity(cm/sec) ± SEM
15
10
5
0
Forced Swim Test

Figure 2.3: OEA treatment improves cognitive function, reduces fatigue and disinhibition type behavior in GWI mice. Mean ± SEM of control (n = 12), GWI mice (n = 11), control+OEA (n=12) and GWI+OEA (n=12). (A) One month after OEA treatment (6-months post-exposure to GW chemicals), acquisition trials were conducted to train mice to escape into the TH. In GWI mice treated with OEA, total distance to the TH was smallest, particularly on days 1 and 2, indicative of learning. As expected GWI mice on normal chow had the worst performance having the largest total distance to the TH. Control mice treated with OEA had a higher latency to find the TH compared to control mice on normal diet on day 2 only. (B) For the probe trials, conducted at 2-months post-treatment (7-months post-exposure), OEA treated GWI mice had similar frequency of the visits to the TH as control mice on normal chow and on OEA but higher frequency of visits than GWI mice. (C) The immobile time was significantly increased in GWI mice compared to controls which was reduced in OEA treated GWI mice. (D) There was no change in average speed among all the different group. (E) An examination of the time in open arms of the EPM showed an increase of disinhibition in GWI mice on normal chow compared to both control groups and OEA treated GWI mice. (F) Time in closed arm was decreased in GWI mice compared with control groups and OEA treated GWI mice. ANOVA with post-hoc tukey *$p \leq 0.05$.

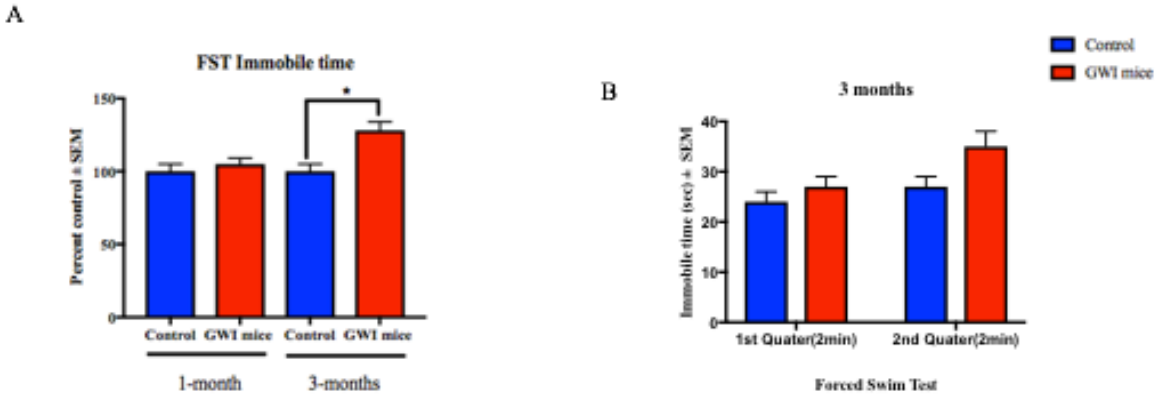

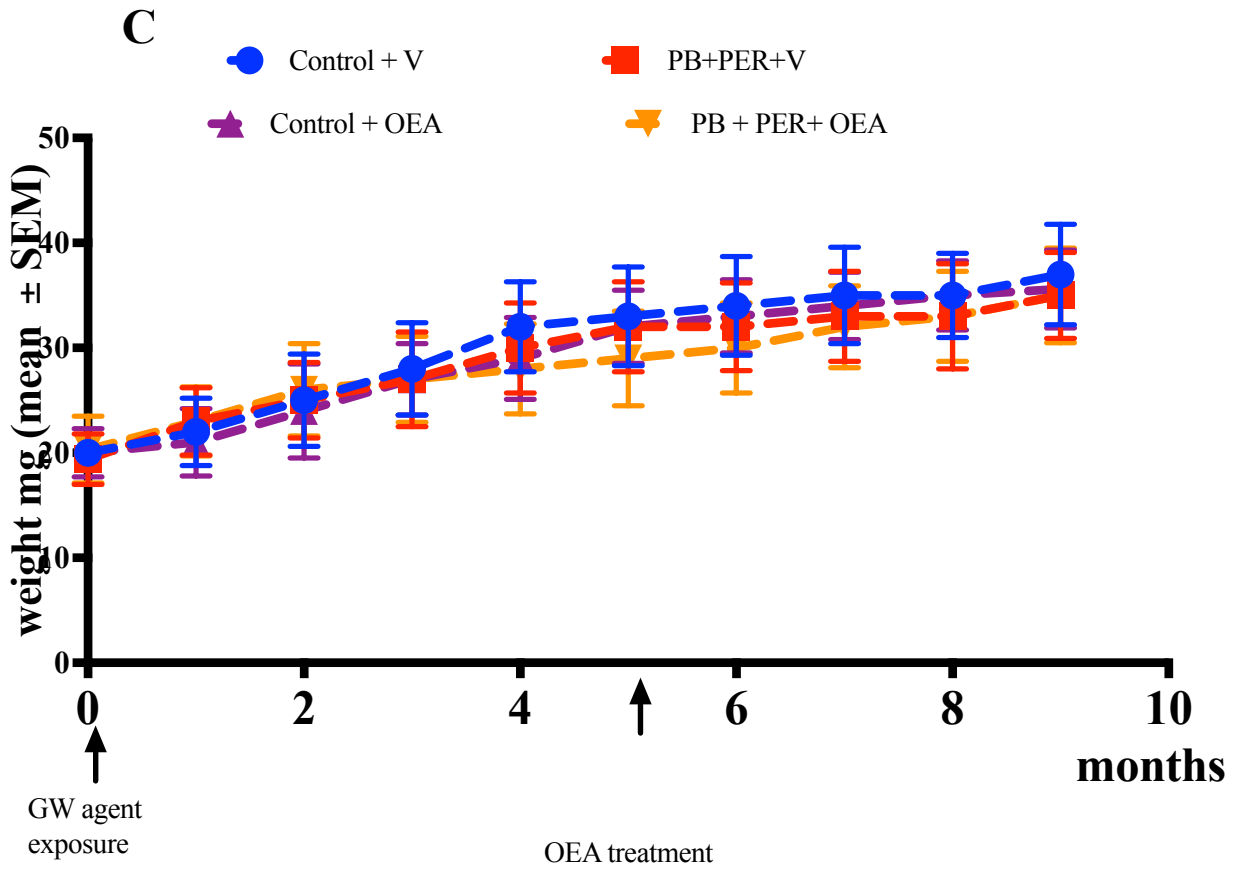

Figure 2.4 Fatigue-like presentation is observed in GWI-exposed mice. (A) FST data expressed as percent control of immobile time ± SEM (n = 24 per group). Total immobile time was significantly decreased in GWI mice at 3-months post-exposure, but no effect was seen at 1-month post-exposure. (B) At 3-months post-exposure, immobility was similar between control and GWI mice for the first 2 min, but the immobility increased in GWI mice with time.(C) Body weight showed no change across all 4 hroups. ANOVA with post-hoc tukey *$p \leq 0.05$.

2.3.3 Elevated levels of VLCFA in the brains of GWI mice were reduced by OEA treatment

Levels of VLCFA were significantly elevated in the brains of GWI compared to all other groups ($F_{(1,13)} = 4.4$, $p = 0.045$; Figure 2.5). Compared to GWI mice on normal chow, those treated with OEA had lower levels of VLCFA ($p < 0.05$) and were similar to control mice on normal chow (Figure 2.5B, $p < 0.05$for VLCFA). Level of TBARS were also different between

all experimental groups ($F_{(1,11)}$=12.4, p = 0.015; Figure 2.5). *Post-hoc* analysis showed a statistically significant increase in TBARS in the brains of GWI mice compared to controls ($p < 0.05$) and these levels were lower in GWI mice treated with OEA (Figure 2.5C, $p < 0.05$). Several omega-3 and omega-6 FFA were altered in GWI compared to control mice on normal chow (Figure 2.5). OEA-treated GWI mice had levels similar to those observed in control mice on a normal diet, whereas levels of these FFA were elevated in control mice treated with OEA (Figure 2.5A). Individual species are shown in heatmap below.

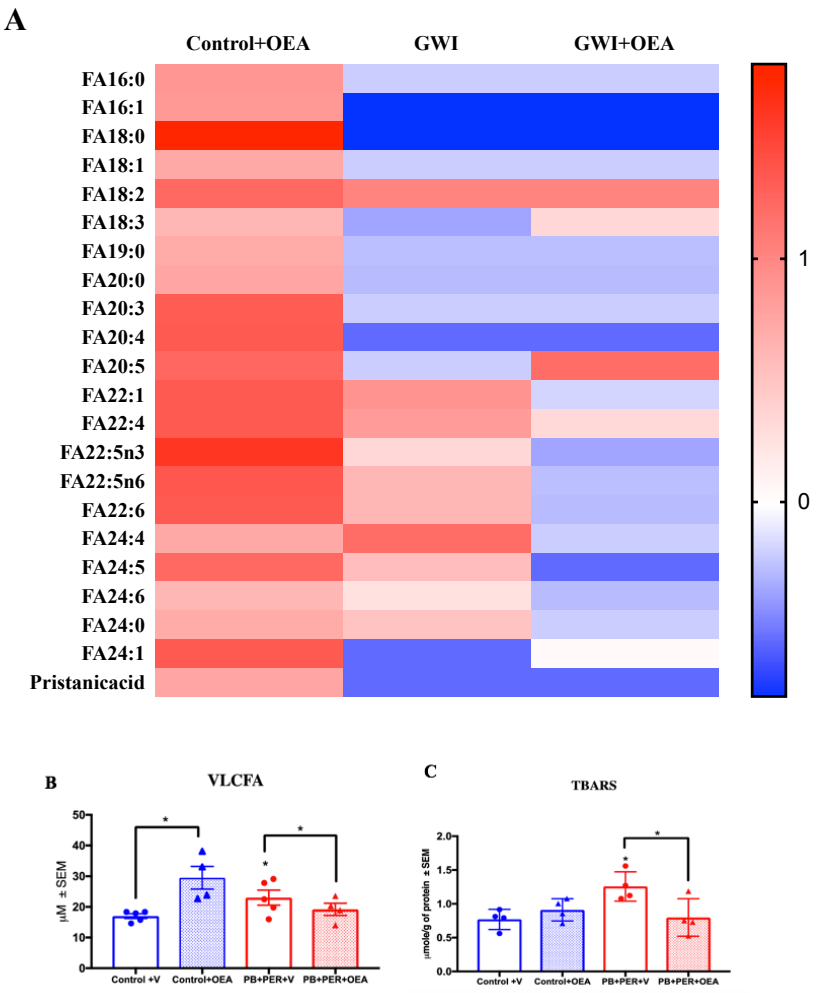

Figure 2.5: Brain lipid profiles show OEA improves fatty acids profile in the brain of GW agent exposed mice relative to controls. Mean ± SEM expressed as percent control of mice on normal chow (n = 4/5 per group). (A) Compared to controls, GWI mice had higher levels of several major omega-6 and omega-3 FA (FA20:4, FA22:4. FA22:5, FA24:5 and FA24:6). Treatment with OEA decreased the levels of these FA in GWI mice (B) Levels of VLCFA were increased in the brains of GWI mice compared to control mice. OEA treated GWI mice had similar levels as in control mice. However, control mice treated with OEA had significantly higher levels of VLCFA compared to control mice which received normal diet). (C) Quantification of lipid peroxidation product TBARS showed that levels were significantly elevated in GWI compared to control mice on normal chow but were lower in OEA treated GWI mice compared to all other groups. ANOVA with post-hoc tukey *$p \leq 0.05$

2.3.4 OEA reduces astroglia and microglia activation in GWI mice

Astroglia and microglia, which participate in protecting the brain and modulating inflammation [164–167], were upregulated in the brains of GWI mice at long-term post-exposure timepoints. Using immunohistochemistry followed by confocal microscopy, an increase in the GFAP staining of astroglia was observed in the cerebral cortex ($F_{(1,8)} = 4.8$, $p = 0.034$) and the dentate gyrus (DG) ($F_{(1,8)} = 6.3$, $p = 0.021$) of GW chemical exposed mice compared to all other group. *Post-hoc* analysis showed significant decreased in GFAP staining in OEA-treated GWI mice compared to GWI mice on a normal diet ($p < 0.05$, Figure 2.6, $p < 0.05$ for the hippocampus and $p < 0.001$ for the cortex). Immunohistochemistry staining with ionized calcium binding adaptor molecule 1 (Iba1) staining followed by light microscopy was used to examine microglia proliferation and activation, respectively. There was an elevation of microglia staining with Iba1 in the dentate gyrus (DG) of GWI mice compared to all other groups ($F_{(1,6)} = 10.2$, $p = 0.018$; Figure 2.7), whereas OEA-treated GWI mice had much lower staining with Iba1 compared to GWI mice on control diet (Figure 2.7, $p < 0.05$).

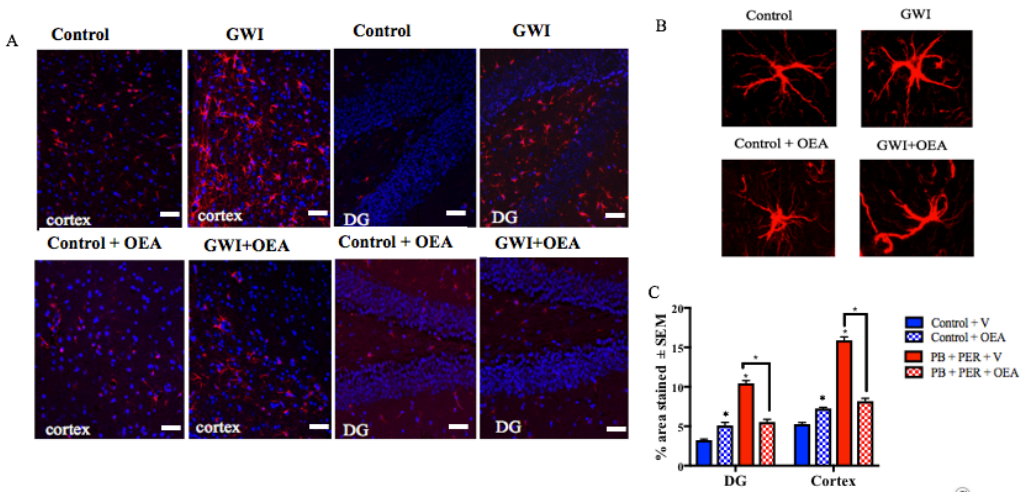

Figure 2.6: OEA treatment reduced elevated astroglia activation in GWI mice. Confocal microscopy images showing staining of astroglia with GFAP (n = 4 per group, 4 serial sections for each animal). Scale bar 50µm. (A) Images show 20x GFAP staining (red) and DAPI (blue) in the cortex and the DG of mice from all 4 treatment groups. (B) Images show 100x magnification of GFAP stained astroglia in the cortex of each study treatment group. (C) Quantification of GFAP staining from 20x images. There significant increases in GFAP staining for both the cortex and the DG within the hippocampus of GWI compared to control mice. GWI mice treated with OEA had similar levels as control mice on normal chow. Control mice treated with OEA had higher levels than control mice on normal diet. *ANOVA with post-hoc tukey* * $p \leq 0.05$

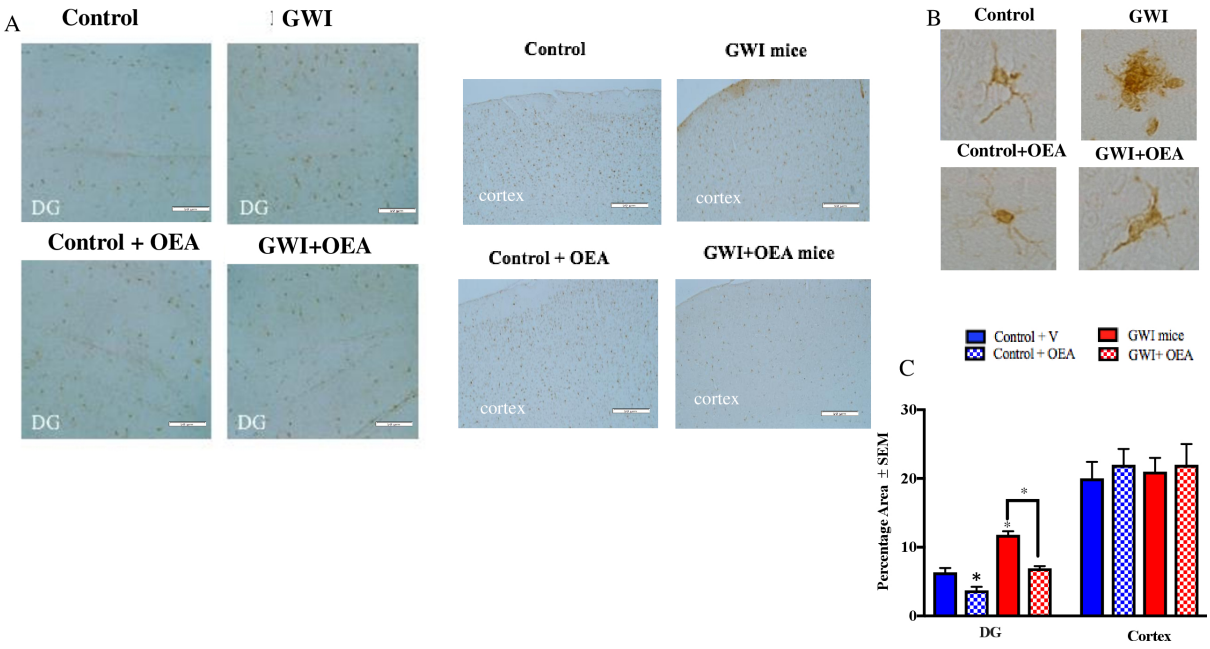

Figure 2.7: OEA treatment reduced microglia proliferation in GWI mice

Light microscopy images showing staining of microglia with IBA-1 (n = 4 per group, 4 serial section for each brain). Scale bar 50µm. (A) Images show 20x Iba1 staining in the cortex and DG of mice from all 4 treatment groups. (B) Images show 100x magnification of Iba1 stained astroglia in the cortex of each study treatment group. (C) Quantification of Iba1 staining from 20x images. Levels of Iba1 staining within the DG was lower in OEA treated GWI mice compared to GWI mice on normal chow. Levels of Iba1 in GWI mice were higher in the DG compared to control mice. There were no differences in the cortices of GWI mice compared to control or OEA treated GWI mice. ANOVA with post-hoc tukey * $p \leq 0.05$.

2.3.5 OEA treatment reduces chronic brain inflammation in GWI mice

In order to determine if NFκB-mediated pro-inflammatory pathways could be inhibited by OEA in the brains of GWI mice, I examined the ratios of pNFκB at the p65 subunit to total NFκB, pSTAT3, and several pro-inflammatory cytokines. At 11-months post-exposure to GW chemicals, corresponding to 6-months of OEA treatment, there was a significant increase in the

ratio pNFκB/NFκB in the brains of GWI compared to all other groups $F_{(1,6)} = 8.2$, $p = 0.012$; Figure 2.8A), whereas OEA-treated GWI mice had lower ratios compared to GWI mice on normal chow ($p < 0.001$, Figure 2.8 A and B). Since pSTAT3 is thought to enhance the activation of NFκB, I examined this protein and found it to be increased in the brains of GWI mice across all 4 experimental groups ($F_{(2,10)} = 12.42$, $p = 0.033$), and reduced in OEA-treated GWI mice compared to GWI mice on normal diet following post-hoc ($p < 0.05$, Figure 2.8 C and D) analysis. Furthermore, several pro-inflammatory cytokines, including IL-1β ($F_{(3,9)} = 7.2$, $p = 0.011$), IL-6 ($F_{(2,8)} = 8.31$, $p = 0.032$), and IFN-γ ($F_{(1,7)} = 6.12$, $p = 0.028$), were affected by GWI status and OEA treatment, where post-hoc analyses showed that these cytokines were elevated in GWI mice compared to all other groups and were significantly lower in GWI mice treated with OEA ($p < 0.05$, Figure 2.8E). We also observed significant effect of the GWI status and OEA treatment was observed for CCR2 ($F_{(2,8)} = 11.32$, $p = 0.031$) and CCL2 ($F_{(2,10)} = 11.14$, $p = 0.03$) at 11-months post-exposure to GW chemicals (Figure 2.8) with *post-hoc* analyses showing increases in the brains of GWI mice compared to control mice and lower levels in OEA treated GWI mice (Figure 2.8F, $p = 0.049$ for CCL2 and $p = 0.056$ for CCR2). Also, Figure 2.9 shows an effect of OEA treatment on PPARα ($F_{(4,10)} = 4.12$, $p = 0.041$) and PPARγ co-activator 1α (PGC-1α)($F_{(2,8)} = 16.11$, $p = 0.039$) expression, irrespective of GWI status. *Post-hoc* analysis showed that OEA treatment increases PPARα ($p<0.05$) and PGC-1α ($p<0.05$) in control and GWI mice.

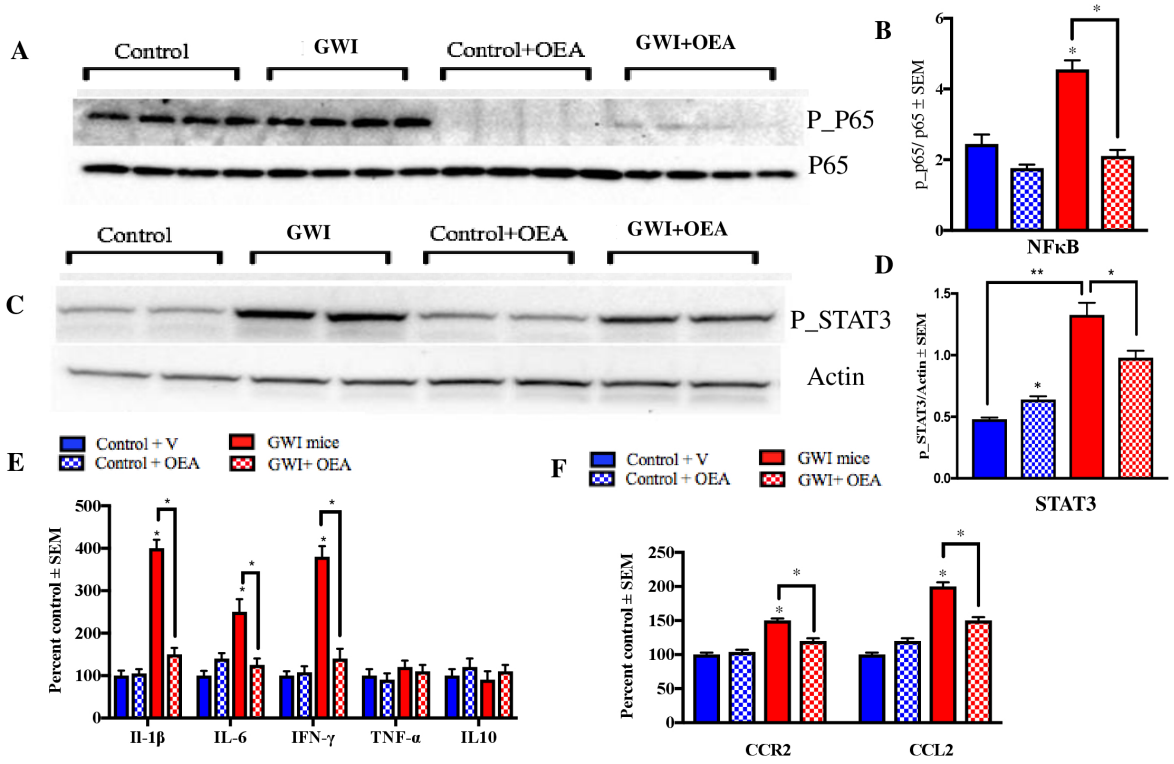

Figure 2.8: **Levels of phosphorylated NFκB and STAT3 were reduced by OEA treatment in GWI mice**. Mean ± SEM (shown as densitometric arbitrary units, n = 4 per group). (A-B) Ratio of p-P65)/P65 was elevated in GWI mice at 11-months post-exposure. At this time-point, which corresponded with 6-months of OEA treatment, GWI mice having OEA treatment had a significantly lower ratio compared to GWI mice on normal chow. Control mice treated with OEA had non-significantly lower ratios compared to control mice on regular diet. (C-D) Similarly, p-STAT3/Actin levels were significantly elevated in GWI compared to control mice and were also lower in OEA treated GWI mice compared to those on normal chow. Levels of STAT3 were also elevated in control mice treated with OEA compared control mice on normal diet. (E) Among the cytokines examined in the brain, IFN-γ, IL-6, and IL-1β were lower in OEA treated GWI mice compared to GWI mice on normal chow. Mice with GWI had elevated levels of these pro-inflammatory cytokines compared to control mice. These cytokines did not differ between control mice treated with OEA compared to control mice on normal diet. (F) Treatment with OEA decreased the levels of CCR2 and CCL2 in the brain of GWI mice compared to GWI mice on normal chow. ANOVA with post-hoc tukey *$p \leq 0.05$.

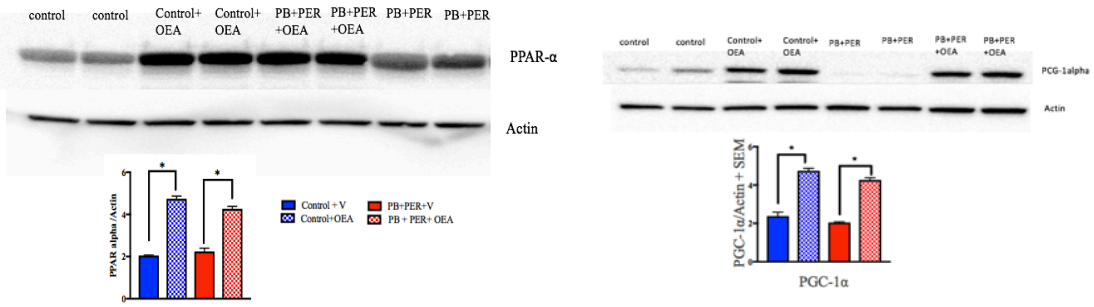

Figure 2.9 Western blot analysis of PPAR-α and PGC-1 α protein expression in the brain. Mean ± SEM (shown as densitometric arbitrary units, n = 4 per group). There was significant increase in PPAR-α and PGC-1 α level in the mice feed with OEA compared to non OEA controls. Histogram showing relative levels of each of the PPAR-α and PGC-1 α protein in all four groups. ANOVA with post-hoc tukey *p ≤ 0.05

2.3.6 In vitro screening of the drug that reduces Lipopolysaccharides induced NFkB activation

I used OEA, DHEA and PGE2EA at 10μM, 1μM and 100nM along with LPS (10μg/ml) to determine if these compounds were able to decrease NFκB phosphorylation induced by LPS. There were no significant differences in LDH release from cells treated with vehicle (DMSO), LPS and all three tested ethanolamides ($p > 0.05$). I observed that LPS treated cells had a significant increase in pNFκB relative to total NFκB levels when compared to DMSO treated cells ($F(5,18) = 13$, $p = 0.012$, Figure 2.10). Compared to LPS alone, LPS with OEA, PGE2EA and DHEA treatment had a lower ratio of pNFκB to total NFκB protein levels at 10μM and 1μM ($p < 0.001$). Also, OEA at all dose decreased NFκB phosphorylation relative to LPS treatment ($p < 0.05$, Figure 2.10). However, 100nM PEA along with LPS had a decreasing trend in NFκB phosphorylation ($p > 0.056$, Figure 2.10) when compared to LPS treated cells. (Figure 2.10). In this study the most potent drug was OEA and IC 50 of OEA was determined as shown in figure 2.11

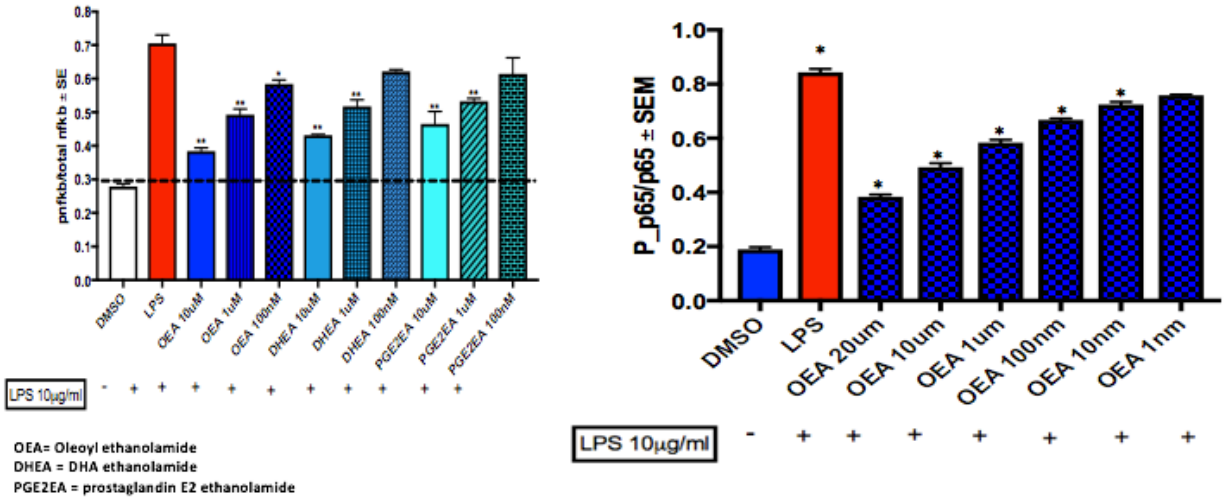

Figure 2.10: Effects of OEA on the NFκB inflammatory signaling pathway in LPS-induced RAW cells. Modulation of NFκB activation by ethanolamides. Activation of NFκB, induced by LPS, was reduced by different ethanolamides in vitro. Compared to LPS alone, LPS along with OEA, PGE2EA, and DHEA significantly decreased this ratio of p-NFκB to NFκB. Cytotoxicity results showed no significant toxicity associated with ethanolamide compounds at all doses tested. ANOVA with post-hoc tukey *$p \leq 0.05$

2.3.7 Modulation of NFκB and STAT 3 activation by ethanolamides is depended on PPARα

Above, I used OEA at 100nM along with LPS to determine if OEA is able to decrease NFκB phosphorylation induced by LPS. I next tested whether NFκB inhibition by OEA is PPARα dependent. As expected, LPS treament significantly increased NFκB phosphorylation when compared to all other groups ($F_{(3,16)} = 16.14$, $p = 0.003$, Figure 2.11). *Post-hoc* analysis showed that normalization of OEA effect on NFκB phosphorylation were depended on PPARα but not on PPARγ ($p < 0.05$, Figure 2.11) since only the pretreatment of cells with PPARα antagonist blocked the anti-inflammatory effects of OEA. Similarly, LPS treated cells had a

significant increase in STAT3 ($F_{(3,12)} = 18.31$, $p = 0.012$, Figure 2.11) and JAK2 phosphorylation ($F_{(3,14)} = 21.23$, $p = 0.002$, Figure 2.11) across all four groups. Post-hoc analyses showed that these effects were similar to those observed for NFκB where only pretreatment with PPARα antagonist was able to abolish phosphorylation of STAT3 and JAK2 (Figure 2.11).

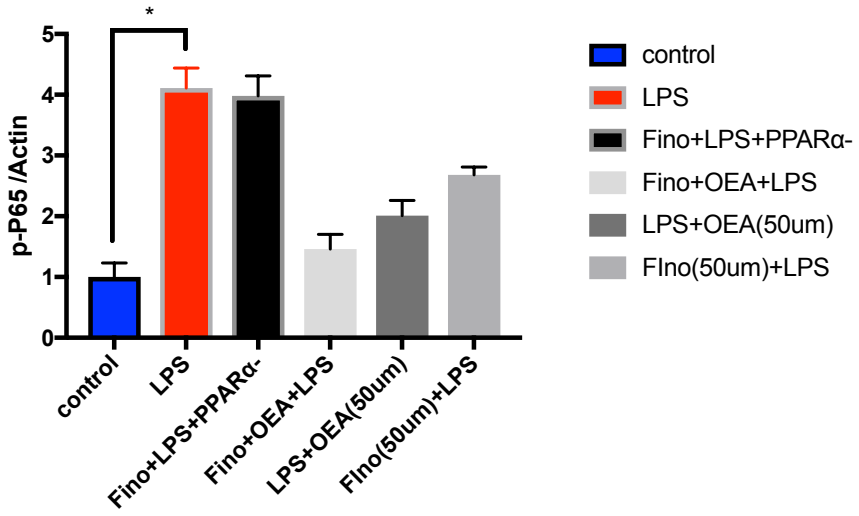

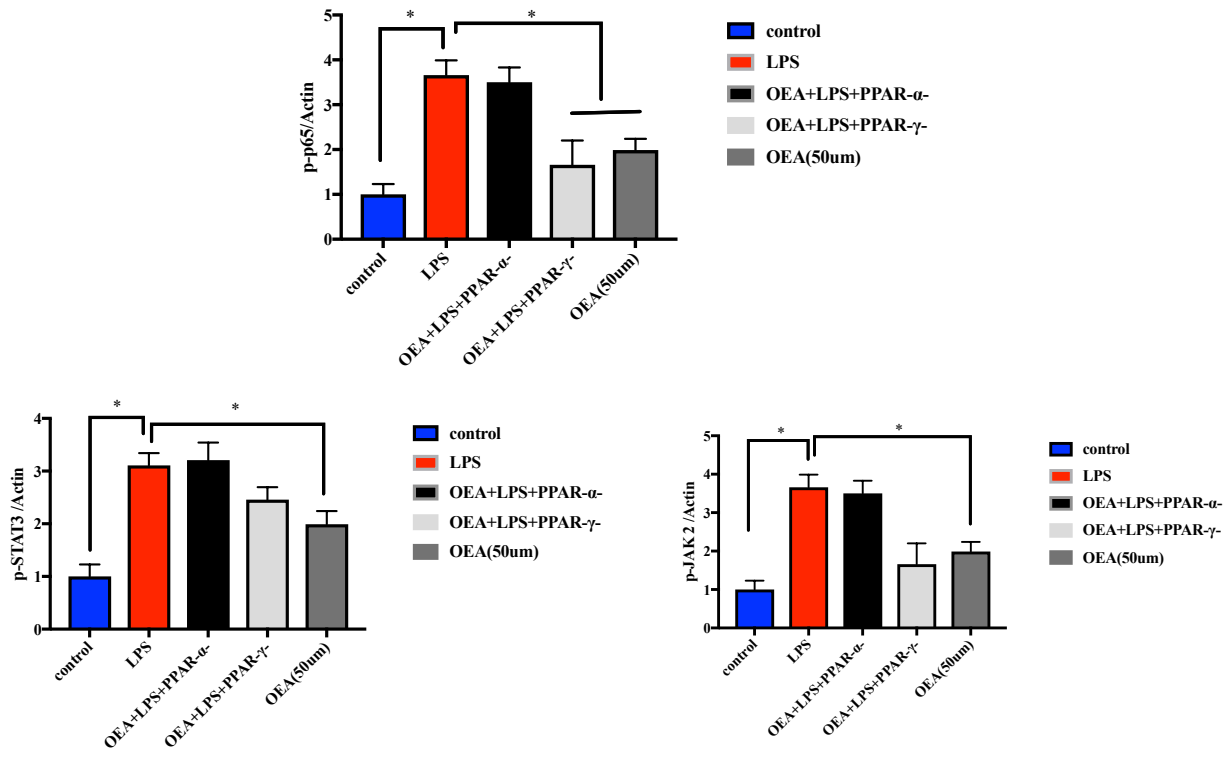

Figure 2.11: Anti-inflammatory effect of OEA is depended on PPAR-alpha. OEA shows more potent than commercially available PPARα agonist at similar concentration. PPARα blockade showed no anti-inflammatory effect of OEA and fenofibrate in LPS induced murine macrophage cell. No such effect was seen in PPAR-gamma blockade cell line. Cells were pretreated with PPAR-alpha inhibitor (GW 6471) and PPAR-gamma inhibitor (GW 1929) for 3 hours and then treated with LPS and OEA. ANOVA with post-hoc tukey *p ≤ 0.05

2.4: Discussion

Our studies showed that lipids which are specially metabolized in peroxisomes, including VLCFA, pristanic acid, and DHA, were altered in plasma from veterans with GWI. These findings were supported by our previous studies showing that omega-3 DHA and ether-containing PL were disturbed in veterans with GWI [76]. Our preclinical mouse model studies also showed that VLCFA were also elevated in the brains of GWI mice compared to control mice. Further supporting possible relevance of impaired peroxisomal β-oxidation or aberrantly active biosynthesis of these fatty acids to the pathogenesis of GWI. Currently, there are no approved therapies that can treat the underlying pathology of GWI. The present treatment strategies mostly focus on pain management with non-steroidal anti-inflammatory drugs or opioids, reducing fatigue with vitamins/antioxidants and targeting mood/cognitive issues with antidepressants. These symptom management approaches do not modify the underlying disease process associated with GWI. Hence, there remains a need for developing treatments which target the underlying pathobiology of GWI. I used OEA as a stimulator of peroxisomal β-oxidation and showed that abnormal increases in brain VLCFA, tetracosahexaenoic (a precursor of DHA) and DHA levels in GWI mice were normalized after OEA treatment. It is well-known that OEA is a potent PPARα ligand, which in itself has various health benefits which include weight loss and reduced fatigue [168]. These post-treatment changes in GWI mice corresponded with reduced brain glia activation and inflammation and improvement in neurobehavioral deficits relevant to the clinical symptom presentation of GWI.

Memory impairment is one of the major complaints among veterans with GWI, and a recent meta-analysis comparing results of neuropsychological functioning in veterans with GWI across 14 studies has shown that veterans with GWI consistently report cognitive deficits in both learning and memory [47,169–175]. This is further supported by imaging studies showing damage to the brain hippocampal regions in veterans with GWI which may possibly contribute

to memory problem observed in ill GW veterans [176–178]. Another recent study of neuropsychological functioning in military pesticide applicators from the GW reported worse memory functioning in veterans exposed to pesticides and personal repellents during the war compared to healthy GW veterans [179]. Animal studies have consistently shown chronic impairment in learning and memory in several rodent models of GWI [44,51,53,54,157,180]. Our current studies show that even after a couple of months of OEA treatment, GWI mice performed far better on both learning and memory-related tasks compared to all other groups, which is consistent with the currently known effects of OEA on cognition [145,149,181] and may be of therapeutic value in GWI.

Other non-cognitive behavioral features were examined in this study with a particular emphasis on fatigue since clinical studies show that fatigue is one of the major symptoms of GWI, reported by nearly 79% of veterans with GWI [1,154,172,173]. This is supported by an imaging study showing altered axial diffusion patterns within brain areas which link cortical regions involved in pain, fatigue, and cognition in a subset of veterans with GWI [22]. At 1-month post-exposure, there was no difference between GWI and control mice on immobility during the FST, indicating no change in fatigue parameters. Interestingly, I detected increased immobility in GWI mice with repeated exposure to the FST apparatus at 3-months and a further increase at 10-months post-exposure. Interesting, such effects were alleviated in GWI mice after 5-months of OEA supplementation. At this 10-month post-exposure timepoint, there were no indications of anxiety on the EPM and no locomotor problems or increased perimeter activity on the OFT in GWI mice. Instead, our findings on the EPM indicate disinhibition in GWI mice, evident by the fact that GWI mice were spending more time in the open arms of the EPM, which is consistent with a previous study reporting disinhibited behavior in the same model at 13-months post-exposure to GW chemicals [53]. Disinhibition is suggested to be a consequence of lesions in the hippocampus and inhibition of dorsal hippocampal functioning[182,183]. Collectively,

these behavior studies suggest that OEA treatment may help with reducing cognitive deficits and fatigue in veterans with GWI.

Consistent with previous studies [51,53,157], I observed astroglia activation in both the cortex and hippocampus of GWI mice which were reduced by OEA treatment. As before, Iba1 staining was increased in the hippocampus of GWI mice when it was examined at 16-months post-exposure [54]. This increase was also normalized after OEA treatment in GWI mice. As can be seen, astroglia to be key pathologies in GWI along with microglia proliferation with age. These finding are replicated in several rodent models of GWI [51,53,54,157]. We do observe, astroglial activation was observed at 5-, 16- and 22-months post-exposure [54,184], whilst increased Iba1 staining, generally associated with microglia proliferation can only be seen at 11-months post exposure but not at any earlier timepoints, despite the presence of robust neuroinflammation. In fact, a role of astroglia involvement in GWI was suggested by an imaging study showing abnormal lactate utilization in subsets of GWI veterans [22,110]. While previously thought to serve in a supportive capacity within the CNS, recent studies have shown that astroglia also play a prominent role in regulating the innate immune responses in the brain by releasing chemokines which facilitate activation, migration, and proliferation of microglia [185,186]. Given that astroglia activation in this GWI model precedes changes in microglia, it is possible that the observed increase of microglia cells in the hippocampus may be a result of increased migration to control ongoing immune and inflammatory responses, which warrant further investigation. However, it is unclear why microglia activation is undetectable in this model until very late stages.

While both astroglia and microglia can release monocyte chemoattractant protein-1 (MCP-1/CCL2), in conditions with an active immune component and an absence of obvious neuronal damage, astroglia appears to be the major producers of CCL2 [187]. Our current study shows that

CCL2 levels are chronically elevated in GWI compared to the control which is consistent with findings of increased mRNA of this protein in another mouse model of GWI that was exposed to an organophosphate pesticide[179]. Release of CCL2 helps recruit brain macrophage/microglia to the damaged area and attracts CCR2 expressing monocytes from the periphery in response to injury or chemical exposure [188,189], contributing to inflammation via CCR2 activation through NFκB and STAT3 pathways [190,191]. Given that myself and my colleagues do not observe an overt neuronal death in our GWI mice at any of the chronic post-exposure timepoints [53,54,157], the increase in CCL2 is likely due to inflammation rather than cell death. Consistent with these studies, I also observed increases in phosphorylation of NFκB and STAT3 in the brains of GWI mice, which corresponded with an increase in several pro-inflammatory cytokines, such as IL-1β, IL-6, and IFN-γ. Increases in serum levels of these cytokines are also observed in veterans with GWI compared to control veterans [103,104,192].

Treatment with OEA can potentially alleviate the inflammatory aspects of GWI described above. This can be supported by our studies showing that OEA exerts anti-inflammatory effects in GWI by inhibiting NFκB activity and downregulating many pro-inflammatory cytokines. However, metabolism of OEA by fatty acid amide hydrolase (FAAH) may target the brain cannabinoid receptors and, as such, some of the observed effects of OEA could be mediated by these alternative pathways and warrant further evaluation [193]. Furthermore, given this impact of OEA on the endocannabinoid system, translation of OEA treatment into humans in the context of cannabinoid use may produce adverse effects and will require close monitoring. One limitation of this study is that OEA also affected the lipid homeostasis in control mice treated with OEA which corresponded with the lowered anxiolytic response and higher immobility in the FST. Despite that, I did not observe any adverse effect on memory or increase in lipid peroxidation and inflammation in these mice. However, given the role of OEA in lipid

metabolism and reducing inflammation, increasing its level in the absence of underlying inflammation or metabolic dysfunction warrants further examination. Our work into the mechanism of these effects suggests that PPARα and PGC-1α elevation could have contributed to possible increases in peroxisome proliferation and mitochondria biogenesis and that increases in lipids could be a reflection of these changes [194–196]. I do expect that additional pharmacokinetics and pharmacodynamic studies will help identify a safe and effective dose for chronic administration in veterans with GWI.

The recent study in Roskamp institute support that activation of astroglia along with lipid dysfunction corresponds with peroxisomal dysfunction. As I already know peroxisome is a very important site for metabolism of VLCFA. I also see some evidence of peroxisome dysfunction in our study from the total fatty acid. As I observe the change in branched chain fatty acid (pristanic acid) which suggests peroxisomal dysfunctions. Phytanic acid in the human body is mainly derived from diet is still unknown how they are translocated in the peroxisome [197,198]. Once inside the peroxisome, phytanoyl-CoA is metabolized by phytanoyl-CoA hydroxylase and is converted into 2-hydroxyphytanoyl-CoA, which again metabolized by aldehyde dehydrogenase to form pristanic acid [198]. Decrease in pristanic acid suggest decrease in expression or activity of these enzyme which are specific to peroxisome.

I also investigated other ethanolamides which act as PPARα agonist to improve peroxisomal functions [199]. PPARα activation leads to NFκB inhibition so, I also checked this *in vitro* to select an appropriate bioactive compound [200]. I used OEA, AEA, PGE2EA at 10μm, 1μm, and 100nM concentration to investigate their anti-inflammatory properties, evident by reduced NFκB activation. Our study suggests that most of these compounds reduce LPS induced activation of NFκB phosphorylation. Among all of them OEA was the most potent in reducing LPS induced NFκB activation via PPAR-α [199].

As reported by other studies, I also observed that OEA ability to reduced inflammation was depended on PPARα. This was confirmed because since our *in vitro* studies showed that PPARα inhibition prior to OEA administration did not reduce NFκB phosphorylation after LPS treatment. But I do not see a similar effect of OEA if PPAR-γ was inhibited. Peroxisomes and mitochondria are related with each other in term of function specially metabolizing fatty acid. They both interact with each other and play a major role in cell metabolism of the different metabolite. As mentioned above, mitochondria and peroxisomes are small organelles ubiquitously present in every cell and are functionally coupled, despite differences in their general physiological roles. The interaction of these two organelles is necessary for optimal cell function and maintain lipid homeostasis. Also, I observed this in our study that PGC1α increased with targeting PPAR-α. It is well known that PGC1α is master regulator of mitochondrial function and biogenesis [201]. Taken together, our finding supports the idea that peroxisomal and mitochondrial activity are co-regulated at the transcriptional level in a PPARα and PGC1α-dependent manner. Since preclinical and clinical studies have suggested an imbalance of lipid homeostasis and lipid metabolism dysfunction. So, another strategy to treat this disease to target mitochondrial function and biogenesis.

2.5 Conclusion:

This study provides support for restoration of lipid profiles associated with improved peroxisome function following OEA treatment, which corresponds with improvements in neurobehavioral symptoms relevant to GWI. These studies also show that OEA treatment leads to a reduction of brain inflammation in our well-characterized mouse model of GWI, a pathology that is highly relevant to the etiology of GWI. These data provide critical support for future translational studies to find an optimal and safe dose of OEA for treating subjects with GWI.

2.6 Graphical summary of our working hypothesis

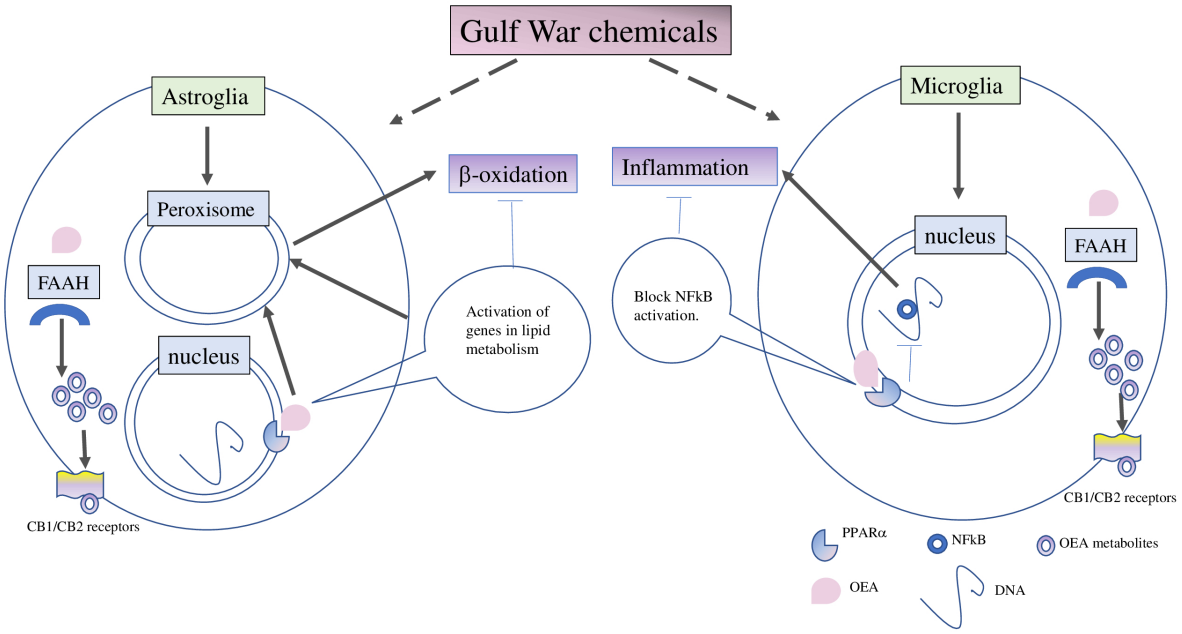

Figure 2.12. OEA reduces brain inflammation in GWI mice. We propose that targeting peroxisome with OEA reduces astroglia activation which corresponds with normalization of peroxisomal lipid metabolism.

Chapter 3: Mitochondrial function and/or biogenesis as a potential target for therapeutics of Gulf War Illness (GWI)

3.1 Introduction

Mitochondria are responsible for the maintenance of cellular bioenergetics and reduction oxidation (redox) balance and also play a critical role in lipid metabolism. Impairment of mitochondrial function can cause homeostatic dysfunction, impeding the normal physiological processes of the cell. Mitochondrial dysfunction can lead to chronic activation of the proinflammatory cellular cascades [202]. As discussed in Chapter I, mitochondrial dysfunction is a consistent feature of GWI and has been suggested in multiple studies as an explanation for the most common symptoms of GWI, which include memory and learning impairments and chronic fatigue [1]. These findings are in line with our previous studies showing a persistent presence of cognitive deficits and fatigue-like behavior over several chronic post-exposure timepoints in our well-characterized mouse model of GWI [78]. Therefore, development of interventions that restore a healthy physiological bioenergetic profile represents a promising and potentially beneficial strategy for altering GWI associated lipid dysfunction and cognitive and behavioral deficits.

Mitochondrial disturbances in patients with GWI are characterized by changes in plasma acylcarnitine levels indicative of disturbances in fatty acid transport or metabolism and bioenergetic processing, such as the inability to recover phosphocreatine levels in muscle after exercise as well as impaired lactate utilization in the brain[22,54,91,203]. Additional evidence for the CNS bioenergetic disturbances in GWI comes from animal studies showing decreases in the Krebs cycle intermediary compounds[54], and downregulation of pathways related to the conversion of pyruvate to lactate and gluconeogenesis. Collectively, these studies suggest that mitochondrial bioenergetic disturbances following exposure to GW chemicals is a critical

aspect of GWI pathogenesis[104–107,204,205]. Mitochondrial bioenergetic disturbances lead to an accumulation of ROS via a decline in complex I activity, which coincides with increased lipid peroxidation followed by increased production of inflammatory cytokine via activation of NFκB [206–208]. We hypothesize that GW chemicals disturb CNS bioenergetics performed by mitochondria which may impair cellular redox balance and promote chronic neuroinflammation. As such, the focus of this current work is to identify interventions that can target the brain bioenergetics and determine the efficacy of such therapies in treating the CNS symptoms and pathology of GWI in a mouse model.

One of the treatment strategies that I tested as part of my thesis work was to supplement mouse diet with the NAD+ precursors, nicotinamide riboside (NR). In the cell, NR is converted to NAD+ by an enzyme nicotinamide riboside kinase (NRK) [209]. Treatment with NR may be a valuable therapeutic approach due to its high bioavailability, minimal toxicity, and evidence of its ability to cross the BBB [210]. In a pilot human study, level of NAD+ rose by 3-fold after a single oral dose of 300mg of NR [210]. NAD+ is a critical component in a plethora of cellular functions performed within mitochondria. NAD+ and its reduced forms, including NADH are crucial in cellular metabolism and energy production [211,212]. NAD+ is used in energy-generating catabolic reactions such as the Krebs cycle, where it is initially reduced to NADH which then serves as an electron rich molecule that take part in OXPHOS ultimately contributing to ATP generation. During OXPHOS, NAD+/NADH only shuttle electrons and they are not consumed during this process. However, NAD+ is actively consumed during the enzymatic processes that are carried out by sirtuins (Sir T), which are deacetylase enzymes that catalyze protein deacylation reactions. Sirtuins are able to bind NAD+, and deacetylation of acetyllysine in cellular protein occurs by nucleophiles reaction via deacetylase [213]. In this deacetylation reaction, nicotinamide and 2'-O-acetyl-ADP-ribose are generated [214]. Sirtuins undergo alternative pathway where NAD + is also used as a substrate to generate ADP-ribosylated

products and nicotinamide via mono-ADP-ribosyl transferase [215]. Nicotinamide can be recycled back to NAD+ by first being converted to nicotinamide mononucleotide by nicotinamide phosphorybosyltransferase (NAMPT) and then eventually to NAD+ by nicotinamide mononucleotide adenylyltransferase (NMNAT)[216]. As NAD+ and NADH are required for Krebs cycle and ETC respectively, an ideal NAD+/NADH ratio is needed for proficient mitochondrial metabolism. Many studies have shown that metabolic disease are influenced by mitochondrial NAD+/NADH ratio [217,218]. Intervention with NR is able to restore NAD+ availability and improve oxidative metabolism, resuting in a significant enhancement of mitochondrial NAD+/NADH ratios [219,220]

Literature suggests that NAD+ increases the expression of the sirtuin protein family (SirT1 and SirT3)[219]. The increased expression of these proteins has the potential to reduce inflammation via NFκB mediated pathways and increase mitochondrial health and biogenesis by PGC-1α dependent pathway[220–222]. Supplementation with NR reduces inflammation and attenuates neuropathological phenotypes through SirT1-mediated deacetylation of the NFκB pathway in animal models of neurological disorders such as alzheimer's Disease[220,223]. Administration of NR decreases oxidative stress via the NAD+/ SirT1 signaling or via increasing autophagy [224,225]. Hence NAD+ is critical for mitochondrial function, health, and biogenesis, as well as in the ETC [226]. As described above, GWI is associated not only with mitochondrial dysfunction but also neuroinflammation and glia activation is a common feature of the chronic CNS pathology of GWI. Others have shown that NR treatment enhances cognitive functioning and reduces neurotoxicity and glial cell activation[220,227]. As such, I believe that by targeting mitochondrial dysfunction with NR, I may be able mitigate neuroinflammation and improve mitochondrial functioning in GWI mice.

While glucose is the primary energy source which fuels the Krebs cycle in the brain, availability of free fatty acids in neurons and their subsequent metabolism fulfills bioenergetic requirements when glucose supply is low or during high neuronal activity [228]. β-oxidation of FFA yields acetyl-CoA molecules for the Krebs cycle to generate ATP [228]. Lipid peroxidation often follows lipid accumulation due to reduced fat oxidation capacity [229]. As a consequence, lipid metabolites may become unavailable to meet neuronal energy demands. As lipid accumulation and peroxidation was observed in our GWI mouse model as well as reduced levels of several compounds from the Krebs cycle[54,65,78], we opted to explore ketogenic diet (KD) as another approach for targeting mitochondrial bioenergetics. This type of diet mimics the metabolic profile of fasting and has provided some promising results when tested as an intervention in animal models of neurological disorders [230,231]. Ketogenic diets generally contain high fat and low carbohydrate content[232]. Prolonged feeding with KD leads to ketosis which increases the ketone bodies specially β-hydroxybutyrate (βHB) in the liver[233–235], which are subsequently used as the source of acetyl-CoA to fuel the Krebs cycle, thereby replacing the need for glycolysis of glucose to generate acetyl-CoA[236]. We therefore also investigated if KD can reduce the CNS pathology in our mouse model of GWI.

Work described below examines how the NAD+ and βHB levels were affected in veterans with GWI and in GWI mice. We also show an impact of NR and KD interventions on these metabolites, markers of mitochondria function and biogenesis as well as glia activation and neuroinflammation in a GWI mouse model.

Hypothesis: Mitochondrial dysfunction is associated with numerous CNS illnesses including GWI. Mitochondria dysfunction in GWI is associated with decreased in bioenergetics specially NAD+ and BHB which in turns effects lipid metabolism. Since there is sufficient data to suggest that certain aspects of mitochondrial specific lipid metabolism are altered in our GWI mouse model and in GWI patients, we hypothesized intervention that increases NAD+ and BHB may lead to potential therapies for this complex and chronic disease.

Specific Aim 1: To determine if therapeutic intervention that increase NAD+ such as NR is beneficial for GWI

Aim 1A: To determine if NR treatment increases bioenergetic along with improves lipid metabolism in mice model.

Aim 1B: To determine if NR treatment increases decreases chronic inflammation as well as neuropathology associated with GWI.

Aim 1C: To identify possible mechanism of action associated to NR treatment in GWI mice model.

Specific Aim 2: To determine if therapeutic intervention that increase BHB such as ketogenic diet is beneficial for GWI

Aim 1A: To determine if KD treatment increases bioenergetic in mice model.

Aim 1B: To determine if NR treatment increases decreases chronic inflammation as well as neuropathology associated with GWI.

Aim 1C: To identify possible mechanism of action associated to NR treatment in GWI mice model.

3.2 Methods:

3.2.1 Human subject:

Recruitment process is previously described in chapter 2. The study was approved by the Institutional Review Board (IRB) at Roskamp Institute. The protocol and procedures were carried out in accordance with the Declaration of Helsink [237]. An IRB-approved informed consent was provided to each potential participant, and a signed consent was obtained from all participants. Six healthy GW-deployed veterans and 12 GWI veterans volunteered in this study. The Kansas GWI criteria were used to diagnose GWI [6]. It is assumed that all the subject were fasting when blood was withdrwan, no data on Diabetes medation were avilable. Diagnostic and recruitment criteria is also explained previously in chapter 1. The Kansas GWI criteria require

that GW veterans show symptoms in at least 3 out of 6 symptom domains (fatigue/sleep problems, somatic pain, neurological/cognitive/mood symptoms, gastrointestinal symptoms, respiratory symptoms, and skin abnormalities). Study participants were excluded if they reported being diagnosed with another medical condition that could explain their chronic health symptoms. Veterans who volunteered for the study were interviewed in person. After the interview blood samples were obtained as described previously. Detailed demographics of the study are provided below in table 3.

Table 3. Demographics of the Gulf War veteran cohort.

	Control (GW veteran)	**GWI**
N total	6	12
Age (Mean ± SEM)	59.3 ± 2.6	56.1 ± 1.6
Male (%)	100	100
Ethnicity		
Caucasian	5(50%)	8(66.6%)
African American	1(10%)	2(16.7%)
Hispanic	0(0%)	2(16.7%)
Asian	0(0%)	0(0%)

3.2.2: Animal Handling:

All procedures on mice were approved by the Roskamp Institute's Institutional Animal Care and Use Committee and were conducted in compliance with the Office of Laboratory Animal Welfare and Laboratory Animal Care guidelines performed as previously described

[53,157]. Mice were maintained with a 12h light/dark cycle in a temperature-controlled environment (21± 2 ℃). Male C57BL/6 mice (3 months of age, weight 25 g ± 0.7 SD) were co-administered 0.7 mg/kg of PB (Fisher Scientific, Hanover Park, IL) with 200 mg/kg of PER (Sigma Aldrich, St. Louis, MO) in a single 50µl intraperitoneal injection in dimethyl sulfoxide (DMSO) (Sigma Adrich, St. Louis, MO) or DMSO alone (*as* control) daily for 10 consecutive days.

After 6 months post-exposure to GW chemicals, a treatment regimine was initiated where mice were either on normal chow diet (Teklad rodent diet , Envigo, Madison, # 2018) that comprised of 58.2% carbohydrate, 10.6% fat and 19% protein by calorie was used as regular chowfed with NR (100µg/kg) in their diet (MedKoo Biosciences, Research Triangle Park, North Carolina # 329479) or fed with NR in the same diet. Mice were separated into 4 groups; one cohort receive NR treatment in their diet for two months. Mice were divided into 4 groups: control mice +regular diet, control mice+NR, GWI mice+regular diet and GWI+NR. Mice were euthanized 2 months after the NR treatment; a timeline of the study procedures is provided as Figure 3.1A. All animals were randomized to the various groups and were not deprived of food before eutheneisa. Average food intake was 5.32 ± 0.09 g/day/mouse, and the average consumption of diets was 0.09 ± 0.015 g/day/mouse. Randomization was performed in all neuro behavioural experiment, experimenter were blinded GW treatment but not diet. Mice were not deprived of food before euthenesia.

For another cohort, 6 months after GW chemical exposure, mice were fed with either the KD or normal chow diet listed above. Mice were divided into 4 groups: control mice + normal diet, control mice +KD, GWI mice+ normal diet and GWI mice+KD. The Ketogenic Diet (Envigo, Madison, # TD.96355) was comprised of 0.5% carbohydrate, 67% fat and 13.4% protein by calorie. Mice were euthanized approximately 1.5 months after the KD treatment; a timeline of the study procedures is provided as Figure 3.1B. All animals were randomized to the various groups and were not deprived of food before eutheneisa.

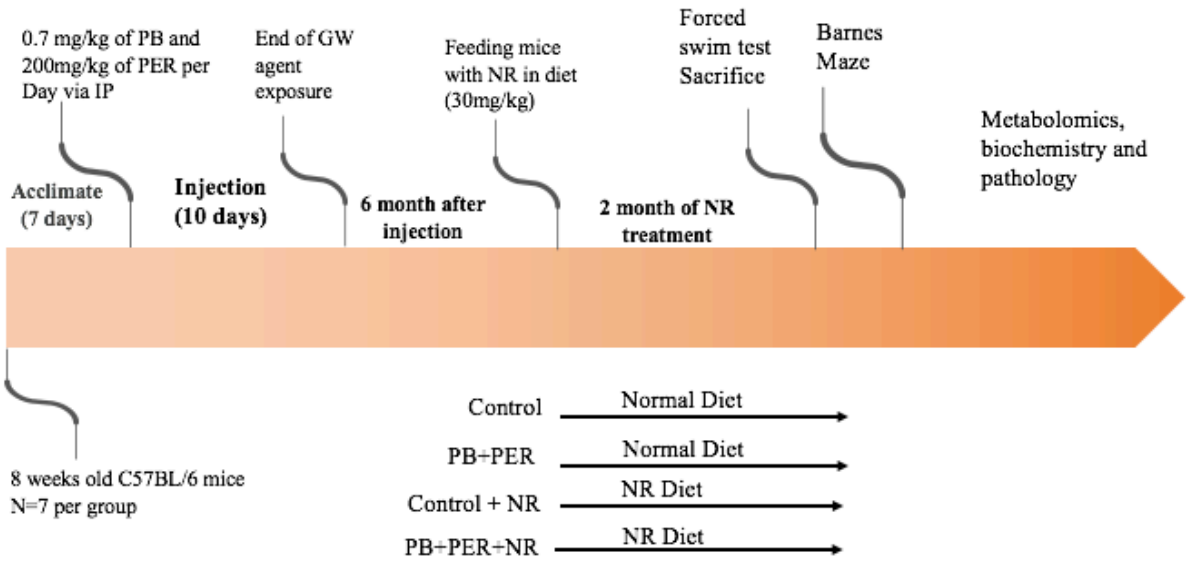

Figure 3.1A: Timeline of NR study design

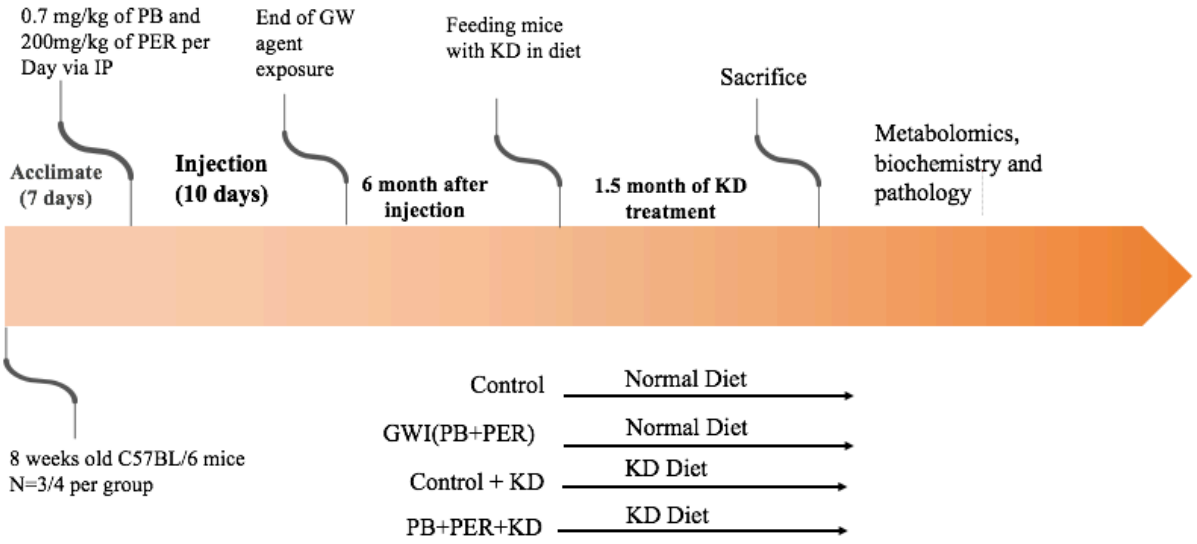

Figure 3.1B: Timeline of KD study design

Forced swim test

We performed FST as described in chapter 2 and as described elsewhere[78], Since our previous work showed that fatigue-type behavior emerges after a few minutes of swimming during the FST, we split the entire duration of FST into two halves, first half (2-4min) and second half (4-6min). The difference between the two halves is denoted as delta immobile time (Δ). Δ immobile time = immobile time[second half-first half].

3.2.3 Sample preparation

Mice were exsanguinated via cardiac puncture using an 18-gauge wide-bore needle to prevent hemolysis of RBC during blood collection. Blood samples were collected into 1.5ml Eppendorf tubes containing 10 units of EDTA to a final concentration of 1x. Samples were immediately centrifuged at 3000 x g for 5 min, and the plasma was transferred to a new 1.5 ml Eppendorf tube and snap frozen in liquid nitrogen. Plasma samples were stored at -80˚C until further biochemical studies were performed. Subsequently, all animals were perfused with PBS, and right hemispheres were immediately frozen in liquid nitrogen and transferred to a -80˚C freezer until further use. Using a dounce homogenizer, brains were homogenized in chilled lysis buffer containing a protease inhibitor cocktail (Roche, Indianapolis, IN) and phosphatase inhibitor (Pierce, Grand Island, NY) cocktails. The total protein content of each sample was determined by the bicinchoninic acid assay (BCA assay, Pierce, Grand Island, NY).

3.2.4 Western Blot

Western blotting was performed as described in previous chapter. List of primary antibodies used is provided in the table below. Horseradish peroxidase–conjugated appropriate secondary antibodies and loading control anti–β-actin antibody was obtained from Cell Signaling, Danvers, MA. The blots were analyzed as described previously.

Table 4A: List of Antibodies used for Western Blot analysis:

Antibody used	Dilution	Company
SirT1	1:1000	Cell Signaling
Sir T3	1:1000	Cell signaling
Phospho p65 (NF-κB subunit)	1:1000	Cell signaling
Total p65(NF-κB subunit)	1:1000	Cell signaling
Phospho STAT3(Signal transducer and activator of transcription 3)	1:1000	Cell signaling
Total STAT3	1:1000	Cell signaling
Uncoupling protein 2(UCP-2)	1:800	Cell signaling
PGC-1 alpha	1:800	Cell signaling
Cytochrome C	1:1000	Cell signaling
Acetylated lysine	1:500	Cell signaling
Actin	1:5000	Cell signaling

3.2.5 Mitochondrial isolation and protein analysis

Mitochondria were isolated by a commercially available kit from Miltenyl Biotech (Gladbach, Germany). After tissue lysis mitochondria was isolated according to manufacture protocol. Briefly, mitochondria was magnetically labelled with translocase of the outer membrane (anti-TOM-2) antibody; this antibody recognizes mitochondrial surface proteins.

These samples were then allowed to pass through a column under the magnetic field of MidiMACS (Miltenyl Biotech, Gladbach, Germany). After several washes, only magnetically labelled mitochondria remain in the column which was finally eluted to obtain functional mitochondria. These mitochondrial preps were used in Western Blots against different mitochondrial proteins involved in mitochondria biogenesis, such as PGC-1α (1:1000, Cell Signaling, Danvers, MA) and uncoupling protein 2 (UPC-2) (1:1000, Cell signaling, Danvers, MA), whereas cytochrome C (1:1000, Cell Signaling, Danvers, MA) was used for normalization. Mitochondrial biogenesis was measured by expression of PGC-1α in mitochondrial fraction[238].

3.2.6 Immunoprecipitation of SirT1, PGC-1α and p65

Sirtuin 1 is an NAD+ dependent deacetylase which regulates metabolism and inflammation[239]. To determine if SirT1 interacts and deacetylates PGC-1α and p65 (NFκB subunit), we performed pull down experiments. Briefly, using a dounce homogenizer, left hemisphere was homogenized in 1ml of mPER (Thermo Fisher Scientific, Waltham, MA) containing a protease inhibitor cocktail (Thermo Fisher Scientific, Waltham, MA). 200µl of PBS was added in 100µl brain homogenate and then centrifuged at 21 x g, 4°C, 15 min. Supernatant was collected and combined with 500µl methanol and again centrifuged at 21 x g 4°C, 15 min. 200µl Triethylammonium bicarbonate (TEAB) buffer was added to pellet (cytosolic fraction). Primary antibody (p65 or Sir T1) was added at 1:100 to the cytosolic fraction and incubated with gentle rocking overnight at 4°C. This antibody complex was incubated for 20 min at room temperature with pre-washed magnetic bead pellet (Cell Signaling, Danvers, MA). Beads were pelleted with a magnetic separation rack (Cell Signaling, Danvers, MA). Pellet was washed several times before adding 30µl of 3X SDS sample buffer. Samples were then boiled for 5 minutes, beads were pelleted and the collected supernatant

underwent SDS-PAGE analysis. Proteins were transfer on a PVDF membrane and probed with primary antibody. HRP-conjugatef secondary antibody was used to detect protein of interest. List of antibodies used is provided in the table below

Table 4B: List of Antibodies used for Western Blot analysis:

Antibody used	Dilution	Company
SirT1	1:1000	Cell Signaling
Acetylated p65 (K310)	1:1000	Cell signaling
p65 (NF-κB subunit)	1:1000	Cell signaling
Acetylated-Lysine Antibody	1:500	Cell signaling
PGC-1 alpha	1:1000	Cell signaling

3.2.7 Enzyme-Linked Immunosorbent Assay

To assess the impact of NR diet on inflammatory pathways, we also examined C-C chemokine receptor type 2 (CCR2) and its ligand, CCL2, as well as fractalkine receptor (CX3CR1). Mouse CX3CR1, CCL2 and CCR2 Enzyme-Linked Immunosorbent Assay (ELISA) kits from Lifespan Biosciences were used for the detection of these proteins in the samples. The total protein content of each sample was determined by the bicinchoninic acid assay (BCA assay, Thermo Fisher Scientific, Waltham, MA). These procedures were performed following the manufacturer's instructions. Approximately 1ml of sample diluent was added to the lyophilized protein provided by the manufacturer and allowed to incubate for 10 min with

gentle agitation, and then serial dilutions were performed following the manufacturer's instructions. Sample at 1:4 dilution and standard were added to the capture antibody-coated 96-well plate and then incubated for 90 min at 37°C. Subsequently, biotinylated detection antibody was added to each well and gently agitated to ensure thorough mixing. The ELISA plate was incubated again for 1 hour at 37°C followed by washing, and then HRP-conjugated antibody was added to each well followed by a 30-min incubation at 37°C. Tetramethylbenzidine (TMB) Substrate solution was added to each well and incubated for 15 min, and the reaction was stopped by adding the stop solution. The optical density (OD 450 nm) of each well was then immediately determined using a microplate reader. This procedure was followed for all CX3CR1, CCL2 and CCR2 ELISAs. Intra-Assay: CV<10.6% Inter-Assay: CV<12.6% for all the ELISA. There was no reported cross reactivity with other proteins for the primary antibody used in these kits.

3.2.8 Cytokine Assay

We examined pro-inflammatory cytokine levels, which included IFN-γ, IL-1 β, IL-10, IL-6, and TNF-α, were quantified using commercially available ELISA kits. Lifspan Biosciences (Seattle, WA) ELISA kits were used to quantify IFN-γ (LS-F5065), IL-10 (LS-F9770) and IL-6 (LS-F2478) (Lifspan Biosciences, Seattle, WA). IL-1β and TNF-α (KMC0011 and BMS607-3) were quantified by using commercial ELISA kits (Thermo Fisher Scientific, Waltham, MA). All procedures were performed as per the manufacturer's instructions. Cytokine concentrations were normalized against the total protein content determined by BCA. Results were then expressed as a percentage to control. There was no reported cross-reactivity with other proteins for the primary antibody used in these kits. Intra-Assay: CV<10.6% Inter-Assay: CV<12.6% for all the ELISAs. There was no reported cross-reactivity with other proteins for the primary antibody used in these kits.

3.2.9 Multiplex Cytokine assay

Selected cytokine levels in the plasma and brain were analyzed using Meso Scale Discovery (MSD) 96-Well MULTI-SPOT®Ultra-Sensitive V-PLEX Proinflammatory Panel 1 Mouse Kit, using electrochemiluminescence detection on an MSD Sector Imager™ 6000 with Discovery Workbench software (version 3.0.18) (MSD®, Gaithersburg). Cytokines were measured using the TH1/TH2 8-plex kit, which included 8 markers: IFN-γ, IL-1β, IL-2, IL-4, IL-5, IL-10, IL-13 and TNF-α. All assays were performed according to manufacturer's instructions in duplicates. Plasma samples were diluted 1:2 and added to the plate which contained the capture antibody immobilized on a working electrode. Following incubation for 1 hour, SULFO_TAG labeled detection antibodies were added to the wells. Finally, MSD buffer was added which developed electrochemiluminescence, and the plate was loaded into an MSD instrument for reading. Data were acquired using a SECTOR S 6000 plate reader (MSD). Results were then expressed as the percentage to control.

3.2.10 Thiobarbituric Acid Reactive Substance assay

Plasma and brain levels of malondialdehyde (MDA) were measured using a Thiobarbituric Acid Reactive Substance (TBARS) formed during the reaction of MDA with thiobarbituric acid. Oxidative stress in the cellular environment results in the formation of highly reactive and unstable lipid hydroperoxides. TBARS are formed as a byproduct of lipid peroxidation (i.e. as degradation products of fats) which can be detected by the TBARS assay. Levels of MDA in brain homogenates were measured using a TBARS Assay Kit (Cayman Chemical, Ann Arbor #10009055) as per the manufacturer's protocol. At boiling temperature, oxidized lipids produce MDA which can be measured calorimetrically at 530–540 nm.

3.2.11 β-Hydroxybutyrate (β-HB) assay

β-Hydroxybutyrate are ketone bodies generated following complete beta-oxidation of fat and, they are expected to be generated following ketogenic diet given the high fat content. We examined β-HB levels in the brain, liver and plasma were determined by using commercially available kits as per manufacture's instruction (BioVision, San Francisco#K632). Brain and liver concentrations were normalized to total protein content determined by BCA.

3.2.12 Nicotinamide adenine dinucleotide (NAD+) assay

Nicotinamide adenine dinucleotide (NAD+) is a co-enzyme and is involved in redox reactions. As a result of electron transfer, NAD+ is reduced to NADH, and NADH is oxidized to NAD+ forms. NAD+ levels were measured using a commercially available quantitation kit (Cloud Clone, Houston# CEG409Ge). Briefly, NAD+ were extracted by using extraction buffer supplied with the kit. The amount of NAD+ present in the samples were determined by NAD cycling enzyme. Brain NAD+ levels were normalized against total protein content determined by BCA.

3.2.13 Acylcarnitine analyses

Acylcarnitine profiling was performed for the biochemical screening of disorders of fatty acid oxidation (FAO) and in some metabolic disorders. Acylcarnitine analysis is also a process that is dependent on positive identification of biomarkers through mass spectrometry. Aclycarnitine was extracted as described previously[54]. Briefly, 5 µl of labeled internal standard mix (Nsk-b-1, Cambridge isotope laboratories, MA, USA) were spiked into 100µl of brain homogenate. Carnitine was extracted by adding 1000µl of 25% methanol in acetonitrile (ACN) followed by centrifugation at 20,000 x g for 20 min at 4 °C. Extracts were dried and then resuspended in 100µl of mobile phase A and centrifuged for 5 min at 10,000 x g. Supernatants were subjected to LC/MS using a 2.1mm ID x 50mm Kinetex HILIC column containing 1.7 µm particles (Phenomenex, Torrance, CA, USA). A gradient was run from 95% solvent A (ACN:

water:100mM ammonium formate,90:5:5 v/v) in 5% solvent B (ACN: water:100mM ammonium formate,50:45:5 v/v) to 70% B in 10 min with a 10 min hold at the final conditions. The flow rate was 250µl/min with the column temperature at 40°C. Data was acquired by full scan MS in positive and negative modes with a mass range of 130-2000 m/z (13 uscans/sec, spray voltage: 1500V, resolution: 17,500, max inject time: 200msec).

Tracefinder™ software (Thermo Fisher Scientific, Waltham, MA) was used for peak identification and integration for acylacrnitine species in each run. Target compound lists of expected analytes for each chosen acylcarnitine class were used to find peaks of interest with ion windows of 5 ppm mass accuracy for the expected ions.

Table 5: Gradient Program for acylcarnitine

Time	**% Solvent A**	**% Solvent B**	**Flow Rate (ml/min)**
0.10	80	20	0.250
5.00	88	22	0.250
10.00	60	40	0.250
13.00	40	60	0.250
15.00	20	80	0.250
15.01	1	99	0.250
20.00	1	99	0.250
20.01	80	20	0.250
25.00	80	20	0.250

3.2.13 Statistical analyses

For the human study, the Student's t-test was used to examine the group differences between GWI case and control. Neuropathological, Western Blot and ELISA data for protein markers described above were analyzed using ANOVA to determine statistical significance. Normally distributed data were analyzed using parametric tests; otherwise non-parametric tests were used. For multiple groups, we used one-way analysis of variance (ANOVA) followed by the Tukey *post-hoc* test. A p value < 0.05 was considered statistically significant. These analyses were performed using GraphPad Prism7 (San Diego, CA, USA), and data were expressed as means ± standard errors. All graphs were generated using GraphPad Prism7 (San Diego, CA,). For lipidomics study after data analysis using MLM, Fisher's least significant difference (LSD) correction and the Benjamini–Hochberg procedure (B-H) were used for multiple-test correction and control of false discovery rate (FDR) for all species between all groups. All data were analyzed using SPSS version 22.0.0 (IBM Corporation, Armonk, NY). B-H ($\alpha = 0.05$) was calculated using Excel. Since human NAD+ data were not normally distributed, Kolmogorov-Smirnov test (K-S test) were performed on them to check if they were statically significant.

3.3 Result

3.3.1 GWI is associated with low NAD+ and β-HB levels in the plasma

We examined blood levels of mitochondria specific metabolties NAD+ and β-HB in a pilot cross-sectional study of age- and gender-matched healthy GW veterans (n = 6) and those with GWI (n = 12). These studies showed that levels of NAD+ (K-S test, $p = 0.002$, Figure 3.2A) and β-HB (t-test $_{(df= 16)} = 2.75$, $p = 0.013$, Figure 3.2B) were significantly decreased in veterans with GWI compared to controls.

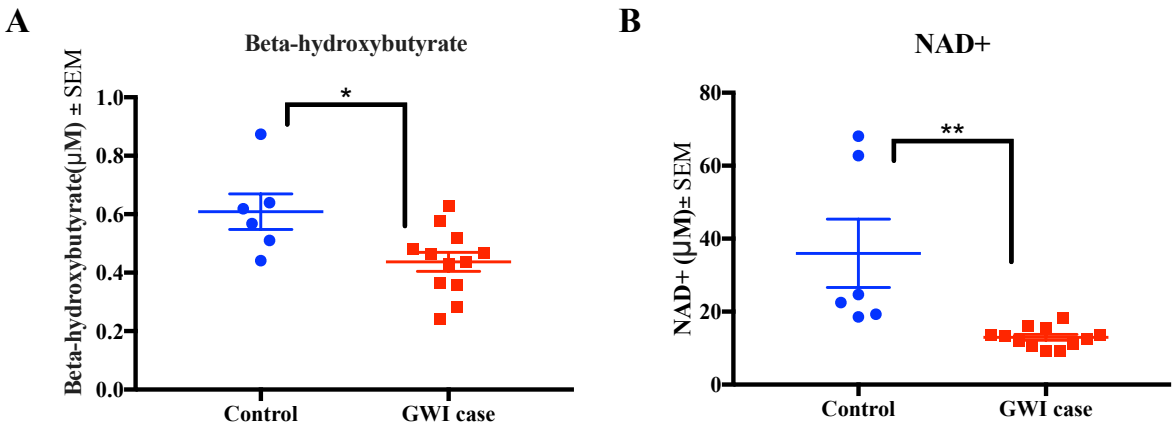

Figure 3.2. Plasma NAD⁺ and β-HB levels in veterans with GWI compared to GW control veterans. Mean ± SEM (n=6 for controls and n=12 for GWI). (A) NAD⁺ and (B) β-HB are altered in plasma from veterans with GWI. * $p \leq 0.05$,**<0.001.

3.3.2 Nicotinamide riboside improves fatigue like behavior in GWI mice

To determine whether NR corrected fatigue-like behavior in GWI mice, we performed the FST at 2-months post-treatment with NR. At 2-months post-treatment (8-months post-exposure), there was no change in total immobile time ($F_{(3,26)} = 1.32$, $p = 0.28$, Figure 3.3A) and frequency of immobility ($F_{(3,22)} = 3.62$, $p = 0.98$, Figure 3.3A) between all experimental groups. Also, the mean velocity did not differ between groups (Figure 3.3A). There were signficiant differences between the groups when Δ immobile time between first and second half of the FST was analyzed ($F_{(3,22)} = 4.2$, $p = 0.01$;Figure 3.3B). *Post-hoc* analysis showed a significant difference between GWI and control mice as well GWI mice treated with NR compared to GWI treated with control diet ($p = 0.05$). NR treatment has no effect on memory and learning as measured by Barnes Maze(Figure 3.3).

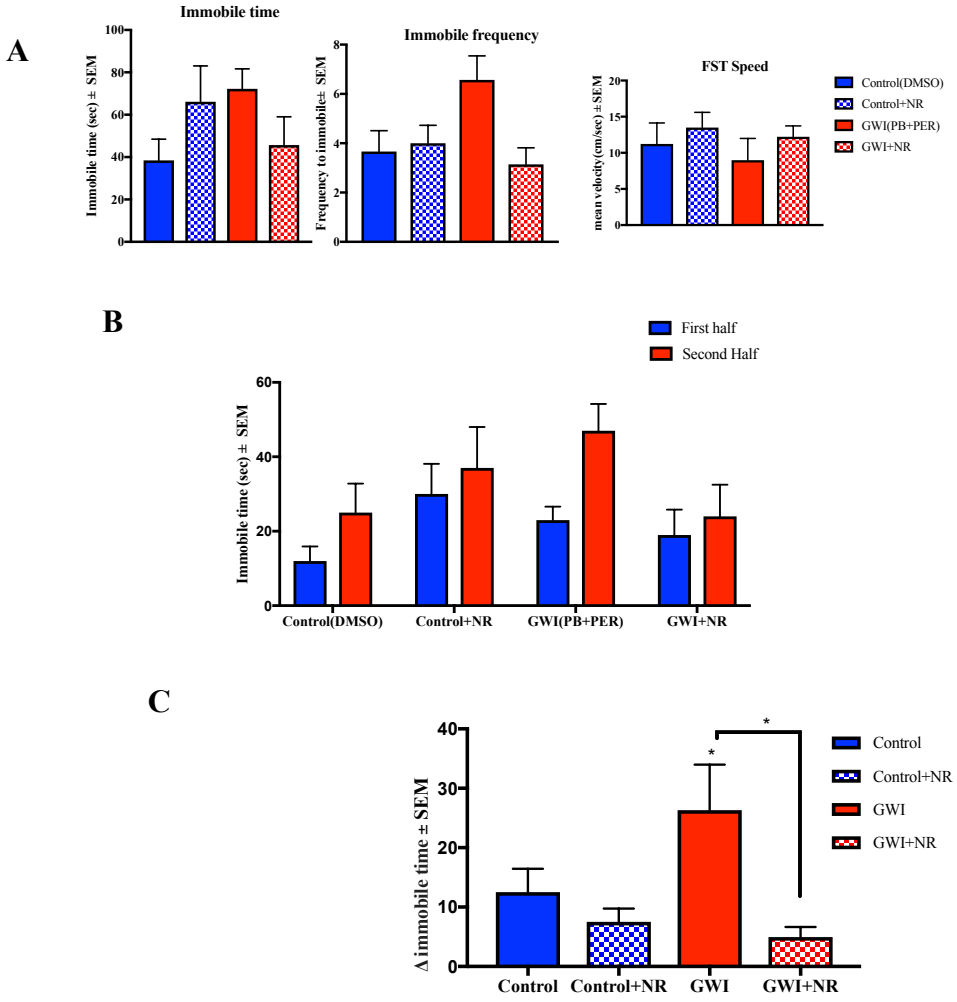

Figure 3.3: Forced swim test data showed NR treatment reduces fatigue-like behavior in GWI mice. Mean ± SEM of control (n = 8), GWI mice (n = 8), control+NR (n = 7) and GWI+NR (n = 8). (A) two months after NR treatment (7-months post-exposure to GW chemicals), the frequency and immobile time had increasing trend in GWI mice compared to controls and was reduced in NR treated GWI. (B) Comparing two halves showed GWI performed worst among all group in second half which was improved by NR treatment. (C) Δ immobile time representing difference between two halves across all groups where GWI had elevated Δ immobile time than control mice and lower in GWI treated with NR diet compare to GWI mice. ANOVA with post-hoc tukey * $p \leq 0.05$.

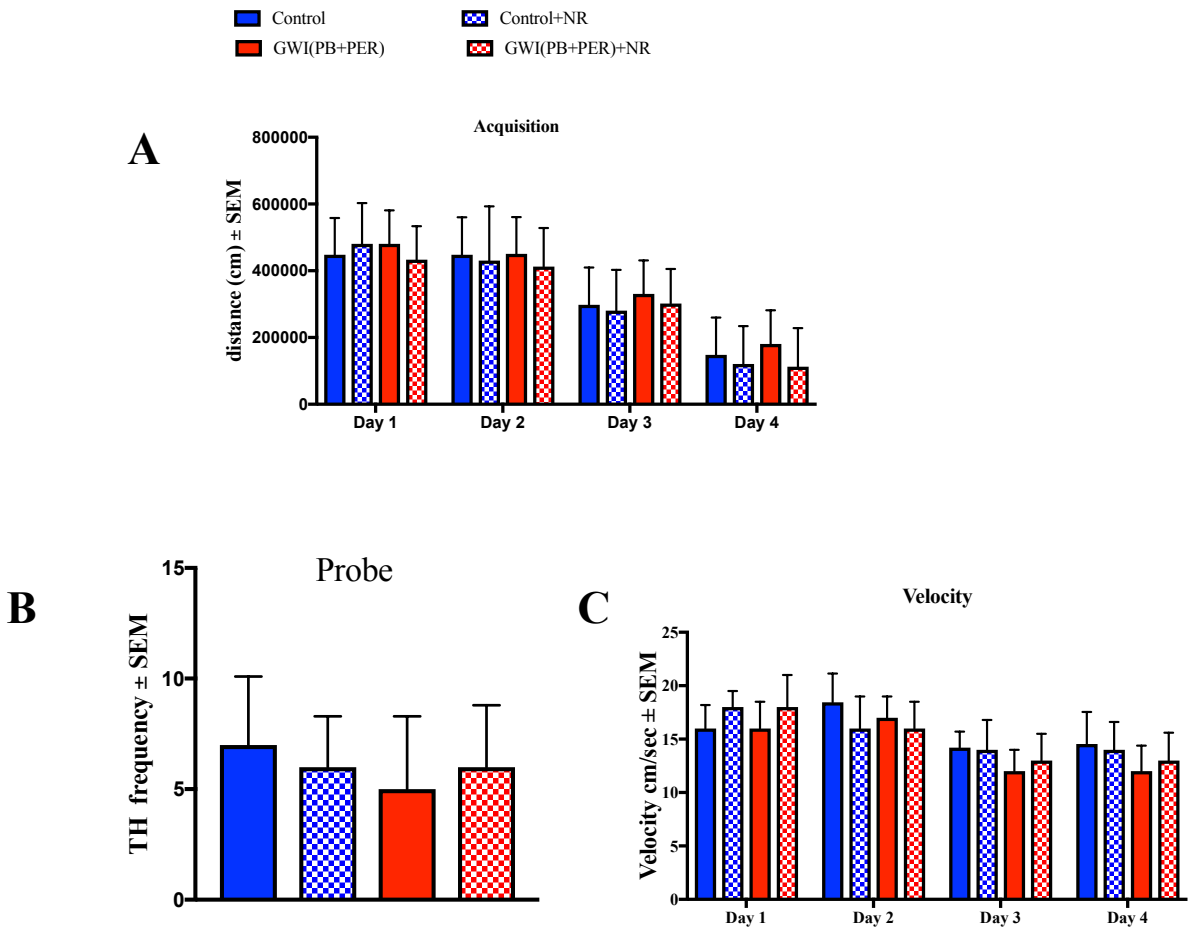

Figure 3.4: NR treatment showed no effect on learning and memory behavior in GWI mice. Mean ± SEM of control (n = 8), GWI mice (n = 8), control+NR (n=8) and GWI+NR (n=8). (A) Two months after NR treatment (8-months post-exposure to GW chemicals), acquisition trials were conducted to train mice to escape into the Target hole (TH). There was no significant difference between any group on total distance to target hole indicative of learning. (B) For the probe trials, conducted at 5-day of BM (8-months post-exposure), there was no significant difference in the frequency of the visits to the TH across all groups. *ANOVA with post-hoc tukey* * $p \leq 0.05$.

3.3.3 Nicotinamide riboside treatment helps recover normal NAD+ levels in GWI mice

There was a significant effect of GWI status and NR treatment on NAD+ levels in the brain ($F_{(3,12)} = 7.33$, $p = 0.004$) and plasma ($F_{(3,12)} = 12.33$, $p = 0.0005$). In brain, *post-hoc* analyses showed no differences in NAD+ levels between control and GWI mice on regular diet ($p > 0.05$), whereas NR treatment increased NAD+ levels in both control ($P < 0.05$) and GWI

mice ($p < 0.05$). In plasma, *post-hoc* analysis showed that NAD+ levels were significantly decreased in GWI mice compared to control mice ($p < 0.05$) and NR treatment significantly increased NAD+ levels in GWI mice ($p < 0.01$; Figure 3.4). There was no change in the brain β-HB levels between all four groups ($F_{(3,12)} = 1.83$, $p = 0.4$). However, we do observe significant differences in the liver β-HB levels across all four study groups ($F_{(3,12)} = 7.83$, $p = 0.004$) with *post-hoc* analysis showing that statistical significance was limited to GWI compared to control mice, and there was no affect of NR treatment on these levels ($p > 0.05$; Figure 3.4). NR treated mice showed decresing trends for weight in both GWI and control mice (Figure 3.5C).

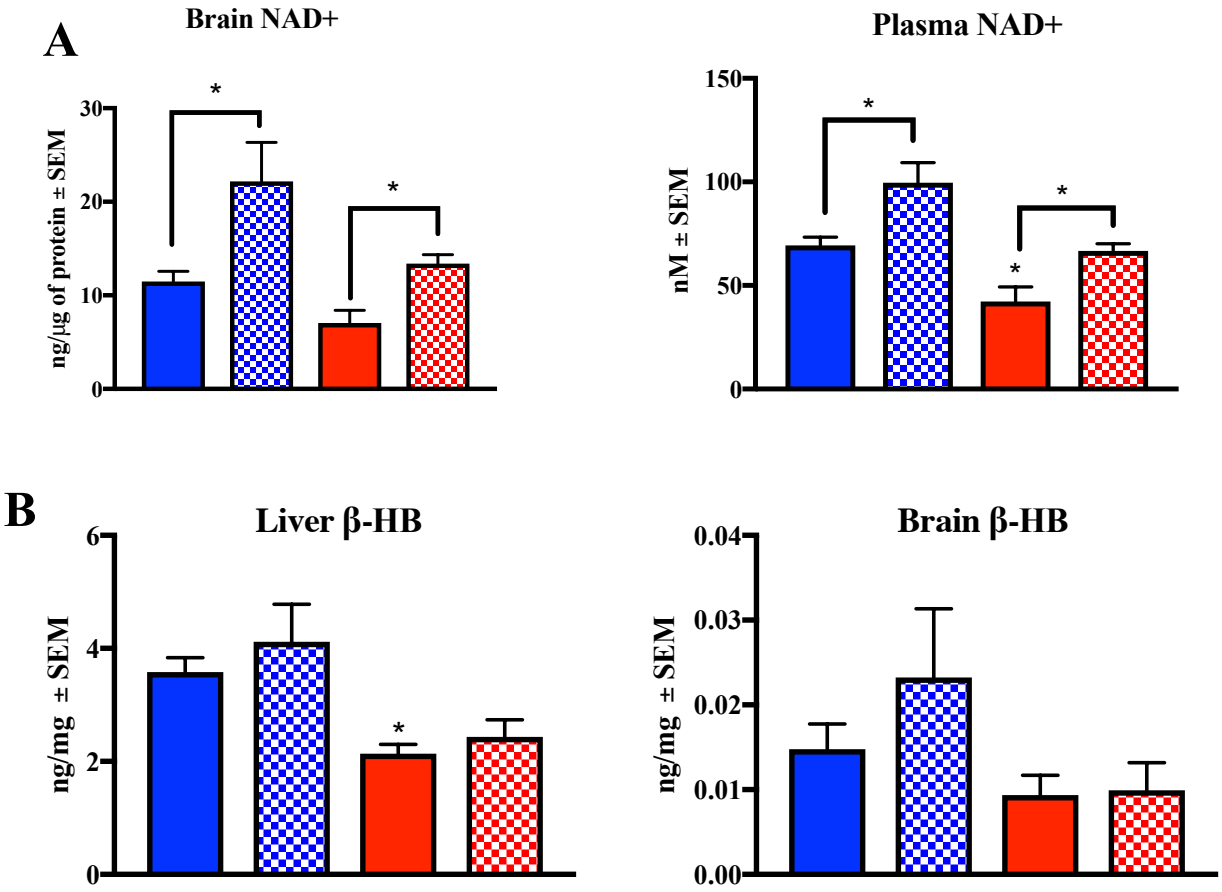

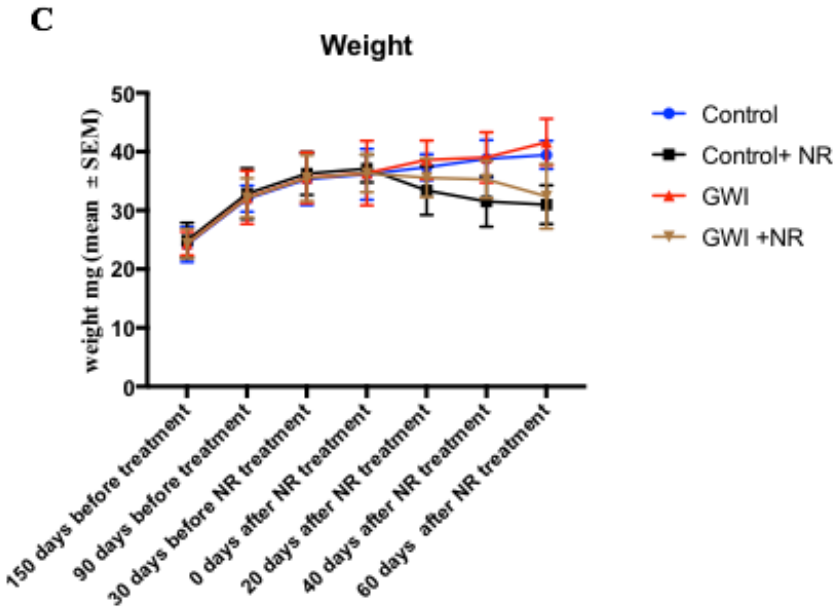

Figure 3.5: Effects of NR supplementation on the NAD+ and β-HB concentration. Mean ± SEM (n = 6 per group). (A)Brain and plasma NAD+ levels across all 4 groups.NAD+ level was decreased in both brain and plasma of GWI. Intervention with NR increases increases NAD+ level in GWI and control. (B) Liver β-HB levels were decreased in GWI mice compared to and NR treatment failed to recover β-HB level in the liver. There were no differences between the experimental groups for brain β-HB levels. Weight change across all 4 groups(C). *ANOVA with post-hoc tukey* * $p \leq 0.05$.

3.3.4 Nicotinamide riboside increases PGC-1α, UCP-2 and SirT3 activity associated with mitochondrial biogenesis in control and GWI mice

PGC-1α is not just a master regulator of mitochondrial biogenesis but also regulates UCP-2 [240]. Uncoupling protein 2 is a mitochondrial inner membrane protein that reduces mitochondria-derived ROS generated by mitochondrial respiration. There was a significant elevation of UCP-2 in the brain across GWI and NR treatment groups ($F_{(3,8)} = 13.068$, $p = 0.01$; Figure 3.5A), while *post-hoc* analysis showed no change in UCP 2 expression between control and GWI mice on regular diet ($p > 0.05$), NR treatment increased UCP-2 expression in both control ($p < 0.05$) and GWI mice ($p < 0.05$; Figure 3.5). Levels of PGC-1α were elevated in the brain following NR treatment ($F_{(3,9)} = 0.14$, $p = 0.009$; Figure 3.5B) and while *post-hoc* analysis

showed no change in PGC-1α expression in GWI compared to control ($p > 0.05$), PGC-1α protein levels were increased by NR treatment in both control ($p < 0.01$) and GWI mice ($p < 0.01$; Figure 3.5B). We further examined acetylated lysine residue of PGC-1α, which was used as a surrogate for SirT3 activity. Immunoprecipitated PGC-1α from mitochondrial fraction were examined for lysine acetylation. I observed a significant impact of NR and GWI status on acetylated PGC-1α levels across all groups ($F_{(3,9)} = 7.14$, $p = 0.001$; Figure 3.5C).The *post-hoc* analyses showed a significant increase in acetylated PGC-1α levels in GWI compared to control mice ($p < 0.05$) which was significantly decreased in GWI mice treated with NR ($p < 0.05$,Figure 3.5C).

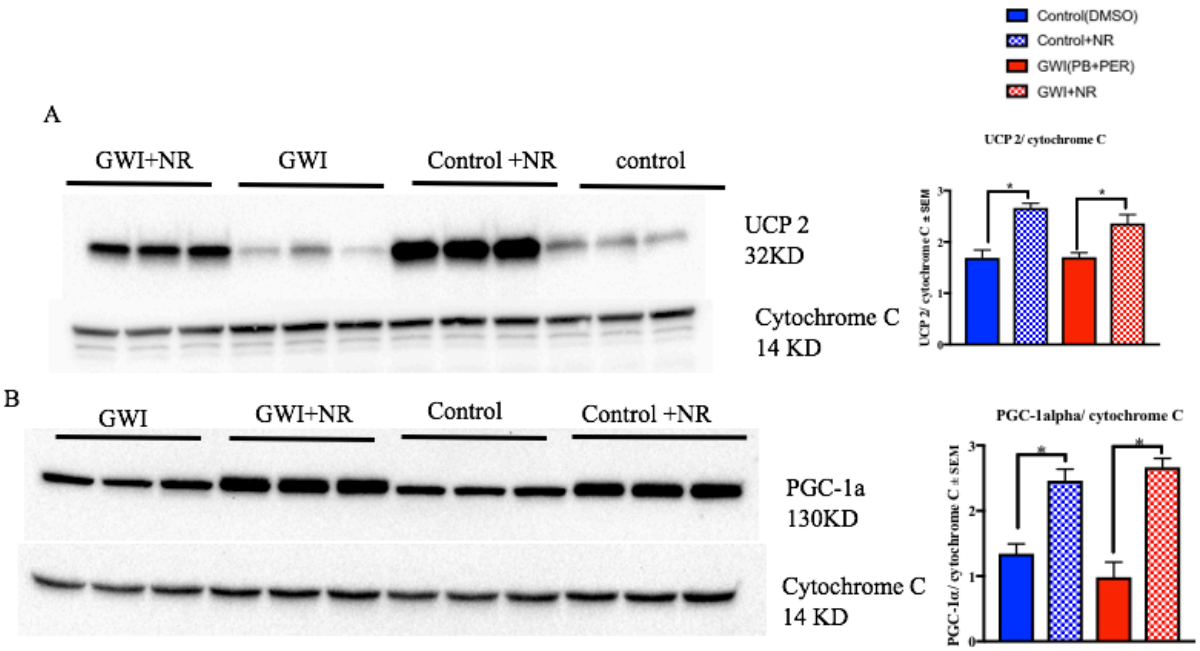

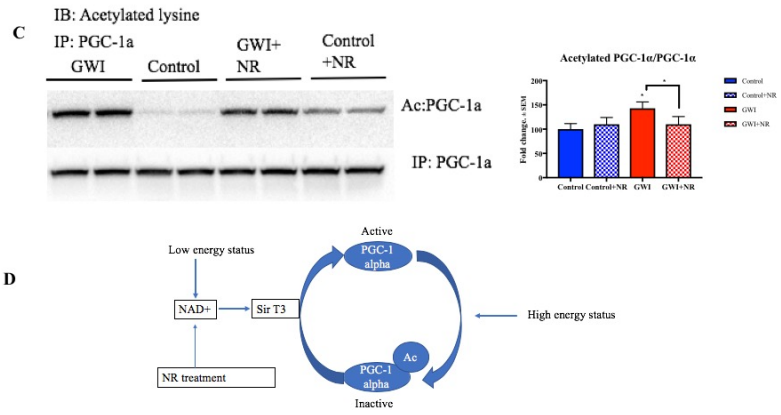

Figure 3.6: Representative images of UCP 2 and PGC-1alpha Western blot of whole brain mitochondria. Mean ± SEM (shown as arbitrary units, n = 6 per group). (A) NR treatment increased UPC-2 levels in both GWI and control mice compared to those on regular diet within respective groups. (B) Levels of PGC-1α were elevated in NR-treated GWI and control mice compared to their respective groups on normal diet. (C) Acetylation assays were performed, PGC-1α immunoprecipitation showed increased acetylated PGC-1α in GWI mice, NR treatment increased deacetylated PGC-1α in GWI mice. (D) Regulation of PGC-1α by acetylation. ANOVA with post-hoc tukey * $p \leq 0.01$.

3.3.5 Nicotinamide riboside treatment elevates SirT1 and SirT3 expression

Sirtuins are a family of proteins that use NAD+ for deacetylation reactions[241]. I observed a significant impact of NR and GWI status on SirT1 protein levels across all groups ($F_{(3,20)} = 37.48$, $p = 0.001$; Figure 3.6) and *post-hoc* analyses showed significant decreases in SirT1 levels in GWI compared to control mice ($p < 0.05$) which was significantly increased in GWI mice treated with NR ($p < 0.05$; Figure 3.6). We also observed change in SirT3 levels across all groups ($F_{(3,12)} = 5.48$, $p = 0.001$) with *post-hoc* analyses showing that while there were no differences between GWI and control mice for SirT3 levels ($p > 0.05$), NR treatment increased SirT3 levels by 4-fold in both control ($p < 0.001$) and GWI mice ($p < 0.001$; Figure 3.6).

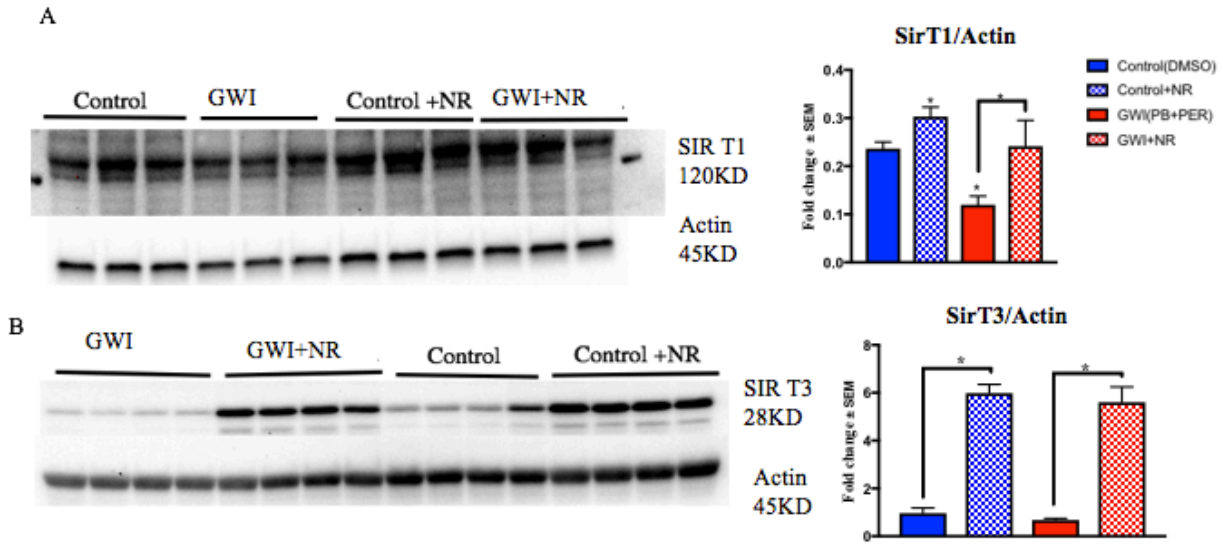

Figure 3.7: Sirtuin 1 and 3 (targets of NR) changes in GWI mice. Mean ± SEM (arbitrary value n = 6 per group) (A-B)Western blot analysis demonstrates decline in Sir T1 in GWI and no change in SirT3 levels between control and GWI. The expression of SirT1 and SirT3 were upregulated by NR treatment on both control and GWI. *ANOVA with post-hoc tukey* * $p \leq 0.001$

3.3.6 SirT1 directly interacts with p65 and deacetylated p65

Increased expression of SirT1 reduces acetylation of p65 (NFκB subunit). Acetylation of p65 leads to phosphorylation of p65, subsequently leads to activation NF-κB. Following immunoprecipitation of SirT1, immunoblotting of this percipipate showed significant group differences in SirT1 interactions with p65 across GWI and NR treatment groups ($F_{(3,12)} = 8.068$, $p = 0.0026$; Figure 3.7A). *Post-hoc* analyses showed that this interaction was significantly decreased in GWI mice as compared to control mice ($p < 0.05$) and this interaction was partially restored by NR treatment in GWI mice compared to GWI mice on normal diet ($p < 0.05$). This interaction of Sir T1 and p65 can lead to deacetylation of p65. Examination of acetylated lysine at residue 310 of p65 subunit showed that significant group differences ($F_{(3,12)} = 5.068$, $p = 0.01$; Figure 3.7B) and *post-hoc* analyses showed that GWI mice had a significant increase in acetylated lysine compared to control mice ($p < 0.05$). In addition, NR treatment

significantly reduced p65 acetylation at this lysine residue in GWI mice compared to nontreated GWI mice ($p < 0.05$) and in NR treated control mice compared to control mice on normal diet ($p < 0.05$).

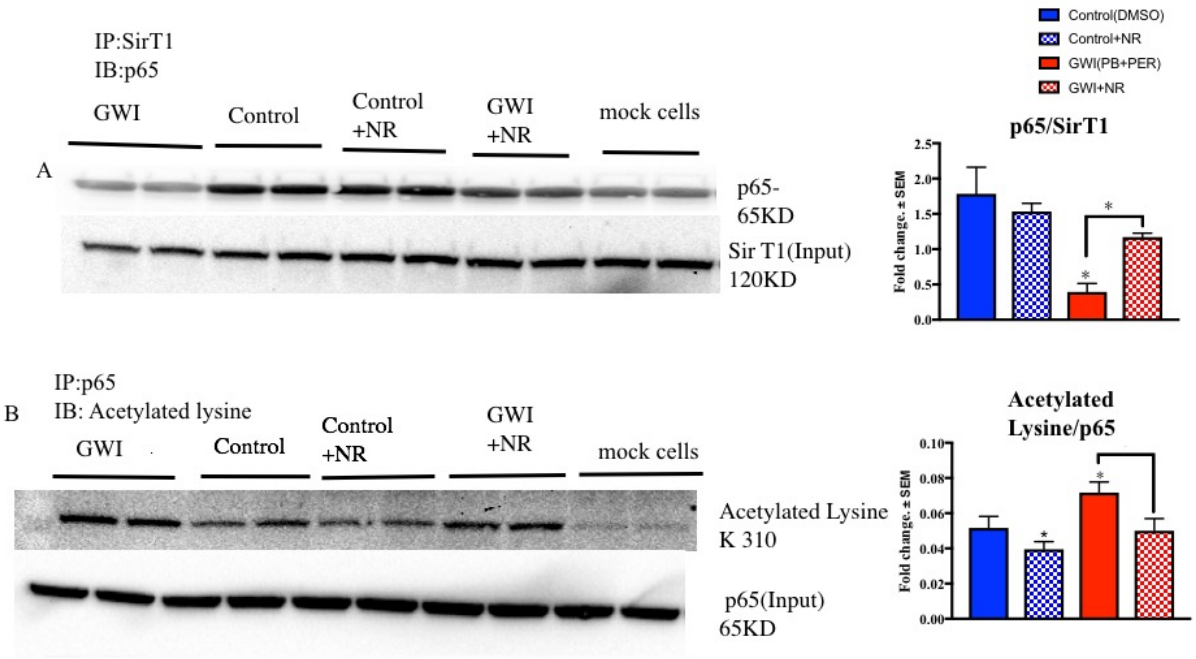

Figure 3.8: SirT1 deacetylates p65 and inactivates NFkB. Mean ± SEM (shown as arbitrary units n = 6 per group). (A)p65 immunoblotting analysis on SirT1 immunoprecipitation demonstrates the NR treatment increases interaction of SirT1 and p65. (B)Acetylation assays were performed, and p65 immunoprecipitation showed increased in acetylated lysine in GWI mice and NR deacetylated p65 at k 310 in treated GWI mice. *ANOVA with post-hoc tukey* * $p \leq 0.05$.

3.3.7 Nicotinamide riboside treatment reduces chronic brain inflammation in GWI mice.

To assess an impact of NR on NFκB activation, we examined p65 protein levels and found significant group differences ($F_{(3,8)} = 8.68$, $p = 0.001$; Figure 3.8) with *post-hoc* analyses

showing higher phosphorylated p65 to total p65 ratios in GWI compared to control mice ($p < 0.05$), whereas NR-treated GWI mice had lower ratios of phosphorylated p65 over total p65 protein levels compared to GWI mice on control diet ($p = 0.034$; Figure 3.8). Cytokines, especially IL-1β ($F_{(4,16)} = 8.68$, $p = 0.001$; Figure 3.9), IFN-γ ($F_{(3,12)} = 5.16$, $p = 0.003$; Figure 3.9) and IL-6 ($F_{(2,8)} = 7.86$, $p = 0.03$; Figure 3.9) were significantly different across all four groups. *Post-hoc* analyses showed that the brains of GWI mice had increased expression of these pro-inflammatory cytokines compared to controls ($p < 0.05$), whereas the brains of NR-treated GWI mice had significantly lower levels compared to GWI mice on normal diet ($p < 0.05$; Figure 3.9). Since chronic upregulation of IL-6 leads to activation and phosphorylation of STAT3, we examined p-STAT3 levels in the brains of GWI and control mice with or without NR treatment. We observed significant changes in p-STAT3 with respect to GWI and NR treatment ($F_{(3,8)} = 19.068$, $p = 0.01$; Figure 3.8) with its levels being elevated in the brains of GWI mice which were normalized in NR-treated GWI mice ($p=0.034$).

We also observed significant effects of NR and GWI status on the brain CCL2 ($F_{(1,4)} = 7.46$, $p = 0.041$, Figure 3.9) CCR2 ($F_{(3,9)} = 7.068$, $p = 0.01$, Figure 3.9) levels with *post-hoc* analyses showing their levels to be increased in the brains of GWI mice compared to control and NR-treated GWI mice ($p<0.05$; Figure 3.9). The TBARS levels, indicative of lipid peroxidation, was altered in the brains of GWI and NR treated mice ($F_{(3,8)} = 65.068$, $p = 0.0001$; Figure 3.9). Post-hoc analyses showed high TBARS levels in the brains of GWI mice compared to control mice ($p < 0.05$) and these levels were lower in the brains of NR treated GWI mice compared to GWI mice on regular diet ($p < 0.05$).

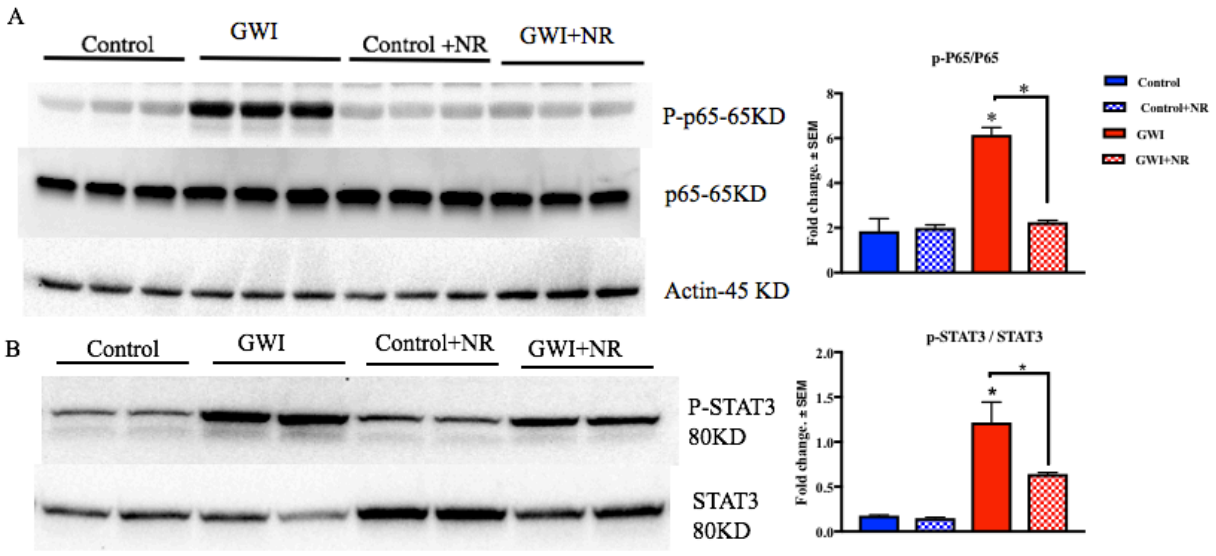

Figure 3.9: Representative images of P65 and STAT 3 western blot of whole brain homogenate. Mean ± SEM (shown as arbitrary units n = 6 per group). (A)The ratio of p-p65/p65 as well as p-STAT3/STAT3 was significantly increased in GWI mice. NR treatment normalizes both P65 and STAT3 phosphorylation in GWI mice. ANOVA with post-hoc tukey $* p \leq 0.05$.

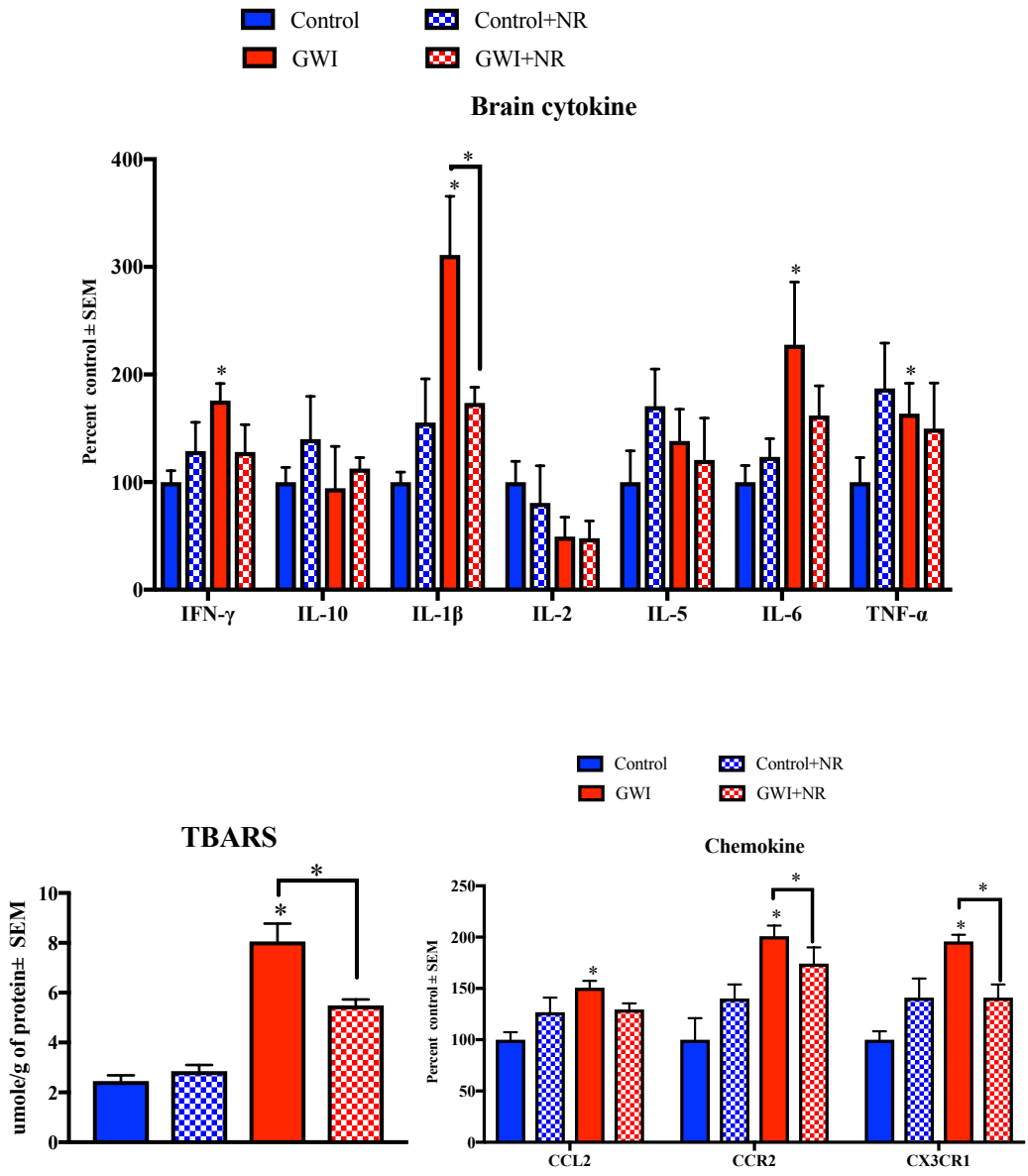

Figure 3.10: NR-normalized inflammatory cytokine, chemokine and lipid peroxidation in the brain of GWI mice. Mean ± SEM (n = 6 per group). MSD cytokine assay showed significant increased in the the brain, IFN-γ, IL-6, and IL-1β level. Among these cytokines examined in the brain, IFN-γ, IL-6, and IL-1β were lower in NR-treated GWI mice compared to GWI mice on normal chow. Similarly, CCR2 and CX3CR2 chemokine levels were elevated in GWI mice compared to control mice, but these levels were reduced in mice treated with NR. Lipid peroxidation measured by TBARS showed GWI mice higher TBARS level compared all other groups. ANOVA with post-hoc tukey * $p \leq 0.05$.

3.3.8 Brain acylcarnitine alterations in GWI mice were normalized by NR treatment

We examined acylcarnitines, which are mitochondria-specific lipids that transport LCFA for β-oxidation in mitochondria and shuttle short- and medium-chain fatty acid between peroxisomes and mitochondria. Short-chain acylcarnitine (SCAC) species were affected across all groups ($F_{(3,8)} = 22.068$, $p = 0.01$; Figure 3.10). *Post-hoc* analyses showed that SCAC were significantly upregulated in the brains of GWI mice compared to conrols ($p = 0.01$; Figure 3.10). This effect in GWI mice was normalized to similar levels in control mice after 2 months of NR treatment in GWI mice ($p=0.03$). However, there were no significant differences between the study groups for medium-chain acylcarnitine (MCAC; 6–14 carbons)($F_{(2,11)} = 4.14$, $p = 0.61$; Figure 3.10) or long-chain acylcarnitine species (LCAC; (14–20 carbons) ($F_{(4,12)} = 2.84$, $p = 0.041$; Figure 3.10). Very Long chain acylcarnitine species (VLCAC; >22 carbons) were changed across all four experimental groups ($F_{(3,12)} = 10.29$, $p = 0.002$) and *post-hoc* analysis showed a significant increased in these acylcarnitine species in the brains of GWI mice compared to control mice ($p = 0.009$), and these levels were reduced to control levels in NR-treated GWI mice ($p = 0.03$). Indiviual species along with fold change to control is shown in the heatmap below. After BH correction these events were either partially or fully normalized in GWI mice by treating them with NR for 2 months. Gamma-butyrobetaine hydroxylase (GBBH) is a key enzyme in the biosynthesis of carnitine which catalyzes L-carnitine formation from GBB. We observed a signficanst effect of GWI status and NR treatment on free L-carnitine ($F_{(3,8)} = 12.22$, $p = 0.002$) and carnitine/gamma-butyrobetaine (GBB) ratio ($F_{(3,12)} = 7.29$, $p = 0.02$) with *post-hoc* analysis showing that L-carnitine and carnitine to GBB ratios were elevated in GWI mice, but these levels were lower in GWI mice treated with NR diet ($p < 0.05$). Trimethylamine *N*-oxide (TMAO) is an organic compound, and its concentrations are increased after consuming foods containing carnitine (i.e. red meat and fish). There were significant group differences for brain TMAO levels ($F_{(3,8)} = 11.32$, $p = 0.001$; Figure 3.10) with *post-hoc* analysis showing increases in GWI mice compare to control and lower levels in NR-treated GWI mice ($p=0.032$).

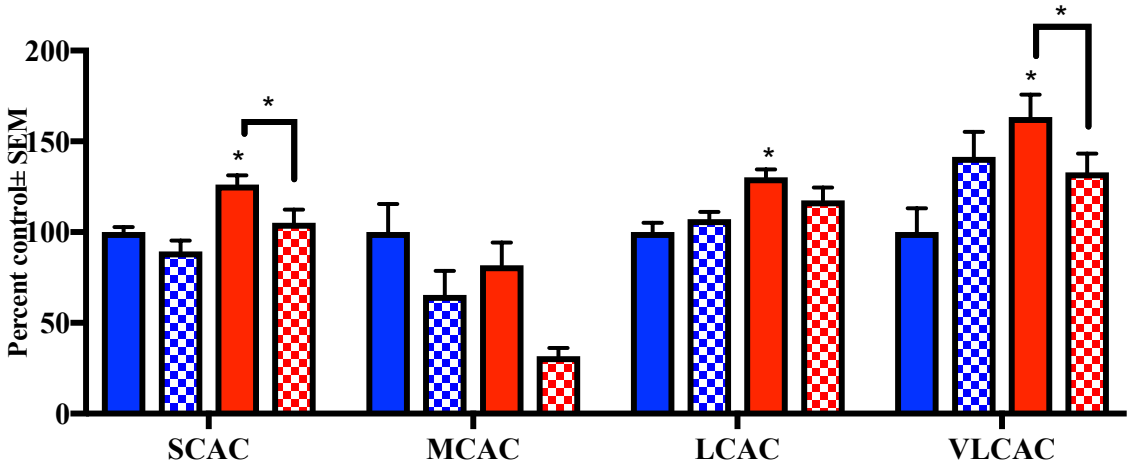
Percent control± SEM
200
150
100
50
0
SCAC
MCAC
LCAC
VLCAC

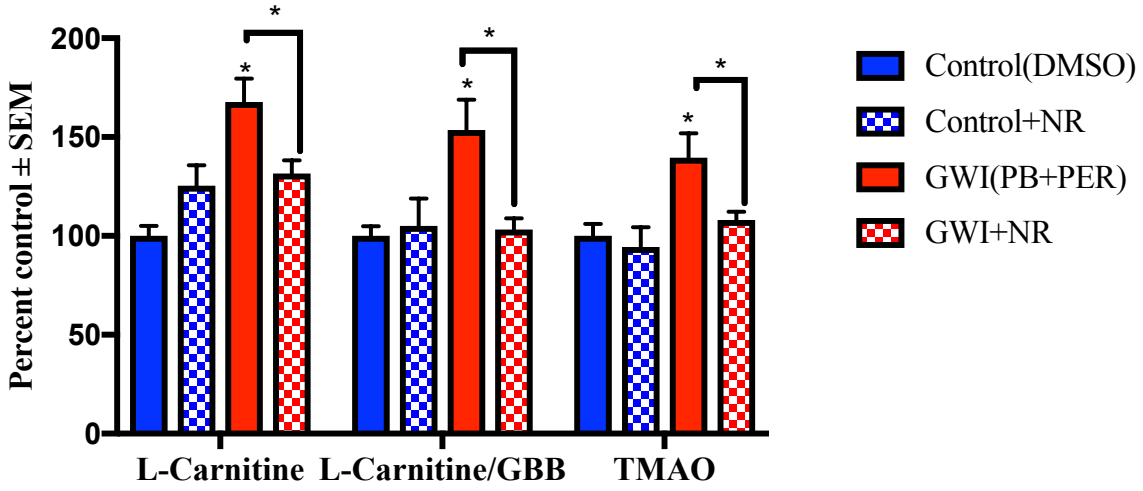
Percent control ± SEM
200
150
100
50
0
L-Carnitine
L-Carnitine/GBB
TMAO
Control(DMSO)
Control+NR
GWI(PB+PER)
GWI+NR

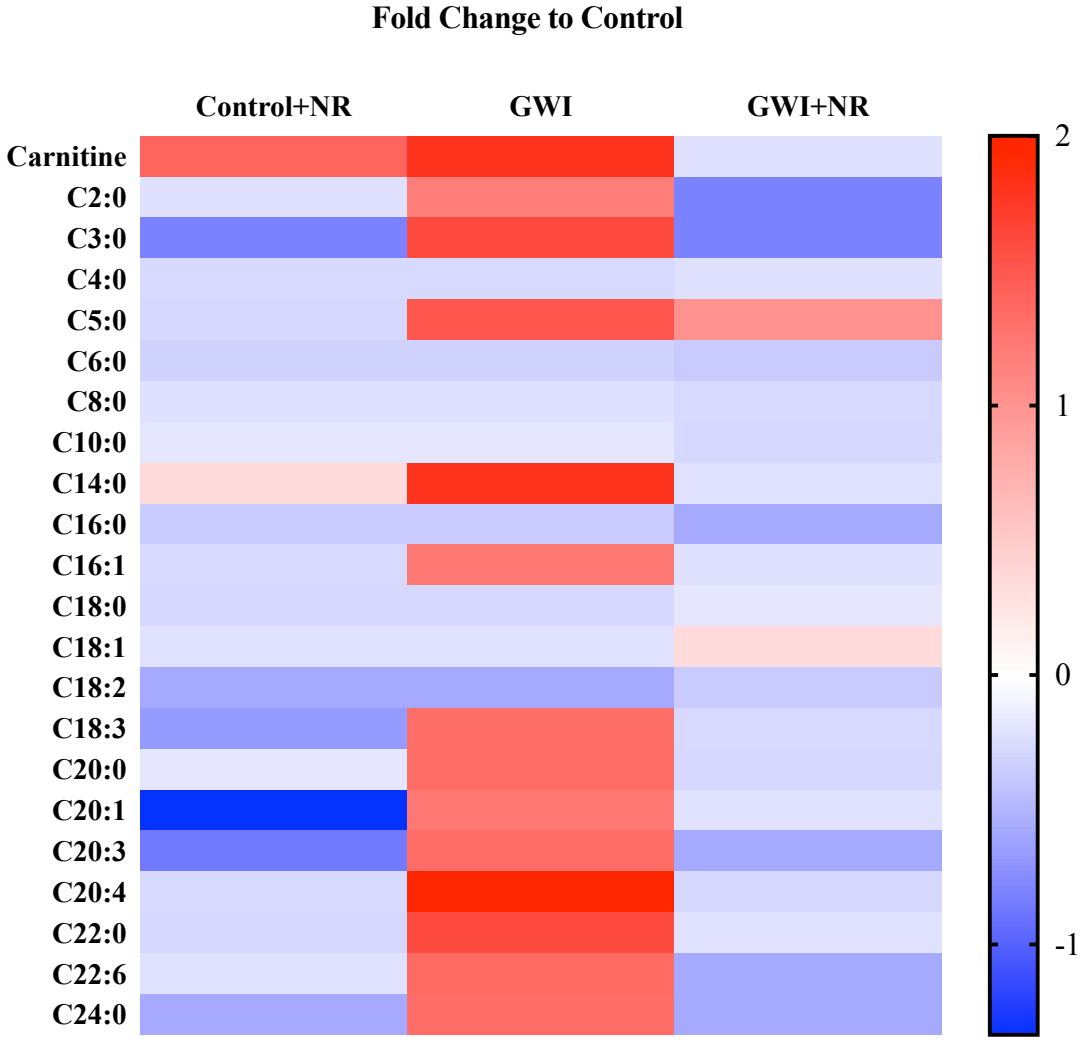

Figure 3.11 NR treatment normalizes increased Acylcarnitine in the brain of GWI mice. Mean ± SE (n = 4 per group).(A) Several short-, medium- and long-chain FA containing acylcarnitine species were elevated in the brains of vehicle-treated GWI mice and were reduced in GWI mice treated with NR. (B)Compared to vehicle-treated GWI mice, NR-treated GWI mice had lower GBBH activity in the brain.(C)Heatmap showing foldchange to control for individual acetylcarnitine species. Mixed linear model with BH correction * $p \leq 0.05$.

3.3.9 Nicotinamide riboside reduced astroglia proliferation in GWI mice

Astroglia and microglia participate in protecting the brain and modulating inflammation. In our mouse models using immunohistochemistry, we observed differences in GFAP staining in GWI and NR-treated mice within the DG ($F_{(3,12)} = 15.29.48$, $p = 0.002$, Figure 3.11) and *post-hoc* analysis showed a significant increase in GFAP staining within the DG of GWI mice compared to control mice ($p < 0.05$). Treatment with NR reduced brain GFAP staining in GWI mice as compared to GWI mice on a normal diet ($p < 0.05$, Figure 3.11). Levels of GFAP staining in the cortex also showed significant change across all groups ($F_{(3,12)} = 4.19.48$, $p = 0.42$; Figure 3.11B), and *post-hoc* analysis showed a significant difference between GWI and control as well as GWI mice treated with NR compared to GWI treated with control diet ($p < 0.05$). There were no differences across any of the experimental groups for microglia staining with Iba1in the DG ($F_{(3,8)} = 6.98$, $p = 1.72$;Figure 3.12) or cortex ($F_{(3,10)} = 4.19$, $p = 3.42$;Figure 3.12).

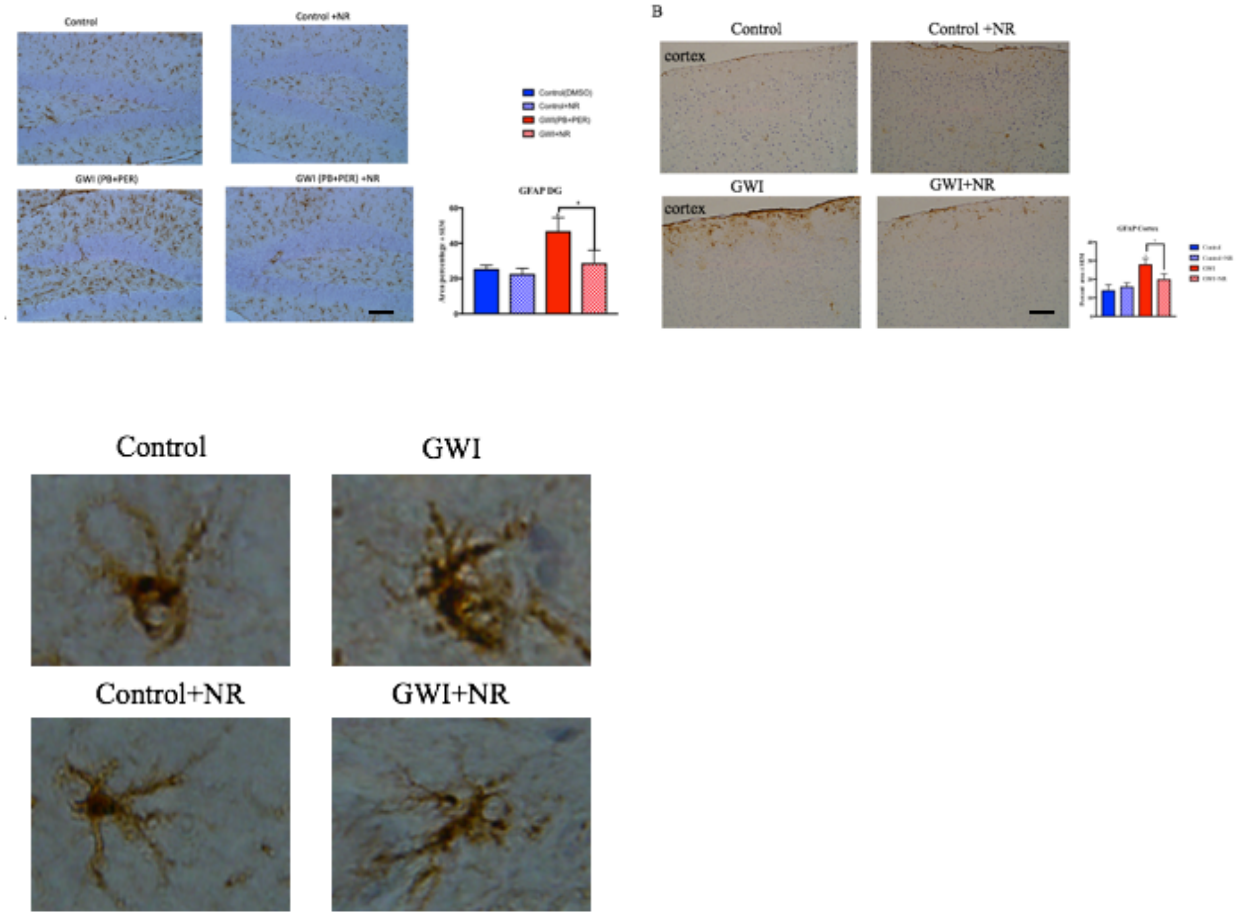

Figure 3.12: Representative images of GFAP staining in the DG and Cortex regions. Sagittal sections of the mouse brain at 0.8 mm lateral to midline in the brainstem. 20x images of astroglia GFAP staining in the hippocampus showed a significant increase in GFAP within the DG of GWI mice compared to controls and NR-treated GWI mice. Quantitative analysis of GFAP staining intensity indicated an increased area of GFAP immunoreactivity in the DG(A) and cortex (B)of GWI mice. Mean ± SEM (n = 4 per group) ANOVA with post-hoc tukey * $p \leq 0.05$. scale bar 100µm

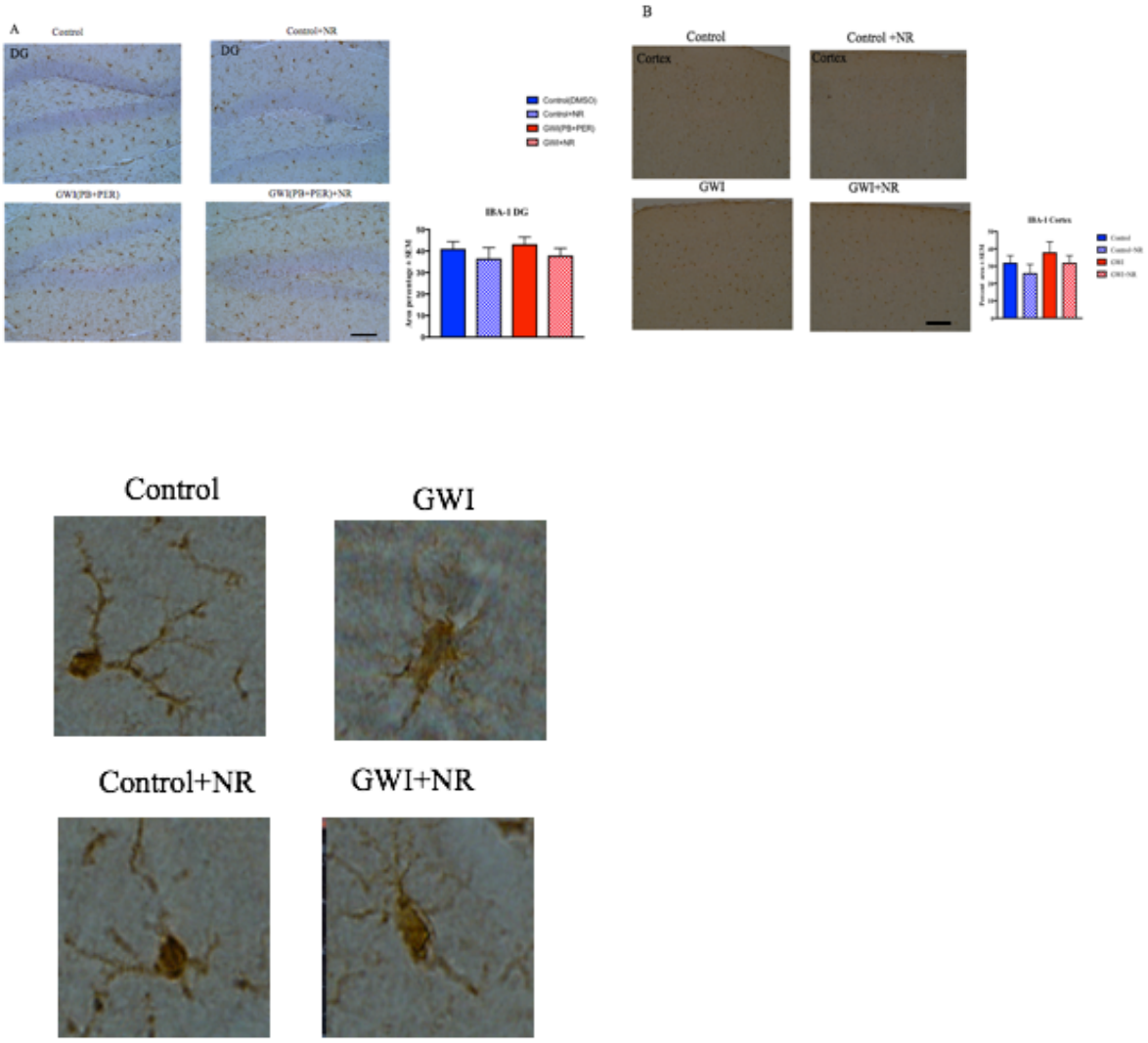

Figure 3.13: Representative images of IBA-1 staining of DG and cortex regions. Sagittal sections of the mouse brain at 0.8 mm lateral to midline in the brainstem. 20x images of microglia marker Iba1 staining within the DG showed no significant change among all four groups. Quantitative analysis of IBA-1 staining intensity indicated no change in the IBA-1immunoreactivity in the DG(A) and cortex(B) of GWI mice. Mean ± SE (n = 4 per group). ANOVA with post-hoc tukey * $p \leq 0.05$. Scale bar 100µm

3.3.10 Ketogenic Diet restores decreased NAD+ and β-HB levels in GWI mice

We also tested whether targeting mitochondrial dysfunction with a ketogenic diet can restore β-HB and NAD+ levels. Administration of KD significantly increased liver β-HB levels across all groups ($F_{(2,6)} = 6.14$, $p = 0.023$, Figure 3.13) with *post-hoc* analyses showing that liver β-HB levels were significantly decreased in GWI mice compared to control mice but restored to normal levels in GWI mice with KD treatment ($p < 0.05$). Brain β-HB level did not differ between the 4 experimental groups ($F_{(2,8)} = 30.88$, $p > 0.05$). There was a significant decrease in plasma NAD+ levels in GWI mice compare to all other groups ($F_{(4,8)} = 14.13$, $p = 0.01$; Figure 3.13). *Post-hoc* analysis showed that NAD+ levels in plasma were significantly decreased in GWI mice compared to control mice and KD treatment significantly increased plasma NAD+ levels in GWI mice ($p < 0.05$). Brain NAD+ level were unchanged in all 4 groups ($F_{(4,8)} = 10.11$, $p = 1.01$; Figure 3.14). There was no significant change in weight across all 4 groups.

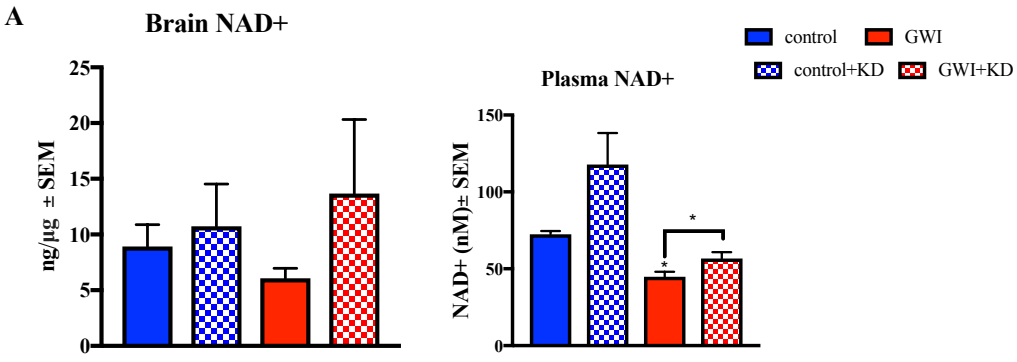
A
Brain NAD+
control
GWI
control+KD
GWI+KD
Plasma NAD+
ng/µg ± SEM
NAD+ (nM)± SEM
25
20
15
10
5
0
150
100
50
0
*
*

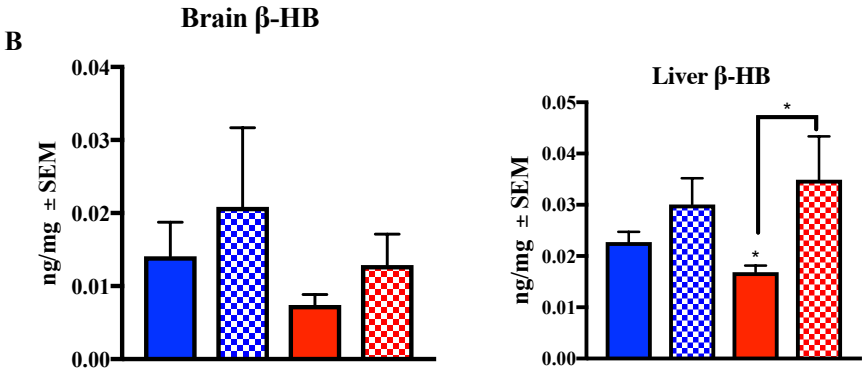
B
Brain β-HB
Liver β-HB
ng/mg ± SEM
0.04
0.03
0.02
0.01
0.00
0.05
*
*

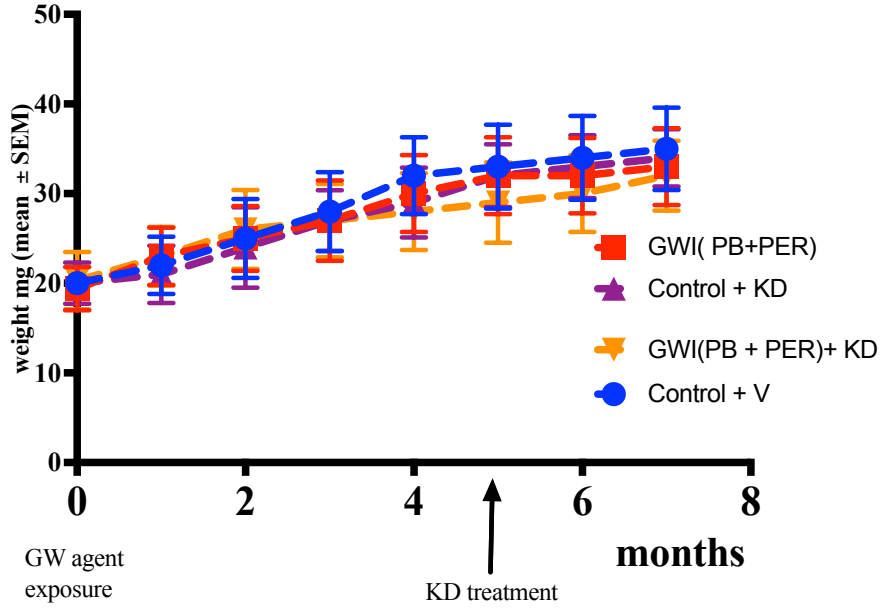
C
weight mg (mean ± SEM)
50
40
30
20
10
0
0
2
4
6
8
months
GW agent exposure
KD treatment
GWI(PB+PER)
Control + KD
GWI(PB + PER)+ KD
Control + V

Figure 3.14: Effects of KD treatment on the NAD+ and β-HB concentration. Mean ± SEM (n = 3/4 per group). (A)Brain and plasma NAD+ levels on all 4 groups showed decreased in plasma NAD+ level in GWI. Treatment with KD increases NAD+ in both plasma and brain among control and HWI(B)Liver and brain β-HB level on all 4 groups. There was no change in brain β-HB among all groups. Liver β-HB levels were decreased in GWI mice, which was significantly increased after KD treatment. Chronic KD treatment had an increasing trend for β-HB in the liver * $p \leq 0.05$.

3.3.11 Ketogenic diet increases marker of mitochondrial function and reduces mitochondria-derived reactive oxygen species

There were significant differences in UCP-2 levels across all experimental groups ($F_{(2,6)} = 6.14$, $p = 0.023$, Figure 3.14) with *post-hoc* analyses showing that 2 months of KD treatment increased its levels in GWI and control mice ($p < 0.05$), despite there being no differences between untreated GWI and controls mice ($p > 0.05$). Levels of PGC-1α in the brain were different across all 4 group treatment groups ($F_{(3,8)} = 6.14$, $p = 0.023$, Figure 3.14), and *post-hoc* analyses showed that while its brain levels in GWI and control mice did not differ significantly, treatment with KD increases protein levels of PGC-1α in the brains of GWI and control mice ($p < 0.05$).

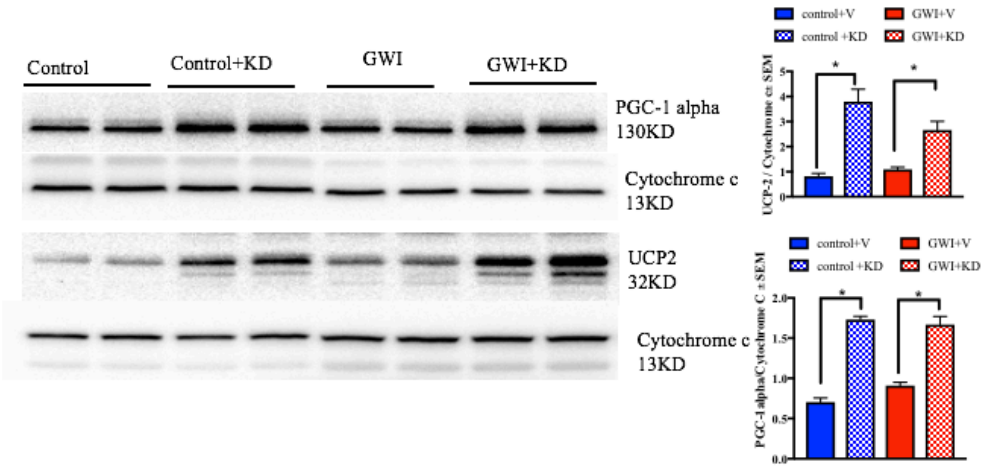

Figure 3.15: Representative images of UCP-2 and PGC-1alpha Western blot of whole brain mitochondria. Mean ± SEM (shown as arbitrary units, n = 3/4 per group). KD treatment increased UPC-2 levels in both GWI and control mice compared to those on regular diet within each respective group. Similarly, levels of PGC-1α were elevated in KD-treated GWI and control mice compared to their respective groups on normal diet. ANOVA with post-hoc tukey * $p \leq 0.05$

3.3.12 Ketogenic Diet treatment had no effect on SirT1 and SirT3 expression

To determine if KD treatment also affects the SirT levels since NAD+ levels were increased with this treatment, we analyzed the expression of SirT1 and SirT3. There were group differences for SirT1 protein levels in the brain ($F_{(3,8)} = 3.08$, $p = 0.05$, Figure 3.15), and post-hoc analyses showed that while SirT1 levels differed between control and GWI mice ($p < 0.05$), there was no significant effect of KD on SirT1 levels ($p > 0.05$). There were no differences in SirT3 protein levels between the experimental groups ($F_{(3,9)} = 0.8$, $p = 0.49$, Figure 3.15).

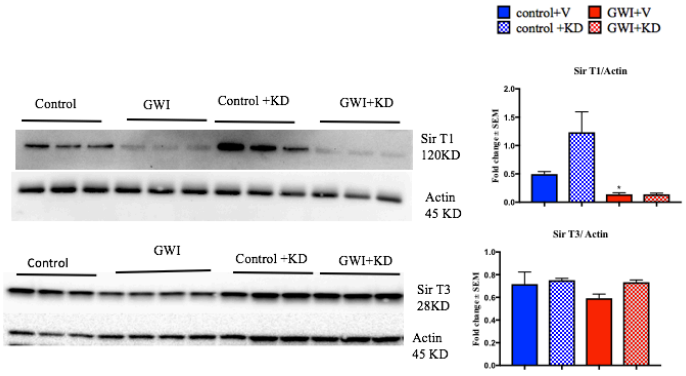

Figure 3.16: Sirtuin 1 and 3 changes in GWI mice. Mean ± SEM (arbitrary value n =3 per group) Western blot analysis demonstrates the expression of SirT1 and Sir T3 were not changed by KD treatment. SirT1 levels were decreased in GWI mice compared to control. Sir T3 levels were unchanged across all the experimental groups. *ANOVA with post-hoc tukey * $p \leq 0.05$*

3.3.13 Ketogenic Diet treatment reduces chronic brain inflammation in GWI mice.

We examined if NFκB activity was affected following KD diet and observed an overall effect of KD and GWI status on p65 phosphorylation ($F_{(2,7)} = 4.08$, $p = 0.032$, Figure 3.16) with *post-hoc* analysis showing that p65 phosphorylation was significantly increased in GWI mice, ($p < 0.05$) and KD treatment partially normalized p65 phosphorylation in the brain of GWI mice ($p < 0.05$). We also observe that chronic KD treatment and GWI status affected STAT3 activation/phosphorylation across all groups ($F_{(2,8)} = 10.08$, $p = 0.02$, Figure 3.16). *Post-hoc* analysis showed that KD treatment reduces STAT3 phosphorylation in the brains of GWI mice ($p < 0.05$) which were elevated in the brains of GWI mice compared to control mice ($p < 0.05$).

Cytokines, specially IL-1β ($F_{(2,7)} = 4.08$, $p = 0.032$, Figure 3.17), IFN-γ ($F_{(2,7)} = 4.08$, $p = 0.032$, Figure 3.18) and IL-6 ($F_{(2,7)} = 4.08$, $p = 0.032$, Figure 3.17) were affected in the brain across all groups (Figure 3.17). *Post-hoc* analysis showed that IL-1β ($p < 0.01$), IFN-γ ($p <0.05$) and IL-6 ($p <0.05$) were significantly upregulated in the brains of GWI mice compared to controls. These cytokines levels were also partially normalized by KD treatment in the brain of GWI mice ($p<0.05$). Along with cytokine levels, KD treatment also affected chemokine and chemokine receptors such as CCR2 ($F_{(2,8)} = 7.08$, $p = 0.02$, Figure 3.17) and CX3CR1($F_{(2,8)} = 6.86$, $p = 0.03$, Figure 3.17) in the brain across all 4 groups. Chronic treatment of KD normalized levels of CCR2 ($p < 0.05$) and CX3CR1 ($p < 0.05$) in the brain of GWI mice which were elevated in the brains of GWI mice compared to control mice ($p < 0.05$). Lipid peroxidation measured by TBARS were also changed across all 4 groups ($F_{(4,10)} = 14.08$, $p = 0.033$;Figure 3.17). *Post hoc* analysis showed significant increased in GWI compared to all other groups and KD diet decreased TBARS levels in GWI mice compared to GWI mice on normal diet ($p < 0.05$, Figure 3.17).

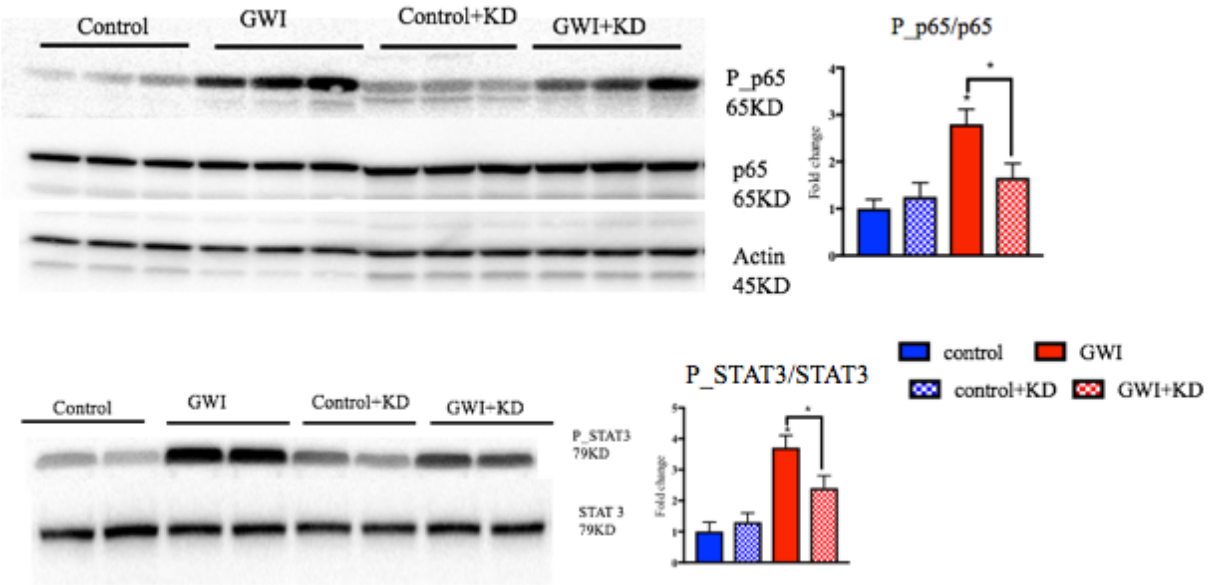

Figure 3.17: Representative images of p65 and STAT3 Western blot of whole brain homogenate. Mean ± SEM (shown as arbitrary units n = 3/4 per group). The ratio of p-p65/p65 is higher in the GWI mice compared to all 4 groups. The ratio of p-STAT3/STAT3 is higher in GWI mice compred to all 4 groups. ANOVA with post-hoc tukey * $p \leq 0.05$

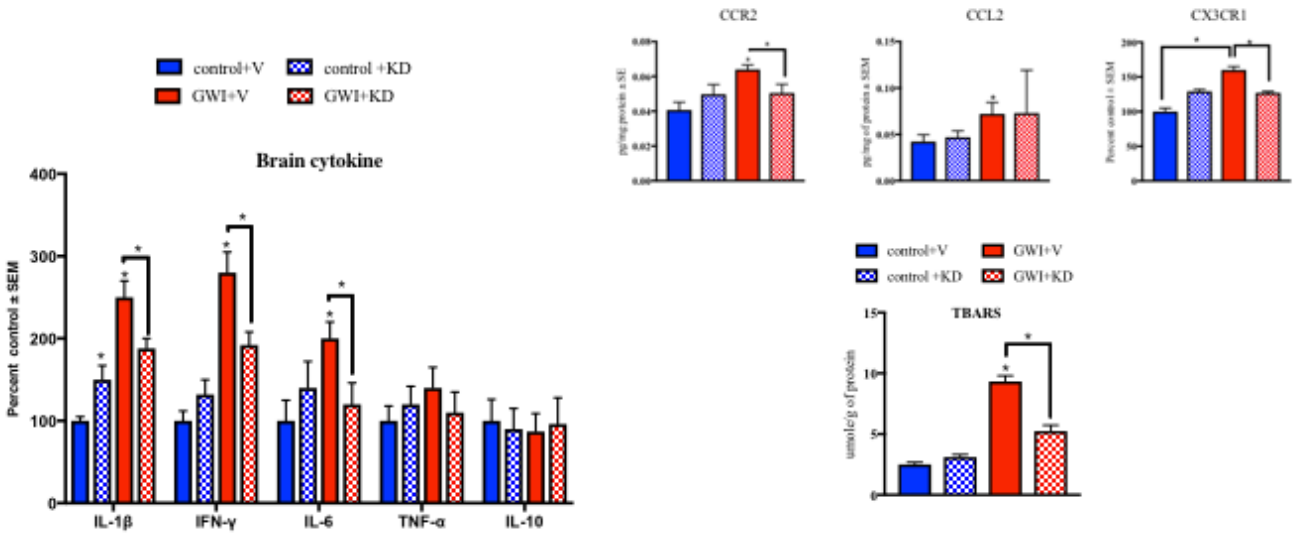

Figure 3.18: KD normalized inflammatory cytokine and chemokine levels in the brain of GWI mice. Mean ± SEM (n = 6 per group). Among the cytokines examined in the brain, IFN-γ, IL-6 and IL-1β were lhigher in GWI mice compared to control, KD treatment reduced these cytokines levels in GWI mice compared to GWI mice on normal chow. Similarly, CCR2 and CX3CR2 chemokine levels were elevated in GWI mice compared to control mice, but these levels were reduced in mice treated with KD. Lipid peroxidation measured by TBARS. Increased TBARS levels in GWI brain were normalized in after KD treatment. ANOVA with post-hoc tukey * $p \leq 0.05$.

3.3.14 Ketogenic Diet reduces astroglia activation in GWI mice

Similar to my previous result, we do see a change in astroglia proliferation in DG across all groups ($F_{(3,8)} = 8.18$, $p = 0.001$, Figure 3.18A). *Post-hoc* analysis showed significant increases in astroglia proliferation in GWI mice compared to control mice ($p < 0.05$) that were normalized by KD treated GWI compared to GWI mice on control diet ($p < 0.05$). GFAP staining in cortex did not affect all experimental groups ($F_{(3,8)} = 6.31$, $p = 0.71$, Figure 3.18B). Also consistent with our previous result, we did not observe any microglia activation or proliferation in GWI mice at 7-months post exposure time point in DG ($F_{(2,9)} = 4.11$, $p = 0.87$, Figure 3.19A) and cortex ($F_{(3,8)} = 10.31$, $p = 1.54$, Figure 3.19B).

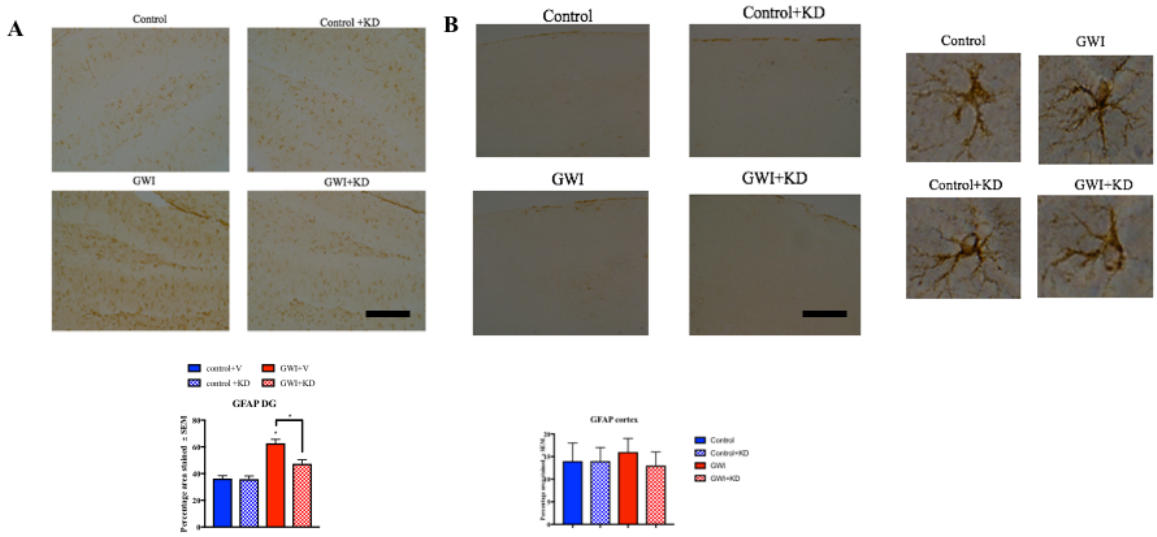

Figure 3.19: Representative images of GFAP staining of DG and Cortex regions. Sagittal sections of the mouse brain at 0.8 mm lateral to midline in the brainstem. 20x images of astroglia GFAP staining in the DG(A) and Cortex (B) showed a significant increase in GFAP immunoreactivity within the DG, observed in GWI compared to controls and KD treated GWI mice. ANOVA with post-hoc tukey*=p<0.05.Scale bar 100µm

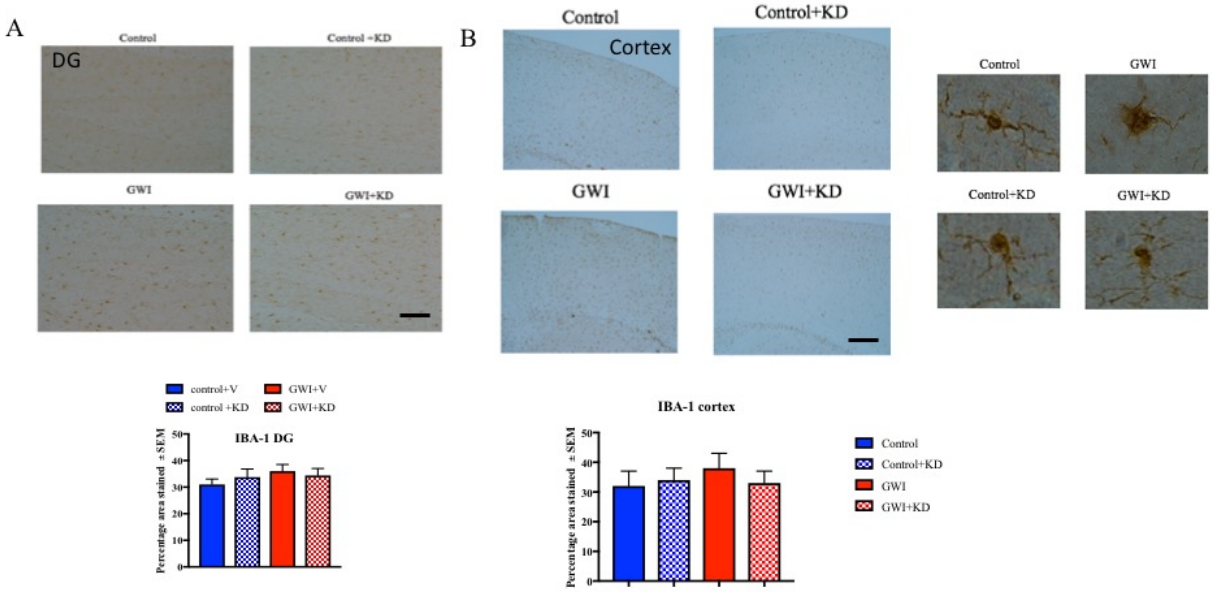

Figure 3.20: Representative images of IBA-1 staining of DG and Cortex regions. Sagittal sections of the mouse brain at 0.8 mm lateral to midline in the brainstem. Quantitative analysis of IBA-1 staining intensity indicated no change in IBA-1 immunoreactivity in the DG(A) and Cortex(B) of GWI mice. Mean ± SE (n = 3/4 per group). ANOVA with post-hoc tukey * $p \leq 0.05$. Scale bar 100μm

3.4 Discussion

Previous proteomic and metabolomic investigations in our labs suggested that exposure to GW chemicals similar to those utilized in this research to generate a GWI mouse model have the potential to disrupt multiple mitochondrial pathways, including; the Krebs cycle, glycerol-3 phosphate shuttling and gluconeogenesis I [54]. The work described in this chapter mechanistically explores whether targeting cellular bioenergetics using NR and KD can restore mitochondrial function and furthermore, whether these bioenergetic changes may also help attenuate neuroinflammation, reduced fatigue like behavior, and improve mitochondrial specific lipid metabolism. In this current study, we demonstrate that treatment with NR rescues mitochondrial bioenergetics, the data in this study are supported by several other studies in the literature which show efficacy of NR in enhancing mitochondrial oxidative phosphorylation [242] and increasing mitochondrial biogenesis [226]. We also demonstrated that the effects of NR and KD are associated with an increase in UPC-2 and PGC-1α protein, supporting mitochondria biogenesis and ultimaltey improving OXPHOS.

I observed a decrease in fatigue-like behavior in GWI mice after NR treatment. Chronic fatigue is one of the primary symptoms of GWI [6], among veterans deployed to the 1991 GW, 23% continue to suffer from fatigue [6]. Decreased levels of NAD+ (indicative of lower bioenergetics capacity) in veterans with GWI may be one of the reasons why chronic fatigue has persisted in ill veterans. Although the underlining mechanism is not well understood, study links CFS to reduced NAD+ level [243]. There are now several clinical studies which have shown that chronic oral treatment with NR has an excellent safety profile and is generally well tolerated [244,245], and furthermore, chronic treatment with NR is associated with decreased fatigue intensity

and improved quality of life [210,246]. Therefore, an intervention that increases NAD+ levels in GWI patients may decrease fatigue intensity.

I did not observed any change in memory and learning as measured by Barnes Maze in this cohort. While other cohort showed significant decline in both learning and memory in GWI mice as measured by BM at similar time point. Although exact reason is not well understood but it could be due to order of neuro behaviour experimnets. I did FST a week before BM, FST increases stress and might have affect memory in these mice.

Along with the critical role of oxidized and reduced forms of NAD in ATP generation, NAD+ activates sirtuins, which are critical regulators of mitochondrial function and biogenesis. Among the seven mammalian sirtuins that have been identified, SirT1 is localized to the nucleus, whereas SirT3 is found explicitly in mitochondria [247]. SirT1 is also ubiquitously expressed in the rodent prefrontal cortex, hippocampus, and basal ganglia. Recent evidence has supported the concept that sirtuin expression is regulated by the availability of free NAD+ and NADH [248]. We, therefore, examined SirT1 and SirT3 protein levels after GW chemical exposure and after NR treatment. We found that SirT1 levels were significantly decreased in the brains of GWI mice and were increased in the brains of GWI mice treated with NR. While SirT3 levels did not differ between GWI and control mice, NR treatment significantly increased SirT3 expression in the brains of both control and GWI mice. It is, therefore, possible that increased protein levels of sirtuins along with increased availability of NAD+ could result in improved mitochondrial function, mitochondrial biogenesis, and reduced inflammation.

More recently, sirtuins have been shown to influence inflammatory processes via the deacetylation of cellular p65 protein and inhibition of NFκB activation [249,250]. SirT1 deacetylates p65 subunit of NFκB, in an NAD+ dependent manner, resulting in suppression of NFκB transcription which subsequently leads to a decreased production of pro-inflammatory cytokines [249,251]. Consistent with these findings, in our immunoprecipitation studies, we observed lower levels of p65 bound to SirT1 in the brains of GWI mice compared to control mice and these levels

are similar to control in GWI mice treated with NR. These results suggest regular interaction between SirT1 and p65 interaction is reduced and therefore reduced deacetylation of p65 resulting in increased phosphorylation and translocation to the nucleus.

Furthermore, NR treatment seems to increase the interaction between p65 and SirT1, corresponding with reduced acetylation of p65. Given the well-known effects of NF-kB activation in inflammation and observations of increased downstream effects of inhibiting NFkB were examined by measuring cytokines and chemokines that are involved in promoting inflammation. Treatment with NR was able to reduce several cytokines, IL-1β, IFN-γ and IL-6, levels and STAT3 phosphorylation in the brains of GWI mice. In addition to cytokines, we also observed decreases in chemokine CCL2 levels as well as its receptor CCR2 along with CX3CR1 after NR treatment in the brains of GWI mice. These findings suggest that NR treatment can target multiple aspects of GWI pathology, including lipid and mitochondrial dysfunction along with reducing inflammation. Increases in cytokine and chemokine levels lead to reactive astroglial activation and proliferation[252,253]. Consistent with other studies, we observed a noticeable decrease in reactive astrocytes and astroglial proliferation following NR treatment[220]. Furthermore, changes in sirtuin levels after NR treatment are consistent with the well-known effects of NAD on sirtuin activity and; therefore, some of these positive effects on mitochondria function are likely facilitated through sirtuin mediated pathways.

While glucose is the primary molecule supporting CNS bioenergetics, under certain conditions or in some diseases, β-oxidation of fatty acids can serve as an alternative energy source for the CNS [254]. Since carnitine and acylcarnitines contribute to fatty acid metabolism and maintain appropriate ratios of acyl-CoA to free CoA, changes in their levels could provide some insight into brain bioenergetics, particularly in disorders with metabolic disturbances. Furthermore, carnitine/acylcarnitine transporter (CACT) can be deacetylated by SirT3, resulting in increased CACT activity [255]. Since our previous studies have found an alteration in blood and brain acylcarnitine levels in GWI mice and veterans with GWI [54], we, therefore, evaluated

acylcarnitine levels following NR or sham treatment to obtain an indirect measure of CNS bioenergetics. We observed that VLCAC and SCAC were particularly affected and their levels were restored to that of control mice following NR treatment. Furthermore, an increase in C14:0 acylcarnitine was detected in the brains of GWI mice, which is generally associated with very long-chain acyl-CoA dehydrogenase deficiency. After NR treatment, levels of this acylcarnitine were reduced in the brains of GWI mice.

Interestingly, the final product of fatty acid β-oxidation, βHB, was unaffected by NR treatment, suggesting that changes in acylcarnitine profiles may not directly translate into metabolites that support Krebs cycle processes. However, it is possible that acetyl-CoA that is generated from chain shortening may enter the Krebs cycle, which would prove a useful mechanism for monitoring NR mediated mitochondrial bioenergetics. While the exact mechanism of how NR diet improves acylcarnitine profiles requires further investigation, the effects of NR shown in this research could be due to improved mitochondrial metabolic function [256]. Therefore, these results suggest that the restoration of acylcarnitine profiles in GWI mice following NR treatment may be indicative of improved fatty acid transport and metabolism. Further examination of this acylcarnitine transport and metabolism, as well as other bioenergetics related compounds, is needed to better understand the effects of NR on the brain mitochondria function and bioenergetics recovery in GWI mice.

In recent years, many studies have suggested that sirtuins are critical regulators of mitochondrial biogenesis, a process that is regulated by PGC-1α and UCP-2 [257]. Uncoupling proteins play an essential role in the regulation of fatty acid metabolism and ROS elimination and have also been reported to maintain mitochondrial membrane potential [258]. PGC-1α increases mitochondrial biogenesis by increasing gene transcription of factors, such as AMPK (adenosine monophosphate-activated protein kinase), that activate mitochondrial transcription factor A[257]. Both SirT1 and SirT3 have been shown to deacetylate PGC-1α, promoting

increased mitochondrial biogenesis [259,260]. In our study, while levels of PGC-1α and UCP2 did not differ between GWI and control mice, NR treatment increased PGC-1α and UCP2 protein levels in both control and GWI mice, suggesting that some of the beneficial effects of NR treatment may be mediated through this mechanism [226,239,242]. PGC-1α is also deacetylated by SirT3[261]. We observed that the acetylated form of PGC-1α in the mitochondrial fraction was elevated in GWI compared to control mice and that NR treated GWI mice had lower levels, generally similar to those observed in control mice. Since SirT3 is mitochondria specific deacetylase, it might be possible that the observed effects on PGC-1α are due to the changes in SirT3 acitivty after exposure to GW chemicals. In addition, PGC-1α deacetylation by SirT3 increases PGC-1α activity contributing to increased mitochondria biogenesis and mitochondrial and peroxisomal lipid metabolism[201,261–263]. As such SirT3-mediated deacetylation and activation of PGC-1α is an important cellular response to restore cellular metabolic function, particularly in conditions like GWI, where there might be energy deprivation or low bioenergetics function. Together, these studies suggest that activation of sirtuins in combination with increases in PGC-1α and UCP2 may help recover impaired mitochondria function seen in veterans with GWI by increasing mitochondrial function after NR treatment may be a useful therapeutic approach for improving the general well-being of veterans with GWI.

Mitochondria are the primary source of ROS production within the cell, excess accumulation or dysfunctional clearance of ROS has been shown to result in the impairment of mitochondrial bioenergetics and metabolic function[206–208]. Our previous works have identified the importance of lipid peroxidation and oxidative stress in our GWI model[78]. Oxidative stress in the cellular environment results in the formation of highly reactive and unstable lipid peroxides[264]. Because reactive oxygen species (ROS) have extremely short half-lives, they are difficult to measure directly. Instead, what can be measured are several products of the damage produced by oxidative stress, such as TBARS. Thiobarbituric acid reactive substances - TBARS - are formed as a byproduct of lipid peroxidation (i.e., as degradation products of fats) which can

be detected by the TBARS assay [265]. In the current study, we observed the levels of TBARS were partially normalized by NR treatment in GWI mice, supporting the anti-inflammatory potential of this compound.

Trimethylamine N-oxide is an amine metabolite generated from choline and carnitine oxidation by gut microbes [266]. Although the mechanism is not clearly understood, recently TMAO been identified as a novel risk factor for promoting atherosclerosis and vascular inflammation [267]. More recently, TMAO has been found to induce phosphorylation of the NFκB resulting in increased inflammatory cytokine production such as Il-6 and IL-1β [268]. Increased in TMAO induces inflammation leading to mitochondrial ROS via inhibition of SirT3 activity [267]. In our study, we do see increased in TMAO and L-carnitine in GWI brain. Studies have shown that TMAO and L-carnitine level are accumulated and correlated in metabolic disorder [269]. Chronic NR treatment decreases both L-Carnitine and TMAO. As such, further investigation is required to confirm our finding, especially in the human population. The final step of L-carnitine synthesis involves the conversion of GBB to L-carnitine by GBB hydroxylase (GBBH). In this study, we showed that NR treatment reduces GBBH activity in GWI mice.

As with the studies above, an examination of NAD+ and βHB showed a decreasing trend in the brains of GWI mice. This allowed me to investigate KD as a potential therapeutic approach since it is know that both NAD+ and βHB levels are increased after KD[222]. In this treatment strategy we performed long term treatment with KD. However, NAD+ in plasma were increased following KD. Levels of βHB were low in the liver of GWI mice but increased following treatment with KD in GWI mice. These studies suggest that KD produces peripheral effects on molecules that support bioenergetics. Since there are transporters are present at the BBB and transport βHB to the brain, it is possible that βHB generated by the liver is transported to the brain to support bioenergetics [270]. Ketone body specially βHB can cross BBB by two mechanism (1) lipid-mediated free diffusion through the BBB or (2) carrier- or receptor-mediated transport

through the BBB While the exact mechanism behind NAD+ increase following KD is currently being investigated, the literature suggests that calorie restriction and KD increase NAD+ levels by possibly stimulating ATP production [271,272].

Since NAD+ levels were elevated in the blood of GWI mice after KD, we explored whether sirtuin levels were also increased as with the NR diet. We observed the expected decrease of SirT1 in the brains of GWI mice, neither SirT1 nor SirT3 were affected by KD. We examined PCG-1α and UCP2 because studies have shown that KD or fasting increases these proteins[222]. We observed increases in their levels in the brains of GWI mice after KD. While the molecular mechanism behind this remains poorly understood, one possible mechanism might be that KD may increase βHB which may increases expression of PGC-1a, a master regulator of mitochondrial biogenesis and function[273]. β-Hydroxybutyric acid not only provides energy but also attenuates neuroinflammation via the inhibition of NFκB activation, bilaterally reducing cytokine such as IL-1β [274,275]. Increased NFκB correlates with increasing in astroglia activation and pro-inflammatory cytokines and chemokines in GWI mice [78]. However, 2-months of KD intervention was able to decrease the activation of astroglia and pro-inflammatory cytokines such as IL-1β, IL-6, IFN-γ in the brain of GWI.

One key limitation of these studies is small sample size and lack of neurobehavioral data. This study needs to be repeated with a larger sample size, along with memory and anxiety evaluation. Overall, these preclinical findings suggest that chronic oral NR and KD treatments restore GWI pathology. In conclusion, this study suggests that NR can target several aspects of GWI, including mitochondrial biogenesis, fatigue, lipid peroxidation, and inflammation. This current study supports that βHB regulates inflammation and stimulates mitochondrial functioning. Once confirmed using larger studies, we propose that strategies to increase βHB levels via KD and NAD+ levels via NR intervention will likely be therapeutically beneficial in GWI.

Chapter 4: A permethrin metabolite is associated with adaptive immune responses in Gulf War Illness

4.1 Introduction:

As discussed in previous chapters, several clinical studies suggest that immune dysfunction and chronic inflammation are among the key causes of the symptoms experienced by ill GW veterans [2]. Studies using the rodent models of GWI implicate both the CNS and peripheral immune systems in contributing to the pathogenesis of this illness [179]. However, a better understanding of these immune responses in GWI would further contribute towards the development of biomarkers and therapies for the CNS symptoms and pathology of GWI.

As discussed in chapter 1, it is now well established that pesticide exposure played a significant role in the manifestation of GWI [1,276]. Statistics reported by the DoD have suggested that a large proportion of the ground troops deployed to the GW reported using any kind of pesticides [33]. Among these, 44% were pesticide sprays that contained pyrethroids, such as PER [1]. Recently emerging evidence suggests that exposure to pesticides in humans can be associated with autoimmune disorders [277]. In particular, several case reports documented that acute pyrethroid intoxication in humans is associated with autoimmune clinical phenotype, including disorders like scleroderma and myasthenia-like syndromes [278–280]. The most compelling evidence for autoimmune abnormalities in GWI comes from studies showing increases in immunoglobulin G (IgG) and T- and B-cells in the blood of veterans with GWI compared to healthy GW veterans [107] and is supported by a study showing elevated autoantibodies against brain-specific proteins, such as GFAP and tau in blood from veterans with GWI [110].

Low molecular weight chemicals can form adducts with endogenous proteins, and these chemically modified proteins can elicit an adaptive immune response [281]. Studies have shown that a 3-phenoxybenzoic acid (3-PBA) is a common metabolite of PER, which is generated by esterase cleavage followed by enzymatic oxidation [282]. It is shown that 3-PBA can undergo glucuronidation in the liver for excretion in urine to form 1-O-(3-phenoxybenzoyl)-ß-D-

glucopyranuronate (Glu-3-PBA) [282]. This Glu-3-PBA has been shown to further react to form an amide with lysine in proteins [282]. Others have shown that chemically-haptenated proteins can reach the lymphatic system, where they encounter immune cells that are involved in antigen presentation to T- and B-cells [283]. These studies suggest a role of haptenated proteins in promoting autoimmune responses. As such, an activation of autoimmune responses in GWI could be downstream of PER exposure that occurred during the GW conflict.

Autoantibodies against brain proteins are a part of a continuum of many autoimmune disorders [284]. For example, in Sydenham's chorea, a neurological manifestation of rheumatic fever where peripheral autoantibodies against Group A β-hemolytic streptococcus cross-reacts with neuronal proteins [284]. In systemic lupus erythematosus (SLE), peripherally generated anti-DNA antibodies enter the brain and cross-react with N-methyl-D-aspartate (NMDA) receptors [285]. In other autoimmune disorders, such as multiple sclerosis (MS), studies suggest that a breach in the BBB allows CNS proteins to leak into the periphery where immune cells first encounter them. Alternatively, these immune cells can gain antigen experience within the cervical lymph nodes where CNS antigens drain [286]. While the exact mechanisms behind brain and peripheral immune cross-talk remain unknown in GWI, the presence of autoantibodies against brain proteins and evidence of glia activation in GWI mouse models do suggest an involvement of adaptive immune system in promoting the CNS pathology of GWI [54,78,110].

Previous studies including my own work shows increases in astroglia activation, NFκB phosphorylation and proinflammatory cytokines are commonly observed in the brains of GWI rodent models [51,53,54,78,157,180], also supporting a role of adaptive immune cells in the CNS pathology of GWI. Elevated proinflammatory cytokines can increase matrix metalloproteinase 9 (MMP9) activity at the BBB and enhance the transmigration process, potentially promoting the infiltration of peripheral immune cells into the CNS [287]. Among these, Ly6C+ monocytes are capable of converting to macrophages upon CNS infiltration [288,289]. As mentioned in

chapters 2 and 3, I observed increases in C-C chemokine receptor type 2 (CCR2) and its ligand, CCL2, in the brains of GWI mice [78]. In neuroinflammatory conditions, CCL2 released by astroglia recruits CCR2-expressing peripheral monocytes into the parenchyma, leading to the activation of NFκB-mediated inflammatory pathways [188,191,290–292]. These studies suggest that peripheral adaptive immune responses could be involved in promoting neuroinflammation in GWI.

I hypothesize that exposure to PER results in 3-PBA haptenation of proteins and that haptenated proteins presented by antigen-presenting cells (APC) could activate T- and B-cells, resulting in autoantibody production. The presence of haptenated proteins in the CNS may promote infiltration of peripheral immune cells, which would further contribute to neuroinflammation. In this study, I determined the presence of 3-PBA-Lys in proteins and 3-PBA recovered from protein hydrolysis in the brains and livers of a GWI mouse model developed using combined PB and PER exposure. I examined the presence of autoantibodies against 3-PBA-haptenated albumin in plasma from GWI mice and in veterans with GWI. I investigated the ability of 3-PBA-haptenated albumin to activate peripheral T- and B-cells and determined that these immune cells are elevated in the blood of GWI mice and in veterans with GWI. I determined that proinflammatory monocytes capable of tissue infiltration are present in the blood of GWI mice. I also examined infiltrating monocytes and macrophages derived from these monocytes in the brains of GWI mice. Collectively, these studies will help determine the role of PER metabolites in activating adaptive immune responses in GWI. This work is published in the journal brain behavior and immunity[293].

We ***hypothesize*** that peripheral 3-PBA-haptenated proteins activate adaptive immune responses resulting in the production of autoantibodies against them. These autoantibodies promote antigen presentation by perivascular macrophages and promote brain entry of T-cells perviously primed by 3-PBA haptenated proteins. We propose that these T-cells encounter 3-PBA-haptanted protein primed memory B-cells in the cervical lymph nodes or in the periphery

which promotes the expansion of plasma B-cells that now produce autoantibodies against brain proteins that are similar to the peripheral 3-PBA-haptenated proteins and contribute to aberrant brain autoimmune responses in GWI.

Specific Aim 1: To identify peripheral autoantibodies against peripheral 3-PBA-haptenated proteins that also cross-react with normal proteins. To identify peripheral 3-PBA-haptenated proteins and autoantibodies against them in human and GWI mice

Specific aim 2: To identify 3-PBA-haptenated protein reactive B- and T-cells in the blood of GWI mice and in veterans with GWI.

Specific aim 3: To identify B- and T-cells which cross-react with normal brain proteins that are similar to 3-PBA-haptenated proteins.

4.2 Material and methods

4.2.1 Human subjects

Plasma and/or peripheral blood mononuclear cells (PBMC) were utilized from 3 different cohorts: (1) GWI and GW control veterans recruited at the Roskamp Institute Clinics (2) GWI cases and GW controls from the Boston Gulf War Illness Consortium (GWIC) and (3) subjects from Thailand who were farm workers or consumed pyrethroid-infested fruits and vegetables and either had positive or negative urine 3-PBA measurements. Plasma from age- and gender-matched GWI and control GW veterans were used for this study. Sample collection at the Roskamp Institute Clinics was approved by the WIRB, and all protocols were conducted in accordance with relevant guidelines and regulations. Recruitment of study subjects and blood collection to obtain plasma and PBMC has been described previously in chapter 1 [76,78,294]. Plasma and PBMC collection at the Boston GWIC were approved by the Boston University IRB. The Kansas GWI criteria [6] were used to diagnose GWI. The Kansas GWI criteria require that GW veterans show symptoms in at least 3 of 6 symptom domains (fatigue/sleep problems, somatic pain, neurological/cognitive/mood symptoms, gastrointestinal symptoms, respiratory symptoms, and skin abnormalities). Study participants were excluded if they reported being

diagnosed with another medical condition that could explain their chronic health symptoms. A detailed demographic table is provided in Table 5A and 5B. Subjects were also excluded from the study if they were currently on any steroid medication, to minimize interferences from the effects of these medications at the time of the blood draw. Controls were veterans deployed to the 1991 GW who did not meet the Kansas GWI criteria or any of the exclusionary criteria listed above. Self-report of pesticide exposure was based on questions which inquired whether they had worn a uniform saturated with pesticide and/or used pesticide cream/spray. Using these data, a summary variable was generated which assigned yes/no to pesticide exposure. Since the exposure status of GW veterans is based on self-report, we also examined plasma from samples obtained from farm and non-farm workers with documented exposure to pyrethroids and measurements of 3-PBA in urine. These were occupational health worker who were expose to different pesticides during their occupation. These were used as positive and negative controls for a 3-PBA-albumin autoantibody detection assay. All the participants gave their written consent, and the study was approved by their respective IRBs. A detailed demographic table is provided in Table 6. Many of these age- and gender-matched people had been exposed to pyrethroids during their occupation, and half of them had 3-PBA detected in their urine (n = 5 positive and n = 5 negative).

Table 5A. Demographics of the Gulf War veteran autoantibody cohort

	Controls (GW veteran)	GWI cases
N total	10	14
Age (Mean ± SEM)	54.3 ± 7.6	52.4 ±7.5
Male (%)	79.7%	86%
Self-report of pesticide exposure during war	5(50%)	95% (12)
Self-report of PB exposure during war	60% (6)	100% (14)
Ethnicity		
Caucasian	8 (70%)	11 (78.4%)
African American	2 (3%)	2 (14.2%)
Other/Multiracial	-	1 (7.13%)

Table 5B. Demographics of the Gulf War veteran Boston consortium cohort

	Controls (GW veteran)	GWI cases
N total	12	12
Age (Mean ± SEM)	51.23 ± 8.56	54.3 ±7.4
Male (%)	83.33%	100%
Self-report of pesticide exposure during war	25% (3)	83.33% (10)
Self-report of PB exposure	83.33%(10)	100%(12)
Ethnicity		
Caucasian	9 (75%)	10 (83.4%)
African American	2 (16.67%)	1 (8.3%)
Other/Multiracial	1 (8.33%)	1 (8.3%)

Table 6. Demographics of the subjects from Thailand.

	Negative Controls (no urine 3PBA detected)	Positive cases (urine3-PBA detected)
N total	5	5
Age (Mean ± SEM)	57.3 ± 7.6	61.4 ± 6.33
Male (%)	80%	80%
Pesticide exposure	20% (1)	66.6%(3)
PB exposure	0	0
Occupation		
Farm worker	60%(3)	60%(3)
Non-farm worker	40%(2)	40%(2)

There was no significant difference in age among two groups in all 3 tables above

4.2.2 Animals:

All procedures on mice were approved by the Roskamp Institute's Institutional Animal Care and Use Committee (IACUC) and were conducted in compliance with the Office of Laboratory Animal Welfare and laboratory animal care guidelines as previously described [53,157]. Mice were maintained with a 12h light/dark cycle in a temperature-controlled environment (21± 2 °C). Male C57BL/6 mice (3 months of age, weight 25 g ± 0.7 SD) were co-administered 0.7 mg/kg of pyridostigmine bromide (PB) (Fisher Scientific Hanover Park, IL) and 200 mg/kg of PER (Sigma Aldrich, St. Louis, MO, USA) in a single 50µl i.p. injection in dimethyl sulfoxide (DMSO) (Sigma Aldrich, St. Louis, MO,USA) or DMSO alone (control) daily for 10 consecutive days. Mice were divided in two groups, with the control group receiving vehicle only (DMSO) and the GWI group receiving vehicle along with PB and PER.

4.2.3 Detection and quantification of 3-PBA using LC/MS reverse phase analysis

Levels of 3-PBA in plasma, brain and liver were quantified as described by Ahn et al [295]. Briefly, 400mg of liver and 100mg of brain from both control and GWI mice were homogenized in 1mL of PBS, and a protein crash was then performed via the addition of 4mL of acetone. Samples were then subjected to acid hydrolysis by 1mL 6N HCL at 100°C for 2 hrs to hydrolyze covalent bonds between 3-PBA and proteins [295]. These samples were subjected to solid-phase extraction (SPE) using 8B-S100-UBJ Strata™-X 33µm polymeric reversed phase, 60mg/3mL spin columns (Phenomenex, Torrance, CA, USA) for clean-up and spiked with 10µM phenoxy-$^{13}C_6$-3-PBA (Cambridge Isotope, Tewksbury, MA, USA) internal standard (IS). Samples were analyzed by reverse-phase liquid-chromatography/mass spectrometry (LC/MS) using a Shimadzu LC-20AT HPLC system, with a 2.6µm EVO C18 100A 100 x 2.1mm Kinetex column (Phenomenex, Torrance, CA, USA). The mobile phases used were as follows: A (10 mM ammonium formate in water); B (100% Acetonitrile. A gradient was run from 90%

solvent A in 10% solvent B to 50% B in 6 min with a 4 min hold at 100% solvent B. with a flow rate of 100µL/min and column temperature at 40°C. Mass spectrometry analyses were conducted with high mass accuracy and parallel reaction monitoring (PRM) using a Q-Exactive (QE) hybrid quadrupole-Orbitrap mass spectrometer (Thermo Fisher Scientific, Waltham, MA, USA). Negative ion electrospray spectra were acquired at 17,500 resolution with a scan range from m/z 150 to 600. All spectra were obtained with a 100ms maximum ion injection time and 5 microscans. The 3-PBA IS (Cambridge Isotope Laboratories, Tewksbury, MA, USA) was monitored with m/z 219.1 as the precursor mass and product ions at m/z 99.053 and 175.084. For 3-PBA, I used m/z 213.1 as the precursor ion and m/z 93.033 and 169.065 as product ions.

4.2.4 Quantification of 3-PBA peptide using LC/MS reverse phase analysis

Levels of 3-PBA bound lysine in plasma, brain and liver were quantified as described by Noort et al [282]. Briefly, 400mg of liver and 100mg of brain from both control and GWI mice were homogenized in 1mL of PBS, and protein was precipitated by the adding 4mL of acetone at -20°C for 3 hrs. Precipitated protein was digested with 100µL of pronase solution (10mg/mL, 50mM NH4HCO3) for 1 hr at 37°C, then analysis with LC-tandem MS as explained above. In-house synthesis of 3-PBA-albumin (described below) was as standard. The 3-PBA-lysine was monitored with m/z 343.12 as the precursor mass and product ions at m/z 197.06.

4.2.5 Detection of 3-phenoxybenzoic in urine using GC-ECD

The first urine samples of the morning were collected and frozen at -20°C until they were analyzed for 3-PBA in urine samples and was detected as described by Pakvilai et al. (2014)[296]. Briefly, 50µL of 3-PBA (1µg/mL), as internal standard, was added to 2mL of urine sample, then mixed for 30 s. The urine samples were subjected to acid hydrolysis by adding 500µL of concentrated hydrochloric acid (37%) at 100°C for 2 hrs. Each sample was extracted

twice with 2mL of ethyl acetate (EA), followed by centrifugation at 2,500rpm for 5 min. The organic phase was separated, and sample cleanup was then performed on pre-conditioned C18– cartridges. The resulting solution was dried and dissolved in acetonitrile. The 3-PBA was analyzed by using a Hewlett-Packard 7890B-electron capture detector (GC-ECD) and Autosampler G4513A (Agilent Technology, CA, USA) equipped with HP-5 (5% phenylmethyl polysiloxane with 30m × 0.25mm, 0.25µm film thickness) after derivatization by 1,1,1,3,3,3-Hexafluoroisopropanol (HFIP) and N,N'-Diisopropylcarbodiim (DIC).

4.2.6 Preparation of 3-PBA-albumin conjugate

It has been shown that the 3-PBA metabolite of PER forms covalent adducts with albumin, and, due to its high abundance, albumin is often the major target of drug haptenation [56,297]. I chose albumin to test our hypothesis that 3-PBA can also haptenate albumin (3-PBA-albumin) and stimulate immune responses. I prepared a 3-PBA-albumin conjugate as described by Ahn et al, [298]. Briefly, 65mg of 3-PBA (Sigma Aldrich, St. Louis, MO, USA) and 92mg 1,3-dicyclohexylcarbodiimide (DCC) (Sigma Aldrich, St. Louis, MO, USA) was dissolved in 4mL of N,N-Dimethylformamide (DMF)(Sigma Aldrich, St. Louis, MO,USA). The active ester in 3-PBA was formed by adding 52mg of N-hydroxysuccinimide (NHS) (Thermo Fisher Scientific, Waltham, MA USA) and allowed to react for 5 hrs at room temperature after which, 10mL of 50mM bovine or human serum albumin in pH 8 borate buffer was added to the solution and allowed to react overnight. The resulting precipitate containing 3-PBA-albumin was collected and dialyzed (12,000 Da) against PBS for 3 days to remove low molecular weight contaminates. For mouse studies (including blood culture studies), bovine albumin was used as previous studies have shown that mouse and bovine serum albumin (BSA) share 72% amino acid homology, and BSA is immunologically inactive in mice [299]. For human studies, human albumin was used.

4.2.7 3-PBA-albumin autoantibody detection in GWI plasma:

Both free albumin and 3-PBA-albumin were subjected to sodium dodecyl sulfate (SDS) polyacrylamide gel electrophoresis in 4-20% Criterion™ TGX Stain-Free™ Precast Gels (Bio-Rad, Hercules, CA, USA). These proteins were then transferred to a polyvinylidene difluoride (PVDF) membrane for 4 hrs at 60mA. After blocking in 5% milk for 1 hr, GWI mouse plasma and control mouse plasma was used as a source of antibody. The membrane was incubated in GWI mice or control mice plasma (1:300) overnight at 4°C. Membranes were then incubated in HRP-linked mouse secondary anit-IgG antibody, and the blot was developed using SuperSignal West Femto Maximum Sensitivity Substrate (Thermo Fisher Scientific Waltham, MA USA) and visualized using a chemiluminescence imager (Bio-Rad, Hercules, CA, USA) as described previously [78].

4.2.8 *Ex vivo* whole blood flowcytometry studies

To test our hypothesis that 3-PBA albumin can stimulate immune response and activate T and B lymphocytes, blood from control mice was collected following a cardiac puncture**.** Blood was then combined with 2% EDTA and cultured in RPMI media (Gibco, Carlsbad, CA, USA) at 37°C in a humidified atmosphere containing 5% CO^2 supplemented with 1% of penicillin-streptomycin solution and 10% FBS. Cultured blood was then treated with 5µm 3-PBA-albumin, 5µm 3-PBA and 5µm albumin for 12 hrs followed by red blood cell (RBC) lysis and stained with antibodies against the cell surface markers: CD4 (Thermo Fisher Scientific, Waltham, MA, USA), CD8 (Thermo Fisher Scientific, Waltham, MA USA), CD3 (Thermo Fisher Scientific, Waltham, MA USA), CD19 (Thermo Fisher Scientific, Waltham, MA USA), CD27 (Thermo Fisher Scientific, Waltham, MA USA) and CD45R (B220) (Thermo Fisher Scientific, Waltham, MA, USA). These cells were analyzed using Attune® NxT Acoustic Focusing Flow Cytometer (Thermo Fisher Scientific, Waltham, MA USA). Flow cytometry analyses were done using Attune® NxT software version 2.7 (Thermo Fisher

Scientific, Waltham, MA, USA). Flow cytometry data were presented as total percentage change, and graphs were generated using GraphPad Prism7. CD4+CD3+ staining was used to identify T-helper cells while CD3+CD8+ staining was used to identify cytotoxic T-cells [73]. CD19+ and CD27+ were used to distinguish memory and naïve B-cell population [300].

4.2.9 Detection of mouse blood monocytes and lymphocyte (B- and T-cells) using flow cytometry

Whole blood was drawn from mice and 100µL was subjected to red blood cell (RBC) lysis using 1mL of RBC lysis buffer (Thermo Fisher Scientific, Waltham, MA USA), washed twice with PBS-containing 5mM EDTA and 0.5% FBS and stained with CD45 (Thermo Fisher, Waltham, MA USA), CD115 (BD bioscience, NJ, USA), Ly6C (BioLegend, San Diego, USA) and CD11b (BD Bioscience NJ, USA) antibodies for flow cytometry analysis. Monocytes were identified by gating cells that were positive for both CD11b and CD115 [57,301]. Patrolling and infiltrating monocyte populations were identified by CD11b+ CD115+ with Ly6C- and CD11b+ CD115+ with Ly6C+ respectively [302]. Ly6C+ monocytes are defined as proinflammatory and tissue-infiltrating while Ly6C++ are phagocytic monocytes[301]. Flow cytometry analysis was conducted using combinations of these monoclonal antibody using Attune® NxT Acoustic Focusing Flow Cytometer (Thermo Fisher Scientific, Waltham, MA USA).

In another experiment, 150µL of whole blood from the same mice was lysed via addition of 1500µL of RBC lysis buffer (Thermo Fisher Scientific, Waltham, MA, USA). The monocytes and lymphocytes were pelleted by centrifugation at 700 x g for 10min and resuspended in 500µL of FACS buffer (PBS, 0.5-1% BSA or 5-10% FBS, 0.1%), to which 10µL of CD4/CD8 antibody cocktail (Thermo Fisher Scientific, Waltham, MA USA) was added. Cells were incubated with the cocktail for 20min at room temperature. Lymphocyte populations were gated, and CD4+ and CD8+ cells were analyzed using Attune® NxT Acoustic

Focusing Flow Cytometer (Thermo Fisher Scientific, Waltham, MA USA). CD3+CD4+ are used to identify T-helper cells while CD3+CD8+ cells are used to identify cytotoxic T-cells. These cells were analyzed as described above. For B lymphocytes, a combination of CD27, CD19 and CD45R (B220) stains were used as described previously; detail on antibodies used is provided above. As described previously, these were used to distinguish memory and naïve B-cell population [300].

4.2.10 Labeling of human PBMC for T- and B- lymphocytes:

The peripheral mononuclear cells provided by GWIC(Boston) were treated with monoclonal antibodies conjugated to different fluorophores. To find the T-cell population, cells were incubated with Anti-human CD3/CD4/CD8 Cocktail (Biolegend, San Diego, CA USA). To find memory B-cell population, a combination of CD19 (Thermo Fisher Scientific, Waltham, MA, USA) and CD27 (Thermo Fisher Scientific, Waltham, MA, USA) antibodies were used and analyzed using Attune® NxT Flow Cytometer as described above.

4.2.11 Flowcytometry studies of the brain myeloid and microglia cells

A single cell suspension was generated from adult mouse brains, using the Adult brain dissociation kit from Miltenyi Biotec (Cologne, Germany) and closely following the manufacturer instructions. Briefly, mouse brains were collected in serum-free media and chopped finely with a sterile scalpel blade. The brains were subjected to a combination of enzymatic Papain (1 ug/uL) mechanical digestion (pipetting up and down 20 times) to yield a single cell suspension, the brain homogenate was then passed through a 70µm strainer, and the cell suspension was centrifuged for 10min at 1000xG and 4°C. Cell pellets were then resuspended in debris removal solution and carefully overlaid with 4ml D-PBS as per manufacturer instructions; the samples were then centrifuged at 3000xG for 10 minutes at 4°C in a swinging bucket rotor with minimal brake. Following centrifugation four phases were

formed in the tube, the upper 2 phases were aspirated, the remaining (glial cell containing) fraction was then resuspended in D-PBS, inverted multiple times and centrifuged at 1000xG for 10 minutes to generate a pellet containing a mixed glial cell population. The microglia population was then isolated by magnetically activated cell sorting (MACS), using anti-CD11b conjugated magnetic microbeads (Miltenyi Biotec, Cologne, Germany) according to the manufacturer's protocol. Briefly, cells were incubated with 10μL CD11b microbeads for 15min at 4 °C. Cells were then washed and placed on a new LS magnetic column (Miltenyi Biotec, Cologne, Germany) in a magnetic holder. The CD11b-ve fraction was washed through the column, and the CD11b+ve cell fraction was eluted from the column by removing the column from the magnetic field, adding buffer and emptying the column with a plunger. Cells were incubated with Rat anti-mouse Fc-block (1:100 BD bioscience) for 5min at room temperature. These cells were then stained with monoclonal antibodies for desired surface markers. The antibodies used were CD11b (BioLegend San Diego, USA), CX3CR1(BioLegend, San Diego, USA), Ly6c (BioLegend San Diego, USA) and CD206 (BioLegend San Diego, USA). Details on the antibodies used are provided in the supplementary table S6. These cells were analyzed as described above using an Attune® NxT Acoustic Focusing Flow Cytometer (Thermo Fisher Scientific, Waltham, MA USA). A combination of CD11b+, CX3CR1+, CD206+, and Ly6C+ staining was used to analyze brain macrophages, and cells stained with CD11b+, CX3CR1+, and CD206- were classified as microglia [303–306]

4.2.12 Immunostaining for microglia and astrocytes:

The left-brain hemispheres were fixed in 4% paraformaldehyde (PFA), dehydrated and embedded in paraffin. Sagittal sections (8μm) were prepared using Leica RM2235 microtome (Leica, Buffalo grove, IL). Approximately 8 to 10 slices of each mouse brain were incubated in blocking buffer (10% donkey serum and 0.3% Triton X-100 in PBS) for 60min at room temperature. Samples were then incubated overnight with the primary antibody Rabbit anti-IBA-1 (Wako, Osaka, Japan) and Chicken anti-GFAP (Aves Lab, Tigard, Oregon) at 4°C. The

following day, slices were incubated with the appropriate fluorescent probe-conjugated secondary antibodies for 1 hr at room temperature. Nuclei were counterstained with DAPI. The entire DG was scanned using an Axiovert 200M Zeiss microscope (Zeiss) equipped with AxioVision 4.8.3.0 software. ImageJ software was used to analyze the stained sagittal sections. The stained areas were calculated and expressed as a percentage of the field.

4.2.13 Enzyme-Linked Immunosorbent Assay

Using a Dounce homogenizer, brains were homogenized in ice cold mPER, which contained protease (Roche, Indianapolis, IN, USA) and phosphatase inhibitor (Pierce, Grand Island, NY, USA) cocktails. The total protein content of each sample was determined by the bicinchoninic acid (BCA) assay (Pierce, Grand Island, NY, USA). Enzyme-Linked Immunosorbent Assay (ELISA) kits for mouse CCR2 (Lifspan Biosciences, Seattle, WA,USA), CCL2 (Lifspan Biosciences, Seattle, WA, USA), Matrix Metalloproteinase-9 (MMP-9) (Bosterbio, Pleasanton, CA, USA) and fractalkine (CX3CL1) protein (MyBiosource, San Diego, CA,USA) were used to study levels of these proteins in the brain using the manufacturer's protocol. Soluble CX3CL1(Thermo Fisher Scientific, Waltham, MA USA) in human plasma were quantified using commercial ELISA kit. The level of IgG protein in blood was quantified by IgG ELISA (Cayman Chemical, Ann Arbor, MI, USA) according to the manufacturer's instruction. MMP-9 is proteolytic protein capable of degrading tight junction protein leading to BBB impairment [307,308]. Results were normalized to total protein quantification obtained from BCA. Intra-Assay: CV<10.6% Inter-Assay: CV<12.6% for all the ELISAs. There was no reported cross-reactivity with other proteins for the primary antibody used in these kits.

4.2.13 Western Blot analyses

CX3CR1 (Abcam, Cambridge, MA, USA), p- NFκB phosphorylated at Ser536 (Cell Signaling, Danvers, MA, USA), total p65 NFκB (Cell Signaling, Danvers, MA, USA), tubulin (Abcam, Cambridge, MA, USA), major histocompatibility complex-II (MHC-II) (Abcam Cambridge, MA, USA), actin (Cell signaling, Danvers, MA, USA) and occludin (Santa Cruz biotechnology**,** Santa Cruz, CA, USA) were analyzed using Western Blotting. MHC-II are markers of antigen-presenting cells [309,310]. In the brain, microglia and macrophages are the main cells expressing MHC-II [309]. Occludin is a tight junction protein used to analyzed BBB impairment [311,312]. Western Blotting was performed as described previously [78]. Horseradish peroxidase–conjugated appropriate secondary antibodies and loading control anti–β-actin or tubulin antibody was obtained from Cell Signaling. The blots were analyzed as described previously in chapter 2[78].

4.2.14 Multiplex cytokine assay

Selected cytokine levels in the plasma were analyzed using Meso Scale Discovery (MSD) 96-Well MULTI-SPOT® Ultra-Sensitive V-PLEX Proinflammatory cytokine Panel 1 mouse Kit (MSD, Rockville, MD, USA), using electrochemiluminescence detection on an MSD Sector Imager™ 6000 with Discovery Workbench software (version 3.0.18) (MSD®, Gaithersburg, MD, USA). Cytokines were measured using the TH1/TH2 8-plex kit which included interleukin-1β (IL-1β), IL-6, interferon-γ (IFN-γ) and tumor necrosis factor-α (TNF-α). All assays were performed according to the manufacturer's instructions, in duplicates as described previously [78]. Human plasma were analyzed using V-PLEX Proinflammatory cytokine Panel 1 Human Kit **(**MSD, Rockville, MD, USA) according to manufacturer protocol.

4.2.15 Statistical analyses

Normally distributed data were analyzed using parametric tests; otherwise non-parametric tests were used. As applicable, the Student's t-test was used to examine the group

differences between GWI and control mice for cytokines, chemokines and percentage of specific cells identified using flow cytometry and protein levels of p-NFκB, occludin, MMP9, IgG and MHC-II. Murine cytokine data were analyzed by using the Student's t-test. Human cytokine data were not normally distributed, so Kolmogorov-Smirnov test (K-S test) was performed on them to check if they were statistically significant. For autoantibody analysis in the GW veteran cohort, the Chi-square test was performed to determine statistical significance. For multiple groups in blood culture studies, I used one-way analysis of variance (ANOVA) followed by the Tukey *post-hoc* test. A p value < 0.05 was considered statistically significant. These analyses were performed using GraphPad Prism7 (San Diego, CA, USA), and data were expressed as means ± standard errors. All graphs were generated using GraphPad Prism7 (San Diego, CA, USA).

4.3 Results

4.3.1 Detection of 3-PBA released following protein hydrolysis and 3-PBA-modified lysine residues from peptides in the brain, liver and plasma of GWI mice

For an acute post-exposure timepoint, I examined 3-PBA modified proteins in liver, brain and plasma of GWI mice euthanized at 1-day post-exposure. I also examined a serum sample of a subject positive for 3-PBA in urine as a positive control. Figure 4.1A shows PER metabolite structures and detected ions that correspond with the presence of 3-PBA lysine residues after pronase digestion that was performed to release these adducts from peptides (Figure 4.1B). I also quantified 3-PBA released post-protein-hydrolysis which showed the presence of 3-PBA in the livers and brains of GWI mice at 1.5 months post-exposure (Figure 4.1C and 4.1D). However, free 3-PBA was detected only in the livers but not in the brains of GWI mice. As expected, no 3-PBA was detected in control mice. Neither free nor protein-conjugated 3-PBA was detected in the brains or livers of GWI mice at 3- or 7-months post-exposure.

Figure 4.1A

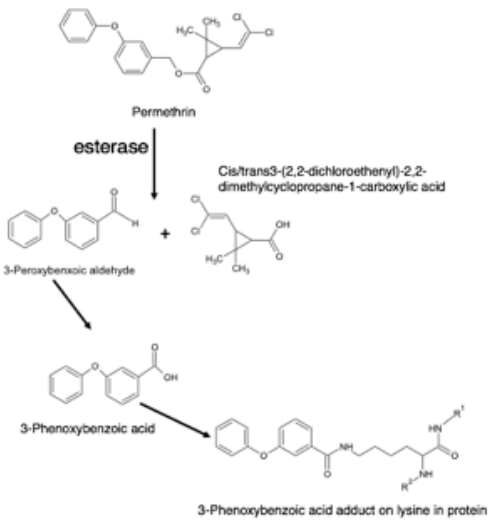

Figure 4.1B

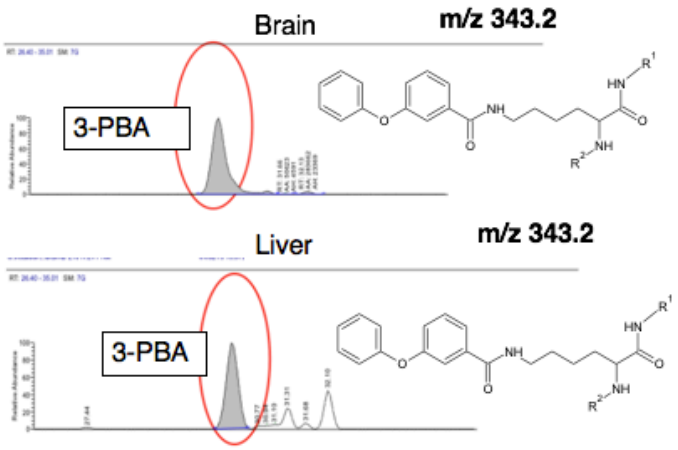

Sample	Precursor ion (m/z 343.2)	Production (m/z 197.060)
GWI mice (Liver and brain)	Detected at 30 min retention time	Detected at 30 min retention time
Control mice (Liver and brain)	Not detected	Not detected

Figure 4.1C

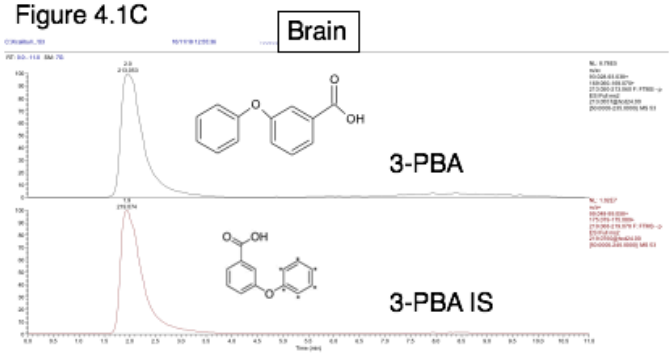

Figure 4.1D

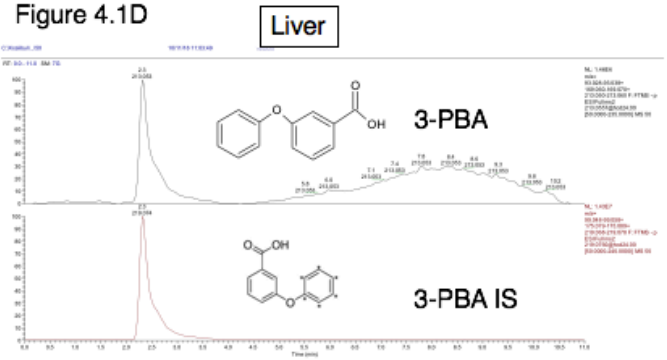

Analyte	Precursor ion	Production
3-PBA IS	(m/z 219.1) detected at 3 min retention time	m/z 99.050,1and 175.08 detected at 3 min retention time
3-PBA	(m/z 213.1) detected at 3 min retention time	m/z 93.03and 169.06 detected at 3 min retention time

Figure 4.1E

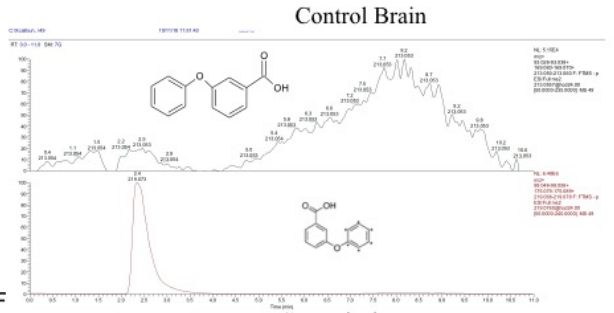

Figure 4.1F

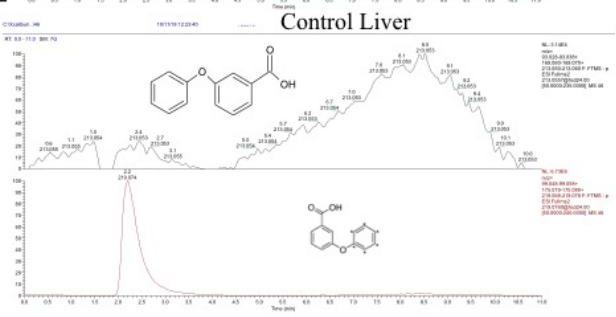

Figure 4.1: Metabolites of PER pesticide is detected as protein adducts in the brain and liver homogenates. (A) A schematic of PER metabolites. (B) Detection of precursor and product ion of 3-PBA lysine (343.2) and its product ions (197.06) in the brain and liver homogenates from a GWI mouse sample. (C and D) Using LC-MS and LC-MS/MS, I detected 3-PBA (m/z 213.055 at 2.3min) and its PRM product ion (m/z 213.1 > 93.033 at that same time) in the brain and liver (mean ± SE (n = 4 or 5/group). While only protein-conjugated 3-PBA recovered after hydrolysis was detected in the brain, free 3-PBA and protein-conjugated 3-PBA were detected in the liver at 1.5 months post-exposure.(E-F) Peak plots show absence of 3-PBA (m/z 213.055 at 3min) and its transition ion (m/z 93.033) ions in control mice (E)brain and (F)liver. These peak plots show presence of 3-PBA internal standard 219.1 at 3min and its transition ion (m/z 93.033) ions in control mice

Table 7: Final concentration of 3-PBA elimination in the urine

code no.	3-PBA conc. (mg/L)	Sex
SPT-C-1-001	ND	male
SPT-C-1-002	ND	female
SPT-C-1-004	ND	Female
SPT-C-1-012	ND	Male
SPT-C-1-013	ND	Male
SPT-C-1-003	0.02740	Male
SPT-C-1-005	0.01080	female
SPT-F-1-019	0.14520	Male
SPT-F-1-024	0.05236	Male
SPT-F-1-026	0.06011	male

Note: These data were generated by collaborator (Dr. Hongsibsong) who gave permission to publish these data.

4.3.2 3-PBA-albumin autoantibodies in plasma from GWI mice and in GWI veterans

Western blot analyses showed that while plasma from control mice did not have immunoreactivity to free albumin or 3-PBA-albumin, plasma from GWI mice showed a strong immunoreactivity with 3-PBA-albumin but not with free albumin (Figure 4.2A). We then examined if 3-PBA-human albumin-reactive autoantibodies were detectable in plasma from GW veterans. Plasma from 10 out of 12 GW veterans diagnosed with GWI showed immunoreactivity to 3-PBA-albumin, and 1 out of 10 healthy GW veterans had immunoreactivity to 3-PBA albumin ($\chi^2 = 11.73$, df = 1, $p = 0.001$, Figure 4.2 B). None of the plasma samples from GW veterans showed any immunoreactivity to albumin alone (Figure 4.2 B). There was a significant association between self-report of pesticide exposure and 3-PBA-albumin autoantibody presence among veterans with GWI ($\chi^2 = 9.46$, df = 1, $p = 0.03$). Only one control GW veteran had 3-PBA-albumin autoantibodies and was exposed to pesticides.

Two additional controls who didn't have autoantibodies did report pesticide exposure, where one subject had an exposure to fogged area whereas the other subject did report exposure to pesticide imbedded uniforms, creams and sprays. In another cohort from Thailand, I detected 3-PBA- albumin autoantibodies in serum of 5 subjects who had positive 3-PBA urine levels, whereas 5 control serum samples with undetectable urinary 3-PBA levels did not show immunoreactivity to 3-PBA-albumin (Figure 4.2C).

Figure 4.2

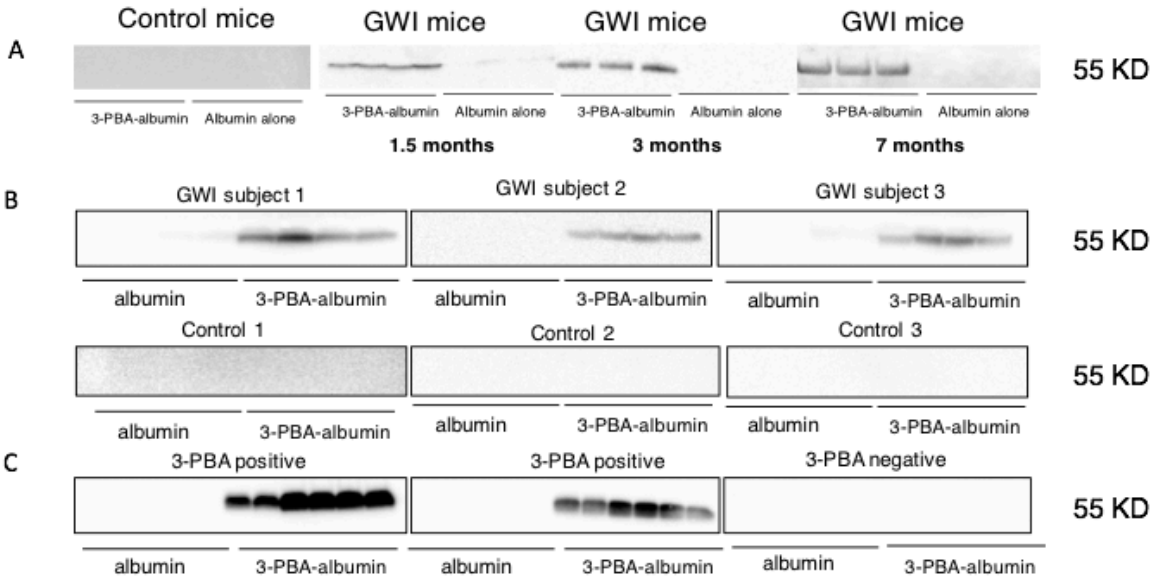

Figure 4.2: Chronic elevation of autoantibodies against 3-PBA-albumin in plasma of GWI mice, in veterans with GWI and in farm workers exposed to pyrethroids. Western Blot showed that control mice had no cross-reactivity to 3-PBA-albumin or albumin alone, but cross-reactivity in GWI mice plasma was observed for 3-PBA-albumin at 1.5-, 3- and 7-months post-exposure in GWI mice (n = 4 or 5/group). (B) Autoantibodies against 3-PBA-albumin were detected in 12 out of 14 veterans with GWI and 1 out of 10 control GW veterans. (C) Immunoreactivity of plasma with 3-PBA-albumin was observed in 5 out of 5 pyrethroid-exposed farm workers or ate pyrethroid tainted fruits and vegetables (as confirmed using 3-PBA measurements in urine), and a lack of immunoreactivity in controls in whom urine 3-PBA was undetected.

4.3.3 Peripheral T-cells and B-cells activated following 3-PBA-albumin treatment

Murine blood was cultured overnight to examine if 3-PBA-albumin as compared to albumin alone, 3-PBA alone and control treatments can activate B-cells, T-cells and monocytes. Antigen-responsive CD19+ CD27+ B-cells were significantly different between the four groups ($F_{(3,12)}$=12.2, p = 0.001, Figure 4.3A), with the 3-PBA-albumin group being significantly elevated compared to all other groups (*post-hoc* $p < 0.05$). Group comparisons for CD3+ CD4+ T-helper cells showed significant differences between treatments ($F_{(3,16)}$ = 61.19, p = 0.001, Figure 4.3B) with *post-hoc* analyses showing increases in CD3+CD4+ T-helper cells by 3-PBA-albumin treatment as compared to controls, 3-PBA and albumin alone ($p < 0.05$). There were no differences in CD3+CD8+ T-lymphocytes when treated with 3-PBA-albumin compared to all other treatments ($p > 0.05$). Total monocyte population gated by CD11b+ and CD115+ differed significantly between the groups ($F_{(3,12)}$ = 20.48, p = 0.001, Figure 4.3C), and *post-hoc* comparisons showed an increase in these cells in the 3-PBA-albumin group compared to others ($p < 0.05$). Consistently, IgG levels were increased by 3-PBA-albumin treatment compared to all other groups ($F_{(3,12)}$ = 221.8, p = 0.001 Figure 4.3D).

Figure 4.3A

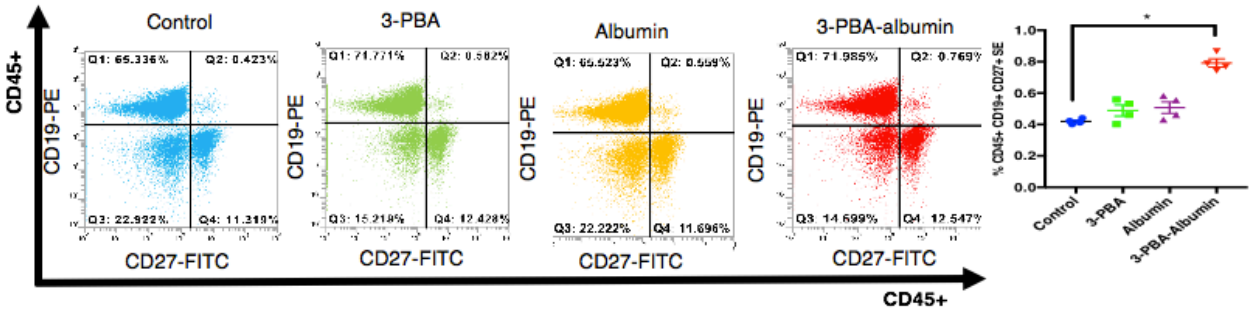

Figure 4.3B

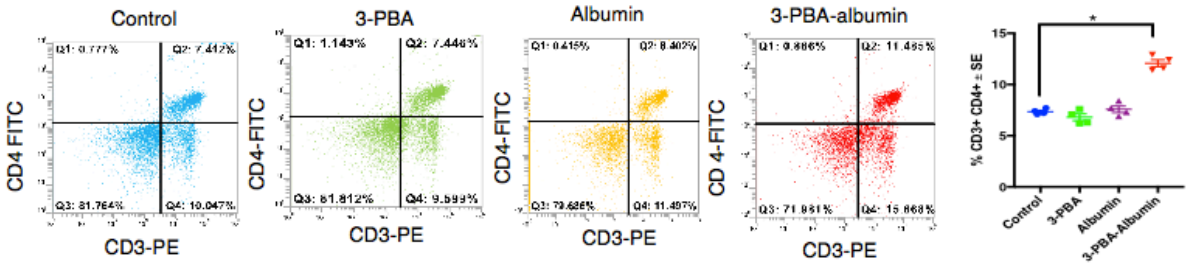

Figure 4.3C

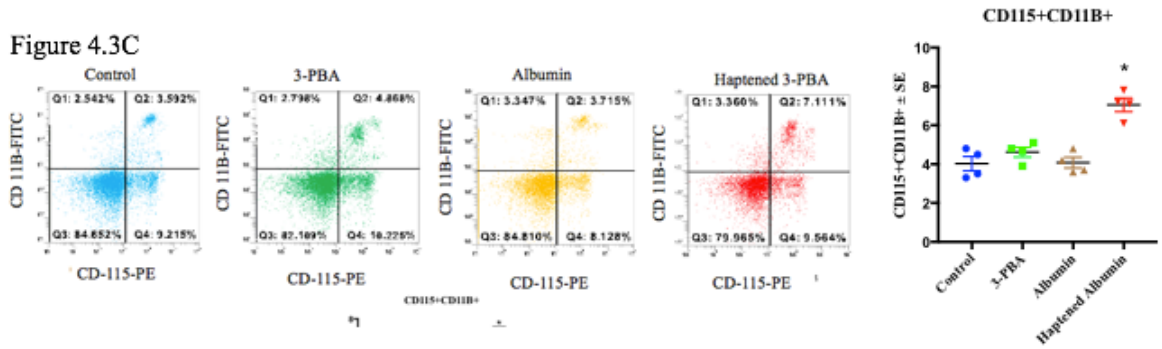

Figure 4.3D

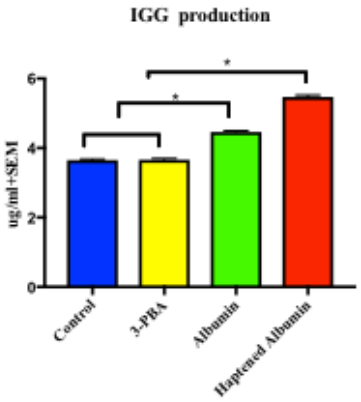

Figure 4.3: 3-PBA-albumin treatment increased memory B-cell and T-helper cells in murine blood. Mean ± SE (n = 4 per group). (A) After overnight incubation of murine blood with 3-PBA, albumin and 3-PBA-albumin, antigen-responsive CD45+ CD19+ CD27+ B-cells are significantly elevated in 3-PBA-albumin compared to all other treatments. (B) T-helper cells, CD3+CD4+, were also elevated upon 3-PBA-albumin treatment. Comparisons between 3-PBA and controls and albumin and controls were not significant. (C) antigen responsive CD11B+ CD115+ cells are significantly elevated in 3-PBA-albumin compared to all other treatments (D) Quantification of IgG in blood by ELISA. *ANOVA with post-hoc tukey* $*p < 0.05$

4.3.4 Activated peripheral immune cells and plasma proinflammatory cytokines are increased in the blood of GWI mice and veterans with GWI

An antigen-reactive B-cell population positive for CD45+CD19+ CD27+ was elevated in the blood of GWI compared to control mice ($t\text{-test}_{(df=6)} = 5.7$, $p = 0.0012$, Figure 4.4A). However, the CD19+ CD27- population did not differ between the two groups ($p > 0.05$) suggesting that while total B-cell population doesn't change, antigen responsive B-cells

proportionally increase. Higher levels of IgG were present in blood from GWI mice compared to controls (t-test$_{(df=5)}$ = 4.5, p = 0.008). I analyzed CD4+ and CD8+ markers after gating on the blood lymphocyte population. This study revealed that CD4+ T-helper cell population was significantly higher in the lymphocytes of GWI mice compared to control (t-test$_{(df=7)}$ = 2.7, p = 0.024, Figure 4B). T-helper cells expressing CD3+CD4+ were also elevated in the blood of GWI mice (t-test$_{(df=6)}$ = 5.3, p = 0.0017, Figure 4B). Although CD8+ lymphocytes didn't differ between the two groups (p > 0.05), the ratios of CD4+ to CD8+ cells were elevated in GWI compared to control mice (t-test$_{(df=6)}$ = 3.7, p = 0.0014, Figure 4.4B). In addition, at 7 months post-exposure, several proinflammatory cytokines, including IL-1β, IL-6, IFN-γ and TNF-α and a chemokine CX3CL1 were elevated in the brain and plasma from this GWI mouse model (Figure 4.3C).

Figure 4.4A

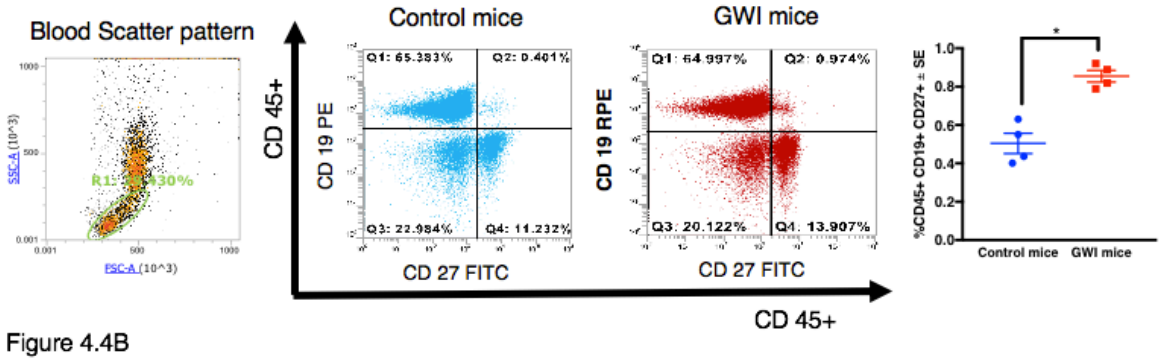

Figure 4.4B

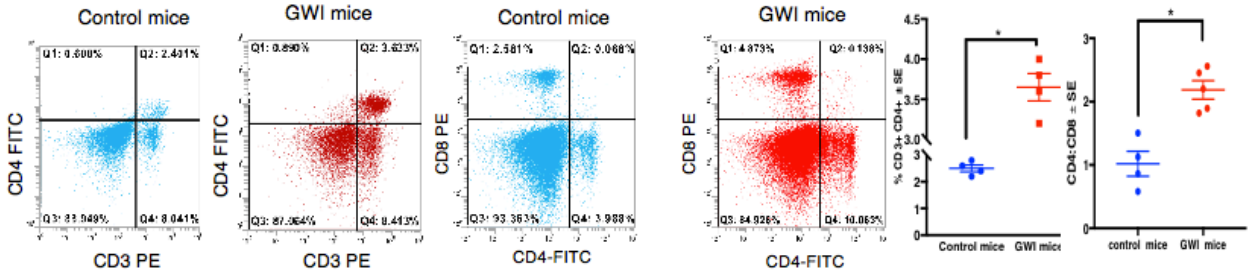

Figure 4.4C

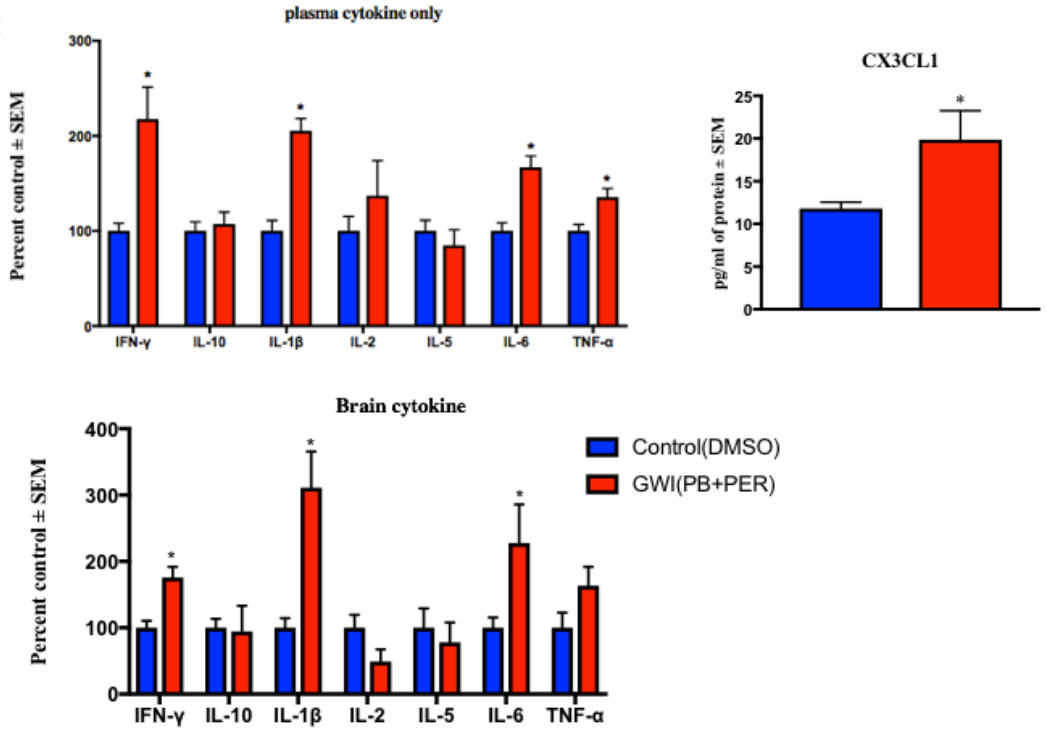

Figure 4.4: Antigen-activated B- and T-cells are increased in blood of GWI mice at 7 months post-exposure. Mean ± SE (n = 4/5 per group). (A) Increased staining of antigen-responsive CD19+ CD27+ B-cells were detected in GWI compared to control mice. (B) Panel B shows that CD3+CD4+ T.cells are increased in blood of GWI mice. However, CD8+ T.cells did not differ between the two groups. Ratios of CD4:C8 was significantly elevated in GWI mice.(C) Pro-inflammatory cytokines and chemokines are chronically elevated in plasma and brain in GWI mice. T-test *$p < 0.05$

I also examined peripheral T- and B-cells in PBMCs from GWI and control GW veterans. The memory B-cell population, as defined by CD19+CD27+ cells, was significantly increased in GWI compared to healthy GW veterans ($t\text{-test}_{(df = 20)} = 5.01$, $p = 0.0014$, Figure 4.5A). T-helper cells expressing CD3+CD4+ are also elevated in GWI veterans ($t\text{-test}_{(df = 28)} = 8$, $p = 0.001$, Figure 4.5B). Although CD3+ CD8+ T-cells didn't differ between the two groups ($p > 0.05$), the ratios of CD4+ to CD8+ cells were elevated in GWI compared to control GW veterans ($t\text{-test}_{(df= 20)} = 3.7$, $p = 0.0014$). Compared to healthy GW veterans, plasma levels of proinflammatory cytokine IL-1β and CX3CL1 were higher in veterans with GWI (Figure 4.5C).

Figure 4.5A

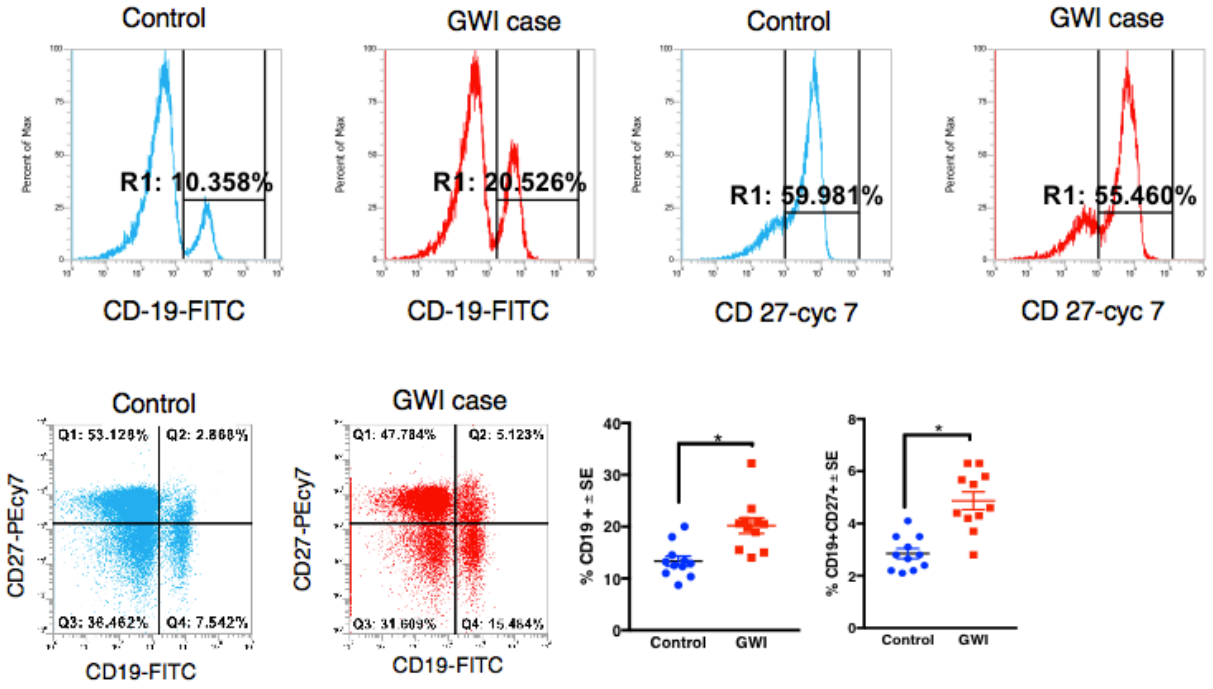

Figure 4.5B

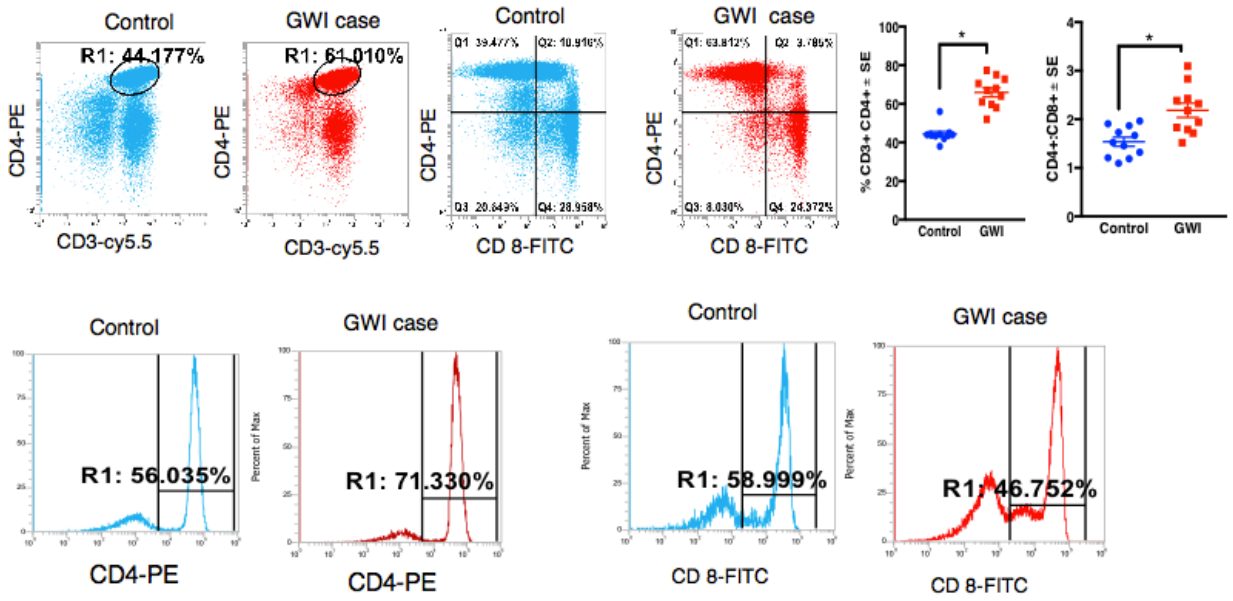

Figure 4.5C

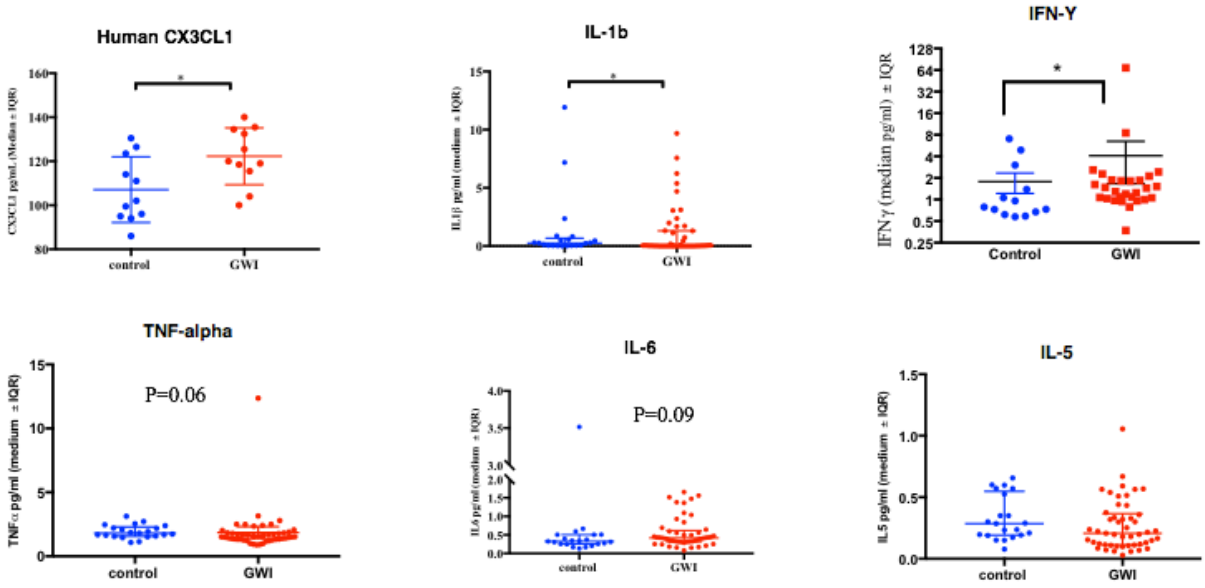

Figure 4.5: Memory B- and CD4 T-cells are increased in blood of veterans with GWI. Mean ± SE (n = 12 per group). (A) Increased staining CD19+ and CD19+ CD27+ memory B-cells in blood of veterans with GWI compared to healthy GW control veterans. (B) CD3+CD4+ T_H cells are increased in blood of veterans with GWI. However, CD8+ T_H cells did not significantly differ between control and GWI veterans. However, there were no group differences for CD3+CD8+ T_H cells.(C) Pro-inflammatory cytokines and chemokines are chronically elevated in plasma in GWI human. Kolmogorov–Smirnov **test** *$p < 0.05$

4.3.5 Disruption of the BBB in GWI mice

Since MMP-9 is increased during inflammation, I examined MMP-9 levels in the brain homogenates from GWI and control mice. MMP-9 was significantly higher in the brains of GWI mice ($t\text{-test}_{(df=10)} = 2.81$, $p = 0.018$, Figure 6B). Assessment of BBB integrity examined using occludin showed a significant decrease in GWI compared to control mice ($t\text{-test}_{(df=10)} = 2.5$, $p = 0.029$, Figure 4.6A). As increases in brain IgG levels are generally indicative of BBB impairment. Levels of IgG were increased in the brains of GWI mice compared to controls ($t\text{-test}_{(df=10)} = 2.61$, $p = 0.026$, Figure 4.6B).

Figure 4.6

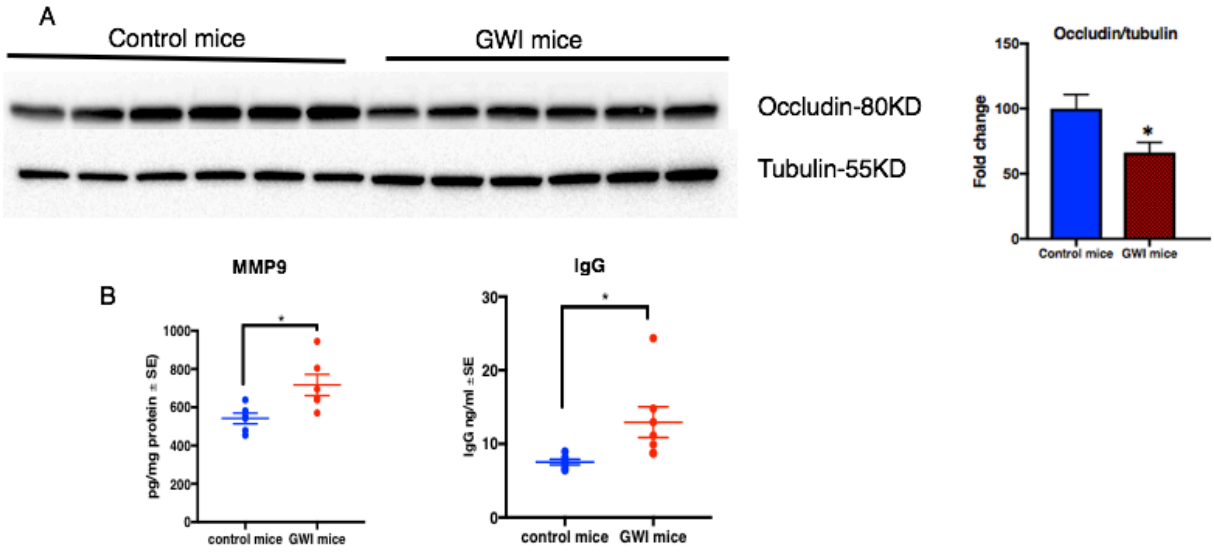

Figure 4.6: GWI mice showed evidence of BBB impairment. Mean ± SE (n = 6 per group). (A) Occludin was decreased in the brains of GWI mice whereas (B) MMP-9 and IgG were increased in GWI mice brain. T-test *$p < 0.05$

4.3.6 Infiltrating monocyte population in the blood and brain of GWI mice

Monocytes staining with CD11b+ CD115+ and Ly6C+ classified as proinflammatory and infiltrating were elevated in GWI blood compared to control mice (t-test$_{(df= 11)}$ = 3.7, p = 0.0032, Figure 4.7A). Macrophages were detected using Cd11b+ CD206+ Ly6C+ positive stains were increased in the brains of GWI compared to control mice (t-test $_{(df= 2.8)}$ = 4.7, p = 0.04, Figure 4.7B). The microglia population characterized by CD11b+, CX3CR1+, CD206- Ly6C- showed no differences between the two groups (Figure 4.7C). Infiltrating monocytes detected by CD11b+ CX3CR1- Ly6C+ were significantly increased in the brains of GWI mice compared to controls (t-test$_{(df= 4)}$ = 4.7, p = 0.01, Figure 4.7D). We also observed increased MHC-II protein levels in the brains of GWI mice compared to controls (t-test $_{(df= 6)}$ = 6.2, p = 0.0007, Figure 7E).

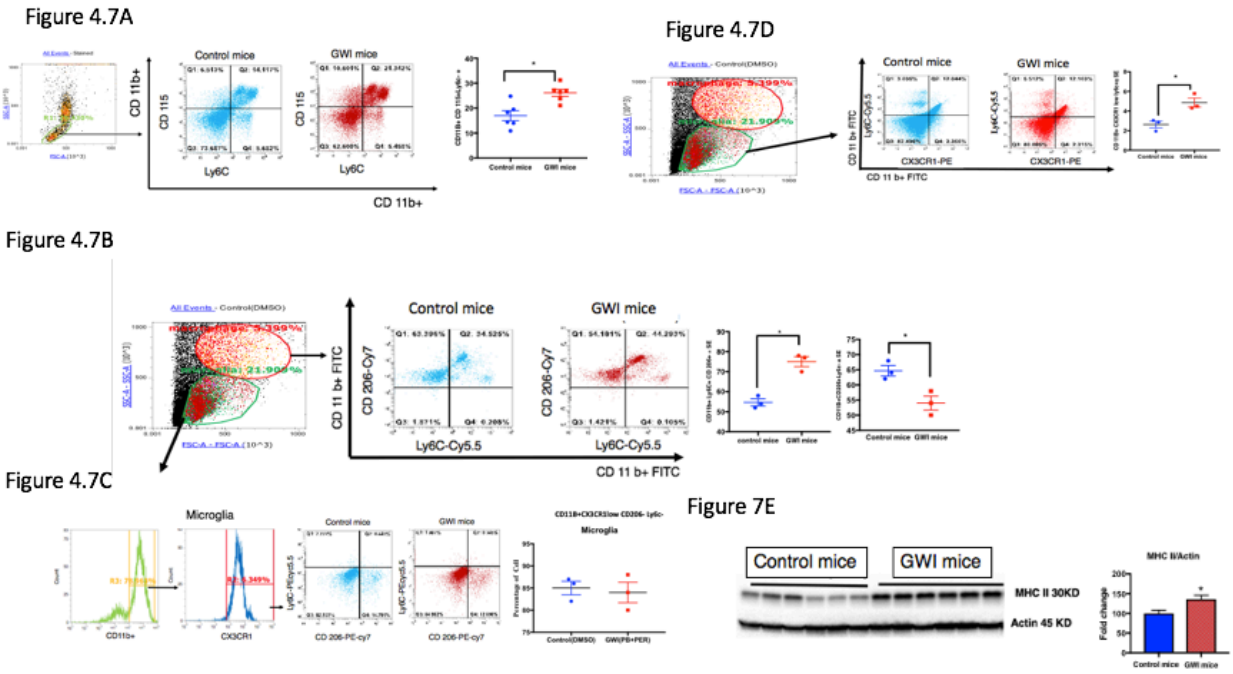

Figure 4.7: Infiltrating monocytes are increased in blood and brains of GWI mice at 7-8 months post-exposure. Mean ± SE (n = 12 per group) (A) Increases in blood monocyte gated by CD11B+ CD115+ and Ly6C+ in GWI mice were observed. (B) GWI mice brain showed increased macrophage population as detected by CD11b+CD 206+Ly6C+ but (C) no change in microglia population detected by CD11b+CX3CR1+ and CD206-. (D) Infiltrating monocytes converting to macrophage (CD11b+, CX3CR1- and Ly6C+) were also increased in the brains of GWI mice. (E) Increase in MHC-II in the brain of GWI mice was detected by Western Blot. T-test $*p < 0.05$

4.3.7 Chemokines and their receptors that promote CNS and peripheral immune cross-talk in are increased in GWI mice

Since plasma CX3CL1 levels were increased in GWI mice and in veterans with GWI, I examined its receptor CX3CR1 in the brain homogenates from GWI and control mice at 7 months post-exposure. Levels of CX3CR1 were elevated in GWI mice compared to control mice ($t\text{-test}_{(df=5)} = 3.1$, $p = 0.03$, Figure 4.8A). There were no differences in the membrane fraction of the brain homogenates for CX3CL1 levels between GWI and control mice at 7

months post-exposure ($p = 0.86$, Figure 4.8B). Levels of CCR2 (t-test$_{(df= 10) = 4.71}$, $p = 0.0008$, Figure 4.8C) and its ligand CCL2 (t-test$_{(df= 10)} = 3.9$, $p = 0.003$, Figure 4.8D) were increased in the brains of GWI compared to control mice. Immunohistochemistry work showed astroglia activation in the cortex and hippocampus of GWI compared to control mice[53]. I examined the ratios of p- NFκB to NFκB in GWI mice to assess inflammation. There was a significant increase in p- NFκB / NFκB ratios (t-test $_{(df = 5)} = 2.2$, $p = 0.06$, Figure 4.8A) *Post-hoc* analyses showed that the ratios of p- NFκB / NFκB were increased in GWI mice at this 7-months post-exposure timepoint.

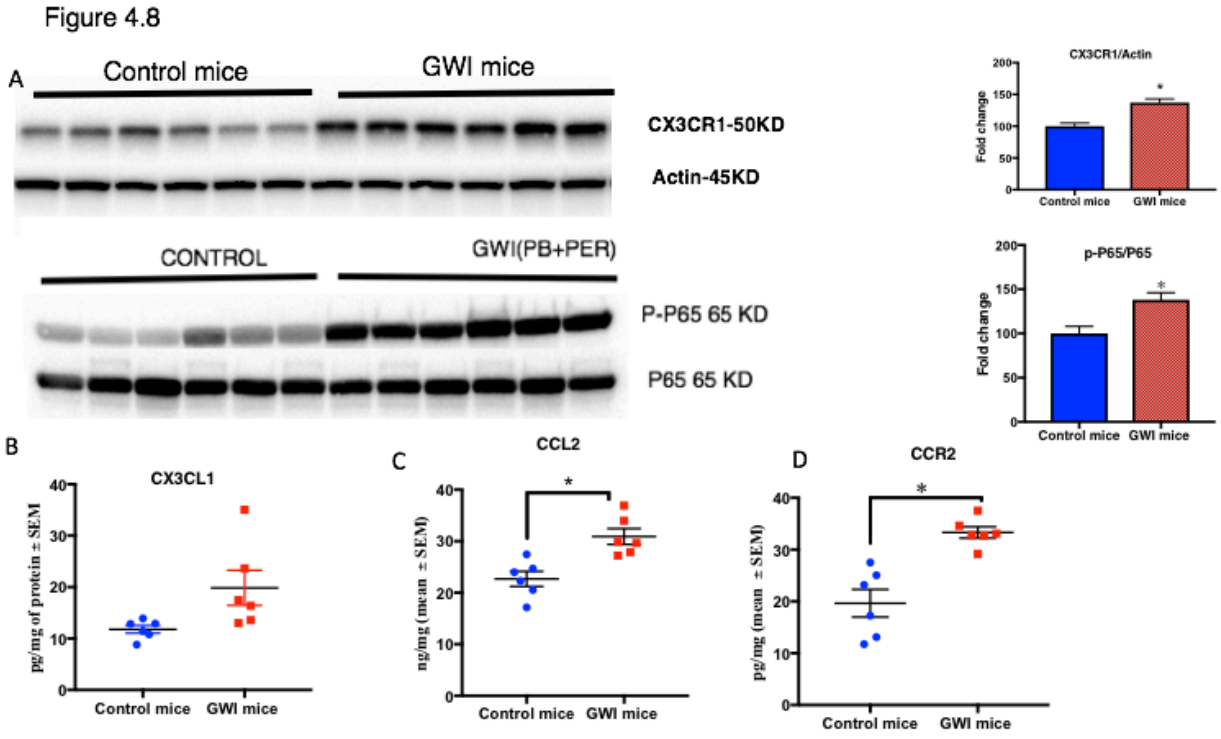

Figure 4.8: CCR2 and its ligand CCL2 are chronically increased in the brains of PB+PER-exposed mice leading to inflammation. Mean as % control ± SEM (n = 6 per group). (A) Western Blot showing CX3CR1/actin and pNFκB/NFκB is increased in the brains of PB+PER-exposed mice. (B) No change in CX3CL1 level as measured by ELISA. (C) Levels of CCL2 were also increased in PB+PER-exposed mice at 7-months post-exposure. (D) CCR2 levels were increased in the brains of GWI mice. T-test *$p < 0.05$

4.3.8 Astrocyte and Microglia Responses in the GWI mice Brain

Morphological changes to astroglia in the GWI brain at 7 months post exposure specially DG and cortex were observed. Robust activation of astroglia cells typified by an increase in cell density and expression of cell surface markers, such as, GFAP is evident in the GWI DG and cortex (Figure 4.9). The microglial cells show no change in number as well as in morphology in GWI brain at similar time point.

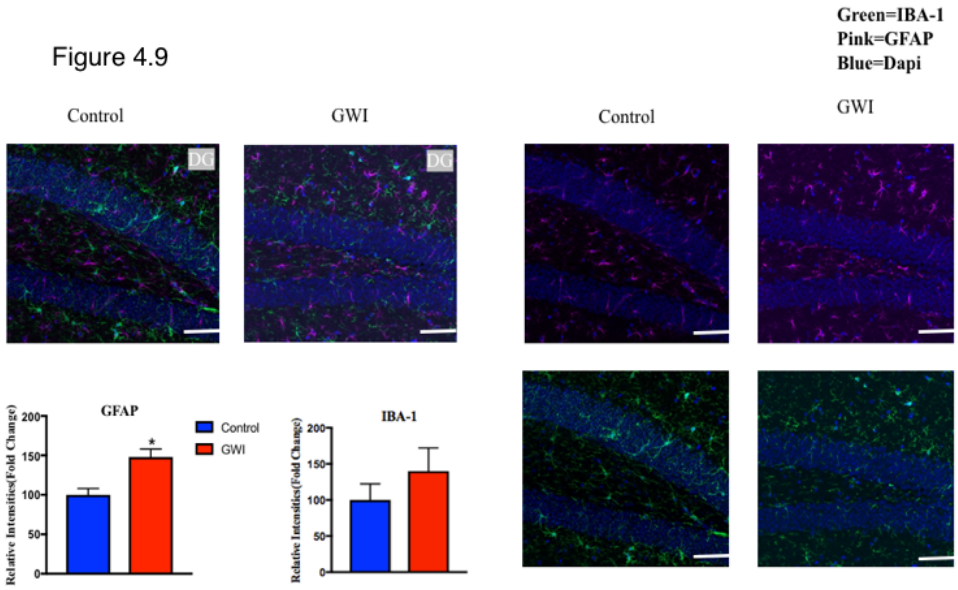

Figure 4.9: Representative images of GFAP and IBA-1 staining in the DG regions. Sagittal sections of the mouse brain at 0.8 mm lateral to midline in the brainstem. 20x images of astroglia GFAP staining(pink) and IBA-1(green) in the DG showed a significant increase in GFAP within the DG was observed in GWI compared to controls. Quantitative analysis of GFAP and IBA-1 staining intensity indicated an increased area of GFAP immunoreactivity in the DG of GWI mice. Mean ± SEM (n = 4 per group). T-test * $p \leq 0.05$ Green=IBA-1, Pink=GFAP, Blue=Dapi

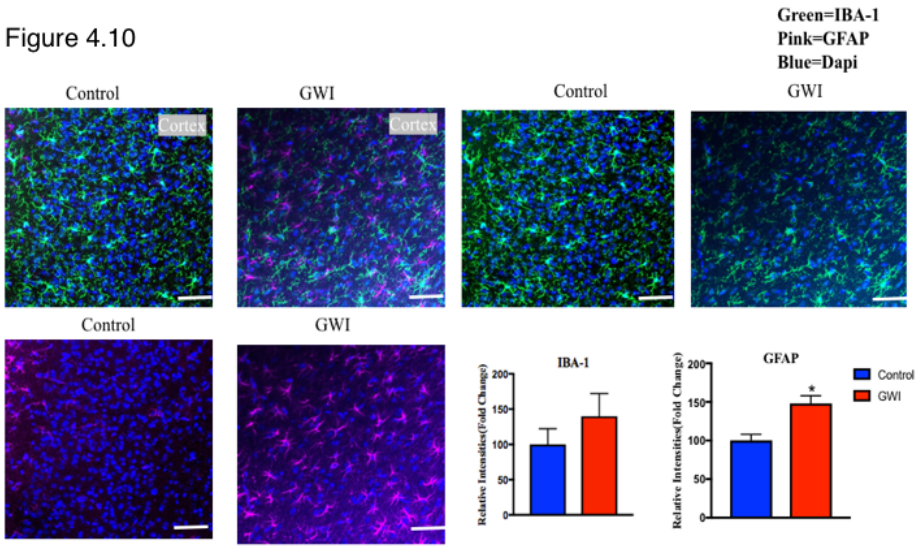

Figure 4.10: Increased GFAP in the cortex of GWI exposed mice. GFAP staining (Pink) and IBA-1(green) visualized with confocal microscopy (20x image) show increased staining in the GFAP staining in the GWI mice. Quantification of relative intensities of IBA-1 and GFAP exposed vs. control mice. Mean ± SE*M* (n = 4 per group).T-test *p < 0.05. Scale Bar=100um Green=IBA-1, Pink=GFAP, Blue=Dapi.

4.4 Discussion:

Evidence suggests that overexposure to PB and pesticides, which included pyrethroids and organophosphates, was one of the etiological factors in GWI [1,2,276]. Exposure to these compounds has been shown to induce chronic immune dysfunction [192,313,314]. While clinical symptoms of GWI resemble those of autoimmune diseases, the exact mechanism by which GW chemicals caused immune activation remains unknown. In this translational study, we show that a common pyrethroid metabolite, 3-PBA, can haptenate albumin, which activates CD4+ T-helper and antigen-responsive B-cells. These immune cells were elevated in PB+PER exposed mice and in veterans with GWI. We observed autoantibodies against 3-PBA-albumin in our PB+PER mouse model and in veterans with GWI at chronic post-exposure timepoints. In this PB+PER mouse model, we also show that brain macrophages thought to be derived from

peripheral blood monocytes were increased in the brains of PB+PER mice. These studies suggest that activation of autoimmune responses against endogenous proteins modified by 3-PBA corresponds with activation of brain macrophages and neuroinflammation in PB+PER mice. The work described herein could aid in the development of sensitive and specific biomarkers for diagnosing GWI in order to provide appropriate care and treatment to veterans with GWI.

During the 1991 GW, a large proportion of veterans were using pyrethroid-based pesticides routinely [1,276]. To date, accurate diagnosis of GWI remains an unmet need for ill GW veterans. One reason it is difficult to accurately diagnose GWI is because the diagnosis is based on self-report of symptoms and exposures. Since studies have shown that 3-PBA can form adducts with lysine residues on endogenous proteins [282,315,316], we performed this experiment and found a presence of 3-PBA-lysine residues in the brain, blood and liver of PB+PER mice acutely after GW chemical exposure. We also examined 3-PBA recovered after protein hydrolysis and found it to be present at 1.5 months after exposure to PB and PER but not at later post-exposure timepoints. This suggests that 3-PBA-haptenated proteins are eventually eliminated. Small molecules which haptenate endogenous proteins can elicit adaptive immune responses, ultimately resulting in B-cell activation and autoantibody production [317,318]. Since albumin is easily haptenated by drugs due to its abundance in blood and availability of lysine residues that can be covalently modified[297], albumin was chosen for haptenation studies with 3-PBA. Our observations of autoantibodies against 3-PBA-albumin in blood from PB+PER mice, veterans with GWI and pyrethroid-exposed subjects suggest that 3-PBA-albumin is capable of provoking autoimmune responses. These studies for the first time provide evidence of autoantibodies following pyrethroid exposure in veterans with GWI. The specificity of these autoantibodies to pyrethroid exposure is further supported by the observation of 3-PBA-albumin autoantibodies in subjects with detectable urinary 3-PBA levels and observable 3-PBA-lysine adducts in their serum. While it remains to be determined if autoantibodies against

3-PBA-albumin have a pathological role in GWI, a higher prevalence of these autoantibodies in GWI veterans compared to control GW veterans suggests that they could be useful biomarkers of GWI.

Our animal and human studies suggest that autoantibodies against 3-PBA-albumin persist for a long time, despite the fact that 3-PBA is not detected in the brain or the liver beyond 1.5 months post-exposure. Studies have shown that proteins haptenated by other chemicals can directly interact with APC, which then travel to the lymphatic system where they present these antigens to T- and B-cells [283]. This may result in the production of autoantibodies against haptenated proteins [283,319,320]. While the exact mechanism behind the persistence of autoantibodies against 3-PBA-albumin remains to be investigated, it may involve a similar mechanism which requires memory B-cell activation and subsequent autoantibody production by plasma B-cells [73,321]. As mentioned above, we show that autoantibodies against 3-PBA-albumin are generated in our PB+PER mouse model. Furthermore, results of our *in vitro* blood culture studies suggest that the adaptive immune system is engaged in promoting immune cell activation after 3-PBA-albumin treatment, which is characterized by an elevation of antigen-presenting monocytes, CD3+CD4+ T-helper cells and antigen-responsive CD19+ CD27+ B-cells. Interestingly, these cells did not react to 3-PBA or albumin alone, further strengthening the concept that chemical haptenation of albumin is required to elicit adaptive immune responses and that 3-PBA alone cannot promote immune activation. Increases of CD3+ CD4+ T-helper and CD19+CD27+ B-cells, together with the presence of autoantibodies against 3-PBA-albumin in PB+PER mice and in GWI veterans, further support an autoimmune-type response in GWI. These studies provide support for an activation of the adaptive immune system in GWI and are consistent with those conducted by Vojdani and colleagues [107], showing an elevation of CD4+ T-helper cells and B-cells in the blood of veterans with GWI. Together, these findings suggest that 3-PBA-albumin can stimulate peripheral immune cell activation.

While most veterans deployed in the GW conflict self-report the use of PB, it is unlikely that PB alone is a major contributing factor in the overactive immune responses noted in veterans with GWI. Previous research has suggested that PB is able to suppress inflammation in rodent models [322], with exposure to PB alone resulting in decreased production of pro-inflammatory cytokines such as IL-6, IFN-y and TNF-α at chronic time points [323]. However, we, along with others, have shown that these cytokine levels are upregulated in plasma from veterans with GWI [104,106]. The mechanism of PB is well defined in the literature, acting as a reversible acetylcholinesterase (AchE) inhibitor [324], while offering prophylactic protection against nerve agents. PB use would likely result in an increase in acetylcholine (ACh) levels in the periphery [324]. Recent evidence suggests a role of ACh in stimulating anti-inflammatory responses in the periphery via a direct interaction with nicotinic receptors on peripheral immune cells [325,326]. As such, one would expect a dampened immune response in GWI mice. However, since we observe activated immune responses and the presence of 3-PBA-albumin autoantibodies in plasma of both human and PB+PER exposed mice, it is possible that PB was unable to suppress immune cell activation that occurs in the presence of combined PB+PER exposure [78]. Additional research is needed to clarify if PB metabolites may also form haptenated proteins, which may promote synergistic interactions resulting in the observed adverse adaptive immune response.

Under normal physiological conditions, the BBB largely restricts entry of peripheral immune cells into the brain, which helps maintain the immune privilege status of the CNS[327]. However, peripheral immune cells have been shown to migrate into the brain parenchyma during inflammation resulting from the increases in proinflammatory cytokines and MMP9 activity which weakens the BBB [287,327,328]. We observed elevated proinflammatory cytokines, such as IL-1β and/or TNF-α, in the brains and blood of PB+PER mice [78]. Similarly, other studies also support an elevation of proinflammatory cytokines in rodent models of GWI as

well as in plasma from veterans with GWI [78,103,104,329]. As such, our observations of increases in these proinflammatory cytokines and in MMP9 and a loss of occludin in PB+PER mice suggests BBB disruptions. Studies on other autoimmune disorders show that autoantibodies against peripheral antigens can enter the brain when the BBB is compromised. Upon entering the brain, they may cross-react with brain proteins, as in the case of SLE where peripherally generated anti-DNA autoantibodies can cross-react with NMDA receptors [330,331]. Hence, a similar mechanism could explain the CNS pathology of GWI, but this requires further investigation.

We also detected 3-PBA-lysine and 3-PBA recovered after protein hydrolysis in the brain. Hence, it is possible that a presence of 3-PBA-protein adducts in the brain could elicit an immune response. While the exact mechanism of how 3-PBA-proteins in the brains of PB+PER mice initiate an immune response is unknown, persistent activation of astroglia suggests that these cells are involved in modulating CNS immune responses following 3-PBA-protein adduct formation. Alternatively, astroglia activation may be secondary to BBB damage as observed in this and other GWI rodent models [50,54,60,78].

Evidence of adaptive immune responses in GWI comes from our observations of increased CCL2 chemokines in the brains of PB+PER mice, which is also reported in other models of GWI [329,332]. In other autoimmune conditions and in a pesticide-induced mouse model of Parkinson's disease, release of CCL2 by astroglia is shown to promote an ingress of bone-marrow-derived CCR2-expressing monocytes into the brain parenchymal space [188,290,333]. We also observed increases in CX3CR1 in the brain homogenates of PB+PER mice. Ligation of this receptor by its ligand CX3CL1 promotes monocyte migration survival and promotes chronic inflammation [188,334]. It is now well-documented that peripheral monocytes are a source of brain macrophages that are distinct from brain-resident microglia, which develop during embryogenesis [335–337]. Within this population, tissue-infiltrating monocytes can be further characterized by their expression of Ly6C+; monocytes positive for this marker are able to

migrate into the brain parenchyma and convert into macrophages that are capable of participating in antigen-presentation [338,339]. These studies collectively suggest an infiltration of monocytes into the CNS after GW pesticide exposure. These data suggest a cross-talk between astroglia and peripheral adaptive immune cells in promoting neuroinflammation, which is further supported by our studies showing activation of NFκB-mediated inflammatory signaling pathways that may be downstream of CCL2-CCR2- and CX3CR1-CX3CL1 ligation, among other pro-inflammatory receptor systems in the brain [292,340–342]. These studies also suggest further examination of these co-stimulatory pathways for the pathogenesis of the CNS pathology of GWI.

Conclusions:

These explorative studies provide strong evidence that PER metabolite 3-PBA can haptenate proteins and promote adaptive immune responses. We also observe autoantibodies against 3-PBA-haptenated proteins in PB+PER mice and in veterans with GWI. While the exact mechanisms associated with these aberrant autoimmune responses and their effects on the CNS pathology of GWI remain to be elucidated, the work presented herein suggests a cross-talk between the brain immune cells and peripheral adaptive immune cells, which may ultimately promote the entry of peripheral immune cells into the brain and promote neuroinflammatory responses. We anticipate that these studies will help guide future development of biomarkers and therapies for the CNS pathology of GWI.

Chapter 5: Discussion

5.1 Summary:

Approximately 30% of GW veterans have been suffering from GWI for nearly three decades. To date, a significant number of GW veterans still do not have a proper diagnosis for their condition since there are no biomarkers for this multisymptomatic illness that can assist clinicians with objectively diagnosing GWI. Furthermore, to identify veterans with GWI, currently available diagnostic methods rely on self-reports of symptoms (fatigue, pain, neurological-cognitive-mood, skin, respiratory, and gastrointestinal) and self-reports of exposure to the chemicals known to have contributed to development of GWI. The problems for patients with GWI are not limited to the lack of objective biomarkers; the clinical presentation of GWI is complex and heterogenous and the pathogenesis is not understood and thus there are no effective therapies to target the underlying mechanisms. While significant advances have been made in understanding the role of GW chemical exposure on the adverse clinical presentation of GWI, the exact pathology of GWI remains to be dissected fully so that appropriate biomarkers and treatments can be developed for GWI. The research contained in this dissertation sought to identify and explore different GWI pathogenic mechanisms, and therefrom to validate a range of therapeutic targets for this currently untreatable illness.

5.2 Field advances from this dissertation research

Previous work from the Roskamp Institute GWI research team has identified abnormalities in peroxisome function characterized by the abnormal accumulation of ether phospholipids and VLCFA containing SM species in both the brain and blood of GWI rodent models [65,76,180]. The work described in Chapter 2 provided additional evidence for peroxisomal dysfunction in GWI where we showed that certain VLCFA were elevated in the blood of veterans with GWI and the same elevations can be seen in the brains of our GWI mouse model. My successful attempts to rescue this peroxisomal dysfunction by regulation of peroxisomal

lipid metabolism with OEA support its potential as a promising candidate for therapeutic intervention. Treatment with OEA reduced the accumulation of peroxisome specific VLCFA in the brains of GWI mice and, furthermore, OEA treatment modified multiple major pathological hallmarks of GWI, including reduction of neuro-inflammation and astroglial pathology. Treatment with OEA also had beneficial effects on cognitive function as assessed by behavioral analyses.

Although our study provides evidence that OEA treatment may have potential for treating GWI, further studies are still needed to fully explore the mechanism of action of OEA against GWI pathogenesis and its suitability as a treatment for GWI. Although OEA is currently sold as a nutraceutical to aid in weight loss it may have potential side effects such as lipolysis at high doses[343]. In addition, very little information is available on its pharmacodynamic and pharmacokinetic properties, and it is known to be rapidly hydrolyzed by FAAH and therefore formulation work is also needed to improve its bioavailability. Therefore, further investigations of these parameters are required for optimal dosing strategies of OEA in order for it to be developed as a therapy for treating GWI. The work described in Chapter 2 provides sufficient support to further examine the translational potential of targeting peroxisomes with OEA. Based on our work, the Department of Defense has funded a pilot clinical trial of OEA in GWI patients recruited through the Roskamp Institute Clinic. This trial is due to commence in late 2019, and will examine if OEA corrects plasma lipid profiles, reduces inflammation and improves the overall health of affected GW veterans. As such, my work is entirely consistent with the translational goals of the Roskamp Institute and may result in significant advances in treatment for the GWI patient population.

Many previously published papers have identified mitochondrial dysfunction as a major hallmark of GWI and mitochondrial dysfunction has been shown to be a consistent feature across several animal models of the illness[94,203]. Based on these findings, and the evidence for bioenergetic and mitochondrial function in our animal model [53], I investigated this second

avenue for therapeutic intervention (Chapter 3). This study provided further information about underlying mitochondrial bioenergetic disturbance, as well as neuroinflammation, in a GWI mouse model. My findings suggest that SirT1 may be a novel target for GWI treatment, which in turn inhibits activation of NFκB mediated pathways in a SirT1 deacetylation-mediated dependent manner.

First, I examined NAD+ and βHB levels in plasma from GW veterans which were significantly decreased in ill veterans compared to healthy controls. As previous metabolomics study did suggest decreased in mitochondrial metabolite related to bioenergetics in GWI mice and in veterans with GWI [54]. In small case-control study, I tested the levels of NAD+ and βHB and these metabolites to be lower in ill compared to control GW veterans. Next, in a pilot animal study, I tested two treatments which are known to increase the levels of these metabolites: nicotinamide riboside (NR), which is the precursor for NAD+; and a ketogenic diet (KD), which increases βHB levels in the liver. I observed that although both treatments work via different mechanisms they achieved similar outcomes relevant to GWI pathology. For instance, both interventions were helpful in reducing inflammation and increasing mitochondrial bioenergetics. Chronic treatment of NR is safe and does not have any potentially harmful side effects [245]. It is currently used as a nutraceutical for vitamin deficiency. The KD intervention has been used for decades to help control diabetes and epilepsy [270,344]. Thus, safe human use data is available for both of these potential GWI treatments, expediting their translational potential. Our findings demonstrate that NR and KD treatments attenuate brain and systemic inflammation and induce mitochondrial biogenesis in the GWI mouse brain; since inflammation and mitochondrial dysfunction are involved in the pathophysiology of GWI, our study has potential clinical benefits if these findings are confirmed in human clinical studies.

Based on recent findings from Abou-Donia and colleagues showing presence of autoantibodies against brain specific proteins in veterans with GWI and the fact that many of the clinical features of GWI are similar to those of patients with autoimmune diseases [345], I

examined if exposure to GW-related pesticides activate peripheral adaptive immune responses which may correspond with BBB disruption and CNS immune activation (Chapter 4). My work demonstrated for the first time that a 3-PBA-protein conjugate (a pyrethroid metabolite) is present in the brain, liver and plasma of our GWI mouse model at acute post-exposure timepoints. Moreover, I also demonstrated the clinical relevance of this finding by detecting autoantibodies against 3-PBA-albumin in the plasma of GWI mice and of veterans with GWI. Although these studies need to be repeated in a larger cohort, if confirmed the presence of these autoantibodies can serve as future potential biomarkers not only for GWI but also for occupational exposure to pyrethroid or other types of pesticides that are capable of forming adducts with proteins. The production of autoantibodies is a major pathological hallmark of autoimmune diseases with underlying adaptive immune dysfunction, such as multiple sclerosis and Traumatic brain injuries[346,347]. These studies suggest that pesticide exposure associated with GWI may have resulted in the activation of adaptive immune responses, which possibly contributed to an autoimmune type phenotype in veterans with GWI and may have contributed to the activation of CNS immune cells and neuroinflammation.

Although our work is focused on GWI, and the pesticide exposure to which the military was subjected during the 1991 GW, our findings have relevance for a much broader potential patient population as pyrethroids have been used in civilian settings for decades to control household and agricultural pests. Most of the pyrethroid toxicity cases have arisen from occupational health exposure due to poor understanding of its toxicity and lack of knowledge about precautions that need to be taken [348]. The use of organophosphate pesticides has decline in past decades but pyrethrin and pyrethroids use has increased during this period (Source:EPA.gov). Although these pesticides are used to protect crops, pesticide residue in food is potentially toxic to humans, particularly if they can accumulate in the body. Exposure to these pesticides from contaminated food may have acute and chronic health problems depending on the quantity of exposure. Professor Hammock and his team at the University of

California, Davis, have developed several assays to detect the presence of pyrethroids and their metabolites in human blood, urine and tissue and these appear to be useful in detecting acute exposure. Our work could potentially complement these studies in civilian situations where we may assist by detecting *chronic* pyrethroid exposure. As can be seen from the samples from the Thailand cohort (in Chapter 4), autoantibodies against 3-PBA-albumin were detected in subjects in whom 3-PBA urine levels were positive. It is still unclear if these antibodies play a positive or negative role, nevertheless, their detection suggests that they might be objective biomarkers of pyrethroid exposure. This proof of concept study has not only provided a foundation for developing biomarkers and appropriate therapies for targeting immunological aspects of GWI, but also provides a platform for further investigating pesticide-induced abnormal adaptive immune responses.

The main objectives of this thesis are to find effective therapies against GWI that target underlying pathology of GWI. Along with finding possible therapies, these data provide an insight into possible mechanisms underlying cognitive impairments observed in soldiers with GWI. I hope that the work described in this thesis provides a groundwork for the development of objective biomarkers and therapies for GWI. In Chapters 2, I focused on targeting peroxisomal function as potential target for GWI. While chapter 3 dealt with mitochondrial function and biogenesis as potential target for GWI. Chapter 4 investigates the immunological dysfunction related with pesticide exposure in GWI human and mice. These studies suggest that pesticide exposure associated with GWI may have resulted in the activation of the peripheral and CNS adaptive immune responses, possibly contributing to autoimmune type phenotype in veterans with GWI.

5.2 Limitations of the study:

While animal studies enable investigation of the pathobiological consequences of toxic exposures at any timepoint from exposure throughout the subsequent lifespan, they are limited by their inability to model all aspects of a disease, including the inherent heterogeneity of the

patient population and, in the case of GWI, the heterogeneity of GW agent exposure, for which we can only base our models on self-reporting surveys. Furthermore, samples from human subjects are influenced by various factors that are not typically included in animal models, and this can particularly affect outcomes in immunological studies. For instance, cytokine measurements can be easily influenced by factors such as allergies or viral infections (G. Izaguirre. Molecular Mediators, Cytokines I: Lecture I). Another potential confounding factor when comparing human and mouse data is that, while controlled standard laboratory diets allow researchers to minimize variables, it has been reported that the severity of disease in humans is heavily influenced by lifestyle and diet which further contributes to the heterogeneity of data in GWI research. Similarly, while age- and gender-matched cloned lines of genetically manipulated rodents provides the opportunity to explore the influence of specific genetic risk factors, this is not representative of the large genetic variation that exists amongst humans and which can modulate disease etiology. Nonetheless, this body of work in our PB+PER mouse model provides insights into the pathogenesis of GWI; if we wish we could now introduce additional variables (guided by data from our populations of GW veterans) into our laboratory model paradigms to see how they influence the pathogenic pathways that we have identified as contributing to GWI.

One major limitation of Chapter 2 is that OEA affected lipid homeostasis in control mice treated with OEA, which corresponded with lowered anxiolytic response in the EPM test and higher immobility in the FST. Despite that, we did not observe any adverse effect on memory or an increase in lipid peroxidation and inflammation in these mice. However, given the role of OEA in lipid metabolism and reducing inflammation, increasing its level in the absence of underlying inflammation or metabolic dysfunction warrants further examination to anticipate any adverse events in patients where these are not the most prominent pathogenic features. We do expect that additional pharmacokinetics and pharmacodynamics studies will help identify a safe and effective dose for chronic administration in veterans with GWI. The

limitation of Chapter 3 is the small sample size and lack of neurobehavioral data. This study needs to be repeated in a larger cohort of mice along with memory and anxiety evaluation. One major experiment lacking in this study is analysis of mitochondrial metabolites which might give us more insight into bioenergetic disturbance following exposure to GW agents. Similar limitations exist in Chapter 4, where our pilot human data needs to be replicated in a larger cohort to confirm a correlation between the pesticide exposure and presence of hapten antibodies.

Animal models are used in preclinical studies of drugs with the potential for human application in order to determine the safety, efficacy and reproducibility of a treatment paradigm. An animal model is a simplified representation of a complex system. Consequently, an animal model for a human disease like GWI is by no means an attempt to reproduce the human disease in all its complexity, but rather to model specific aspects of a disease. When designed and conducted appropriately, animal models can provide valuable information regarding systems biology, pathology and target identification, and drive the development of new drugs. There will be no single, all-encompassing model for GWI, owing to the mixed etiology and the heterogeneity of human populations. The clinical presentation is very complicated, and includes features of a more subjective natures such as pain and fatigue, which increase the difficulty of replication in animal models. If a single particular animal model is not a good representation of human physiology or disease, one possibility is to generate different models which attempt to recapitulate different aspects of the human pathology. Because of these caveats, it would be foolish to rely solely on one GWI animal model to assess whether or not an intervention will have a favorable clinical outcome in human subjects. As such, the OEA, NR and KD interventions should ideally be tested in several different animal models of GWI before moving to human studies. That said, when dealing with widely used dietary supplements or repurposed drugs with a history of safe usage, the primary concern of Safety is

largely addressed, and so moving straight into human testing presents less of a challenge; hence we are advancing to a human clinical trial with OEA in GWI patients.

5.3 Future directions:

Both clinical and animal studies now suggest an association between peroxisomal and mitochondrial dysfunction in GWI and therefore further evaluation of the enzymatic processes and proteins involved in their function is required. This work would also benefit greatly by examining the influence of genetic factors involved in the transport and metabolism of these lipids as these could influence human response both to the toxic exposures and to the treatments targeting these systems. Both NR and OEA are naturally occurring compounds, and chronic supplementation of these compounds has been shown to be well tolerated in humans [245,349]. However, I do propose that additional pharmacokinetics and pharmacodynamics studies should be performed to identify a safe and effective dose for chronic administration of OEA and NR in veterans with GWI. Furthermore, given the complexity of this illness, and the different pathogenic mechanisms which likely need to be targeted in tandem for greater overall health benefits to the sick veterans, preclinical testing of combinations of treatments is needed to maximize the translational potential.

My major research highlights from Chapter 4 include: 1) the detection of 3-PBA in the livers and brains of our PB+PER GWI mouse model, and 2) the presence of autoantibodies against 3-PBA-albumin in GWI mice and GWI veterans at chronic post-exposure timepoints, where pesticide exposure was correlated with detection of autoantibody. While the assessment of levels of these molecules is a good way to gain information about the association of such molecules in a disease state, this study should be replicated in a larger cohort, especially if the presence of these molecules is to be used as a biomarker. Moreover, further research needs to be conducted focusing on the enzymes that metabolize PER, not only analyzing the expression level of these enzymes but also their enzymatic activity. Additionally, the location of the

molecule could contribute to its role in the disease; therefore, studying certain organs/tissues (e.g. brain, adipose tissue, liver) and specific cell types may shed light on the toxic function of the molecule. Finally, further studies should be conducted on protein modifications, investigating the reversible or irreversible chemical alterations of a protein after its haptenization, as these are believed to play a great role in the toxicological effect of pesticide such as permethrin. Future work must focus on identifying all the proteins that 3-PBA can bind, and its presence in different organs might help us to understand the mechanism behind immune activation led by 3-PBA.

5.4 Conclusion:

The work presented in this thesis describes novel and diverse approaches to treat GWI. It is my assessment that these approaches have good potential efficacy as therapeutic interventions, as they target the underling disease pathology. This thesis also contributes to the existing cumulative knowledge of peroxisome and mitochondrial dysfunction in GWI. Furthermore, the findings of this thesis focus on the identification of biomarkers in GWI. The diagnosis of this multisymptom illness relies heavily on self-report, supporting the need for an objective biomarker. The human pilot study on fatty acid profiles suggested an increase in plasma VLCFA, a marker which could help in clinical diagnosis; however, more research is needed before we move to clinical trials. The presence of autoantibodies in GWI indicated pesticide exposure in this cohort of veterans, and if replicated with additional positive and negative controls these autoantibodies could also serve as novel biomarkers for GWI. Collectively, these studies provide new targets for discovering treatments for GWI and additional information on biochemical and molecular abnormalities that persist long after the GW chemical exposure. I anticipate that my work may provide useful insight into the persistent pathology of GWI and lead to the development of diagnostic markers and novel therapeutics for GWI and other toxic environmental exposures.

Reference:

1. Binns J, Barlow C, Bloom F, et al. Gulf War Illness and the Health of Gulf War Veterans: Scientific Findings and Recommendations. 2008:1-465.
2. White RF, Steele L, O'Callaghan JP, et al. Recent research on Gulf War illness and other health problems in veterans of the 1991 Gulf War: Effects of toxicant exposures during deployment. *Cortex*. 2016;74:449-475. doi:10.1016/j.cortex.2015.08.022.
3. Unwin C, Blatchley N, Coker W, et al. Health of UK servicemen who served in Persian Gulf War. *Lancet*. 1999;353(9148):169-178. doi:10.1016/S0140-6736(98)11338-7.
4. Proctor SP, Heeren T, White RF, et al. Health status of Persian Gulf War veterans: Self-reported symptoms, environmental exposures and the effect of stress. *International Journal of Epidemiology*. 1998. doi:10.1093/ije/27.6.1000.
5. Binns JH. Gulf War Illness and the Health of Gulf War Veterans : Research Update and Recommendations , 2009-2013 Updated Scientific Findings and Recommendations Research Advisory Committee on Gulf War Veterans ' Illnesses. 2013:2009-2013.
6. Steele L. Prevalence and patterns of Gulf War illness in Kansas veterans: Association of symptoms with characteristics of person, place, and time of military service. *American Journal of Epidemiology*. 2000. doi:10.1093/aje/152.10.992.
7. Binns JH, Golomb B, Graves J, Haley RW. RAC-GWVI Minutes 2005. *RAC-GWVI Meeting Minutes*. 2005;48(9):800-809.
8. Brian E. Engdahl, Lisa M. James, Ryan D. Miller, Arthur C. Leuthold, Scott M. Lewis, Adam F. Carpenter APG. Brain Function in Gulf War Illness (GWI) and Associated Mental Health Comorbidities. *Journal of Neurology & Neuromedicine*. 2018.
9. Fukuda K, Nisenbaum R, Stewart G, et al. Chronic multisymptom illness affecting Air Force veterans of the Gulf War. *JAMA : the journal of the American Medical Association*. 1998;280(11):981-988. doi:10.1001/jama.280.11.981.
10. Kang HK, Mahan CM, Lee KY, Magee CA, Murphy FM. Illnesses among united states

veterans of the gulf war: A population- based survey of 30,000 veterans. *Journal of Occupational and Environmental Medicine*. 2000. doi:10.1097/00043764-200005000-00006.

11. Spencer PS, McCauley LA, Lapidus JA, Lasarev M, Joos SK, Storzbach D. Self-reported exposures and their association with unexplained illness in a population-based case-control study of Gulf War Veterans. *Journal of Occupational and Environmental Medicine*. 2001. doi:10.1097/00043764-200112000-00006.
12. Steele L. Prevalence and patterns of Gulf War illness in Kansas veterans: Association of symptoms with characteristics of person, place, and time of military service. *American Journal of Epidemiology*. 2000;152(10):992-1002. doi:10.1093/aje/152.10.992.
13. Schwartz DA. Self-reported illness and health status among Gulf War veterans: A population-based study. *Journal of the American Medical Association*. 1997. doi:10.1001/jama.277.3.238.
14. Spencer PS, McCauley L a, Lapidus J a, Lasarev M, Joos SK, Storzbach D. Self-reported exposures and their association with unexplained illness in a population-based case-control study of Gulf War veterans. *Journal of occupational and environmental medicine / American College of Occupational and Environmental Medicine*. 2001;43(12):1041-1056. http://www.ncbi.nlm.nih.gov/pubmed/11765675.
15. Toomey R, Alpern R, Vasterling JJ, et al. Neuropsychological functioning of U.S. Gulf War veterans 10 years after the war. *Journal of the International Neuropsychological Society*. 2009. doi:10.1017/S1355617709990294.
16. Janulewicz PA, Krengel MH, Maule A, et al. Neuropsychological characteristics of Gulf War illness: A meta-Analysis. *PLoS ONE*. 2017. doi:10.1371/journal.pone.0177121.
17. Maule AL, Janulewicz PA, Sullivan KA, et al. Meta-analysis of self-reported health symptoms in 1990-1991 Gulf War and Gulf War-era veterans. *BMJ Open*. 2018;8(2). doi:10.1136/bmjopen-2017-016086.

18. Haley RW, Marshall WW, McDonald GG, Daugherty MA, Petty F, Fleckenstein JL. Brain abnormalities in Gulf War syndrome: evaluation with 1H MR spectroscopy. *Radiology*. 2000;215(3):807-817. doi:10.1148/radiology.215.3.r00jn48807.

19. Menon PM, Nasrallah HA, Reeves RR, Ali JA. Hippocampal dysfunction in Gulf War Syndrome. A proton MR spectroscopy study. *Brain Research*. 2004;1009(1-2):189-194. doi:10.1016/j.brainres.2004.02.063.

20. Heaton KJ, Palumbo CL, Proctor SP, Killiany RJ, Yurgelun-Todd DA, White RF. Quantitative magnetic resonance brain imaging in US army veterans of the 1991 Gulf War potentially exposed to sarin and cyclosarin. *NeuroToxicology*. 2007. doi:10.1016/j.neuro.2007.03.006.

21. Chao LL, Rothlind JC, Cardenas VA, Meyerhoff DJ, Weiner MW. Effects of low-level exposure to sarin and cyclosarin during the 1991 Gulf War on brain function and brain structure in US veterans. *NeuroToxicology*. 2010;31(5):493-501. doi:10.1016/j.neuro.2010.05.006.

22. Rayhan RU, Stevens BW, Raksit MP, et al. Exercise Challenge in Gulf War Illness Reveals Two Subgroups with Altered Brain Structure and Function. *PLoS ONE*. 2013;8(6). doi:10.1371/journal.pone.0063903.

23. Aquilonius SM, Eckernas SÅ, Hartvig P, Lindström B, Osterman PO, Stålbergt E. Clinical pharmacology of pyridostigmine and neostigmine in patients with myasthenia gravis. *Journal of Neurology, Neurosurgery and psychiatry*. 1983. doi:10.1136/jnnp.46.10.929.

24. Chao LL, Abadjian L, Hlavin J, Meyerhoff DJ, Weiner MW. Effects of low-level sarin and cyclosarin exposure and Gulf War Illness on Brain Structure and Function: A study at 4T. *NeuroToxicology*. 2011;32(6):814-822. doi:10.1016/j.neuro.2011.06.006.

25. Haley RW. Is Gulf War syndrome due to stress? The evidence reexamined. *American Journal of Epidemiology*. 1997. doi:10.1093/oxfordjournals.aje.a009343.

26. Madsen JM, Hurst CG, MacIntosh R RJ. Clinical Considerations in the Use of Pyridostigmine Bromide as Pretreatment for Nerve-agent Exposure. *US Army Medical Research Institute of Chemical Defense*. (USAMRICD-SP-03-01).

27. Fricker RD, Reardon E SD. Pesticide Use During the Gulf War A Survey of Gulf War VeteransNo Title. *National Defense Research Institute (RAND);* . 2000.

28. Steele L, Sastre A, Gerkovich MM, Cook MR. Complex factors in the etiology of Gulf War illness: Wartime exposures and risk factors in veteran subgroups. *Environmental Health Perspectives*. 2012;120(1):112-118. doi:org/10.1289/ehp.1003399.

29. SCHUMM WR. SELF-REPORTED CHANGES IN SUBJECTIVE HEALTH AND ANTHRAX VACCINATION AS REPORTED BY OVER 900 PERSIAN GULF WAR ERA VETERANS. *Psychological Reports*. 2005. doi:10.2466/pr0.90.2.639-653.

30. Boyd KC, Hallman WK, Wartenberg D, Fiedler N, Brewer NT, Kipen HM. Reported exposures, stressors, and life events among Gulf War Registry veterans. *Journal of occupational and environmental medicine / American College of Occupational and Environmental Medicine*. 2003;45(12):1247-1256. doi:10.1097/01.jom.0000099980.38936.09.

31. Bloomquist JR, Barlow RL, Gillette JS, Li W, Kirby ML. Selective effects of insecticides on nigrostriatal dopaminergic nerve pathways. In: *NeuroToxicology*. Vol 23. ; 2002:537-544. doi:10.1016/S0161-813X(02)00031-1.

32. Degennaro M. The mysterious multi-modal repellency of DEET. *Fly*. 2015;9(1):45-51. doi:10.1080/19336934.2015.1079360.

33. Winkenwerder W. *Environmental Exposure Report: Pesticides Final Report. U.S. Department of Defense, Office of the Special Assistant to the Undersecretary of Defense(Personnel and Readiness) for Gulf War Illnesses Medical Readiness and Military Deployments,*. Washington, D.C; 2003.

34. Casida JE, Quistad GB. Serine hydrolase targets of organophosphorus toxicants. In:

Chemico-Biological Interactions. ; 2005. doi:10.1016/j.cbi.2005.10.036.

35. Maxwell DM, Brecht KM, Koplovitz I, Sweeney RE. Acetylcholinesterase inhibition: Does it explain the toxicity of organophosphorus compounds? *Archives of Toxicology*. 2006. doi:10.1007/s00204-006-0120-2.

36. Pancetti F, Olmos C, Dagnino-Subiabre A, Rozas C, Morales B. Noncholinesterase effects induced by organophosphate pesticides and their relationship to cognitive processes: Implication for the action of acylpeptide hydrolase. *Journal of Toxicology and Environmental Health - Part B: Critical Reviews*. 2007. doi:10.1080/10937400701436445.

37. Trevisan R, Uliano-Silva M, Pandolfo P, et al. Antioxidant and acetylcholinesterase response to repeated malathion exposure in rat cerebral cortex and hippocampus. *Basic and Clinical Pharmacology and Toxicology*. 2008. doi:10.1111/j.1742-7843.2007.00182.x.

38. Kaur P, Radotra B, Minz RW, Gill KD. Impaired mitochondrial energy metabolism and neuronal apoptotic cell death after chronic dichlorvos (OP) exposure in rat brain. *NeuroToxicology*. 2007. doi:10.1016/j.neuro.2007.08.001.

39. Prendergast MA, Terry A V., Buccafusco JJ. Effects of chronic, low-level organophosphate exposure on delayed recall, discrimination, and spatial learning in monkeys and rats. *Neurotoxicology and Teratology*. 1998. doi:10.1016/S0892-0362(97)00098-6.

40. Raheja G, Dip Gill K. Altered cholinergic metabolism and muscarinic receptor linked second messenger pathways after chronic exposure to dichlorvos in rat brain. *Toxicology and Industrial Health*. 2007. doi:10.1177/0748233707072490.

41. Terry A V., Gearhart DA, Beck WD, et al. Chronic, Intermittent Exposure to Chlorpyrifos in Rats: Protracted Effects on Axonal Transport, Neurotrophin Receptors, Cholinergic Markers, and Information Processing. *Journal of Pharmacology and*

Experimental Therapeutics. 2007. doi:10.1124/jpet.107.125625.

42. Terry A V, Stone JD, Buccafusco JJ, Sickles DW, Sood A, Prendergast MA. Repeated Exposures to Subthreshold Doses of Chlorpyrifos in Rats: Hippocampal Damage, Impaired Axonal Transport, and Deficits in Spatial Learning. *The Journal of Pharmacology and Experimental Therapeutics*. 2003;305(1):375-384. doi:10.1124/jpet.102.041897.
43. Abou-Donia MB. Organophosphorus ester-induced chronic neurotoxicity. *Archives of Environmental Health*. 2003. doi:10.3200/AEOH.58.8.484-497.
44. Terry AV. Functional Consequences of Repeated Organophosphate Exposure: Potential Non-Cholinergic Mechanisms. *Pharmacol Ther*. 2012;v(2):265-275. doi:10.1007/s10955-011-0269-9.Quantifying.
45. Steenland K, Jenkins B, Ames RG, O'Malley M, Chrislip D, Russo J. Chronic neurological sequelae to organophosphate pesticide poisoning. *American Journal of Public Health*. 1994. doi:10.2105/AJPH.84.5.731.
46. Dassanayake T, Weerasinghe V, Dangahadeniya U, et al. Cognitive processing of visual stimuli in patients with organophosphate insecticide poisoning. *Neurology*. 2007. doi:10.1212/01.wnl.0000264423.12123.f0.
47. Lange G, Tiersky L a, Scharer JB, et al. Cognitive functioning in Gulf War Illness. *Journal of clinical and experimental neuropsychology*. 2001;23(2):240-249. doi:10.1076/jcen.23.2.240.1208.
48. Nisenbaum R, Barrett DH, Reyes M, Reeves WC. Deployment stressors and a chronic multisymptom illness among Gulf War veterans. *Journal of Nervous and Mental Disease*. 2000. doi:10.1097/00005053-200005000-00002.
49. Lange JL, Schwartz DA, Doebbeling BN, Heller JM, Thorne PS. Exposures to the Kuwait oil fires and their association with asthma and bronchitis among gulf war veterans. *Environmental Health Perspectives*. 2002. doi:10.1289/ehp.021101141.

50. Abdel-Rahman A, Abou-Donia SM, El-Masry EM, Shetty AK, Abou-Donia MB. Stress and Combined Exposure to Low Doses of Pyridostigmine Bromide, DEET, and Permethrin Produce Neurochemical and Neuropathological Alterations in Cerebral Cortex, Hippocampus, and Cerebellum. *Journal of Toxicology and Environmental Health, Part A*. 2004;67(2):163-192. doi:10.1080/15287390490264802.

51. Parihar VK, Hattiangady B, Shuai B, Shetty AK. Mood and memory deficits in a model of Gulf War illness are linked with reduced neurogenesis, partial neuron loss, and mild inflammation in the hippocampus. *Neuropsychopharmacology : official publication of the American College of Neuropsychopharmacology*. 2013;38(12):2348-2362. doi:10.1038/npp.2013.158.

52. Hattiangady B, Mishra V, Kodali M, Shuai B, Rao X, Shetty AK. Object location and object recognition memory impairments, motivation deficits and depression in a model of Gulf War illness. *Frontiers in Behavioral Neuroscience*. 2014. doi:10.3389/fnbeh.2014.00078.

53. Zakirova Z, Tweed M, Crynen G, et al. Gulf War agent exposure causes impairment of long-term memory formation and neuropathological changes in a mouse model of Gulf War Illness. *PLoS ONE*. 2015;10(3). doi:10.1371/journal.pone.0119579.

54. Abdullah L, Evans JE, Joshi U, et al. Translational potential of long-term decreases in mitochondrial lipids in a mouse model of Gulf War Illness. *Toxicology*. 2016;372:22-33. doi:10.1016/j.tox.2016.10.012.

55. Abdel-Rahman a, Abou-Donia S, El-Masry E, Shetty A, Abou-Donia M. *Stress and Combined Exposure to Low Doses of Pyridostigmine Bromide, DEET, and Permethrin Produce Neurochemical and Neuropathological Alterations in Cerebral Cortex, Hippocampus, and Cerebellum.* Vol 67.; 2004. doi:10.1080/15287390490264802.

56. Grigoryan H, Li B, Anderson EK, et al. Covalent binding of the organophosphorus agent FP-biotin to tyrosine in eight proteins that have no active site serine. *Chemico-Biological*

Interactions. 2009. doi:10.1016/j.cbi.2009.03.018.

57. Greter M, Lelios I, Croxford AL. Microglia versus myeloid cell nomenclature during brain inflammation. *Frontiers in Immunology*. 2015. doi:10.3389/fimmu.2015.00249.

58. Prinz M, Priller J, Sisodia SS, Ransohoff RM. Heterogeneity of CNS myeloid cells and their roles in neurodegeneration. *Nature Neuroscience*. 2011. doi:10.1038/nn.2923.

59. Abdel-Rahman A, Shetty AK, Abou-Donia MB. Disruption of the blood-brain barrier and neuronal cell death in cingulate cortex, dentate gyrus, thalamus, and hypothalamus in a rat model of Gulf-War syndrome. *Neurobiology of Disease*. 2002. doi:10.1006/nbdi.2002.0524.

60. O'Callaghan JP, Kelly KA, Locker AR, Miller DB, Lasley SM. Corticosterone primes the neuroinflammatory response to DFP in mice: Potential animal model of Gulf War Illness. *Journal of Neurochemistry*. 2015;133(5):708-721. doi:10.1111/jnc.13088.

61. Grigoryan H, Schopfer LM, Thompson CM, Terry A V., Masson P, Lockridge O. Mass spectrometry identifies covalent binding of soman, sarin, chlorpyrifos oxon, diisopropyl fluorophosphate, and FP-biotin to tyrosines on tubulin: A potential mechanism of long term toxicity by organophosphorus agents. *Chemico-Biological Interactions*. 2008. doi:10.1016/j.cbi.2008.04.013.

62. Hernandez CM, Beck WD, Naughton SX, et al. Repeated exposure to chlorpyrifos leads to prolonged impairments of axonal transport in the living rodent brain. *NeuroToxicology*. 2015. doi:10.1016/j.neuro.2015.01.002.

63. Chen Y. Organophosphate-induced brain damage: Mechanisms, neuropsychiatric and neurological consequences, and potential therapeutic strategies. *NeuroToxicology*. 2012. doi:10.1016/j.neuro.2012.03.011.

64. Parihar VK, Hattiangady B, Kuruba R, Shuai B, Shetty a K. Predictable chronic mild stress improves mood, hippocampal neurogenesis and memory. *Molecular psychiatry*. 2011;16(2):171-183. doi:10.1038/mp.2009.130.

65. Abdullah L, Evans JE, Montague H, et al. Chronic elevation of phosphocholine containing lipids in mice exposed to Gulf War agents pyridostigmine bromide and permethrin. *Neurotoxicology and Teratology*. 2013;40:74-84. doi:10.1016/j.ntt.2013.10.002.

66. Zakirova Z, Reed J, Crynen G, et al. Complementary proteomic approaches reveal mitochondrial dysfunction, immune and inflammatory dysregulation in a mouse model of Gulf War Illness. *Proteomics - Clinical Applications*. 2017. doi:10.1002/prca.201600190.

67. Wanders RJA, Waterham HR. Biochemistry of Mammalian Peroxisomes Revisited. *Annual Review of Biochemistry*. 2006. doi:10.1146/annurev.biochem.74.082803.133329.

68. Fransen M, Lismont C, Walton P. The peroxisome-mitochondria connection: How and why? *International Journal of Molecular Sciences*. 2017. doi:10.3390/ijms18061126.

69. Fransen M, Nordgren M, Wang B, Apanasets O. Role of peroxisomes in ROS/RNS-metabolism: Implications for human disease. *Biochimica et Biophysica Acta - Molecular Basis of Disease*. 2012. doi:10.1016/j.bbadis.2011.12.001.

70. Van Meer G, Voelker DR, Feigenson GW. Membrane lipids: Where they are and how they behave. *Nature Reviews Molecular Cell Biology*. 2008. doi:10.1038/nrm2330.

71. Cipolla CM, Lodhi IJ. Peroxisomal Dysfunction in Age-Related Diseases. *Trends in Endocrinology and Metabolism*. 2017. doi:10.1016/j.tem.2016.12.003.

72. Lodhi IJ, Semenkovich CF. Peroxisomes: A nexus for lipid metabolism and cellular signaling. *Cell Metabolism*. 2014. doi:10.1016/j.cmet.2014.01.002.

73. Alberts B, Johnson A LJ. *Molecular Biology of the Cell.* 4th editio. New York, NY: Garland Science; 2002.

74. Tracey TJ, Steyn FJ, Wolvetang EJ, Ngo ST. Neuronal Lipid Metabolism: Multiple Pathways Driving Functional Outcomes in Health and Disease. *Frontiers in Molecular Neuroscience*. 2018. doi:10.3389/fnmol.2018.00010.

75. Gloerich J, van Vlies N, Jansen GA, et al. A phytol-enriched diet induces changes in fatty acid metabolism in mice both via PPARα-dependent and -independent pathways. *Journal of Lipid Research*. 2005. doi:10.1194/jlr.M400337-JLR200.

76. Emmerich T, Zakirova Z, Klimas N, et al. Phospholipid profiling of plasma from GW veterans and rodent models to identify potential biomarkers of Gulf War Illness. *PLoS ONE*. 2017;12(4). doi:10.1371/journal.pone.0176634.

77. Vasko R, Goligorsky MS. Dysfunctional lysosomal autophagy leads to peroxisomal oxidative burnout and damage during endotoxin-induced stress. *Autophagy*. 2013;9(3):442-444. doi:10.4161/auto.23344.

78. Joshi U, Evans JE, Joseph R, et al. Oleoylethanolamide treatment reduces neurobehavioral deficits and brain pathology in a mouse model of Gulf War Illness. *Scientific Reports*. 2018. doi:10.1038/s41598-018-31242-7.

79. Tymoczko, John L. Berg, Jeremy Mark Stryer L. *Biochemistry. 5th Edition*.; 2002. doi:10.1007/164.

80. Duchen MR. Roles of mitochondria in health and disease. *Diabetes*. 2004.

81. Willems PHGM, Rossignol R, Dieteren CEJ, Murphy MP, Koopman WJH. Redox Homeostasis and Mitochondrial Dynamics. *Cell Metabolism*. 2015. doi:10.1016/j.cmet.2015.06.006.

82. Shen Z, Ye C, McCain K, Greenberg ML. The Role of Cardiolipin in Cardiovascular Health. *BioMed Research International*. 2015;2015. doi:10.1155/2015/891707.

83. Datta K, Sinha S, Chattopadhyay P. Reactive oxygen species in health and disease. *National Medical Journal of India*. 2000.

84. Pettit FH, Pelley JW, Reed LJ. Regulation of pyruvate dehydrogenase kinase and phosphatase by acetyl-CoA/CoA and NADH/NAD ratios. *Biochemical and Biophysical Research Communications*. 1975. doi:10.1016/S0006-291X(75)80185-9.

85. Flanagan JL, Simmons PA, Vehige J, Willcox MD, Garrett Q. Role of carnitine in

disease. *Nutrition & metabolism*. 2010;7:30. doi:10.1186/1743-7075-7-30.

86. Horvath SE, Daum G. Lipids of mitochondria. *Progress in Lipid Research*. 2013. doi:10.1016/j.plipres.2013.07.002.

87. Paradies G, Paradies V, De Benedictis V, Ruggiero FM, Petrosillo G. Functional role of cardiolipin in mitochondrial bioenergetics. *Biochimica et Biophysica Acta - Bioenergetics*. 2014. doi:10.1016/j.bbabio.2013.10.006.

88. Shetty GA, Hattiangady B, Upadhya D, et al. Chronic Oxidative Stress, Mitochondrial Dysfunction, Nrf2 Activation and Inflammation in the Hippocampus Accompany Heightened Systemic Inflammation and Oxidative Stress in an Animal Model of Gulf War Illness. *Frontiers in Molecular Neuroscience*. 2017;10(June):1-20. doi:10.3389/fnmol.2017.00182.

89. Marchi S, Giorgi C, Suski JM, et al. Mitochondria-Ros Crosstalk in the Control of Cell Death and Aging. *Journal of Signal Transduction*. 2011. doi:10.1155/2012/329635.

90. Astiz M, Alaniz MJT de, Marra CA. Effect of pesticides on cell survival in liver and brain rat tissues. *Ecotoxicology and Environmental Safety*. 2009;72(7):2025-2032. doi:10.1016/j.ecoenv.2009.05.001.

91. Chen Y, Meyer JN, Hill HZ, et al. Role of mitochondrial DNA damage and dysfunction in veterans with Gulf War Illness. *PLoS ONE*. 2017. doi:10.1371/journal.pone.0184832.

92. Hokama Y, Empey-Campora C, Hara C, et al. Acute phase phospholipids related to the cardiolipin of mitochondria in the sera of patients with chronic fatigue syndrome (CFS), chronic ciguatera fish poisoning (CCFP), and other diseases attributed to chemicals, gulf war, and marine toxins. *Journal of Clinical Laboratory Analysis*. 2008. doi:10.1002/jcla.20217.

93. Koslik HJ, Hamilton G, Golomb BA. Mitochondrial dysfunction in Gulf War illness revealed by 31phosphorus magnetic resonance spectroscopy: A case-control study. *PLoS ONE*. 2014;9(3). doi:10.1371/journal.pone.0092887.

94. Rayhan RU, Raksit MP, Timbol CR, Adewuyi O, VanMeter JW, Baraniuk JN. Prefrontal lactate predicts exercise-induced cognitive dysfunction in Gulf War Illness. *American Journal of Translational Research*. 2013.

95. Ross JM, Oberg J, Brene S, et al. High brain lactate is a hallmark of aging and caused by a shift in the lactate dehydrogenase A/B ratio. *Proceedings of the National Academy of Sciences*. 2010. doi:10.1073/pnas.1008189107.

96. Mintun MA, Vlassenko AG, Rundle MM, Raichle ME. Increased lactate/pyruvate ratio augments blood flow in physiologically activated human brain. *Proceedings of the National Academy of Sciences*. 2004. doi:10.1073/pnas.0307457100.

97. Alberts Bruce, Johnson Alexander, Julian Lewis, Martin Raff, Keith Roberts and PW. *Lymphocytes and the Cellular Basis of Adaptive Immunity*. New York, NY: Garland Science; 2002.

98. Kulkarni OP, Lichtnekert J, Anders H-J, Mulay SR. The Immune System in Tissue Environments Regaining Homeostasis after Injury: Is "Inflammation" Always Inflammation? *Mediators of Inflammation*. 2016. doi:10.1155/2016/2856213.

99. Zambrano-Zaragoza JF, Romo-Martínez EJ, Durán-Avelar M de J, García-Magallanes N, Vibanco-Pérez N. Th17 Cells in Autoimmune and Infectious Diseases. *International Journal of Inflammation*. 2014. doi:10.1155/2014/651503.

100. Tesmer LA, Lundy SK, Sarkar S, Fox DA. Th17 cells in human disease. *Immunological Reviews*. 2008. doi:10.1111/j.1600-065X.2008.00628.x.

101. Claesson-Welsh L. Vascular permeability - The essentials. *Upsala Journal of Medical Sciences*. 2015. doi:10.3109/03009734.2015.1064501.

102. Peakman M, Skowera A, Hotopf M. Immunological dysfunction, vaccination and Gulf War illness. *Philosophical Transactions of the Royal Society B: Biological Sciences*. 2006. doi:10.1098/rstb.2006.1826.

103. Parkitny L, Middleton S, Baker K, Younger J. Evidence for abnormal cytokine

expression in Gulf War Illness: A preliminary analysis of daily immune monitoring data. *BMC immunology*. 2015;16:57. doi:10.1186/s12865-015-0122-z.

104. Khaiboullina SF, DeMeirleir KL, Rawat S, et al. Cytokine expression provides clues to the pathophysiology of Gulf War illness and myalgic encephalomyelitis. *Cytokine*. 2015;72(1):1-8. doi:10.1016/j.cyto.2014.11.019.

105. Skowera A, Hotopf M, Sawicka E, et al. Cellular immune activation in Gulf War veterans. *Journal of Clinical Immunology*. 2004;24(1):66-73. doi:10.1023/B:JOCI.0000018065.64685.82.

106. Broderick G, Kreitz A, Fuite J, Fletcher MA, Vernon SD, Klimas N. A pilot study of immune network remodeling under challenge in Gulf War Illness. *Brain, Behavior, and Immunity*. 2011;25(2):302-313. doi:10.1016/j.bbi.2010.10.011.

107. Vojdani A, Thrasher JD. Cellular and humoral immune abnormalities in Gulf War veterans. *Environmental Health Perspectives*. 2004;112(8):840-846. doi:10.1289/ehp.6881.

108. Johnson GJ, Slater BCS, Leis LA, Rector TS, Bach RR. Blood biomarkers of chronic inflammation in Gulf War illness. *PLoS ONE*. 2016;11(6):1-14. doi:10.1371/journal.pone.0157855.

109. Giltiay N V., Chappell CP, Clark EA. B-cell selection and the development of autoantibodies. *Arthritis Research and Therapy*. 2012. doi:10.1186/ar3918.

110. Abou-Donia MB, Conboy LA, Kokkotou E, et al. Screening for novel central nervous system biomarkers in veterans with Gulf War Illness. *Neurotoxicology and Teratology*. 2017;61:36-46. doi:10.1016/j.ntt.2017.03.002.

111. Conboy L, Gerke T, Hsu KY, St John M, Goldstein M, Schnyer R. The Effectiveness of Individualized Acupuncture Protocols in the Treatment of Gulf War Illness: A Pragmatic Randomized Clinical Trial. *PloS one*. 2016;11(3):e0149161. doi:10.1371/journal.pone.0149161.

112. Conboy L, St John M, Schnyer R. The effectiveness of acupuncture in the treatment of Gulf War Illness. *Contemporary Clinical Trials*. 2012. doi:10.1016/j.cct.2012.02.006.

113. Donta ST, Engel CC, Collins JF, et al. Benefits and harms of doxycycline treatment for Gulf War Veterans' illnesses: A randomized, double-blind, placebo-controlled trial. *Annals of Internal Medicine*. 2004. doi:10.7326/0003-4819-141-2-200407200-00006.

114. Donta ST, Clauw DJ, Engel CC, et al. Cognitive Behavioral Therapy and Aerobic Exercise for Gulf War Veterans' Illnesses: A Randomized Controlled Trial. *Journal of the American Medical Association*. 2003. doi:10.1001/jama.289.11.1396.

115. Golomb BA, Allison M, Koperski S, Koslik HJ, Devaraj S, Ritchie JB. Coenzyme Q10 benefits symptoms in gulf war veterans: Results of a randomized double-blind study. *Neural Computation*. 2014. doi:10.1162/NECO_a_00659.

116. Golomb BA, Allison M, Koperski S, Koslik HJ, Devaraj S, Ritchie JB. Coenzyme Q10 Benefits Symptoms in Gulf War Veterans: Results of a Randomized Double-Blind Study. *Neural Computation*. 2014;26(11):2594-2651. doi:10.1162/NECO_a_00659.

117. Turunen M, Olsson J, Dallner G. Metabolism and function of coenzyme Q. *Biochimica et Biophysica Acta - Biomembranes*. 2004. doi:10.1016/j.bbamem.2003.11.012.

118. Linnane AW, Zhang C, Yarovaya N, et al. Human aging and global function of coenzyme Q10. In: *Annals of the New York Academy of Sciences*. ; 2002. doi:10.1111/j.1749-6632.2002.tb02110.x.

119. Rodick TC, Seibels DR, Babu JR, Huggins KW, Ren G, Mathews ST. Potential role of coenzyme Q_{10} in health and disease conditions. *Nutrition and Dietary Supplements*. 2018. doi:10.2147/nds.s112119.

120. Ransohoff RM, Engelhardt B. The anatomical and cellular basis of immune surveillance in the central nervous system. *Nature Reviews Immunology*. 2012. doi:10.1038/nri3265.

121. Maes M, Mihaylova I, Kubera M, Uytterhoeven M, Vrydags N, Bosmans E. Coenzyme Q10 deficiency in myalgic encephalomyelitis / chronic fatigue syndrome (ME/CFS) is

related to fatigue, autonomic and neurocognitive symptoms and is another risk factor explaining the early mortality in ME/CFS due to cardiovascular disorder. *Neuroendocrinology Letters*. 2009.

122. Baraniuk JN, El-Amin S, Corey R, Rayhan R, Timbol C. Carnosine Treatment for Gulf War Illness: A Randomized Controlled Trial. *Global Journal of Health Science*. 2013;5(3). doi:10.5539/gjhs.v5n3p69.

123. Rokicki J, Li L, Imabayashi E, Kaneko J, Hisatsune T, Matsuda H. Daily carnosine and anserine supplementation alters verbal episodic memory and resting state network connectivity in healthy elderly adults. *Frontiers in Aging Neuroscience*. 2015. doi:10.3389/fnagi.2015.00219.

124. Baye E, Menon K, De Courten MP, Earnest A, Cameron J, De Courten B. Does supplementation with carnosine improve cardiometabolic health and cognitive function in patients with pre-diabetes and type 2 diabetes? study protocol for a randomised, double-blind, placebo-controlled trial. *BMJ Open*. 2017. doi:10.1136/bmjopen-2017-017691.

125. Chengappa KNR, Turkin SR, DeSanti S, et al. A preliminary, randomized, double-blind, placebo-controlled trial of l-carnosine to improve cognition in schizophrenia. *Schizophrenia Research*. 2012. doi:10.1016/j.schres.2012.10.001.

126. Chez MG, Buchanan CP, Aimonovitch MC, et al. Double-blind, placebo-controlled study of L-carnosine supplementation in children with autistic spectrum disorders. *Journal of Child Neurology*. 2002. doi:10.1177/08830738020170111501.

127. Golier JA, Caramanica K, Michaelides AC, et al. A randomized, double-blind, placebo-controlled, crossover trial of mifepristone in Gulf War veterans with chronic multisymptom illness. *Psychoneuroendocrinology*. 2016. doi:10.1016/j.psyneuen.2015.11.001.

128. Delille HK, Bonekamp NA, Schrader M. Peroxisomes and disease - an overview.

International journal of biomedical science : IJBS. 2006.

129. Farooqui AA, Horrocks LA, Farooqui T. Modulation of inflammation in brain: A matter of fat. *Journal of Neurochemistry*. 2007;101(3):577-599. doi:10.1111/j.1471-4159.2006.04371.x.

130. Ran-Ressler RR, Devapatla S, Lawrence P, Brenna JT. Branched chain fatty acids are constituents of the normal healthy newborn gastrointestinal tract. *Pediatric Research*. 2008. doi:10.1203/PDR.0b013e318184d2e6.

131. Ivashchenko O, Van Veldhoven PP, Brees C, Ho Y-S, Terlecky SR, Fransen M. Intraperoxisomal redox balance in mammalian cells: oxidative stress and interorganellar cross-talk. *Molecular Biology of the Cell*. 2011;22(9):1440-1451. doi:10.1091/mbc.E10-11-0919.

132. Koepke JI, Wood CS, Terlecky LJ, Walton PA, Terlecky SR. Progeric effects of catalase inactivation in human cells. *Toxicology and Applied Pharmacology*. 2008;232(1):99-108. doi:10.1016/j.taap.2008.06.004.

133. Terlecky SR, Terlecky LJ, Giordano CR. Peroxisomes, oxidative stress, and inflammation. *World journal of biological chemistry*. 2012;3(5):93-97. doi:10.4331/wjbc.v3.i5.93.

134. Gao X, Kim HK, Chung JM, Chung K. Reactive oxygen species (ROS) are involved in enhancement of NMDA-receptor phosphorylation in animal models of pain. *Pain*. 2007. doi:10.1016/j.pain.2007.01.011.

135. Anderson MT, Staal FJ, Gitler C, Herzenberg LA, Herzenberg LA. Separation of oxidant-initiated and redox-regulated steps in the NF-kappa B signal transduction pathway. *Proceedings of the National Academy of Sciences of the United States of America*. 1994.

136. Singh I, Singh AK, Contreras MA. Peroxisomal dysfunction in inflammatory childhood white matter disorders: An unexpected contributor to neuropathology. *Journal of Child*

Neurology. 2009. doi:10.1177/0883073809338327.

137. Broderick G, Fletcher MA, Gallagher M, Barnes Z, Vernon SD, Klimas NG. Exploring the diagnostic potential of immune biomarker coexpression in gulf war illness. *Methods in Molecular Biology*. 2012;934:145-164. doi:10.1007/978-1-62703-071-7_8.

138. Zhang Q, Zhou XD, Denny T, et al. Changes in immune parameters seen in Gulf War veterans but not in civilians with chronic fatigue syndrome. *Clinical and Diagnostic Laboratory Immunology*. 1999;6(1):6-13.

139. Bordet R, Ouk T, Petrault O, et al. PPAR: a new pharmacological target for neuroprotection in stroke and neurodegenerative diseases. *Biochem Soc Trans*. 2006;34(Pt 6):1341-1346. doi:BST0341341 [pii]\r10.1042/BST0341341 [doi].

140. Forman BM, Chen J, Evans RM. Hypolipidemic drugs, polyunsaturated fatty acids, and eicosanoids are ligands for peroxisome proliferator-activated receptors and . *Proceedings of the National Academy of Sciences*. 1997;94(9):4312-4317. doi:10.1073/pnas.94.9.4312.

141. Gray E, Ginty M, Kemp K, Scolding N, Wilkins A. Peroxisome proliferator-activated receptor-α agonists protect cortical neurons from inflammatory mediators and improve peroxisomal function. *European Journal of Neuroscience*. 2011;33(8):1421-1432. doi:10.1111/j.1460-9568.2011.07637.x.

142. Jung TW, Lee JY, Shim WS, et al. Rosiglitazone protects human neuroblastoma SH-SY5Y cells against MPP+ induced cytotoxicity via inhibition of mitochondrial dysfunction and ROS production. *Journal of the Neurological Sciences*. 2007;253(1-2):53-60. doi:10.1016/j.jns.2006.11.020.

143. Lehmann JM, Lenhard JM, Oliver BB, Ringold GM, Kliewer SA. Peroxisome proliferator-activated receptors alpha and gamma are activated by indomethacin and other non-steroidal anti-inflammatory drugs. *The Journal of biological chemistry*. 1997;272(6):3406-3410. doi:10.1074/jbc.272.6.3406.

144. D'Agostino G, Cristiano C, Lyons DJ, et al. Peroxisome proliferator-activated receptor alpha plays a crucial role in behavioral repetition and cognitive flexibility in mice. *Molecular Metabolism*. 2015. doi:10.1016/j.molmet.2015.04.005.

145. Yang LC, Guo H, Zhou H, et al. Chronic oleoylethanolamide treatment improves spatial cognitive deficits through enhancing hippocampal neurogenesis after transient focal cerebral ischemia. *Biochemical Pharmacology*. 2015;94(4):257-269. doi:10.1016/j.bcp.2015.02.012.

146. Luo D, Zhang Y, Yuan X, et al. Oleoylethanolamide inhibits glial activation via moudulating PPARα and promotes motor function recovery after brain ischemia. *Pharmacological Research*. 2019. doi:10.1016/j.phrs.2019.01.027.

147. Yang L, Guo H, Li Y, et al. Oleoylethanolamide exerts anti-inflammatory effects on LPS-induced THP-1 cells by enhancing PPARα signaling and inhibiting the NF-κB and ERK1/2/AP-1/STAT3 pathways. *Scientific reports*. 2016;6(September):34611. doi:10.1038/srep34611.

148. Djouadi F, Weinheimer CJ, Saffitz JE, et al. A gender-related defect in lipid metabolism and glucose homeostasis in peroxisome proliferator-activated receptor α-deficient mice. *Journal of Clinical Investigation*. 1998. doi:10.1172/JCI3949.

149. Campolongo P, Roozendaal B, Trezza V, et al. Fat-induced satiety factor oleoylethanolamide enhances memory consolidation. *Proceedings of the National Academy of Sciences of the United States of America*. 2009;106(19):8027-8031. doi:10.1073/pnas.0903038106.

150. Orio L, García-Bueno B, Pavón FJ, Serrano A, Alen F. Oleoylethanolamide, Neuroinflammation, and Alcohol Abuse. *Frontiers in Molecular Neuroscience*. 2019;11(January):1-21. doi:10.3389/fnmol.2018.00490.

151. Cunard R, DiCampli D, Archer DC, et al. WY14,643, a PPAR alpha ligand, has profound effects on immune responses in vivo. *Journal of immunology*.

2002;169(12):6806-6812. doi:10.4049/jimmunol.169.12.6806.

152. Dasgupta S, Roy A, Jana M, Hartley DM, Pahan K. Gemfibrozil ameliorates relapsing-remitting experimental autoimmune encephalomyelitis independent of peroxisome proliferator-activated receptor-alpha. *Molecular pharmacology*. 2007;72(4):934-946. doi:10.1124/mol.106.033787.

153. Gocke AR, Hussain RZ, Yang Y, et al. Transcriptional modulation of the immune response by peroxisome proliferator-activated receptor-{alpha} agonists in autoimmune disease. *Journal of immunology (Baltimore, Md : 1950)*. 2009;182(7):4479-4487. doi:10.4049/jimmunol.0713927.

154. Jones DC, Ding X, Daynes R a. Nuclear receptor peroxisome proliferator-activated receptor alpha (PPARalpha) is expressed in resting murine lymphocytes. The PPARalpha in T and B lymphocytes is both transactivation and transrepression competent. *The Journal of biological chemistry*. 2002;277(9):6838-6845. doi:10.1074/jbc.M106908200.

155. Sayd A, Antón M, Alén F, et al. Systemic administration of oleoylethanolamide protects from neuroinflammation and anhedonia induced by LPS in rats. *International Journal of Neuropsychopharmacology*. 2015;18(6):1-14. doi:10.1093/ijnp/pyu111.

156. Wilks AF. Two putative protein-tyrosine kinases identified by application of the polymerase chain reaction. *Proceedings of the National Academy of Sciences*. 2006. doi:10.1073/pnas.86.5.1603.

157. Abdullah L, Crynen G, Reed J, et al. Proteomic CNS profile of delayed cognitive impairment in mice exposed to Gulf War agents. *NeuroMolecular Medicine*. 2011;13(4):275-288. doi:10.1007/s12017-011-8160-z.

158. Can A, Dao DT, Arad M, Terrillion CE, Piantadosi SC, Gould TD. The mouse forced swim test. *Journal of visualized experiments : JoVE*. 2012;(59):e3638. doi:10.3791/3638.

159. Zhang Z, Ma X, Xia Z, et al. NLRP3 inflammasome activation mediates fatigue-like behaviors in mice via neuroinflammation. *Neuroscience*. 2017;358:115-123.

doi:10.1016/j.neuroscience.2017.06.048.

160. Macanas-Pirard P, Quezada T, Navarrete L, et al. The CCL2/CCR2 axis affects transmigration and proliferation but not resistance to chemotherapy of acute myeloid leukemia cells. *PLoS ONE*. 2017;12(1). doi:10.1371/journal.pone.0168888.

161. FOLCH J, LEES M, SLOANE STANLEY GH. A simple method for the isolation and purification of total lipides from animal tissues. *The Journal of biological chemistry*. 1957;226(1):497-509. doi:10.1371/journal.pone.0020510.

162. Duan FF, Guo Y, Li JW, Yuan K. Antifatigue Effect of Luteolin-6-C-Neohesperidoside on Oxidative Stress Injury Induced by Forced Swimming of Rats through Modulation of Nrf2/ARE Signaling Pathways. *Oxidative Medicine and Cellular Longevity*. 2017;2017. doi:10.1155/2017/3159358.

163. Xu M, Liang R, Li Y, Wang J. Anti-fatigue effects of dietary nucleotides in mice. *Food & Nutrition Research*. 2017;61(1):1334485. doi:10.1080/16546628.2017.1334485.

164. Gadea A, López-Colomé AM. Glial transporters for glutamate, glycine, and GABA: II. GABA transporters. *Journal of Neuroscience Research*. 2001;63(6):461-468. doi:10.1002/jnr.1040.

165. Kacem K, Lacombe P, Seylaz J, Bonvento G. Structural organization of the perivascular astrocyte endfeet and their relationship with the endothelial glucose transporter: A confocal microscopy study. *GLIA*. 1998;23(1):1-10. doi:10.1002/(SICI)1098-1136(199805)23:1<1::AID-GLIA1>3.0.CO;2-B.

166. Gehrmann J, Matsumoto Y, Kreutzberg GW. Microglia: Intrinsic immuneffector cell of the brain. *Brain Research Reviews*. 1995;20(3):269-287. doi:10.1016/0165-0173(94)00015-H.

167. Kreutzberg GW. Microglia: A sensor for pathological events in the CNS. *Trends in Neurosciences*. 1996;19(8):312-318. doi:10.1016/0166-2236(96)10049-7.

168. Chen L, Li L, Chen J, et al. Oleoylethanolamide, an endogenous PPAR-alpha ligand,

attenuates liver fibrosis targeting hepatic stellate cells. *Oncotarget*. 2015. doi:10.18632/oncotarget.6466.

169. Maule AL, Janulewicz PA, Sullivan KA, et al. Meta-analysis of self-reported health symptoms in 1990–1991 Gulf War and Gulf War-era veterans. *BMJ Open*. 2018;8(2):e016086. doi:10.1136/bmjopen-2017-016086.

170. Sullivan K, Krengel M, Proctor SP, Devine S, Heeren T, White RF. Cognitive functioning in treatment-seeking Gulf War veterans: Pyridostigmine bromide use and PTSD. *Journal of Psychopathology and Behavioral Assessment*. 2003;25(2):95-103. doi:10.1023/A:1023342915425.

171. Anger WK, Storzbach D, Binder LM, et al. Neurobehavioral deficits in Persian Gulf veterans: Evidence from a population-based study. *Journal of the International Neuropsychological Society*. 1999;5(3):203-212. doi:10.1017/S1355617799533031.

172. Sillanpaa MC, Agar LM, Milner IB, Podany EC, Axelrod BN, Brown GG. Gulf War veterans: A neuropsychological examination. *Journal of Clinical and Experimental Neuropsychology*. 1997;19(2):211-219. doi:10.1080/01688639708403852.

173. Binder LM, Storzbach D, Anger WK, et al. Subjective cognitive complaints, affective distress, and objective cognitive performance in Persian Gulf War veterans. *Archives of clinical neuropsychology : the official journal of the National Academy of Neuropsychologists*. 1999;14(6):531-536. doi:http://dx.doi.org/10.1016/S0887-6177(98)00047-X.

174. Bunegin L, Mitzel HC, Miller CS, Gelineau JF, Tolstykh GP. Cognitive performance and cerebrohemodynamics associated with the Persian Gulf Syndrome. *Toxicology and Industrial Health*. 2001;17(4):128-137. doi:10.1191/0748233701th100oa.

175. Storzbach D, Campbell KA, Binder LM, et al. Psychological differences between veterans with and without Gulf War unexplained symptoms. *Psychosomatic Medicine*. 2000;62(5):726-735. doi:10.1097/00006842-200009000-00017.

176. Menon PM, Nasrallah HA, Reeves RR, Ali JA. Hippocampal dysfunction in Gulf War Syndrome. A proton MR spectroscopy study. *Brain Research*. 2004;1009(1-2):189-194. doi:10.1016/j.brainres.2004.02.063.

177. Vythilingam M, Luckenbaugh DA, Lam T, et al. Smaller head of the hippocampus in Gulf War-related posttraumatic stress disorder. *Psychiatry Research - Neuroimaging*. 2005;139(2):89-99. doi:10.1016/j.pscychresns.2005.04.003.

178. Weiner MW. Magnetic Resonance and Spectroscopy of the Human Brain in Gulf War Illness. 2005:1-11.

179. Koo BB, Michalovicz LT, Calderazzo S, et al. Corticosterone potentiates DFP-induced neuroinflammation and affects high-order diffusion imaging in a rat model of Gulf War Illness. *Brain, Behavior, and Immunity*. 2018;67:42-46. doi:10.1016/j.bbi.2017.08.003.

180. Abdullah L, Evans JE, Bishop A, et al. Lipidomic profiling of phosphocholine containing brain lipids in mice with sensorimotor deficits and anxiety-like features after exposure to gulf war agents. *NeuroMolecular Medicine*. 2012;14(4):349-361. doi:10.1007/s12017-012-8192-z.

181. Plaza-Zabala A, Berrendero F, Suarez J, et al. Effects of the endogenous PPAR-alpha agonist, oleoylethanolamide on MDMA-induced cognitive deficits in mice. *Synapse*. 2010;64(5):379-389. doi:10.1002/syn.20733.

182. Bannerman DM, Rawlins JNP, McHugh SB, et al. Regional dissociations within the hippocampus - Memory and anxiety. *Neuroscience and Biobehavioral Reviews*. 2004;28(3):273-283. doi:10.1016/j.neubiorev.2004.03.004.

183. Da Cruz e Alves-de-Moraes LB, Ribeiro-Paes JT, Longo BM, Ferrazoli EG, De Andrade TGCS. Effect of the bone marrow cell transplantation on elevated plus-maze performance in hippocampal-injured mice. *Behavioural Brain Research*. 2013;248:32-40. doi:10.1016/j.bbr.2013.03.042.

184. Zakirova Z, Crynen G, Hassan S, et al. A chronic longitudinal characterization of

neurobehavioral and neuropathological cognitive impairment in a mouse model of Gulf War agent exposure. *Frontiers in integrative neuroscience*. 2015;9:71. doi:10.3389/fnint.2015.00071.

185. McKimmie CS, Graham GJ. Astrocytes modulate the chemokine network in a pathogen-specific manner. *Biochemical and Biophysical Research Communications*. 2010;394(4):1006-1011. doi:10.1016/j.bbrc.2010.03.111.

186. Ramesh G, Maclean AG, Philipp MT. Cytokines and chemokines at the crossroads of neuroinflammation, neurodegeneration, and neuropathic pain. *Mediators of Inflammation*. 2013;2013. doi:10.1155/2013/480739.

187. Conductier G, Blondeau N, Guyon A, Nahon JL, Rovère C. The role of monocyte chemoattractant protein MCP1/CCL2 in neuroinflammatory diseases. *Journal of Neuroimmunology*. 2010;224(1-2):93-100. doi:10.1016/j.jneuroim.2010.05.010.

188. Parillaud VR, Lornet G, Monnet Y, et al. Analysis of monocyte infiltration in MPTP mice reveals that microglial CX3CR1 protects against neurotoxic over-induction of monocyte-attracting CCL2 by astrocytes. *Journal of Neuroinflammation*. 2017. doi:10.1186/s12974-017-0830-9.

189. Selenica MLB, Alvarez JA, Nash KR, et al. Diverse activation of microglia by chemokine (C-C motif) ligand 2 overexpression in brain. *Journal of Neuroinflammation*. 2013;10. doi:10.1186/1742-2094-10-86.

190. Chen K, Liu M, Liu Y, et al. Signal relay by CC chemokine receptor 2 (CCR2) and formylpeptide receptor 2 (Fpr2) in the recruitment of monocyte-derived dendritic cells in allergic airway inflammation. *Journal of Biological Chemistry*. 2013;288(23):16262-16273. doi:10.1074/jbc.M113.450635.

191. Jimenez F, Quinones MP, Martinez HG, et al. CCR2 plays a critical role in dendritic cell maturation: possible role of CCL2 and NF-kappa B. *Journal of immunology (Baltimore, Md : 1950)*. 2010;184(10):5571-5581. doi:10.4049/jimmunol.0803494.

192. Craddock TJA, Del Rosario RR, Rice M, et al. Achieving remission in Gulf War Illness: A simulation-based approach to treatment design. *PLoS ONE*. 2015;10(7). doi:10.1371/journal.pone.0132774.

193. Sagar DR, Gaw AG, Okine BN, et al. Dynamic regulation of the endocannabinoid system: Implications for analgesia. *Molecular Pain*. 2009;5. doi:10.1186/1744-8069-5-59.

194. Edvardsson U, Ljungberg A, Lindén D, et al. PPARalpha activation increases triglyceride mass and adipose differentiation-related protein in hepatocytes. *Journal of lipid research*. 2006;47(2):329-340. doi:10.1194/jlr.M500203-JLR200.

195. Garcia-Roves P, Huss JM, Han D-H, et al. Raising plasma fatty acid concentration induces increased biogenesis of mitochondria in skeletal muscle. *Proceedings of the National Academy of Sciences*. 2007;104(25):10709-10713. doi:10.1073/pnas.0704024104.

196. Watt MJ, Southgate RJ, Holmes a G, Febbraio M a. Suppression of plasma free fatty acids upregulates peroxisome proliferator-activated receptor (PPAR) alpha and delta and PPAR coactivator 1alpha in human skeletal muscle, but not lipid regulatory genes. *Journal of molecular endocrinology*. 2004;33(2):533-544. doi:10.1677/jme.1.01499.

197. Verhoeven NM, Roe DS, Kok RM, Wanders RJ, Jakobs C, Roe CR. Phytanic acid and pristanic acid are oxidized by sequential peroxisomal and mitochondrial reactions in cultured fibroblasts. *Journal of lipid research*. 1998;39(1):66-74. http://www.ncbi.nlm.nih.gov/pubmed/9469587.

198. Verhoeven NM, Jakobs C. Human metabolism of phytanic acid and pristanic acid. *Progress in Lipid Research*. 2001. doi:10.1016/S0163-7827(01)00011-X.

199. Fu J, Gaetani S, Oveisi F, et al. Oleylethanolamide regulates feeding and body weight through activation of the nuclear receptor PPAR-α. *Nature*. 2003. doi:10.1038/nature01921.

200. Chinetti G, Fruchart JC, Staels B. Peroxisome proliferator-activated receptors (PPARs): Nuclear receptors at the crossroads between lipid metabolism and inflammation. *Inflammation Research*. 2000. doi:10.1007/s000110050622.

201. Austin S, St-Pierre J. PGC1 and mitochondrial metabolism - emerging concepts and relevance in ageing and neurodegenerative disorders. *Journal of Cell Science*. 2012. doi:10.1242/jcs.113662.

202. Wilkins HM, Weidling IW, Ji Y, Swerdlow RH. Mitochondria-derived damage-associated molecular patterns in neurodegeneration. *Frontiers in Immunology*. 2017. doi:10.3389/fimmu.2017.00508.

203. Koslik HJ, Hamilton G, Golomb BA. Mitochondrial dysfunction in Gulf War illness revealed by 31phosphorus magnetic resonance spectroscopy: A case-control study. *PLoS ONE*. 2014. doi:10.1371/journal.pone.0092887.

204. Halpin P, Williams MV, Klimas NG, Fletcher MA, Barnes Z, Ariza ME. Myalgic Encephalomyelitis/Chronic Fatigue Syndrome and Gulf War Illness patients exhibit increased humoral responses to the Herpesviruses-encoded dUTPase: Implications in disease pathophysiology. *Journal of Medical Virology*. 2017;(November 2016). doi:10.1002/jmv.24810.

205. Zhang Q, Zhou XD, Denny T, et al. Changes in immune parameters seen in Gulf War veterans but not in civilians with chronic fatigue syndrome. *Clinical and diagnostic laboratory immunology*. 1999.

206. Wilkins HM, Carl SM, Greenlief A, Festoff BW, Swerdlow RH. Bioenergetic dysfunction and inflammation in alzheimer's disease: A possible connection. *Frontiers in Aging Neuroscience*. 2014. doi:10.3389/fnagi.2014.00311.

207. Dela Cruz CS, Kang MJ. Mitochondrial dysfunction and damage associated molecular patterns (DAMPs) in chronic inflammatory diseases. *Mitochondrion*. 2018. doi:10.1016/j.mito.2017.12.001.

208. Wang P, Xie K, Wang C, Bi J. Oxidative stress induced by lipid peroxidation is related with inflammation of demyelination and neurodegeneration in multiple sclerosis. *European Neurology*. 2014. doi:10.1159/000363515.

209. Wang S, Wan T, Ye M, et al. Nicotinamide riboside attenuates alcohol induced liver injuries via activation of SirT1/PGC-1α/mitochondrial biosynthesis pathway. *Redox Biology*. 2018. doi:10.1016/j.redox.2018.04.006.

210. Trammell SAJ, Schmidt MS, Weidemann BJ, et al. Nicotinamide riboside is uniquely and orally bioavailable in mice and humans. *Nature Communications*. 2016. doi:10.1038/ncomms12948.

211. Berger F, Ramírez-Hernández MH, Ziegler M. The new life of a centenarian: Signalling functions of NAD(P). *Trends in Biochemical Sciences*. 2004. doi:10.1016/j.tibs.2004.01.007.

212. Ruggieri S, Orsomando G, Sorci L, Raffaelli N. Regulation of NAD biosynthetic enzymes modulates NAD-sensing processes to shape mammalian cell physiology under varying biological cues. *Biochimica et Biophysica Acta - Proteins and Proteomics*. 2015. doi:10.1016/j.bbapap.2015.02.021.

213. Sauve AA. Sirtuin chemical mechanisms. *Biochimica et Biophysica Acta - Proteins and Proteomics*. 2010. doi:10.1016/j.bbapap.2010.01.021.

214. Sauve AA, Wolberger C, Schramm VL, Boeke JD. The Biochemistry of Sirtuins. *Annual Review of Biochemistry*. 2006. doi:10.1146/annurev.biochem.74.082803.133500.

215. Kitada M, Kume S, Takeda-Watanabe A, Kanasaki K, Koya D. Sirtuins and renal diseases: relationship with aging and diabetic nephropathy. *Clinical Science*. 2012. doi:10.1042/cs20120190.

216. Revollo JR, Grimm AA, Imai SI. The NAD biosynthesis pathway mediated by nicotinamide phosphoribosyltransferase regulates Sir2 activity in mammalian cells. *Journal of Biological Chemistry*. 2004. doi:10.1074/jbc.M408388200.

217. Ying W. NAD + /NADH and NADP + /NADPH in Cellular Functions and Cell Death: Regulation and Biological Consequences . *Antioxidants & Redox Signaling*. 2008. doi:10.1089/ars.2007.1672.

218. Stein LR, Imai SI. The dynamic regulation of NAD metabolism in mitochondria. *Trends in Endocrinology and Metabolism*. 2012. doi:10.1016/j.tem.2012.06.005.

219. Cettour-rose P, Gademann K, Rinsch C, Schoonjans K, Sauve AA, Auwerx J. The NAD + precursor nicotinamide riboside enhances oxidative metabolism and protects against high-fat diet induced obesity. *Cell Metabolism*. 2013. doi:10.1016/j.cmet.2012.04.022.The.

220. Hou Y, Lautrup S, Cordonnier S, et al. NAD + supplementation normalizes key Alzheimer's features and DNA damage responses in a new AD mouse model with introduced DNA repair deficiency. *Proceedings of the National Academy of Sciences*. 2018. doi:10.1073/pnas.1718819115.

221. Chong ZZ, Shang YC, Wang S, Maiese K. SIRT1: new avenues of discovery for disorders of oxidative stress. *Expert Opinion on Therapeutic Targets*. 2012. doi:10.1517/14728222.2012.648926.

222. Hasan-Olive MM, Lauritzen KH, Ali M, Rasmussen LJ, Storm-Mathisen J, Bergersen LH. A Ketogenic Diet Improves Mitochondrial Biogenesis and Bioenergetics via the PGC1α-SIRT3-UCP2 Axis. *Neurochemical Research*. 2019. doi:10.1007/s11064-018-2588-6.

223. Chen X, Chen C, Fan S, et al. Omega-3 polyunsaturated fatty acid attenuates the inflammatory response by modulating microglia polarization through SIRT1-mediated deacetylation of the HMGB1/NF-KB pathway following experimental traumatic brain injury. *Journal of Neuroinflammation*. 2018. doi:10.1186/s12974-018-1151-3.

224. Zhu Y, Zhao KK, Tong Y, et al. Exogenous NAD+ decreases oxidative stress and protects H2O2-treated RPE cells against necrotic death through the up-regulation of

autophagy. *Scientific Reports*. 2016. doi:10.1038/srep26322.

225. Hong G, Zheng D, Zhang L, et al. Administration of nicotinamide riboside prevents oxidative stress and organ injury in sepsis. *Free Radical Biology and Medicine*. 2018. doi:10.1016/j.freeradbiomed.2018.05.073.

226. Schöndorf DC, Ivanyuk D, Baden P, et al. The NAD+ Precursor Nicotinamide Riboside Rescues Mitochondrial Defects and Neuronal Loss in iPSC and Fly Models of Parkinson's Disease. *Cell Reports*. 2018. doi:10.1016/j.celrep.2018.05.009.

227. Liu D, Pitta M, Jiang H, et al. Nicotinamide forestalls pathology and cognitive decline in Alzheimer mice: Evidence for improved neuronal bioenergetics and autophagy procession. *Neurobiology of Aging*. 2013. doi:10.1016/j.neurobiolaging.2012.11.020.

228. Guzmán M, Blázquez C. Ketone body synthesis in the brain: Possible neuroprotective effects. *Prostaglandins Leukotrienes and Essential Fatty Acids*. 2004. doi:10.1016/j.plefa.2003.05.001.

229. Schrauwen P, Hesselink MKC. Oxidative capacity, lipotoxicity, and mitochondrial damage in type 2 diabetes. *Diabetes*. 2004. doi:10.2337/diabetes.53.6.1412.

230. Kawamura MJ, Ruskin DN, Masino SA. Metabolic Therapy for Temporal Lobe Epilepsy in a Dish: Investigating Mechanisms of Ketogenic Diet using Electrophysiological Recordings in Hippocampal Slices. *Frontiers in Molecular Neuroscience*. 2016. doi:10.3389/fnmol.2016.00112.

231. Gjedde A. Calculation of cerebral glucose phosphorylation from brain uptake of glucose analogs in vivo: A re-examination. *Brain Research Reviews*. 1982. doi:10.1016/0165-0173(82)90018-2.

232. Barañano KW, Hartman AL. The ketogenic diet: uses in epilepsy and other neurologic illnesses. *Current treatment options in neurology*. 2008.

233. Bergqvist AGC, Schall JI, Gallagher PR, Cnaan A, Stallings VA. Fasting versus gradual initiation of the ketogenic diet: A prospective, randomized clinical trial of efficacy.

Epilepsia. 2005. doi:10.1111/j.1528-1167.2005.00282.x.

234. Lab S, Delaney E, Zenchak J. Research Article: Replacing the ketogenic diet with oral β-hydroxybutyrate. *BIOS*. 2005. doi:10.1893/0005-3155(2005)076[0162:rartkd]2.0.co;2.

235. Hartman AL, Vining EPG. Clinical Aspects of the Ketogenic Diet. *Epilepsia*. 2007. doi:10.1111/j.1528-1167.2007.00914.x.

236. Masino S, Kawamura Jr. M, Wasser C, Pomeroy L, Ruskin D. Adenosine, Ketogenic Diet and Epilepsy: The Emerging Therapeutic Relationship Between Metabolism and Brain Activity. *Current Neuropharmacology*. 2009. doi:10.2174/157015909789152164.

237. Ebihara A. World medical association declaration of Helsinki. *Japanese Pharmacology and Therapeutics*. 2000.

238. Baldelli S, Aquilano K, Ciriolo MR. PGC-1α buffers ROS-mediated removal of mitochondria during myogenesis. *Cell Death and Disease*. 2014. doi:10.1038/cddis.2014.458.

239. Cettour-rose P, Gademann K, Rinsch C, Schoonjans K, Sauve AA, Auwerx J. The NAD + precursor nicotinamide riboside enhances oxidative metabolism and protects against high-fat diet induced obesity. *Cell Metabolism*. 2013;15(6):838-847. doi:10.1016/j.cmet.2012.04.022.The.

240. Chen S Der, Yang DI, Lin TK, Shaw FZ, Liou CW, Chuang YC. Roles of oxidative stress, apoptosis, PGC-1 and mitochondrial biogenesis in cerebral ischemia. *International Journal of Molecular Sciences*. 2011. doi:10.3390/ijms12107199.

241. Carafa V, Rotili D, Forgione M, et al. Sirtuin functions and modulation: from chemistry to the clinic. *Clinical Epigenetics*. 2016. doi:10.1186/s13148-016-0224-3.

242. Canto C, Auwerx J. Targeting Sirtuin 1 to Improve Metabolism: All You Need Is NAD+? *Pharmacological Reviews*. 2011. doi:10.1124/pr.110.003905.

243. Mikirova N, Casciari J, Hunninghake R. The assessment of the energy metabolism in patients with chronic fatigue syndrome by serum fluorescence emission. *Alternative*

Therapies in Health and Medicine. 2012.

244. J. C-M, N. S-F, M.J. S, et al. Effect of coenzyme Q10 plus nicotinamide adenine dinucleotide supplementation on maximum heart rate after exercise testing in chronic fatigue syndrome - A randomized, controlled, double-blind trial. *Clinical Nutrition*. 2016.

245. Martens CR, Denman BA, Mazzo MR, et al. Chronic nicotinamide riboside supplementation is well-Tolerated and elevates NAD+ in healthy middle-Aged and older adults. *Nature Communications*. 2018. doi:10.1038/s41467-018-03421-7.

246. Alegre J, Roses JM, Javierre C, Ruiz-Baques A, Segundo MJ, Fernandez De Sevilla T. Nicotinamide adenine dinucleotide (NADH) in patients with chronic fatigue syndrome. [Spanish] Nicotinamida adenina dinucleotido (NADH) en pacientes con sindrome de fatiga cronica. *Revista clínica española*. 2010. doi:http://dx.doi.org/10.1016/j.rce.2009.09.015.

247. Giralt A, Villarroya F. SIRT3, a pivotal actor in mitochondrial functions: metabolism, cell death and aging. *Biochemical Journal*. 2012. doi:10.1042/bj20120030.

248. Gambini J, Gomez-Cabrera MC, Borras C, et al. Free [NADH]/[NAD+] regulates sirtuin expression. *Archives of Biochemistry and Biophysics*. 2011. doi:10.1016/j.abb.2011.04.020.

249. Yang H, Zhang W, Pan H, et al. SIRT1 Activators Suppress Inflammatory Responses through Promotion of p65 Deacetylation and Inhibition of NF-κB Activity. *PLoS ONE*. 2012. doi:10.1371/journal.pone.0046364.

250. Zakhary SM, Ayubcha D, Dileo JN, et al. Distribution analysis of deacetylase SIRT1 in rodent and human nervous systems. *Anatomical Record*. 2010. doi:10.1002/ar.21116.

251. Croteau DL, Stevnsner T V., O'Connell JF, et al. NAD + supplementation normalizes key Alzheimer's features and DNA damage responses in a new AD mouse model with introduced DNA repair deficiency . *Proceedings of the National Academy of Sciences*.

2018. doi:10.1073/pnas.1718819115.

252. Shiow LR, Favrais G, Schirmer L, et al. Reactive astrocyte COX2-PGE2 production inhibits oligodendrocyte maturation in neonatal white matter injury. *GLIA*. 2017. doi:10.1002/glia.23212.

253. You LH, Yan CZ, Zheng BJ, et al. Astrocyte hepcidin is a key factor in LPS-induced neuronal apoptosis. *Cell death & disease*. 2017. doi:10.1038/cddis.2017.93.

254. Schönfeld P, Reiser G. Why does brain metabolism not favor burning of fatty acids to provide energy-Reflections on disadvantages of the use of free fatty acids as fuel for brain. *Journal of Cerebral Blood Flow and Metabolism*. 2013. doi:10.1038/jcbfm.2013.128.

255. Giangregorio N, Tonazzi A, Console L, Indiveri C. Post-translational modification by acetylation regulates the mitochondrial carnitine/acylcarnitine transport protein. *Molecular and Cellular Biochemistry*. 2017. doi:10.1007/s11010-016-2881-0.

256. Lee CF, Caudal A, Abell L, Nagana Gowda GA, Tian R. Targeting NAD + Metabolism as Interventions for Mitochondrial Disease. *Scientific Reports*. 2019. doi:10.1038/s41598-019-39419-4.

257. Jornayvaz FR, Shulman GI. Regulation of mitochondrial biogenesis. *Essays In Biochemistry*. 2010. doi:10.1042/bse0470069.

258. Nedergaard J, Cannon B. The “novel” “uncoupling” UCP2 and UCP3: What do they really do? Pros and cons for suggested functions. *Experimental Physiology*. 2003. doi:10.1113/eph8802502.

259. Gurd BJ. Deacetylation of PGC-1α by SIRT1: importance for skeletal muscle function and exercise-induced mitochondrial biogenesis. *Applied Physiology, Nutrition, and Metabolism*. 2011. doi:10.1139/h11-070.

260. Zhang X, Ren X, Zhang Q, et al. PGC-1α/ERRα-Sirt3 Pathway Regulates DAergic Neuronal Death by Directly Deacetylating SOD2 and ATP Synthase β. *Antioxidants &*

Redox Signaling. 2015. doi:10.1089/ars.2015.6403.

261. Ansari A, Rahman MS, Saha SK, Saikot FK, Deep A, Kim KH. Function of the SIRT3 mitochondrial deacetylase in cellular physiology, cancer, and neurodegenerative disease. *Aging Cell*. 2017. doi:10.1111/acel.12538.

262. Satterstrom FK, Swindell WR, Laurent G, Vyas S, Bulyk ML, Haigis MC. Nuclear respiratory factor 2 induces SIRT3 expression. *Aging Cell*. 2015. doi:10.1111/acel.12360.

263. Bagattin A, Hugendubler L, Mueller E. Transcriptional coactivator PGC-1 promotes peroxisomal remodeling and biogenesis. *Proceedings of the National Academy of Sciences*. 2010. doi:10.1073/pnas.1009176107.

264. Wijeratne SSK, Cuppett SL. Lipid hydroperoxide induced oxidative stress damage and antioxidant enzyme response in Caco-2 human colon cells. *Journal of Agricultural and Food Chemistry*. 2006. doi:10.1021/jf060475v.

265. Schimke I, Kahl P, Romaniuk P, Papies B. Concentration of thiobarbituric acid reactive substances (TBARS) in serum following myocardial infarct. *Klin Wochenschr ;64(23):1237-9*. 1989;64(23):(2):1237-1239.

266. Velasquez MT, Ramezani A, Manal A, Raj DS. Trimethylamine N-oxide: The good, the bad and the unknown. *Toxins*. 2016. doi:10.3390/toxins8110326.

267. Chen M-L, Zhu X-H, Ran L, Lang H-D, Yi L, Mi M-T. Trimethylamine-N-Oxide Induces Vascular Inflammation by Activating the NLRP3 Inflammasome Through the SIRT3-SOD2-mtROS Signaling Pathway. *Journal of the American Heart Association*. 2017. doi:10.1161/JAHA.117.006347.

268. Seldin MM, Meng Y, Qi H, et al. Trimethylamine N-Oxide Promotes Vascular Inflammation Through Signaling of Mitogen-Activated Protein Kinase and Nuclear Factor-κB. *Journal of the American Heart Association*. 2016. doi:10.1161/JAHA.115.002767.

269. Heianza Y, Sun D, Smith SR, Bray GA, Sacks FM, Qi L. Changes in gut microbiota-Related metabolites and longterm successful weight loss in response to weight-loss diets: The POUNDS lost trial. *Diabetes Care*. 2018. doi:10.2337/dc17-2108.

270. Masino SA, Rho JM. Mechanisms of ketogenic diet action. *Epilepsia*. 2010. doi:10.1111/j.1528-1167.2010.02871.x.

271. Bordone L, Guarente L. Calorie restriction, SIRT1 and metabolism: Understanding longevity. *Nature Reviews Molecular Cell Biology*. 2005. doi:10.1038/nrm1616.

272. Nisoli E, Tonello C, Cardile A, et al. Cell biology: Calorie restriction promotes mitochondrial biogenesis by inducing the expression of eNOS. *Science*. 2005. doi:10.1126/science.1117728.

273. Gao Z, Yin J, Zhang J, et al. Butyrate improves insulin sensitivity and increases energy expenditure in mice. *Diabetes*. 2009. doi:10.2337/db08-1637.

274. Grabacka M, Pierzchalska M, Dean M, Reiss K. Regulation of ketone body metabolism and the role of PPARα. *International Journal of Molecular Sciences*. 2016. doi:10.3390/ijms17122093.

275. Fu SP, Wang JF, Xue WJ, et al. Anti-inflammatory effects of BHBA in both in vivo and in vitro Parkinson's disease models are mediated by GPR109A-dependent mechanisms. *Journal of Neuroinflammation*. 2015. doi:10.1186/s12974-014-0230-3.

276. Sullivan K, Krengel M, Bradford W, et al. Neuropsychological functioning in military pesticide applicators from the Gulf War: Effects on information processing speed, attention and visual memory. *Neurotoxicology and Teratology*. 2018. doi:10.1016/j.ntt.2017.11.002.

277. Thrasher JD, Madison R, Brouchton A. Immunologic abnormalities in humans exposed to chlorpyrifos: Preliminary observations. *Archives of Environmental Health*. 1993. doi:10.1080/00039896.1993.9938400.

278. Proudfoot AT. Poisoning due to pyrethrins. *Toxicological Reviews*. 2005.

doi:10.2165/00139709-200524020-00004.

279. Gangemi S, Gofita E, Costa C, et al. Occupational and environmental exposure to pesticides and cytokine pathways in chronic diseases (Review). *International Journal of Molecular Medicine*. 2016. doi:10.3892/ijmm.2016.2728.

280. Müller-Mohnssen H. Chronic sequelae and irreversible injuries following acute pyrethroid intoxication. In: *Toxicology Letters*. ; 1999. doi:10.1016/S0378-4274(99)00043-0.

281. Warrington R. Drug allergy: Causes and desensitization. *Human Vaccines and Immunotherapeutics*. 2012. doi:10.4161/hv.21889.

282. Noort D, Van Zuylen A, Fidder A, Van Ommen B, Hulst AG. Protein adduct formation by glucuronide metabolites of permethrin. *Chemical Research in Toxicology*. 2008. doi:10.1021/tx8000362.

283. Karlsson I, Samuelsson K, Simonsson C, et al. The Fate of a Hapten - From the Skin to Modification of Macrophage Migration Inhibitory Factor (MIF) in Lymph Nodes. *Scientific Reports*. 2018. doi:10.1038/s41598-018-21327-8.

284. Diamond B, Honig G, Mader S, Brimberg L, Volpe BT. Brain-Reactive Antibodies and Disease. *Annual Review of Immunology*. 2013. doi:doi:10.1146/annurev-immunol-020711-075041.

285. Omdal R, Brokstad K, Waterloo K, Koldingsnes W, Jonsson R, Mellgren SI. Neuropsychiatric disturbances in SLE are associated with antibodies against NMDA receptors. *European Journal of Neurology*. 2005. doi:10.1111/j.1468-1331.2004.00976.x.

286. Stern JNH, Yaari G, Vander Heiden JA, et al. B cells populating the multiple sclerosis brain mature in the draining cervical lymph nodes. *Science Translational Medicine*. 2014. doi:10.1126/scitranslmed.3008879.

287. Song J, Wu C, Korpos E, et al. Focal MMP-2 and MMP-9 Activity at the Blood-Brain

Barrier Promotes Chemokine-Induced Leukocyte Migration. *Cell Reports*. 2015. doi:10.1016/j.celrep.2015.01.037.

288. Miró-Mur F, Pérez-de-Puig I, Ferrer-Ferrer M, et al. Immature monocytes recruited to the ischemic mouse brain differentiate into macrophages with features of alternative activation. *Brain, Behavior, and Immunity*. 2016. doi:10.1016/j.bbi.2015.08.010.

289. Wohleb ES, Powell ND, Godbout JP, Sheridan JF. Stress-Induced Recruitment of Bone Marrow-Derived Monocytes to the Brain Promotes Anxiety-Like Behavior. *Journal of Neuroscience*. 2013. doi:10.1523/jneurosci.1671-13.2013.

290. Harrison-Brown M, Liu GJ, Banati R. Checkpoints to the brain: Directing myeloid cell migration to the central nervous system. *International Journal of Molecular Sciences*. 2016. doi:10.3390/ijms17122030.

291. Gerard C, Rollins BJ. Chemokines and disease. *Nature Immunology*. 2001. doi:10.1038/84209.

292. Bose S, Cho J. Role of chemokine CCL2 and its receptor CCR2 in neurodegenerative diseases. *Archives of Pharmacal Research*. 2013. doi:10.1007/s12272-013-0161-z.

293. Joshi U, Pearson A, Evans JE, et al. A permethrin metabolite is associated with adaptive immune responses in Gulf War Illness. *Brain, Behavior, and Immunity*. 2019. doi:10.1016/j.bbi.2019.07.015.

294. Qiang L, Rao AN, Mostoslavsky G, et al. Reprogramming cells from Gulf War veterans into neurons to study Gulf War illness. *Neurology*. 2017;88(20):1968-1975. doi:10.1212/WNL.0000000000003938.

295. Ahn KC, Gee SJ, Kim HJ, et al. Immunochemical analysis of 3-phenoxybenzoic acid, a biomarker of forestry worker exposure to pyrethroid insecticides. *Analytical and Bioanalytical Chemistry*. 2011. doi:10.1007/s00216-011-5184-z.

296. Pakvilai N, Prapamontol T, Hongsibsong S, Kerdnoi T. A Gc-Ecd Method for Detecting 3-Phenoxybenzoic Acid in Human Urine Samples and Its Application in Real Samples.

2014;8(15):143-148.

297. Tailor A, Waddington JC, Meng X, Park BK. Mass Spectrometric and Functional Aspects of Drug-Protein Conjugation. *Chemical Research in Toxicology*. 2016. doi:10.1021/acs.chemrestox.6b00147.

298. Ahn C ki, Lohstroh P, Gee SJ, Gee NA, Lasley B, Hammock BD. High-throughput automated luminescent magnetic particle-based immunoassay to monitor human exposure to pyrethroid insecticides. *Analytical Chemistry*. 2007. doi:10.1021/ac070675l.

299. Di Domizio J, Dorta-Estremera S, Cao W. Methylated BSA Mimics Amyloid-Related Proteins and Triggers Inflammation. *PLoS ONE*. 2013. doi:10.1371/journal.pone.0063214.

300. Santer DM, Ma MM, Hockman D, Landi A, Tyrrell DLJ, Houghton M. Enhanced Activation of Memory, but Not Naïve, B Cells in Chronic Hepatitis C Virus-Infected Patients with Cryoglobulinemia and Advanced Liver Fibrosis. *PLoS ONE*. 2013. doi:10.1371/journal.pone.0068308.

301. Randolph GJ, Jakubzick C, Qu C. Antigen presentation by monocytes and monocyte-derived cells. *Current Opinion in Immunology*. 2008. doi:10.1016/j.coi.2007.10.010.

302. Chao LC, Soto E, Hong C, et al. Bone marrow NR4A expression is not a dominant factor in the development of atherosclerosis or macrophage polarization in mice. *Journal of lipid research*. 2013. doi:10.1194/jlr.M034157.

303. Zarruk JG, Greenhalgh AD, David S. Microglia and macrophages differ in their inflammatory profile after permanent brain ischemia. *Experimental Neurology*. 2018. doi:10.1016/j.expneurol.2017.08.011.

304. Wong M, Milbrandt J, Head R, et al. Abnormal Microglia and Enhanced Inflammation-Related Gene Transcription in Mice with Conditional Deletion of Ctcf in Camk2a-Cre -Expressing Neurons. . *The Journal of Neuroscience*. 2017. doi:10.1523/jneurosci.0936-17.2017.

305. Zhou T, Huang Z, Sun X, et al. Microglia polarization with M1/M2 phenotype changes in rd1 mouse model of retinal degeneration. *Frontiers in Neuroanatomy*. 2017. doi:10.3389/fnana.2017.00077.

306. Han W, Umekawa T, Zhou K, et al. Cranial irradiation induces transient microglia accumulation, followed by long-lasting inflammation and loss of microglia. *Oncotarget*. 2015. doi:10.18632/oncotarget.12929.

307. Underly RG, Hartmann DA, Grant RI, Levy M, Watson AN, Shih AY. Pericytes as Inducers of Rapid, Matrix Metalloproteinase-9-Dependent Capillary Damage during Ischemia. *The Journal of Neuroscience*. 2016. doi:10.1523/jneurosci.2891-16.2016.

308. Schactae AL, Palmas D, Michels M, et al. Congenital muscular dystrophy 1D causes matrix metalloproteinase activation and blood-brain barrier impairment. *Current Neurovascular Research*. 2017. doi:10.2174/1567202613666161201204549.

309. Lehnardt S, Massillon L, Follett P, et al. Activation of innate immunity in the CNS triggers neurodegeneration through a Toll-like receptor 4-dependent pathway. *Proceedings of the National Academy of Sciences*. 2003. doi:10.1073/pnas.1432609100.

310. Vaure C, Liu Y. A comparative review of toll-like receptor 4 expression and functionality in different animal species. *Frontiers in Immunology*. 2014. doi:10.3389/fimmu.2014.00316.

311. Liebner S, Kniesel U, Kalbacher H, Wolburg H. Correlation of tight junction morphology with the expression of tight junction proteins in blood-brain barrier endothelial cells. *European Journal of Cell Biology*. 2000. doi:10.1078/0171-9335-00101.

312. Yang S, Mei S, Jin H, et al. Identification of two immortalized cell lines, ECV304 and bEnd3, for in vitro permeability studies of blood-brain barrier. *PLoS ONE*. 2017. doi:10.1371/journal.pone.0187017.

313. Jokanović M. Neurotoxic effects of organophosphorus pesticides and possible

association with neurodegenerative diseases in man: A review. *Toxicology*. 2018. doi:10.1016/j.tox.2018.09.009.

314. Broderick G, Ben-Hamo R, Vashishtha S, et al. Altered immune pathway activity under exercise challenge in Gulf War Illness: An exploratory analysis. *Brain, Behavior, and Immunity*. 2013;28:159-169. doi:10.1016/j.bbi.2012.11.007.

315. Noort D, Benschop HP, Black RM. Biomonitoring of exposure to chemical warfare agents: A review. *Toxicology and Applied Pharmacology*. 2002. doi:10.1016/S0041-008X(02)99449-4.

316. Thiphom S, Prapamontol T, Chantara S, et al. An enzyme-linked immunosorbent assay for detecting 3-phenoxybenzoic acid in plasma and its application to farmers and consumers. *Analytical Methods*. 2012. doi:10.1039/c2ay25642h.

317. Palm NW, Medzhitov R. Immunostimulatory activity of haptenated proteins. *Proceedings of the National Academy of Sciences*. 2009. doi:10.1073/pnas.0809403105.

318. Naisbitt DJ, Farrell J, Gordon SF, et al. Covalent binding of the nitroso metabolite of sulfamethoxazole leads to toxicity and major histocompatibility complex-restricted antigen presentation. *Molecular pharmacology*. 2002.

319. Gefen T, Vaya J, Khatib S, et al. The effect of haptens on protein-carrier immunogenicity. *Immunology*. 2015. doi:10.1111/imm.12356.

320. Lanzavecchia A. Antigen-specific interaction between T and B cells. *Nature*. 1985. doi:10.1038/314537a0.

321. Ochsenbein AF, Pinschewer DD, Sierro S, Horvath E, Hengartner H, Zinkernagel RM. Protective long-term antibody memory by antigen-driven and T help-dependent differentiation of long-lived memory B cells to short-lived plasma cells independent of secondary lymphoid organs. *Proceedings of the National Academy of Sciences*. 2000. doi:10.1073/pnas.230417497.

322. Macht VA, Woodruff JL, Maissy ES, et al. Pyridostigmine bromide and stress interact to

impact immune function, cholinergic neurochemistry and behavior in a rat model of Gulf War Illness. *Brain, Behavior, and Immunity*. 2019. doi:10.1016/j.bbi.2019.04.015.

323. Macht VA, Woodruff JL, Grillo CA, Wood CS, Wilson MA, Reagan LP. Pathophysiology in a model of Gulf War Illness: Contributions of pyridostigmine bromide and stress. *Psychoneuroendocrinology*. 2018. doi:10.1016/j.psyneuen.2018.07.015.
324. Musilek K, Roder J, Komloova M, et al. Preparation, in vitro screening and molecular modelling of symmetrical 4-tert-butylpyridinium cholinesterase inhibitors - Analogues of SAD-128. *Bioorganic and Medicinal Chemistry Letters*. 2011. doi:10.1016/j.bmcl.2010.11.051.
325. Ibrahim SM, Al-Shorbagy MY, Abdallah DM, El-Abhar HS. Activation of α7 Nicotinic Acetylcholine Receptor Ameliorates Zymosan-Induced Acute Kidney Injury in BALB/c Mice. *Scientific Reports*. 2018. doi:10.1038/s41598-018-35254-1.
326. Tracey KJ. Fat meets the cholinergic antiinflammatory pathway: Figure 1. *The Journal of Experimental Medicine*. 2005. doi:10.1084/jem.20051760.
327. Van Dyken P, Lacoste B. Impact of Metabolic Syndrome on Neuroinflammation and the Blood–Brain Barrier. *Frontiers in Neuroscience*. 2018. doi:10.3389/fnins.2018.00930.
328. Yabluchanskiy A, Ma Y, Iyer RP, Hall ME, Lindsey ML. Matrix Metalloproteinase-9: Many Shades of Function in Cardiovascular Disease. *Physiology*. 2013. doi:10.1152/physiol.00029.2013.
329. Shetty GA, Hattiangady B, Upadhya D, et al. Chronic Oxidative Stress, Mitochondrial Dysfunction, Nrf2 Activation and Inflammation in the Hippocampus Accompany Heightened Systemic Inflammation and Oxidative Stress in an Animal Model of Gulf War Illness. *Frontiers in Molecular Neuroscience*. 2017. doi:10.3389/fnmol.2017.00182.
330. Diamond B, Huerta PT, Mina-Osorio P, Kowal C, Volpe BT. Losing your nerves? Maybe it's the antibodies. *Nature Reviews Immunology*. 2009. doi:10.1038/nri2529.

331. Brimberg L, Mader S, Fujieda Y, et al. Antibodies as Mediators of Brain Pathology. *Trends in Immunology*. 2015. doi:10.1016/j.it.2015.09.008.

332. Locker AR, Michalovicz LT, Kelly KA, Miller J V., Miller DB, O'Callaghan JP. Corticosterone primes the neuroinflammatory response to Gulf War Illness-relevant organophosphates independently of acetylcholinesterase inhibition. *Journal of Neurochemistry*. 2017. doi:10.1111/jnc.14071.

333. Rothhammer V, Quintana FJ. Control of autoimmune CNS inflammation by astrocytes. *Seminars in Immunopathology*. 2015. doi:10.1007/s00281-015-0515-3.

334. O'Sullivan SA, Gasparini F, Mir AK, Dev KK. Fractalkine shedding is mediated by p38 and the ADAM10 protease under pro-inflammatory conditions in human astrocytes. *Journal of Neuroinflammation*. 2016;13(1):189. doi:10.1186/s12974-016-0659-7.

335. London A, Cohen M, Schwartz M. Microglia and monocyte-derived macrophages: functionally distinct populations that act in concert in CNS plasticity and repair. *Frontiers in Cellular Neuroscience*. 2013. doi:10.3389/fncel.2013.00034.

336. Ginhoux F, Prinz M. Origin of microglia: Current concepts and past controversies. *Cold Spring Harbor Perspectives in Biology*. 2015. doi:10.1101/cshperspect.a020537.

337. Huber T, Ginhoux F, Hoeffel G, Low D, Lim S. Origin and differentiation of microglia. *Frontiers in Cellular Neuroscience*. 2013. doi:10.3389/fncel.2013.00045.

338. Gordon S, Taylor PR. Monocyte and macrophage heterogeneity. *Nature Reviews Immunology*. 2005. doi:10.1038/nri1733.

339. Jakubzick C V., Randolph GJ, Henson PM. Monocyte differentiation and antigen-presenting functions. *Nature Reviews Immunology*. 2017. doi:10.1038/nri.2017.28.

340. Montague K, Simeoli R, Valente J, Malcangio M. A novel interaction between CX 3 CR 1 and CCR 2 signalling in monocytes constitutes an underlying mechanism for persistent vincristine-induced pain. *Journal of Neuroinflammation 2018 15:1*. 2018. doi:10.1186/s12974-018-1116-6.

341. Ferretti E, Pistoia V, Corcione A. Role of fractalkine/CX3CL1 and its receptor in the pathogenesis of inflammatory and malignant diseases with emphasis on B cell malignancies. *Mediators of Inflammation*. 2014;2014. doi:10.1155/2014/480941.

342. Sheridan GK, Murphy KJ. Neuron-glia crosstalk in health and disease: fractalkine and CX3CR1 take centre stage. *Open biology*. 2013;3(12):130181. doi:10.1098/rsob.130181.

343. Guzmán M, Lo Verme J, Fu J, Oveisi F, Blázquez C, Piomelli D. Oleoylethanolamide stimulates lipolysis by activating the nuclear receptor peroxisome proliferator-activated receptor α (PPAR-α). *Journal of Biological Chemistry*. 2004. doi:10.1074/jbc.M404087200.

344. Yancy WS, Foy M, Chalecki AM, Vernon MC, Westman EC. A low-carbohydrate, ketogenic diet to treat type 2 diabetes. *Nutrition and Metabolism*. 2005. doi:10.1186/1743-7075-2-34.

345. Moss JI. Many gulf war illnesses may be autoimmune disorders caused by the chemical and biological stressors pyridostigmine bromide, and adrenaline. *Medical Hypotheses*. 2001. doi:10.1054/mehy.2000.1129.

346. Zhang Z, Zoltewicz JS, Mondello S, et al. Human traumatic brain injury induces autoantibody response against glial fibrillary acidic protein and its breakdown products. *PLoS ONE*. 2014. doi:10.1371/journal.pone.0092698.

347. Pröbstel AK, Sanderson NSR, Derfuss T. B cells and autoantibodies in multiple sclerosis. *International Journal of Molecular Sciences*. 2015. doi:10.3390/ijms160716576.

348. ATSDR. *Toxicological Profile for Pyrethrins and Pyrethroids*.; 2003. doi:10.1177/074823379901500802.

349. Nielsen MJ, Petersen G, Astrup A, Hansen HS. Food intake is inhibited by oral oleoylethanolamide. *Journal of Lipid Research*. 2004. doi:10.1194/jlr.c300008-jlr200.

APPENDIX

Chapter 2

Table showing absolute concentration of human plasma free fatty acid and mice brain free fatty acid.

	Control	SEM	GWI case	SEM
FA19:0	2.246591909	0.12	1.943343	0.25
FA20:0	12.19015685	0.34	10.5978	0.31
FA24:4	1.264909042	0.22	1.265773	0.25
FA24:5	0.994543005	0.11	1.367475	0.10
FA24:6	0.570222951	0.11	0.775772	0.15
FA16:0	655.8729547	3.2	628.3581	9.2
FA16:1	40.54458228	4.3	55.59287	5.3
FA18:0	594.1698374	5.5	515.779	3.5
FA18:1	959.0170044	55.4	1247.565	66.4
FA18:2	384.8887904	50.3	520.0629	70.3
FA18:3	37.24441324	32.3	48.81775	45.3
FA20:3	16.89213982	1.2	21.89752	2.2
FA20:4	56.75493424	1.4	72.25026	2.4
FA20:5	10.1522195	0.71	10.94809	0.51
FA22:1	3.54638816	0.54	1.871912	0.74
FA22:4	11.0888527	1.1	14.55546	1.51
FA22:5n3	10.78242947	1.24	16.95872	1.4
FA22:5n6	5.011327198	0.33	7.128399	0.36
FA22:6	37.53091998	1.2	48.07908	1.42
FA24:0	4.491940173	0.66	3.040707	0.56
FA24:1	0.041859864	0.004	0.028608	0.004
Phytanicacid	2.613029327	0.24	2.318204	0.42
Pristanicacid	0.313721956	0.23	0.272232	0.33

	control(uM/ug)	Control+OEA(uM/ug)	Control+OEA(uM/ug)	GWI (uM/ug)
FA19:0	4.739045128	0.006200183	0.006200183	0.004616551
FA20:0	0.2942313	4.998083067	4.998083067	4.56812933
FA24:4	0.372420263	0.358603938	0.358603938	0.325075834
FA24:5	2.108312343	0.402495544	0.402495544	0.395023328
FA24:6	402.6457587	2.033658105	2.033658105	2.130905512
FA16:0	0.022877354	290.7922474	290.7922474	335.8799076
FA16:1	33.4497406	0.026184025	0.026184025	0.024065568
FA18:0	0.610180401	30.04084201	30.04084201	32.65348571
FA18:1	0.136549656	0.698006756	0.698006756	0.610208317
FA18:2	0.038091028	0.092237605	0.092237605	0.124736518
FA18:3	11.82895541	0.030758311	0.030758311	0.034279802
FA20:3	24.91360256	21.8625	21.8625	14.32595573
FA20:4	0.007381428	25.08444386	25.08444386	25.83356742
FA20:5	0.921089582	0.007018559	0.007018559	0.006623717
FA22:1	20.41432927	0.899825131	0.899825131	0.847879617
FA22:4	0.112785436	25.13103831	25.13103831	27.05969668
FA22:5n3	0.074417373	0.116192749	0.116192749	0.122361611
FA22:5n6	301.8505338	0.048868606	0.048868606	0.059545853
FA22:6	0.003731431	466.6225681	466.6225681	392.3535188
FA24:0	2.886255924	0.003218759	0.003218759	0.002928319
FA24:1	1.234	2.336787565	2.336787565	2.094017094
Pristanic acid	5.148228713	12.3	12.3	8.63

Chapter 3

Table showing absolute concentration of mice brain acetyl carnitine.

Compound	control(nmol/g))	SEM	GWI(nmol/g))	SEM	Control+NR(nmol/g))	SEM	GWI+NR(nmol/g))	SEM
2:0	2.682432764	0.120061792	3.188511339	0.111609334	2.3736135	0.26113185	2.393390094	0.119482704
3:0	0.029290341	0.001599855	0.028601164	0.006777546	0.025921799	0.002696983	0.017205961	0.000780862
4:0	0.011340902	0.000978062	0.010241298	0.001093692	0.008619254	0.001327254	0.007632602	0.001403251
5:0	0.018297939	0.000966713	0.029239519	0.000232218	0.018500723	0.001632812	0.018346825	0.001567656
6:0	0.000514256	0.000107788	0.000307363	9.5093E-05	0.000299893	5.0121E-05	0.000150058	1.8282E-05
14:0	0.088694035	0.003891811	0.164716846	0.007508173	0.082843315	0.004288409	0.090659867	0.001297559
16:0	0.489740936	0.018466255	0.516914768	0.024967277	0.476073147	0.021848491	0.475000858	0.024746998
16:1	0.063409549	0.008315284	0.077207239	0.003035203	0.055698425	0.002559204	0.047361738	0.000757277
18:0	0.106080664	0.007701896	0.114709485	0.007800853	0.097842077	0.005703363	0.115979167	0.006678328
18:1	0.272991139	0.017524292	0.289229948	0.007706301	0.246068785	0.012416752	0.267700955	0.010183048
18:2	0.014253615	0.001519379	0.019992729	0.002807475	0.013167305	0.001240846	0.015377021	0.000828518
18:3	0.018297939	0.000966713	0.027822853	0.000700838	0.018500723	0.001632812	0.018346825	0.001567656
20:0	0.004030584	0.000383579	0.004008381	0.000270507	0.003273265	0.000155776	0.004705451	0.000314129
20:1	0.021441479	0.002397366	0.028243446	0.001976899	0.018606655	0.002242977	0.022775786	0.001496857
20:3	0.008195642	0.000789612	0.008706749	0.000744218	0.006595075	0.000456569	0.006668959	0.001493714
20:4	0.168607080	0.016785426	0.343239399	0.014465694	0.171886958	0.024235004	0.128933708	0.009894133
22:0	0.018297939	0.000966713	0.029239519	0.000232218	0.018500723	0.001632812	0.018346825	0.001567656
22:6	0.020431722	0.003483075	0.028082093	0.003859073	0.026065691	0.004309954	0.026957307	0.002277509
24:0	0.018297939	0.000966713	0.026822853	0.000570623	0.018500723	0.001632812	0.018346825	0.001567656
26:0	ND	ND	ND	ND	ND	ND	ND	ND
free	12.952711273	0.662996618	21.73094677	1.526876128	18.84283135	1.327878073	17.04909219	0.857452665
Gamma-butyrobetaine	0.566499947	0.013736568	0.829801321	0.011298211	0.793481916	0.048624783	0.720075371	0.006411785

Carnitine/GBB	22.95795725	1.116910177	35.27428455	3.492018453	24.13439461	3.162234116	23.69716206	1.305937655